UNIVERSITY OF SOUTHAMPTON

FACULTY OF MEDICINE, HEALTH & LIFE SCIENCES

School of Biological Sciences

The Role of Membrane Proteins in *Arabidopsis* Seedling Development

By

Jonathan Jerram

Thesis for the degree of Doctor of Philosophy

March 2007

UNIVERSITY OF SOUTHAMPTON

ABSTRACT

FACUTLY OF MEDICINE, HEALTH AND LIFE SCIENCES
SCHOOL OF BIOLOGICAL SCIENCES

Doctor of Philosophy

THE ROLE OF MEMBRANE PROTEINS IN *ARABIDOPSIS* SEEDLING DEVELOPMENT

by Jonathan Giles Jerram

Plants have evolved sophisticated mechanisms to perceive changes in their environment and adapt their developmental program. Light is one of the most important factors and is most dramatically illustrated by seedling development. The transition from the dark-grown seedling to the photoautotrophic seedling is called de-etiolation and is accompanied by extensive changes in seedling morphology. Associated with this is a re-distribution of photoassimilates and other vital compounds and it is likely that changes in morphology require changes in the expression of a wide variety of transporter genes. To identify genes that are regulated by phytochrome A (phyA) during far-red light (FR) induced de-etiolation a transcriptomics approach was used. Transporter genes from a range of transport classes were identified using both the Arabidopsis Membrane Transporter (AMT) array (Maathius *et al.*, 2003) and data from previously published array datasets including Wang *et al.* (2002). Examples of FR-light induced genes included the monosaccharide transporter *STP1*, a Ca^{2+} ATPase, *ACA2*, the auxin transporter *PIN4*, a putative anthocyanin transporter *ANM2* and two genes of unknown function, the Niemann-Pick C disease-like protein and *FRIMP1*. Three FR-light repressed candidate transporter genes were also selected, *RAN1* an ATP-dependent copper transporter, *CAT4* an amino acid transporter and *AHA2* an H^{+}-ATPase. Most of the genes were confirmed as being FR-light regulated by FR-light using RT-PCR and real-time PCR. The expression of some genes, including STP1 was also shown to be mediated by other wavelengths of light including blue and red-light. To further study the role of these candidate genes in seedling de-etiolation insertional T-DNA mutants were obtained and characterised. The *stp1*, *aca2*, *cat4* and *aha2* mutants were obtained and interesting phenotypes were shown in some of these mutants. This included a reduced apical hook curvature and a reduction in hypocotyl elongation in the dark-grown *cat4* mutant and a smaller *aca2* seedling when grown in blue and white-light. A gene of unknown function was also established as being FR-light induced and termed FRIMP (**F**ar-**r**ed **I**nduced **M**embrane **P**rotein). The *frimp1* mutant had a number of phenotypic characteristics including the epinastic curling of the leaves, elongated petioles and an elongated hypocotyl in the FR-light grown seedling. A homolog to FRIMP1, termed FRIMP2 was revealed by protein sequence analyses and the phenotype of *frimp2* was less severe than *frimp1* but also has an unusual leaf shape. The induction of *FRIMP1* in the FR-light grown *phyA* seedling indicated another photoreceptor other than phyA is important in perceiving FR-light. This is a unique expression profile. The FRIMP proteins may act directly as components of a light signalling pathway between phytochrome and other effector proteins. Alternatively they might transport a signalling molecule or may be receptors for such a molecule. The transcriptomics approach was successful in identifying FR-light responsive genes and indicated that membrane proteins are important in mediating light-regulated seedling development and changes in morphology.

Contents

Page

Page

Chapter 4 Transporters in *Arabidopsis* Seedling Development

4.1 Introduction

4.2 Results

4.3 Discussion

Acknowledgements

Firstly I would like to thank the BBSRC for the funding throughout my PhD as without this I would not have been able to complete this thesis. I would like to thank The University of Southampton for allowing me to study for my doctorate and making my time at Southampton enjoyable. Many thanks to the countless people at Southampton who have aided me in my research, including Dr Aram Buchanan, Dr Duncan Legge, Rob Holmes, Melissa Doherty and Dave Cook. A massive thanks goes to Dr Alex McCormac without who I would probably not have finished my PhD. Not only would I like to thank Alex for her knowledge and research support, but also for the emotional support she gave always willing to listen especially during the low periods. I thank numerous people for their technical aid, including Anton Page for his aid with the leaf sections. I also thank the project students Sarah and Amy. A huge big up to my friends who have been there for me, I could not ask for such a better group of friends. There are so many to mention but the biggest thanks go to Juicy, Kat, Mikey, Adrian, Julia, Rosie, Tom, Dave and Brenda. The biggest thanks go to my parents and my family. I would not be here finishing this PhD without the support from my mum and dad, thank you so much. Finally I would especially like to thank my supervisors Dr Matthew Terry and Dr Lorraine Williams for their support, expertise and guidance through my research and the writing of this thesis.

Abbreviations

A	Absorbance
AAP	Amino acid permease
ABC	ATPase binding cassette
AMPL	*Arabidopsis* Membrane Protein Library
AMT	*Arabidopsis* Membrane Transporter
ANT	Neutral amino acid transporter
At	*Arabidopsis thaliana*
ATF	Amino acid transporter family
ATP	Adenosine triphoshate
ATPase	Adenosine triphosphatase
AUX	Auxin transporter
B	Blue-light
BLAST	Basic Local Alignment Search Tool
bps	Base pairs
BSA	Bovine serum albumin
Ca	Calcium
CaM	Calmodulin
CAT	Cationic amino acid transporter
CATMA	Complete *Arabidopsis* Transcriptome Microarray
cDNA	Complementary DNA
CNGC	Cyclic nucleotide gated channel
Col-0/Col-8	*Columbia* ecotype
cry	Cryptochrome
C(T)	Cycle threshold
CTP	Cytosine triphosphate
D	Dark
Da	Dalton
dATP	Deoxyadenosine triphosphate
dH_20	Distilled water
DMF	N,N-dimethylformamide
DNA	deoxyribonucleic acid

DNAse	Deoxyribonuclease
dNTP	Deoxynucleotide triphosphate
DTT	Dithiothreitol
EDTA	Ethylene diamine tetra-acetic acid
ER	Endoplasmic reticulum
EST	Expressed sequence tag
EtBr	Ethidium bromide
(F)	Forward primer
FR	Far-red light
FRIMP	FR-light induced membrane protein
gDNA	Genomic DNA
GFP	Green fluorescent protein
GPCR	G-protein coupled receptor
GSP	Gene specific protein
GTP	Guanidine triphosphate
H	Hydrogen
HCL	Hydrogen chloride
HEMA	Glutamyl t-DNA reductase
IAA	Indole-3-acetic acid
K	Potassium
kb	Kilobase
kDa	Kilodalton
Lba1	Left border primer 1
Ler	*Landsberg erecta*
Lhcb	Light-harvesting chlorophyll a/b binding protein
LHT	Lysine histidine transporter
LiCl	Lithium chloride
M	molecular mass
MATDB	MIPS *Arabidopsis thaliana* database
MFS	Major facilitator superfamily
MIPS	Munich Information Centre for Protein Sequences
MOPS	3-(N-morpholino) propanesulphonic acid
mRNA	Messenger RNA
MS	Murashige and Skoog

NaCl	Sodium Chloride
NASC	Nottingham *Arabidopsis* stock centre
NaOAc	Sodium acetate
NaOH	Sodium Hydroxide
NPTII	Neomycin phosphotransferase
Nramp	Natural resistant-associated macrophage protein
OD	Optimal density
oligo	Oligonucelotide
Os	Rice
PCR	Polymerase Chain Reaction
PHOT	Phototropin
phy	Phytochrome
POR	NADPH-Pchlide oxidoreductase
ProT	Proline transporter
qPCR	Quantitative real-time PCR
R	Red-light
(R)	Reverse primer
RNA	Ribonucleic acid
RNAi	RNA interference
rRNA	Ribosomal RNA
RNase	Ribonuclease
rpm	Repeats per minute
RT-PCR	Reverse transcription PCR
SAP	Shrimp Alkaline Phosphatase
SDS	Sodium dodecyl suphate
SSC	Saline sodium citrate
STP	Sugar transporter protein
T-DNA	Transposon DNA
TAE	Tris/acetate/EDTA
TAIR	The *Arabidopsis* Information Resource
TE	Tris/EDTA
T_m	Temperature
Tr	Truncated
Tris	Tris(hydroxymethyl) aminomethane

TTP	Thymine triphosphate
UTP	Uridine triphosphate
UV	Ultraviolet
V	Volt
v/v	Volume per volume
Vol	Volume
W	Wild-type gene
w/v	Weight per volume
WT	Wild-type

Chapter 1

Introduction

1.1 Light Regulation of plant development

As sessile organisms, plants have evolved a multitude of developmental responses to cope with changing environmental conditions that challenge the plant throughout its life cycle (Sullivan and Deng, 2003). Plants have developed sophisticated mechanisms in which to perceive these environmental changes and adapt their developmental pattern. Light is one of the most important environmental conditions that regulate plant development. From determining the developmental program of the emerging seedling and the time of flowering to influencing the organisation of organelles to maximise photosynthesis, light has dramatic effects on development during all stages of plant life (Sullivan and Deng, 2003). Plants have evolved complex methods of sensing the quality, quantity, direction and duration of light and interpreting these signals to produce the appropriate physiological and developmental response (Möller *et al.*, 2000). The light control of plant development is most dramatically illustrated by seedling development. Seedlings can follow one of two developmental pathways according to the light environment. The development of a seedling grown in light is distinct from one grown in the dark; with respect to gene expression and organ morphology (Von Arnim and Deng, 1996).

In darkness, seedlings follow skotomorphogenic (or etiolated) development, characterised by a long hypocotyl and closed cotyledons which are protected by the apical hook (Figure 1.1). The apical hook allows the buried seed to emerge through the soil, while maximum cell elongation in the hypocotyl allows the plant to attempt to reach light conditions sufficient for photoautotrophic growth and to switch to a developmental program optimal for photosynthesis in a process called de-etiolation (Fankhauser and Chory, 1997). In contrast, growth in the light results in photomorphogenic development characterised by a short hypocotyl and expanded cotyledons which are optimally designed to carry out photosynthesis (Figure 1.1). The different developmental patterns are thought

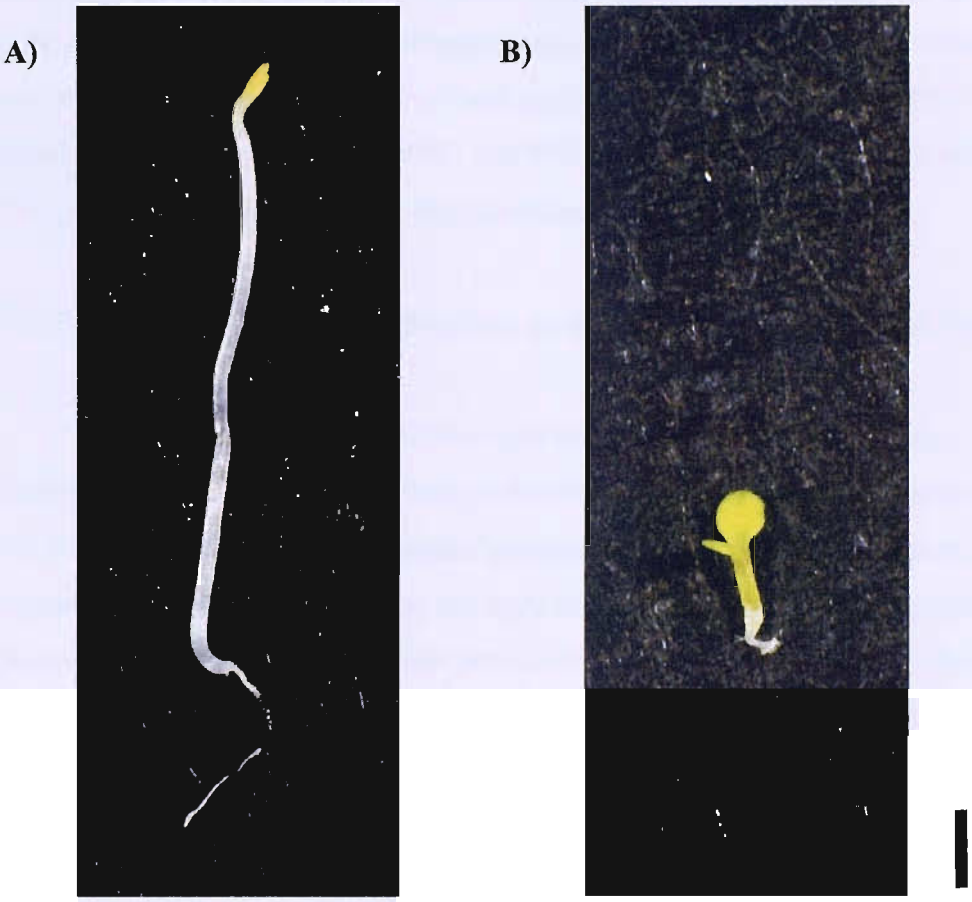

Figure 1.1 *Arabidopsis* seedling development when grown in complete darkness and white light. Phenotypic differences of seedlings as a consequence of the light environment. Seedlings were stratified for 48 h at 4°C, then placed under white light to induce germination. Seedlings were transferred to (A) complete darkness or (B) white light treatment at a fluence of 120 µmol $m^{-2}s^{-1}$ for 96 hours. Bar = 1 mm

to be primarily mediated by changes in the expression of light-regulated genes (Li *et al.*, 1993; Terzaghi and Cashmore, 1995).

The most important component for encoding the complexity of these light-regulated responses are multiple families of photoreceptors. To monitor these changes in the ambient light conditions, different photoreceptor classes have evolved, UVB photoreceptors, the two blue/UVA photoreceptors cry1 and cry2 (Ahmad and Cashmore 1993), the blue-light phototropin photoreceptors, PHOT1 and PHOT2 (Kagawa *et al.*, 2001) and the red/far-red (FR) reversible photoreceptors, phytochromes A-E (Clack *et al.*, 1994).

1.2 Multiple phytochromes contribute to light-regulated plant development

The identification of multiple light-regulated responses responding to a single photoreceptor was one of the initial problems in early phytochrome research. However, in the 1980s spectrophotometric studies indicated that there were two distinct groups of phytochrome, type I (light labile) and type II (light stable). The cloning of multiple phytochrome apoprotein genes has provided vast new insights on the distinct groups and modes of action of phytochrome (Sharrock and Quail 1989). It is now known that there are five distinct phytochromes termed phyA-phyE (Clack *et al.*, 1994).

In dark grown tissues, phyA is by far the must abundant of the five phytochromes, however after exposure to light the level of phyA drops by a factor of 100 fold (Clough *et al.*, 1999). The regulation of phyA protein level by light is therefore the result of co-ordinated transcriptional and post-translational regulation. The rapid intracellular degradation of phyA induced upon its photo-conversion to the Pfr form (representing a 100-fold greater rate for PfrA than PrA) was one of the first molecular properties of the photoreceptor to be recorded in literature (discussed in Clough *et al.*, 1999). The other phytochromes phyB-phyE do not exhibit this dramatic isoform specific difference in degradation and are therefore considered to be more light stable (Somers *et al.*, 1991). In light-grown plants, phyB becomes the most abundant phytochrome, while phyC-phyE are less abundant (Clack *et al.*, 1994; Hirschfield *et al.*, 1998).

1.3 Phytochrome structure

The functional phytochrome molecule exists as a homodimer composed of approximately 124kDa subunits, each of which carries a single covalently attached linear tetrapyrrole chromophore (phytochromobilin) linked via a thioether bond to a conserved cysteine residue in the N-terminal globular domain of the protein (Furuya and Song 1994, Wagner *et al.*, 2005) (Figure 1.2). Evidence from biochemical studies on phyA indicated that the polypeptide consists of two structural domains. The 60kDa N-terminal structural domain has been shown to contain the components for photoreception and is also responsible for the differences in photosensory specificity and photolability between the phytochromes (Quail., 1997, Montgomery and Lagarias, 2002). However the C-terminal is required for the actual transfer of the perceived informational signals downstream to the transduction pathway components and also for the PfrA-specific degradation (Quail., 1997, Rockwell and Lagarias, 2006). Analysis of deletion derivatives of phyA and phyB expressed in transgenic plants have shown a chromophore lyase activity sufficient for attachment of the chromophore within the N-terminal segment between positions 115 and 450 (Deforce *et al.*, 1991; Boylan and Quail 1991). Signalling by phytochromes also involves protein-protein interactions via the N-terminal of phytochrome (Oka *et al.*, 2004). The C-terminal contains two histidine kinase-related domains (HKRD) that have been shown to transfer ATP-dependent protein phosphotransferase activity in many cases (Tasler and Mioises., 2005), and two motifs with homology to PAS (**P**ER-**A**RNT-***S***IM, period clock, ARNT, single minded proteins) domains (Lagarias and Mercurio, 1995; Ponting and Aravind, 1997). These PAS domains are present in various signal transduction molecules which sense environmental signals such as oxygen levels and light conditions (Taylor and Zhulin, 1999). The C-terminal regulatory domains have also been shown to mediate homodimerization and light-modulated nuclear targeting, both of which are required for signal transmission (Matsushita *et al.*, 2003; Chen *et al.*, 2005).

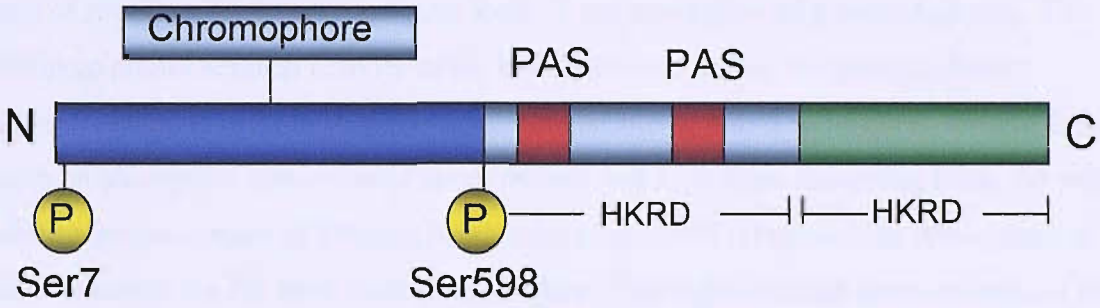

Figure 1.2 Typical structure of a phytochrome. The chromophore is bound to the N-terminal domain. Phytochrome contains two histidine kinase-related domains (HKRD) and two motifs with homology to PAS (PER-ARNT-SIM, period clock, ARNT, single-minded protein) domains. Picture modified from Möller *et al.*, 2002.

1.4 Pr/Pfr conformational changes

The phytochromes are signal transducing photoreceptors that are able to convert between active and inactive forms in response to different light wavelengths. Light signals are used to provide important information of crucial ecological value at many developmental stage of a plants life cycle, in respect to seed germination, seedling development, photosynthetic machinery development, the timing of flowering and responses to neighbouring competition (Smith., 2000). One of the striking properties of the phytochromes is their photoreversibility property of changing colour on photon absorption and of reverting back to the original form on the absorption of a second photon. The intrinsic photochemical activity of the bilin molecule within the protein allows phytochromes to exist in two photointerconvertible forms. A red light absorbing form Pr, with an absorption maximum of about 665nm and a FR-light absorbing form, Pfr with an absorption maximum of 730nm (Braslavsky *et al.*, 1997) (Figure 1.3). Absorption of FR-light converts the Pfr form back to the Pr form. The light-induced interconversions between Pr and Pfr involves a Z-E isomerization of the linear tetrapyrrole chromophore about the C_{15} double bond that links the C and D rings of the tetrapyrrole (Terry *et al.*, 1993). This photoconversion of the chromophore leads to reversible conformational changes throughout the protein moiety of phytochrome (Quail, 1991). The altered protein conformations stabilize the chromophore isomers. Based on both physiological and genetic studies, the Pfr form of phytochrome is generally considered to be biologically active and the Pr form is considered to be inactive. It is these light-induced conformational changes that account for the differences in activity between Pfr and Pr (Whitelam *et al.*, 1998). The absorption spectra of Pr and Pfr show a considerable overlap throughout the visible light spectrum (Figure 1.3), thus as a consequence the phytochromes are present in an equilibrium of the two forms under almost all irradiation conditions. This ensures that no light condition can convert all phytochrome into exclusively one form. Only phytochrome that is synthesised in complete darkness is present exclusively as Pr. It is generally thought that it is the concentration of Pfr, rather than Pr that is responsible for all the photomorphogenic effects of phytochrome (Liscum and Hangarter, 1993b; Reed *et al.*, 1994; Shinomura *et al.*, 1994).

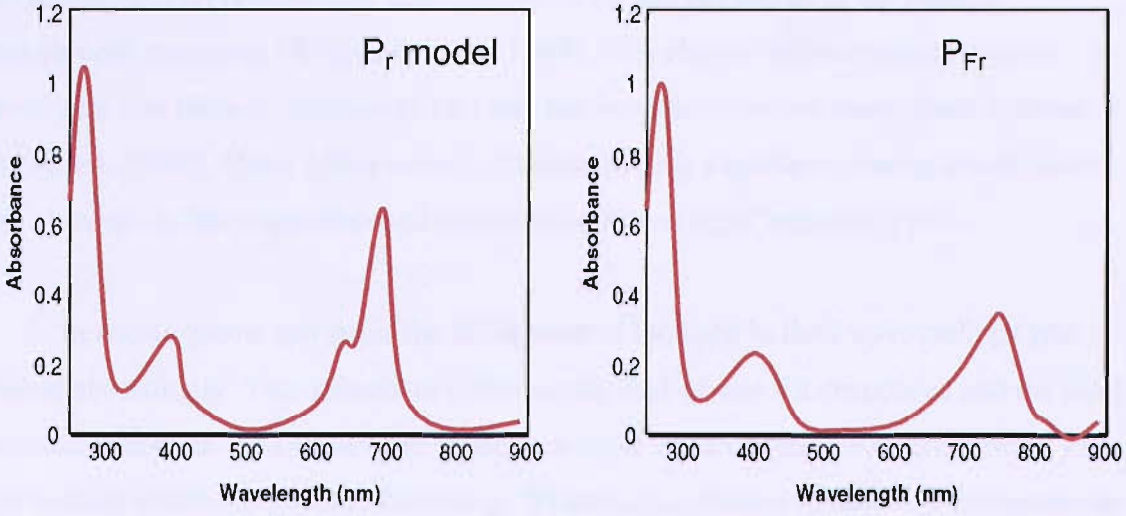

Figure 1.3 Absorption spectra of phytochromes. The absorption spectra of phytochrome which exists in two forms Pr and Pfr (solid red line). The Pr form of phytochrome absorbs at a maximum wavelength of 665 nm, while the Pfr form absorbs maximally at 730 nm. Spectra taken from Rockwell *et al.* (2006).

1.5 Phytochrome responses

One of the major goals in phytochrome research has been to understand the signal transduction pathways that lead to altered plant development. It was found that red light stimulates seed germination, but this induction can be inhibited by subsequent exposure to FR-light. The seeds can be cycled through sequential red or FR-light treatments; however the final germination response is determined solely by the last light treatment. Reciprocity, the dependence of the total number of photons irrespective of the duration of exposure is exhibited in this response, indicating the involvement of a first-order chemical reaction. Red/far-red (R/FR) reversibility and reciprocity are the hallmarks of the classic phytochrome responses (Whitelam *et al.,* 1998). This class of phytochrome responses is known as a low fluence response (LFR) and has been described in many plant systems (Mancinelli, 1994). Other LFRs include changes in gene expression during de-etiolation, stem elongation, leaf expansion and transition to flowering (Cosgrove, 1994).

In reality plants can sense the R/FR ratio of the light in their surroundings and respond accordingly. Two subsets of LFRs are the end-of-day FR-responses and the shade avoidance response. The end-of-day responses occur by detecting the enrichment of FR-light at dusk which then affects flowering. Whereas, the shade avoidance is a response to FR-light under a leaf canopy or reflected light from nearby leaves and is a mechanism for neighbour detection (Aphalo *et al.*, 1999). In this situation FR-light can pass through the leaf canopy, whereas the red light is reflected or absorbed by the leaf. In both of these cases plants respond by elongating their stems and increasing the length to width ratio of the leaves. So both responses are controlled by the R-FR ratio (Smith and Whitlam 1997).

As more phytochrome-mediated processes were discovered it has become clear that there are at least three physiologically distinct modes of phytochrome action. In addition to the classic R/FR reversible LFRs, there are two other responses: the very low fluence responses (VLFRs) and the high irradiance responses (HIRs). These three response modes can be distinguished by the amount of light required, which varies over eight orders of magnitude and are characterised by R/FR reversibility and different fluence rate dependence. VLFRs are mediated by phyA and by light fluences as low as 10^{-9} μmol $m^{-2}s^{-1}$. These responses are therefore saturated by very low concentrations of Pfr and do not show R-FR photoreversibility (Smith and Whitelam, 1990). The VLFR promotes

germination and therefore allows seeds to take opportunistic advantage of very brief pulses of light through the soil. The LFRs are mediated by the phytochromes stable in the Pfr form, namely phyB to phyE. These responses generally require fluence rates between 0.1-100 μmol $m^{-2}s^{-1}$ and are characterised by their R-FR reversibility (Shinomura *et al.*, 1996). In the HIRs, plants generally respond to greater than 1000 μmole/m^2 of light, although it is fluence rate and not total fluence defining these responses. The HIR is characterised therefore by a requirement for continuous irradiation as opposed to being elicited by a single pulse (Casal *et al.*, 1998). Reciprocity is not seen for either VLFRs or HIRs.

1.6 Phytochrome localization

Another striking property of phytochrome that is affected by light is its subcellular localization (Nagatani, 2004). Immunolocalization studies of phyA indicated that it was mainly located in the cytoplasm, however it was later found that a large portion of phyB was located in the nucleus in light-grown plants (Sakamoto and Nagatani 1996). Later expression of the rice phyA green fluorescent protein (GFP) and the tobacco phyB-GFP fusion protein was used to demonstrate that phyA-GFP and phyB-GFP were localized in the cytosol of dark-grown plants, but light treatment led to the nuclear translocation of phyA-GFP and phyB-GFP (Kircher *et al.*, 1999). The fusion proteins formed speckles in the nucleus, indicating the possibility that phytochromes are found in a large complex in the nucleus (Kircher *et al.*, 1999).

The kinetics and light requirements for phyA and phyB nuclear translocation are quite different. For phyB there is evidence that nuclear translocation occurs only in the Pfr conformation (Murphy & Lagarias, 1997). However, phyA does migrate into the nucleus even with FR-illumination, suggesting that phyA in its Pr conformation is capable of nuclear accumulation if it has been recycled through Pfr (Kircher *et al.*, 1999). The Pr-to-Pfr conversion is very rapid but it takes several hours to accumulate significant levels of phyB in the nucleus. However, many phytochrome responses such as changes in hypocotyl growth occurs within minutes, indicating that the nucleus is not the only site of action of phytochromes (Kircher *et al.*, 1999). Phytochrome signalling components have also been identified in the cytoplasm demonstrating that the nucleus is not the only place for phytochromes action (Moller *et al.*, 2002). This indicates that phytochrome responses must

also be mediated by cytoplasmic events and these could include a direct effect on a number of proteins including those functioning in the membrane (Nagy and Schafer, 2002).

1.7 Phytochrome functions indicated by mutant studies

Establishing the roles of the individual phytochrome species has been the subject of extensive research, and much has been revealed from the study of mutants deficient in one or more phytochromes (Whitelam and Devlin, 1997). The unique role of phyA in inhibiting hypocotyl elongation in prolonged FR-light was established through analysis of *phyA*-deficient mutants in a variety of species including *Arabidopsis* (Nagatani *et al.*, 1993) and rice (Takano *et al.*, 2001). When grown in continuous FR, *Arabidopsis phyA* mutants display long hypocotyls and are unable to open and expand their cotyledons and resemble etiolated wild-type seedlings (Nagatani *et al.*, 1993). This phenotype currently forms the basis for screening for mutants involved in phyA signalling (Nagatani *et al.*, 1993; Franklin *et al.*, 2005).

Analyses of *phyB* mutants have revealed a significant role for phyB in the de-etiolation of seedlings in red-light. Under these conditions *phyB* null mutants display elongated hypocotyls and smaller cotyledons compared to wild-type seedlings (Koornneef *et al.*, 1980). *phyB* seedlings respond normally to blue and FR-light, indicating that phyB is the principal photoreceptor for de-etiolation under red light (Reed *et al.*, 1993). In *Arabidopsis* it has been revealed that mutants deficient in both phyA and phyB display longer hypocotyls than either single mutant (Reed *et al.*, 1994). These observations provided early evidence of phyA action in response to red-light and established the redundant nature of phytochromes functions. Redundancy between these two phytochromes has also been reported in the red-light mediated opening and expansion of the cotyledons (Neff and Chory, 1998). The *phyB* mutant seedlings display attenuated responses to a low R/FR ratio, leading to the proposal that phyB plays a key role in the shade avoidance syndrome (Nagatani *et al.*, 1991). The creation of double, triple and quadruple mutants, deficient in multiple phytochromes has revealed that all five phytochromes members promote cotyledon expansion in continuous red-light (Franklin *et al.*, 2003a). Functional redundancy between phyB, D and E has been shown to be involved in controlling flowering time and leaf development (Devlin *et al.*, 1999; Franklin *et al.*, 2003a).

The recent identification of a *phyC* null mutant has provided insights into the role of phyC in seedling de-etiolation (Franklin *et al.*, 2003b). When grown in continuous red-light *phyC* mutants displayed elongated hypocotyls, suggesting a putative role for this phytochrome in modulating growth (Franklin *et al.*, 2003b). The absence of an additive phenotype in the *phyBphyC* double mutant presents the possibility that phyC may operate through modulating phyB function. Even though PHYA and PHYC show a relatively close phylogenetic relationship no role has been identified for phyC in FR-light sensing in *Arabidopsis* (Monte *et al.*, 2003). phyC may perform a significant role in the modulation of other phytochromes and it appears to work with phyA to act redundantly to modulate phyB-mediated inhibition of hypocotyl elongation in red-light and to function together to regulate leaf morphology (Franklin *et al.*, 2003b).

When looking at the *phyAphyBphyD* triple mutant it displays elongated petioles and enhanced elongation of the internodes in response to end-of-day FR-light. These characteristics indicate phyD acts in the shade-avoidance syndrome by controlling flowering time and leaf area (Devlin *et al.*, 1999). Consistent with its phylogenetic relationship to phyB, phyD functions in shade-avoidance responses (Aukerman *et al.*, 1997) and also interacts with cry1, suggesting phyD has a role in modulating blue-light perception (Hennig *et al.*, 1999). phyE has also been shown to participate in light-regulated germination, maintenance of rosette and also in shade avoidance (Devlin *et al.*, 1998). When looking at the *phyE* mutant results indicated that like phyB, phyE participates directly in R/FR reversible regulation of germination and unlike phyB and phyD, phyE did not inhibit phyA mediated germination (Hennig *et al.*, 2000). phyE was in fact found to be required for germination of *Arabidopsis* seeds in continuous FR-light, however in the *phyE* mutant inhibition of hypocotyl elongation and induction of cotyledon unfolding was not affected by FR-light (Hennig *et al.*, 2000). Such results reveal the novel role of phyE in plant development and demonstrates the functional diversity of the closely related phytochromes B, D and E (Hennig *et al.*, 2000).

1.8 Phytochrome signal transduction

Arabidopsis seedlings display contrasting developmental patterns depending on the light environment and recent studies have implicated protein degradation as a means of regulating this developmental switch (Osterlund *et al.*, 2000). The HY5 protein is a positive regulator of photomorphogenesis and acts to promote the light developmental pattern and is subject to control by negative photomorphogenic regulators such as COP1 (CONSTITUTIVE PHOTOMORPHOGENIC 1) and the COP9 signalsome (Osterlund *et al.*, 2000). HY5 is a transcription factor that is localised to the nucleus and has been shown to bind to the G-box motif of multiple light inducible promoters and is necessary for the optimal expression of the corresponding genes (Ang *et al.*, 1998). In darkness COP1 interacts with HY5 preventing it from binding to the promoters of the light inducible genes. Genetic screens for constitutive photomorphogenic or de-etiolated development in darkness resulted in the identification of at least 10 *Arabidopsis COP/DET/FUS* loci (Chory *et al.*, 1989; Deng *et al.*, 1991). All loss-of-function mutations in these genes resulted in similar photomorphogenic phenotypes in the dark and include activation of light-inducible genes, chloroplast development, inhibition of hypocotyl elongation, cotyledon opening and anthocyanin accumulation (Chory *et al.*, 1989). The *COP/DET/FUS* genes are involved in a pathway to repress photomorphogenic development, which acts during darkness to suppress photomorphogenic developmental pattern (Wei *et al.*, 1994).

The nuclear protein COP1, acts to suppress photomorphogenesis in the absence of light (Yamamoto *et al.*,1998). The subcellular localisation of COP1 can be regulated by light as when COP1 is fused with the GUS (β-glucuronidase) reporter protein the fusion protein was observed primarily in the nucleus in the absence of light. After light perception, the fusion protein was not detectable in the nucleus. This results from not a change in the amount of COP1 but by nuclear localization (von Arnim and Deng 1994). COP1 was shown to act autonomously to suppress photomorphogenesis and that this ability is highly dependent on its cellular abundance suggests that COP1 is part of a key regulatory step responsible for the suppression of photomorphogenesis (Torii and Deng, 1997). COP1 regulates photomorphogenesis via the specific targeting of proteins for ubiquitination and proteasome-mediated degradation (Hoecher, 2005). COP1 is an E3 ubiquitin protein ligase which acts downstream of both phytochromes and crytochromes (Ang and Deng, 1994; Hoecher. 2005). In then light, the re-localization of COP1 to the

cytoplasm allows proteins involved in the positive regulation of photomorphogenesis, such as the transcriptional factor HY5 to accumulate and photomorphogenesis to occur. In addition the interaction of both phytochromes and crytochromes with COP1 in a light-dependent manner is believed to repress COP1 activity through direct protein-protein interactions (Wang *et al.*, 2001). The localization of COP1 is controlled by the light where in the light it is primarily cytoplasmic but the protein accumulates in the nucleus during darkness where is directly interacts with HY5. The COP1-HY5 interaction is necessary for the degradation of HY5 (Osterlund *et al.*, 2000). COP1 has also been shown to control photoreceptor levels in the light as recently it has been shown that COP1 is necessary for the red light-induced degradation of phyA (Seo *et al.*, 2003) which is degraded in the light by ubiquitin-mediated proteolysis (Clough and Vierstra, 1997). It has also been shown that COP1 is partly responsible for the targeted degradation of many proteins including HY5, LAR1, HFR1 (Long hypocotyl in far-red) (Osterlund *et al.*, 2000; Saijo *et al.*, 2003; Yang *et al.*, 2003; Yang, 2005; Seo *et al.*, 2003). Therefore COP1 in conjunction with the 26S proteasome complex, functions as a crucial modulator that controls the levels of photoreceptors and downstream transcriptional factors (Huq; 2006).

Recent studies have shown that multiple related bHLH (basic helix-loop-helix) class transcription factors play key roles in phytochrome signal transduction (Duek and Fankhauser 2005). These transcriptional factors primarily act as negative regulators of phytochrome signalling (Duek and Fankhauser 2005). Members of the bHLH family appear to be particularly important because several of them specifically interact with light activated Pfr form (Quail. 2002). This model was derived from early studies based mainly on the analyses of PIF3 **P**hytochrome **I**nteracting **F**actor 3. In the nucleus Pfr can interact with a variety of basic helix-loop-helix including PIF3 and control the expression of a selection of target genes by triggering a transcriptional cascade regulating the expression of 2500 genes in *Arabidopsis* (Ni *et al.*, 1998; Bauer *et al.*, 2004). The binding of phytochrome to bHLH transcriptional factors in the nucleus is believed to form one of the early signalling steps in the de-etiolation of dark grown seedlings. The DNA sequence motif recognised by most bHLH transcription factors is termed the E-box, and the most commonly recognised E-box is the sequence CACGTG, termed the G-box (Toledo-Ortiz *et al.*, 2003). This is an example of direct activation of a transcription factor in the nucleus, and PIF3 binds the G-box motif in the promoter region of *CCA1* (Circadian Clock Associated 1) and *LHY* (Late elongated Hypocotyl) genes resulting in a reduction in their

expression (Moller *et al.*, 2002), which in turn encode MYB transcription factors that regulate developmental genes. This suggests that PIF3 may act as a control point for different branches of photomorphogenesis. The accumulation of PIF3 in the nucleus in the dark requires COP1 as the negative regulator of photomorphogenesis while red and FR-light induces rapid degradation of the PIF3 protein. This rapid light-induced degradation of PIF3 indicates that interaction of PIF3 with phyA, phyB and phyD is transient (Bauer *et al.*, 2004). The degradation of PIF3 is mediated by the 26S proteasome (Park *et al.*, 2004). Many signalling components specific for individual photoreceptors have been identified, among them PIF3, NPDH2, PSK1, COG1, PFT1 and PRR7 are shared by both phyA and phyB; ELF3, ELF4, ARR4, PIF4 and SRR1 are specific for phyB signalling; and FHY1, FHY3, FAR1, PAT1, HFR1, LAF1, LAF3, LAF6, FIN219, SPA1 and EID1 are specific for phyA signalling (Quail *et al.*, 2002).

1.9 Light control of seedling development

Light responses which are known to be mediated by phytochromes include seed germination, chloroplast development, leaf expansion, inhibition of cell elongation, cotyledon opening and expansion, photoperiodic control of flowering and regulation of gene expression (Reed *et al.*, 1994). The most dramatic light-mediated response is shown during seedling photomorphogenesis. Some characteristics of seedling development will be discussed.

1.9.1 Seed germination

Rapid germination of *Arabidopsis* seeds in darkness is controlled by phyB in the Pfr form which is stored in the seeds, whereas phyA contributes a minor secondary role to the decision to germinate in the darkness. The rate of germination is particularly high when the seeds are overexpressing phyB (McCormac *et al.*, 1993). Short pulses of red-light increases germination efficiency of wild-type seeds, suggesting a significant level of phyB is also present in the Pr form (Shinomura *et al.*, 1994). Other phytochromes including phyA gradually begin to accumulate in the seed promoting germination especially under continuous FR-light illumination. However, under FR-light *phyB* mutant seeds germinate more efficiently than the respective wild-type indicating that phyB opposes the action of phyA, a classic example of antagonistic control (Reed et al., 1994; Shinomura *et al.*, 1994).

Light-dependent decisions that affect cell shape and differentiation during *Arabidopsis* seedling development only become apparent two days after germination that then lead to diverging pathways. The first two days in either light or darkness are accompanied by overall cell enlargement in the hypocotyl, cotyledons and roots, and root hairs also develop. On the third day in darkness, cells within the hypocotyl continue to elongate, whereas in the light hypocotyl cell elongation is inhibited and cell type differentiation proceeds. Cotyledon development in darkness is arrested after the first two days, whereas in the light, the cotyledon cells differentiate into the distinct cells types (von Arnim and Deng 1996).

1.9.2 Development and separation of the cotyledons

The separation of the cotyledons and the opening of the apical hook are stimulated by blue and red light (Casal *et al.*, 1994; Liscum and Hangarter 1993a). The cotyledons are folded back on the hypocotyl when initially formed during embryogenesis and the apical hook is maintained at the top of the hypocotyl during etiolation. Under white light phyA and phyB appear to be the main phytochromes involved in cotyledon expansion in *Arabidopsis* (Reed *et al.*, 1994). The full cotyledon expansion in bright blue and red light depends on signals perceived by phyB, shown using the *phyB* mutant (Reed *et al.*, 1994).

1.9.3 Hypocotyl elongation

The same light signals that promote cell expansion in the cotyledons inhibit cell elongation in the hypocotyl. However the inhibition of hypocotyl elongation shows a complex fluence dependence involving phytochrome-photoreversible and high-irradiance responses (Li *et al.*, 1994). Multiple photoreceptors can control hypocotyl elongation. In *Arabidopsis* phytochromes A and B, the blue light receptor CRY1 and a UV-A receptor have the ability to inhibit hypocotyl cell elongation (Whitelam and Harberd 1994). Light strongly inhibits cell elongation but proportionally more in the upper part of the seedling (Le *et al.*, 2005). During hypocotyl elongation, each cell reacts to light as well as hormones in a time and position-dependent manner and although light is the most important environmental factor that inhibits elongation growth, hormones are also vital in this process (Vandenbussche *et al.*, 2005).

At least five classes of plant hormones play a role in regulating hypocotyl growth in the dark, including ethylene and cytokinins which reduce the rate of cell elongation. In contrast gibberellins promote hypocotyl elongation in etiolated seedlings (Vandenbussche *et al.*, 2005). In the light hypocotyl elongation can be counteracted by ethylene and auxin as they are known to stimulate hypocotyl elongation in the light (Boerjan *et al.*, 1995; Le *et al.*, 2005), whereas the rate of elongation is reduced by a reduction in brassinosteroids (Symons and Reid 2003).

1.9.4 Apical hook curvature

Arabidopsis seedlings develop a hook-like structure at the apical part of the hypocotyl when grown in the darkness (Raz and Ecker, 1999). Growth during plant development is governed by the combined activities of cell division and cell elongation. A fast change in growth is exhibited at the apical hypocotyl of etiolated seedlings where cells grow at different rates to form a hook-like structure (Raz and Koornneef, 2001). Seedling apical hook development involves a complex interplay of hormones and light in the regulation of differential growth (Li *et al.*, 2004). Treatment of wild-type seedlings with auxin results in a reduced hook curvature, whereas ethylene enhances curvature (Ecker, 1995; Lehman *et al.*, 1996). The *Arabidopsis* ethylene-regulated HOOKLESS1 (*HLS1*) gene is essential for apical hook formation. *Arabidopsis* hook opening is promoted by blue, red and FR-light, an indication that multiple photoreceptors mediate this response (Liscum & Hangarter 1993b). In *Arabidopsis* the response of the hook to both low fluence red and blue light is mediated by phytochrome and is FR-reversible, involving phyA and a blue light-specific pathway (Liscum and Hangarter 1993a).

1.10 The use of microarrays for investigating genes involved in phytochromes responses

Microarrays are a semi-quantitative method of genome wide analysis of gene expression, which can measure the relative expression of thousands of genes simultaneously (Schena *et al.*, 1996). Recently developed Microarray technology has been adopted to investigate the genome expression profiles in several important plant process (Ma *et al.*, 2001). These include nutrient responses (Wang *et al.*, 2000; Matthius *et al.*, 2003), integrating membrane transport with male gametophyte development (Bock *et al.*,

2006) and toxic metal responses (Weber *et al.*, 2006). A number of arrays have also be conducted to investigate light-responses, these include the regulation of biochemical pathways during photomorphogenesis (Ghassemian *et al.*, 2006), early dark-responses (Kim and von Arnim, 2006), shade avoidance responses (Devlin *et al.*, 2003), light-regulated genome expression (Jiao *et al.*, 2005), regulation of gene expression by blue (Wang *et al.*, 2001; Jiao *et al.*, 2003), far-red (Tepperman *et al.*, 2002) and red (Tepperman *et al.*, 2004) light.

Microarrays when used to measure the expression profiles in both the *Arabidopsis* wild-type and *phyA* null-mutant mutants indicated that 10% of the genes on the array were regulated by phyA in response to continuous FR-light illumination (Tepperman *et al.*, 2001). Of these, 63% were induced and 37% repressed, with 8% exhibiting changes in mRNA abundance within one hour of transfer to FR-light (early response genes) and the remaining 92% first exhibiting changes at a later point during the remainder of the 24 hour irradiation period (late response genes). With 34% of these genes showed a 2-3 fold light induced change and 16% a 10-fold or greater change. It was found that 44% of the genes responding to the signal within 1 hour are predicted to encode multiple classes of transcriptional factors (Tepperman *et al.*, 2001). These observations suggest that phyA may regulate seedling photomorphogenesis by direct targeting of light signals to the promoters of genes encoding a master set of diverse transcriptional regulators. These are then responsible for the expression of multiple downstream target genes in various branches of phyA regulated transcriptional network (Tepperman *et al.*, 2001). Of the genes of known functions over half are classified as being involved in either photosynthesis and chloroplast biosynthesis or general cellular metabolism. Other genes included those involved in transcriptional regulation, stress or defence, signalling, hormone pathways, growth and development and transport processes (Tepperman *et al.*, 2001). The aim of this project is to look at the gene expression profiles of such transporter genes in response to various light treatments using microarray technology.

Further microarray studies have shown 30% of the genes in the *Arabidopsis* genome are involved in plant photomorphogenesis and this massive change in gene expression is the likely result of a transcriptional cascade (Wang *et al.*, 2002). This was shown using by investigating the FR-light controlled genome expression profiles of four *Arabidopsis* wild-type ecotypes (Col, Ler, No-0 and RLD), which when grown are

phenotypically similar. Examination of the expression ratios of the genes in the microarray between FR-light versus dark-grown wild-type seedlings revealed that FR-light regulates the expression of large portions of genes in these four ecotypes. Overall 1083, 825, 971 and 998 out of the 6126 genes displayed a two-fold or more differential expression in the Col, Ler, No-0 and RLD ecotypes respectively (Wang *et al.*, 2002). Light control of *Arabidopsis* development has been shown to entail coordinated regulation of genome expression and cellular pathways (Ma *et al.*, 2001). Similar gene expression profiles have been observed among seedlings in different light qualities, including red, blue and FR-light. Also light/dark transitions have also been shown to trigger similar differential genome expression profiles. The number of regulated genes in all light conditions was estimated to account for approximately one-third of the genome, with three-fifths up-regulated and two-fifths down-regulated (Ma *et al.*, 2001). Analysis of those light-regulated genes revealed more than 26 cellular pathways are regulated by light (Ma *et al.*, 2001), indicating that light is one of the most important environmental factors that govern plant growth and development.

1.11 Plant membrane transport research

The complete genome sequencing of *Arabidopsis thaliana* is a great landmark and the information it contains has provided a large insight to many areas of plant research. *Arabidopsis* was first chosen as a popular model organism due to its rapid life cycle and small size of genome, making it ideal for laboratory studies. The reason for this smaller size is not due to the reduced number of genes but due to the decrease in the proportion of non-coding DNA. The life span of *Arabidopsis* from seed to senescence is only approximately 12 weeks for a wild-type. Achieving an objective set in 1996, the *Arabidopsis* sequencing consortium has sequenced the 118.7 million base pairs of this plants nuclear genome, (Theologis *et al.*, 2000) making it one of the most accurate eukaryotic genome sequence obtained so far (The Arabidopsis Genome Initiative 2000). The *Arabidopsis* genome contains 25,498 genes encoding proteins from 11,000 families, some of which are new protein families but it also lacks several common protein families (The Arabidopsis Genome Initiative 2000).

Transporters in the plasma and intracellular membranes of *Arabidopsis* are responsible for the acquisition, redistribution and compartmentalization of organic

nutrients and inorganic ions, as well as for the efflux of toxic compounds and metabolic end products. Membrane transport processes in *Arabidopsis* have been compared to those of fungi, animals and prokaryotes and have identified over 1700 predicted membrane transport systems in *Arabidopsis* (http://www-biology.ucsd.edu/~ipaulsen/transport). Since the first molecular structures of plant transporters were discovered, considerable advances have been made in the study of plant membrane transport (Barbier-Brygoo *et al.*, 2001). A wide variety of complementary strategies are now available to study plant transport systems, including heterologous expression, forward and reverse genetics, proteomics and RNAi (Barbier-Brygoo *et al.*, 2001).

One of the first methods used to study plant transport systems were patch-clamp techniques which measures ionic currents across a membrane (White *et al.*, 1999). For example the activity of a proton-pumping pyrophosphatase can be determined by expressing the enzyme in yeast and measuring PPi-dependent current across a membrane (Nakanishi *et al.*, 2003). Purification of membrane proteins has also led to the cloning of the first transporters and yeast complementation has led to the discovery and cloning of many secondary transporters (Ludewig and Frommer, 2002). Further still, expression studies using heterologous systems such as yeast and xenopus oocytes have played an important role in studying structure-function relationships through mutational analysis (Frommer and Ninnemann, 1995; Dreyer *et al.*, 1999). Many plant transport proteins have been identified by complementation of yeast mutants that were deficient in certain transport of metabolic functions (Frommer & Ninnemann, 1995).

Major advances in understanding the physiological function of plant transporters came with the generation of T-DNA insertional mutants (Krysan *et al.*, 1999). Before the identification of T-DNA mutant plants, mutants in transporters were available but the number was limited. For further details of how T-DNA mutants are used and studied refer to section 1.12. Further studies into transporter function were conducted using combinations of molecular techniques including antisense expression, reporter genes and RNA interference (RNAi) to investigate the physiological role of transporters. RNAi is a powerful tool for suppressing gene function in many eukaryotes including plants, where the introduction of double-stranded RNA into *Arabidopsis* protoplasts leads to silencing of the endogenous gene of interest (Bosher and Labouesse 2000; An *et al.*, 2005). Advances in molecular technologies include transcriptomics which has allowed the identification of

genes involved in a particular response (Ma *et al.*, 2001). The accurate prediction of promoters has also been fundamental in understanding gene expression patterns. A number of programs can be used to highly predict promoters corresponding to genes which are regulated under a specific response (Shahnuradov *et al.*, 2005).

Proteomics has become a modern techniques used to study plant transporter proteins allowing the examination of changes in morphology at the protein level rather than a genomic level. Proteomics has become a leading technology for analysis of proteins on a genome-wide scale (Kwon *et al.*, 2006). With the completion of genome sequencing and the development of analytical methods for protein characterization, proteomics has become a major field of functional determination (Park, 2004). Such techniques are being used in combination with metabolomics which examines metabolite composition and content (Keurentjes *et al.*, 2006) and when used in combination with mass spectrometry has become a powerful tool for metabolome analysis (Harada *et al.*, 2006). Ionomics has also become a technique to investigate transporter function by studying nutrient ion homeostasis in plants measuring the levels of metals, metalloids and non-metals in an organism (Lahner *et al.*, 2003; Salt, 2004).

Bioinformatics has also become an important part of plant membrane research and there are now a number of websites and tools that can be used. A number of research groups have pioneered the discovery of novel families of membranes proteins from the *Arabidopsis* genome (Ward, 2001). A comprehensive website has been constructed giving concise sequencing and hydropathy plots of all known membranes transporters (http://www.cbs.umn.edu/arabidopsis). A second website MIPS (**M**unich **I**nformation Centre for **P**rotein **S**equences), uses the MATDB (**M**unich **A**rabidopsis **T**haliana **D**ata**b**ase) to provide sequences and hydropathy plots (http://mips.gsf.de/proj.thal). The development of a new novel database for *Arabidopsis* integral membrane protein called ARAMEMNON was designed to facilitate the interpretation of gene and protein sequence data by integrating features that are presently only available from individual sources. This database is found at (http://aramemnon.botanik.uni-koeln.de/) and enables direct comparison of the predictions of seven different transmembrane programs (Schwacke *et al.*, 2003). Such websites are available to those investigating the structure and classification of *Arabidopsis* membrane proteins. Combinations of these molecular and biochemical techniques have provided a vast insight into the structure, function, localization and gene expression profile

of membrane transport proteins and will continue to be vital in understanding the role of unknown proteins which could potentially function as transporters regulating plant growth and development.

Transport proteins can be grouped into three classes: carriers, channels and pumps (Figure 1.4). Carrier proteins bind the specific solute being transported and undergo a conformational change in order to transport the solute across the membrane (Taiz and Zeiger, 2006). Channel proteins form pores that extend across the membrane and allow specific solutes, usually ions to pass through them when open. Ion channels are not continuously open as they have gates that open briefly and then close (Taiz and Zeiger, 2006). Finally pumps which transport solutes against their concentration gradient and are either driven by either chemical or light energy. Active transport is driven by primary transporters and they are responsible for driving secondary transporters which include the carriers and channel proteins (Raven *et al.*, 2005). Transporters also are categorised according to the speed of transport. Pumps are the slowest transport protein transporting fewer than 500 solute molecules per second while carriers and channels are more rapid, transporting 500 – 10,000 and 10,000 to many millions respectively (Taiz and Zeiger 2006). The proteins involved in transport have been classified into families according to what the protein transports. A summary of the transporter families including channels and pumps located on the plasma membrane, tonoplast and chloroplast envelope are summarised in Figure 1.5.

The ATP binding cassette (ABC) transporter superfamily is the largest single family of transporters and is a large diverse group of proteins. The ABC transporters function not only as ATP-dependent pumps but also as ion channels and ion regulators (Theodoulou *et al.*, 2000). These transporters are involved in the transport of a range of unrelated compounds, such as lipids, inorganic acids, peptides, secondary metabolites, toxins and drugs (Martinoia *et al.*, 2002). Recently a group of the ABC transporters have been shown to be involved in auxin transport (Geisler and Murphy 2006).

Amino acids are the currency of nitrogen exchange in plants, so amino acid transport is a fundamental activity in plant growth. Recent molecular cloning of amino acid transporters by functional complementation in yeast have revealed that there are multiple

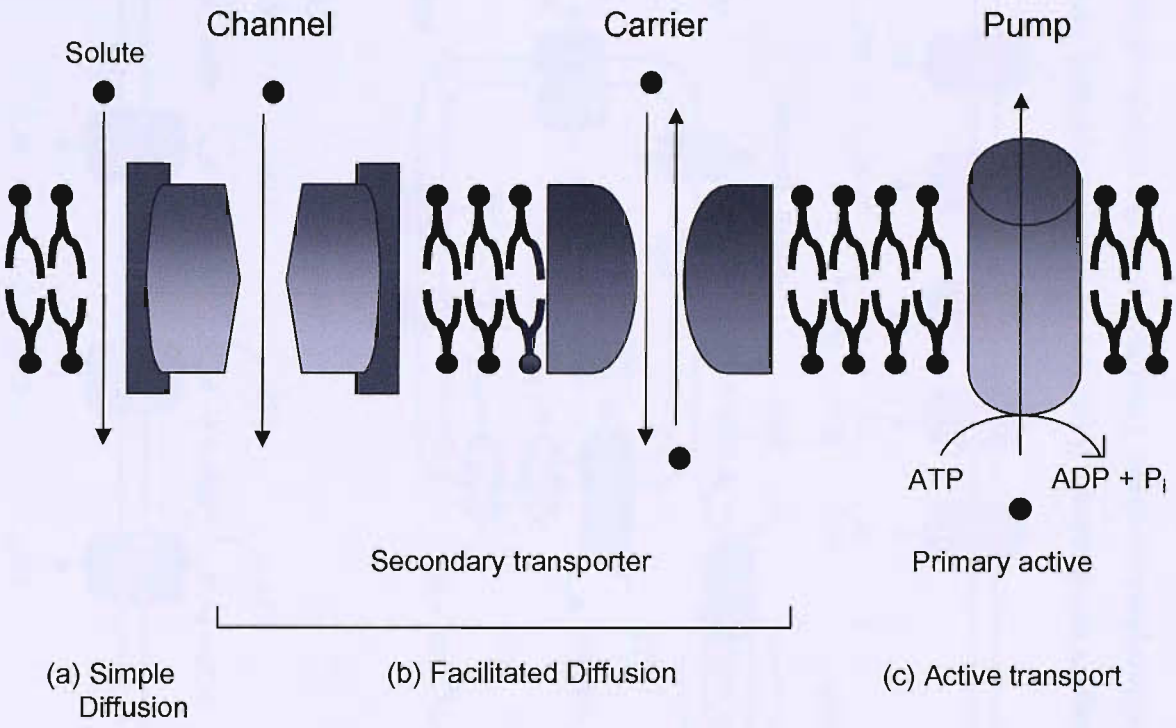

Figure 1.4 Modes of transport through the plasma membrane. Transport through the plasma membrane of plant cells occurs via three different types of membrane transport proteins, channels, carriers and pumps. a) In simple diffusion small molecules pass directly through the lipid bilayer. b) Facilitated diffusion occurs via either channel proteins or carrier proteins. Some carriers are secondary symporters or antiporters. c) Primary active transport moves solutes against their concentration gradient via pumps.

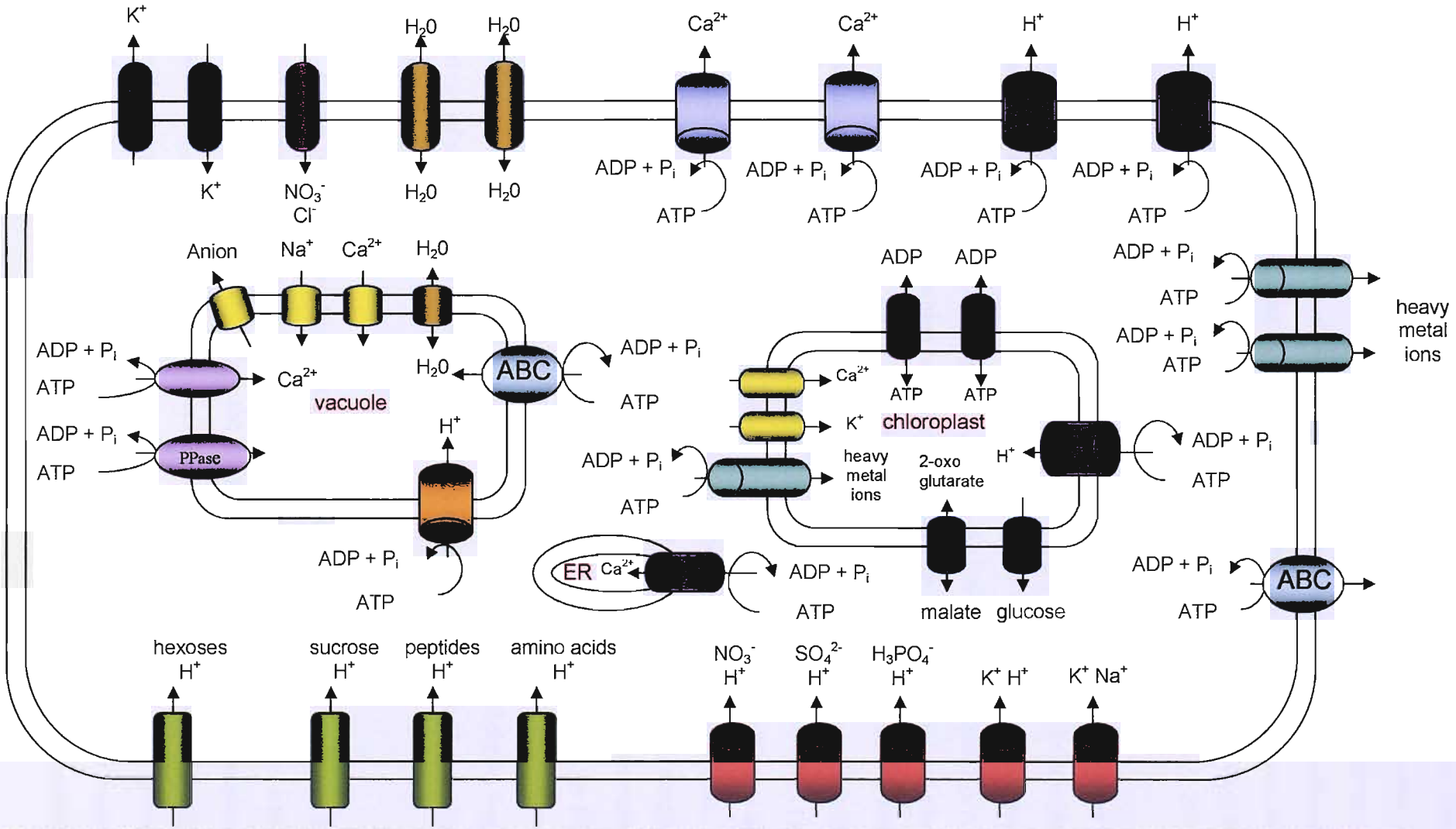

Figure 1.5 Model of a plant cell showing the main transport mechanisms. Summary of some transporters, including pumps, carriers and channels located on the plasma membrane, tonoplast and chloroplast envelope. Transporters on the mitochondrial membrane are not shown. Modified diagram taken from Johansson *et al.*, 2000.

gene families that encode different classes of amino acid transporters in plants (Bush *et al.*, 1996). Two superfamilies of amino acid transporters have been defined; the amino acid, polyamine and choline transporters superfamily (APC) and amino acid transporter family (ATF) superfamily (Fischer *et al.*, 1995). The ATF superfamily has at least five sub-classes of transporters, including the amino acid permeases (AAPs), the lysine, histidine transporters (LHTs), the proline transporters (ProTs), the putative auxin transporters (AUXs) and the aromatic and neutral amino acid transporter (ANT) family (Ortiz-Lopez *et al.*, 2000).

Another large family of transporters is the P-type (phosphorylated) pumps where a total of 45 genes encoding for P-type pump ATPases have been identified in the complete genome sequence of Arabidopsis forming five subfamilies (Figure 1.6). The most predominant families are: P_{1B} ATPases (heavy metal pumps), P_{2A} and P_{2B} ATPases (Ca^{2+} pumps), P_{3A} ATPases (H^{+} pumps) and the P_4 ATPases which have been implicated in aminophospholipid flipping (Figure 1.6) (Axelsen and Palmgren, 2001). There has shown to be eight P_{1B} ATPases, which are involved in the transport of heavy metals (Williams *et al.*, 2000b). These include HMA2, HMA3 and HMA4 which are likely to be Zn^{2+}/ Co^{2+}/ Cd^{2+}/Pb^{2+} ATPases; HMA1 a Cu^{2+} ATPase at the chloroplast and RAN1, HMA5 and PAA1 are Cu^{2+}/Ag^{2+} ATPases and HMA8 (Williams *et al.*, 2000b; Williams and Mills, 2005). The phylogenetic analysis has shown that HMA2-HMA4 form a subcluster, supporting the suggestion that they have a similar function (Figure 1.6). Recent analysis has shown that there are 14 Ca^{2+} ATPases in *Arabidopsis thaliana*, and that these calcium ATPases form two distinct groups; type P_{2A} (or ECA for ER-type Ca^{2+} ATPases) and type P_{2B} (ACA for autoinhibited Ca^{2+} ATPase). Generally plant type IIB calcium ATPases employ an N-terminal calmodulin-binding autoinhibitor, suggesting that the activity of such ATPases is controlled by these autoinhibitory terminal domains (Giesler *et al.*, 2000a).

Higher plants, such as *Arabidopsis* have developed two distinct classes of sugar transport protein carriers: the disaccharide transporters that primarily transport sucrose, and the monosaccharide transports that regulate the transport of a whole range of monosaccharides (Williams *et al.*, 2000a). These transporters are involved in the movement of fluxes of carbohydrate across the plasma membrane of higher plant cells (Sauer *et al.*, 1994). Plants have several monosaccharide and disaccharide transporters to coordinate sugars in diverse tissues, at different developmental stages and varying environmental conditions. Both monosaccharide

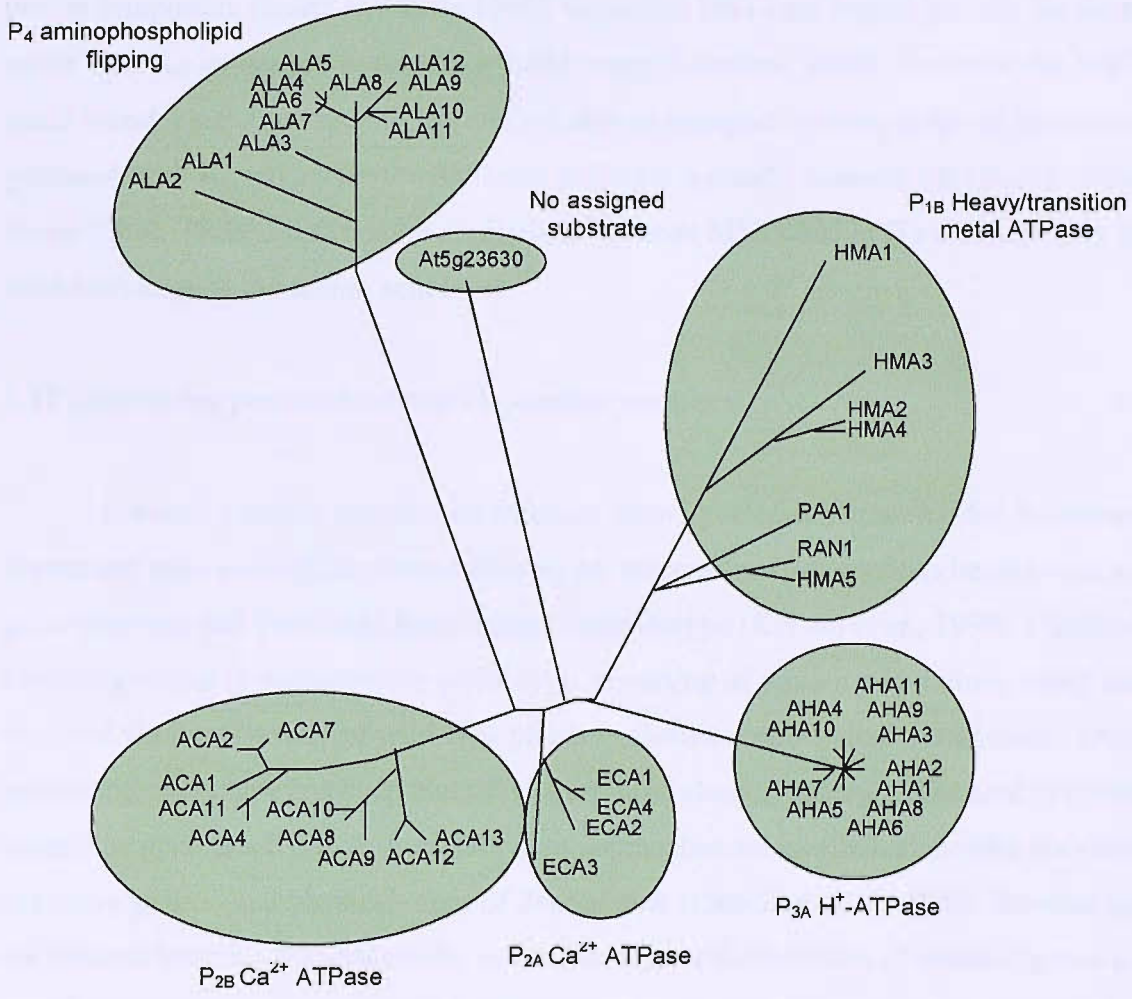

Figure 1.6 Phylogenetic tree diagram of all known *Arabidopsis thaliana* P-type ion pumps, indicating the P_{1B}, P_{2A}, P_{2B}, P_3, P_4 and P_5 subfamilies. Phylogenetic tree taken from Axelson and Palmgren, 2001.

sugar transporters (MSTs) and disaccharide sugar transporters (DSTs) belong to the sugar transporter family of the **M**ajor **F**acilitator **S**uperfamily (MFS), also called the uniporter-symporter-antiporter family (Saier *et al.*, 1999) (Figure 1.7). Heterologous expression in yeast has been carried out for some protein members and evidence suggests that they function as proton symporters (Sauer and Stolz 1994). Generally DSTs are highly specific for sucrose, while their K_m values are in the 0.3-1.0 mM range (Lemoine, 2000). However the MSTs have a much broader substrate specificity, and are able to transport a whole range of hexoses and pentoses, with K_m values for the preferred substrate typically between 10-100μM (Buttner and Sauer 2000). There are structural similarities between MSTs and DSTs although they share little homology at the amino acid level.

1.12 Identifying protein function via mutant analyses

Forward genetics begins with a mutant phenotype and then search for the sequence of the mutant gene causing the altered phenotype, whereas reverse genetics begins with a mutant gene sequence and then looks for a change in phenotype (Krysan *et al.*, 1999). Classical forward genetics is performed by phenotypic screening of mutant populations which have been obtained via the exposure of wild-type plants to chemical or physical mutagenesis. Once an interesting phenotype has been identified a series of cloning strategies are used to identify and isolate the gene. Such conventional forward approaches are inefficient, despite the existence of extensive genetic and physical maps of *Arabidopsis* (Camilleri *et al.*, 1998). Reverse genetics via random insertional mutagenesis, in contrast allows the isolation of mutated genes in a much more direct method. Foreign DNA, either a piece of T-DNA (Krysan *et al.*, 1999) or a transposon (Martienssen., 1998) is introduced into the plant and used to disrupt genes by random integration. This creates loss-of function mutants which are tagged by the interrupting piece of DNA. The potential of these mutants can be fully exploited when using such lines for reverse genetics (Parinov and Sandaresan 2000). The known inserted DNA sequence allows for the relatively easy isolation of any mutant gene by using screening based on PCR (Young *et al.*, 2001). These PCR methods have been developed to allow the easy isolation of individual plants that carry a particular T-DNA mutation (McKinney *et al.*, 1995). PCR primers for both the target gene and the insertion element are used (Bouche and Bouchez 2001). Currently databases are used that contain sequence information of DNA stretches flanking the insertion sites allowing primers to be designed to confirm the T-DNA insertion (Parinov *et al.*, 1999).

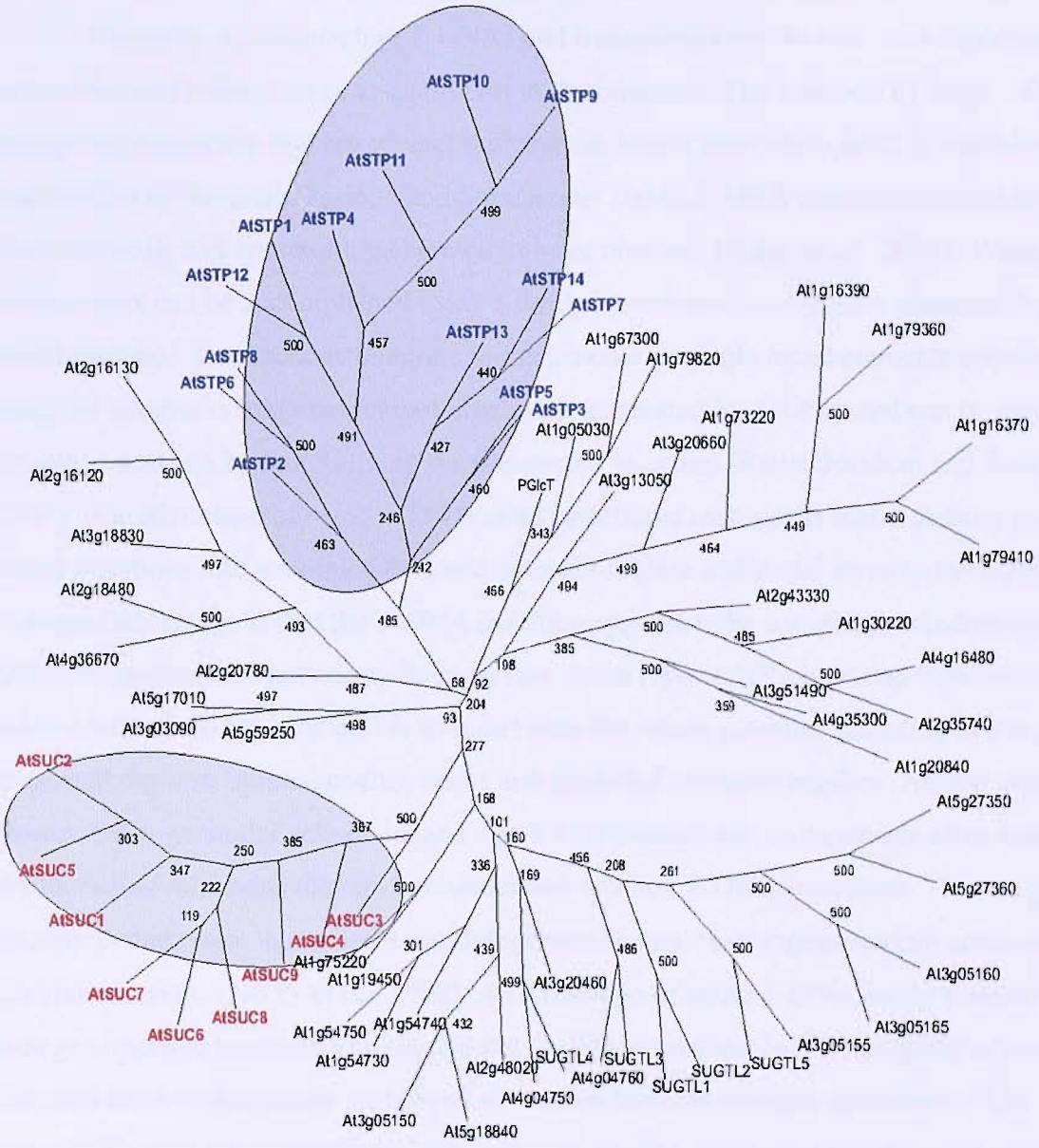

Figure 1.7 Phylogenetic tree of *Arabidopsis thaliana* sugar transporters. All known and putative sugar transporter proteins are shown, showing the sequence identity between the family members. Taken from Legge *et al.*, 2003, unpublished data.

Therefore using reverse genetics screening methods it becomes easier to find an *Arabidopsis* mutant with an insertion in the gene of interest.

1.13 T-DNA verses transposon insertional mutagenesis

Currently *Agrobacterium* T-DNAs and transposons are the two main insertional mutagens used widely for gene disruption in *Arabidopsis*. The insertion of large T-DNA or transposon constructs that are several kilobases in length most often leads to complete inactivation of the gene (Parinov and Sundaresan 2000). T-DNA insertions are easily generated in *Arabidopsis* and are readily generated in large numbers (Raina *et al.*, 2002). Transposon mutagenesis can be accomplished using a limited number of starter lines generated by transformation. Transposons integrate in the genome as single intact elements compared to the complex integration patterns that are frequently generated by T-DNA and can be used for inversion analysis by remobilizing the transposon insertion (Ramachandran and Sundaresan 2001). One advantage of using T-DNA as an insertional mutagen is that it directly generates stable insertions into genomic DNA and does not require additional steps to stabilize the insert. A second advantage is that the T-DNA insertion appears to be completely random as no T-DNA integration hot spots or preferences have been reported (Parinov and Sundaresan 2000). T-DNA insertions have the ability to insert over the whole genome, including 5' and 3' un-translated regions, introns, coding exons and predicted promoter regions (Alonso *et al.*, 2003). However it is generally acknowledged that T-DNA insertional mutagenesis often results in the production of mutations that are not associated with the T-DNA insertions. There is growing awareness that major, sometimes multiple, chromosomal rearrangements can accompany integration events (Nacry *et al.*, 1998). An advantage of using T-DNA as the insertional mutagen opposed to transposons is that the T-DNA insertions do not transpose subsequent to insertion and are chemically and physically stable through multiple generations. The T-DNA not only disrupts the expression of the gene into which it is inserted but also acts as a marker for subsequent identification of the mutation. Since *Arabidopsis* introns are small the insertion of T-DNA on the order of 5 to 25 kilobases in length generally produces a disruption of the gene (Radhamony *et al.*, 2005). Mutations that are homozygous lethal can also be obtained and then maintained in a population in the form of a heterozygous plant. There are a number of advantages of using transposons for insertional mutagenesis. Unlike T-DNA, a transposon can be excised from the disrupted gene in the presence of transposase, resulting in the reversion of

the mutation. This provides a simple method to confirm the observed mutation (Speulman *et al.*, 1999).

Large numbers of T-DNA and transposon insertion lines have been generated by different groups, and when combined these collections represent insertions into most *Arabidopsis* genes (Krysan *et al.*, 1999). The ***Arabidopsis*** **B**iological **R**esource **C**entre (ABRC) of the Ohio State University (http://aims.cps.msu.edu/aims) in cooperation with the **N**ottingham ***Arabidopsis*** **S**tock **C**entre (NASC) (http://masc.nott.ac.uk) are organising the collection, preservation and distribution of transgenic seeds ((Parinov and Sundaresan 2000). Over 225,000 independent Agrobacterium transferred DNA (T-DNA) insertion events in the *Arabidopsis* thaliana genome have been created and the precise locations were determined for T-DNA insertions in more than 21,700 of the 29,454 predicted *Arabidopsis* genes (Alonso *et al.*, 2003).

1.14 Phenotypic analyses of a T-DNA mutant

Mutants can then be phenotyped to help identify a putative function for the protein translated from the mutated gene of interest. Such Phenotypic profiling approaches aim to measure chemical or physical properties of an organism at specific points during its life cycle (Holtorf *et al.*, 2002). Collecting data on a set of morphological and developmental traits allows researchers to put together a comprehensive picture of a mutants phenotype (Boyes *et al.*, 2001) The phenotype of the mutant is compared to the profile of the wild-type plant which is recorded simultaneously. For plants a whole range of phenotypic characteristics can be analysed, including seedling morphology, growth rate, timing of flowering and seed set, root density, leaf shape and number (Holtorf *et al.*, 2002). Although many *Arabidopsis* knockouts have already been obtained, few of them have been reported to present interesting phenotypes that provide a direct clue to gene function. It seems reasonable that functional redundancy could explain the lack of phenotypic alterations in some cases where the phenotype and function of a gene in a family may be masked (Hua and Meyerowitz, 1998). Consequently gene knockout is not sufficient to assess gene function and it must be integrated into a more global approach for determining biological function (Bouche and Bouchez, 2001).

Mutant phenotype can be assessed from germination, to seedling morphology right through to the onset of senescence. Some of the biggest and most dramatic changes in phenotype can be noticed at the seedling level and many aspects of the developing seedlings can be investigated. The easiest seedling phenotype to score is hypocotyl length which can be measured under different light conditions including, dark, white, blue, red and FR-light (Fankhauser and Casal, 2004). Cotyledon size and angle, apical hook angle, time of germination, chlorophyll and anthocyanin content are other factors which can be measured when looking for a seedling phenotype (Fankhauser and Casal, 2004).

1.15 Aims

Plants have evolved sophisticated mechanisms to perceive environmental changes, including light which is most dramatically illustrated by seedling development. Seedlings follow two developmental pathways, skotomorphogenesis (dark grown) and photomorphogenesis (light grown). The contribution of photoreceptors will be investigated using specific light conditions namely FR-light which is perceived by phyA. It is hypothesized that membrane transporters and other proteins are likely to play significant roles in mediating light-regulated growth and development, ranging from specific light regulated sugar transporters involved in the redistribution of sugars around the plant to ABC transporters. The aim of this PhD is to use a functional genomics approach to determine candidate transporter genes which play a crucial role in such light-regulated seedling growth and development, particularly when growth under FR-light. This will involve the combination of two different post-genomic strategies. Firstly specialised microarray technology will be used for the *Arabidopsis* transporter genes as a gateway to determine putative candidate transporter genes that are specifically involved in photomorphogenic processes. The role of these candidate genes will then be confirmed using RT-PCR and real-time PCR by designing primers specific to the chosen genes. Secondly the function of these candidate genes will be assessed by screening, identifying and analysing mutants already generated through large-scale insertional mutagenesis programs. A particular focus will be to investigate light-regulated developmental responses at the seedling stage.

Chapter 2

Materials and Methods

2.1 Plant Material

2.1.1 Seed stock maintenance

Bulking of *Arabidopsis thaliana* seed was achieved by growing plants of the appropriate line in 5 inch diameter planting pots containing a 50:50 mix of Levingtons M2 compost and vermiculite. Seeds were sown onto the surface of water soaked soil and plant pots were sealed with cling film for 3-4 days while seeds germinated. The plants were grown to maturity (approximately 3 months) in a growth room, following a diurnal program of 16 h light at a constant temperature of 23°C, and 8 h dark at 18°C. White light was provided by white fluorescent tubes (400-700nm at a fluence rate of 130 $\mu molm^2s^{-1}$). When siliques had turned brown the entire flower stalks were cut and placed in a paper brown bag to dry out at room temperature. Seeds were then separated from the dried plant material by sieving through a fine mesh and stored at 6°C in the presence of silica gel pellets to maintain dryness.

2.1.2 Seedling growth conditions for RNA extraction

Approximately 200 *Arabidopsis thaliana* Columbia seeds were surface sterilised in 10% (v/v) bleach (Domestos) for 20 min before washing 3 times with RNase-free sterile water. Under sterile conditions the seeds were plated on to Petri dishes containing autoclaved MS medium (Murashige & Skoog, 1962) with 1.0 % (w/v) agar, with no sucrose, and sealed with parafilm. Plates were wrapped in a layer of aluminium foil and stratified at 4°C for 48 h. Following 2-3 h under white light (fluence rate 120 $\mu mol\ m^{-2}\ sec^{-1}$, temperature 23°C) in the white light growth cabinet to initiate seed germination. The white light was provided by LED displays in environmental controlled chambers (Percival Scientific Inc., Boone, IA, USA). Plates were re-wrapped in tin foil and placed in darkness in a growth cabinet at 23°C for 48 h. Seedling plates were then placed in the appropriate

light cabinet (blue, red or FR-light) at 23°C or kept in the dark growth cabinet at 23°C for 12 h prior to RNA extraction.

2.1.3 Light sources

FR-light from the LEDs had a absorption peak at 739 nm and was passed through two filters (#116 and #172; Lee Filters, Andover, UK) to remove wavelengths <700 nm to give a final fluence of 10 $\mu molm^{-2}s^{-1}$ (McCormac *et al.*, 2001). Red light corresponded to a peak at 669 nm with a fluence rate of 80 $\mu molm^{-2}s^{-1}$ and blue light had a peak at 470 nm and a fluence rate of 20 $\mu molm^{-2}s^{-1}$ (McCormac *et al.*, 2001).

2.1.4 Crossing *Arabidopsis* mutant plants back to wild-type lines

Crossing of *Arabidopsis* plants was undertaken using a dissecting mask with very fine tweezers. Plants were grown on soil until the first flowers began to open. A wild-type plant was used as the female plant and the mutant as the male plant. For the female part a terminal inflorescence was chosen where some of the flowers were just starting to show white tips of the sepals. All but three flowering spikes were removed and the apical meristem of the inflorescence was pinched out so no more flowers could develop. Using tweezers the flower was carefully opened checking the anthers were still green. The sepals, petal, and stamens were removed without damaging the stigma. Once flowers were prepared all other developing flowering stems were removed and the plant was left for 2 -3 days for the stigma to become receptive to pollen. At this point the style developed a hairy like surface. Using tweezers a flower was removed from a male plant where the petals were just emerging and the flower was gently opened by squeezing at the base. The anthers were opened and clumps of sulphur yellow colour pollen grains were visible on the inner surface. The female flower was held between thumb and forefinger and the male flower held with the tweezers and the style was dabbed with the anther to transfer as much pollen as possible. This was repeated for each flower with pollen being dabbed from 4 – 5 anthers per plant. The stem on which the crossing was undertaken was labelled by attaching a small section of tape around the stem. Plants were placed in sleeves and the siliques were allowed to develop. When the silique was brown and fully ripe it was removed and seeds were collected.

The same procedure for back crossing was applied to create a double mutant, except that crossing was undertaken in both directions, with each mutant being used as both the male plant and the female plant.

2.2 Physiological analysis of mutant phenotypes

2.2.1 Analysis of seedling phenotypes

Seedlings grown for phenotypic analyses under various light conditions were surface sterilized as in section 2.1.2. Seeds were placed individually on 9 cm MS plates containing no sucrose. Wild-type and T-DNA mutant seeds were sown on the same plates. If just one mutant line was compared to wild-type then the plate was divided into two and approximately 20-25 seeds were plated for each line. This was repeated twice for each light treatment studied. However, if two mutants are compared against wild-type then the plate was divided into three sections and approximately 15-18 seeds were plated for each line. Three replicates were undertaken per light treatment studied. Plate were dried and sealed with parafilm then wrapped in aluminium foil and stratified at 4°C for 48 h. Plates were transferred to white light (130 $\mu molm^{-2}s^{-1}$) for 3-4 h. The period was extended if the germination rate of the line was low. The plates are re-wrapped in silver foil and transferred to the dark cabinet at 23°C for 24 h. Plates are then transferred to the appropriate light treatment for 96 h or continued in the dark, all at 23°C. Identical light fluences were used as with the seedlings grown for RNA extraction. Plates were randomised every 24 h. To record changes in seedling morphology, photographs were taken under the light microscope using a digital camera. Graph paper was placed under the plates when photographs were taken to enable scaling of the seedlings. To take photos of the apical hook angle and hypocotyl length, each seedling was placed on the surface of the agar. Then to photograph the cotyledon area, the hypocotyl was pulled down using tweezers on to the agar surface to open up the cotyledons. Seedling measurements were calculated using the imaging program ImageJ, (http://rsb.info.nih.gov/ij/download.html). Measurements of 30 seedlings were taken per line per light treatment.

2.2.2 Phenotypic analysis of roots

Root length and weights were undertaken by plating seeds on half MS vertical plates containing 1.0 % (w/v) agar, both without and with 1% (w/v) sucrose. Each plate was divided into 3 vertical sections and 4 seeds of either, *frimp1*, *frimp2* and wild-type were sown in a straight line in the corresponding plate section. The position of the seed lines were randomised over different plates. Twelve plates were sown for each treatment. Plates were sealed in parafilm and wrapped tin foil and stratified at 4°C for 48h. Plates were then transferred to a growth chamber following a diurnal growth pattern of 16h day (23°C) and 8h night (18°C). Plates were grown vertically in white light (120-150 $\mu molm^{-2} s^{-1}$) and randomised every 24 hours for between 12 and 14 days. Root lengths were determined by taking photographs of 12 day old seedlings and transferring images to the imaging program (Image J). The weights of the whole seedling, the roots and the aerial tissue were determined by weighing the four seedlings of each line from one plate together. The roots were then removed and the aerial tissues were weighed. This was repeated for each of the 3 lines on the plate.

2.2.3 Analysis of mature plants

To analyse the phenotype of mature *Arabidopsis* plants individual seeds were sown as described in 2.1.1. Plants were monitored at various stages of growth development. Plants were grown in light controlled conditions (2.1.1) and randomised every day with a total of 20 plants per line studied. Basic measurements including the diameter of the rosette and height of the plant were measured using a ruler and the data was recorded. The number of leaves at first bolt, the day of first bolt, flower and silique and the number leaves at different developmental time points was also recorded. To measure the ratio of the petiole to the whole length of the leaf, measurements were taken of the length of the petiole and of the whole leaf, with two leaves per plant. Photographs were also taken of various aspects of plant growth. All photographs were scaled.

2.2.4 Leaf curvature measurements

Three randomly selected leaves of ≥ 2cm were harvested from each of ten plants per line. The mid-point of the longitudinal axis of each leaf was measured and at this point the width of each leaf was taken. Firstly the cross section of the leaf was measured as it was on the plant, ie curled leaf (W_L), and then the leaf was opened up and the total width (W_T) was measured. The width of the leaf in cross section was divided by the total width of the leaf to obtain a ratio as shown below. The ratio varied from 1 for a flat leaf to 0.5 for a highly curled leaf (Booker *et al.*, 2004).

$$\text{Curvature Ratio} = \frac{\text{Width of curled leaf } (W_L)}{\text{Total width of leaf } (W_T)}$$

2.2.5 Measurement of photosynthetic pigments

Ten *Arabidopsis* seedlings per line were placed in a 1.9 ml microcentrifuge tube containing 1 ml of DMF (N,N-Dimethylformamide). Samples were wrapped in aluminium foil and stored at 4°C for 48 hours. Absorbance at 647, 664 and 480 nm was recorded in 100 µl samples using the Hitachi U-2000 spectrophotometer (Biocompare, San Francisco USA). Levels of different photosynthetic pigments were calculated using the following equations (Moran and Porath 1980).

$$\text{Chlorophyll A } (C_a) = (12.7 \times A_{664}) - (2.79 \times A_{647})$$

$$\text{Chlorophyll B } (C_b) = (20.7 \times A_{647}) - (4.62 \times A_{664})$$

$$\text{Chlorophyll A + B} = (17.9 \times A_{647}) + (2.79 \times A_{664})$$

$$\text{Total carotenoids} = (1000 \times A480 - 1.12C_a - 34.07C_b)/245$$

2.3 Nucleotide isolation from *Arabidopsis thaliana*

2.3.1 Precautions taken to minimise RNase contamination

For RT-PCR and microarrays pure non-contaminated and intact RNA is essential. This process is complicated due to the presence of contaminating RNA-degrading enzymes

called RNases that are not only present in the cells from which the RNA is being extracted, but are also likely to be present on all equipment used during the extraction procedure. Therefore important precautions are taken to prevent the likelihood of RNase contamination. All tips, eppendorfs and glassware used in the extraction of RNA were autoclaved for 1 h, as were all buffers and solutions (with the exception of those containing Tris and SDS). All solutions, especially those containing Tris or SDS were prepared using autoclaved RNase-free sterile water. Gloves were worn and changed regularly on all occasions in the extraction and subsequent handling of RNA.

2.3.2 Extraction of total RNA from *Arabidopsis thaliana*

Total RNA was extracted from *Arabidopsis* seedlings or other tissues using a phenol:extraction buffer and LiCl precipitation based on the method of Verwoerd *et al* 1989. Approximately 2g (2 x 5cm plates) of total seedling material was ground in liquid nitrogen in a pre-chilled pestle and mortar and then transferred to a 50ml plastic centrifuge tube containing 15ml of 1:1 (v/v) phenol (pH 4.8)/extraction buffer (1M Tris-HCl (pH 8.0), 4M LiCl, 0.5M sodium EDTA and 10% (w/v) SDS). This was carried out in a dark room under a green safelight. Samples were vortexed for 2 min forming a slurry, then a 0.5 x vol chloroform (approximately 7.5 mls) was added followed by a second vortex for 2 min. Samples were centrifuged at 3000x *g* at room temperature for 10 min. The aqueous (top) layer was added to a 1.0 x vol (approximately 7.0 mls) of 1:1 (v/v) phenol (pH 4.8)/chloroform buffer and vortexed for 2 mins, followed by a second centrifugation at 3000x *g* at room temperature for 10 min. 0.75 ml aliquots of the aqueous phase were added to a 1.0 x vol 4M LiCl in 1.9ml microcentrifuge tubes, mixed gently and stored at -20°C overnight. Microcentrifuge tubes were centrifuged at 3000x *g* at room temperature for 10 min and the pellets from 2 tubes were combined and dissolved in 0.25 ml of RNase-free water. To each sample, 0.1 x vol NaOAc (pH 5.2) and 2.0 x vol of 100% ethanol was added and stored for 2-20 h at -20°C. Samples were centrifuged at 3000x *g* at room temperature for 10 mins, the pellet was then air dried for 2-3 h and samples for each treatment were combined and re-suspended in the appropriate amount of RNase-free sterile water and stored at -80°C.

2.3.3 Removal of genomic DNA contamination from total RNA

Contaminating DNA was removed from RNA using the TURBO DNase kit (Qiagen, Crawley, UK). A 0.1X vol of 10 x DNase1 buffer and 1 µl of DNase1 was added to approximately 100 µg of RNA. The sample was mixed gently and incubated at 37°C for 20-30 mins. To cease the reaction, 5 µl of DNase inactivation reagent was added to each sample. The inactivation reagent requires re-suspension by vortexing the tube vigourously. The samples were incubated for 2 min at room temperature and flicked once during the incubation to re-disperse the DNase inactivation reagent. Samples were then centrifuged at 3000x *g* for 1 min to pellet the inactivation reagent. The RNA solution was removed from the pellet with a pipette and stored at -80°C.

2.3.4 Removal of polysaccharide contamination from total RNA

Approximately 50 µg of the contaminated RNA pellet was dissolved in a total volume of 500 µl sterile distilled water. 50 µl of 1M sodium acetate/acetic acid (pH 4.5) was added and mixed thoroughly. To precipitate out the polysaccharide 200 µl of 2-butoxyethanol (2-βE ethylene glycol monobutylether) was added and mixed thoroughly and then incubated on ice for 30 min. The sample was centrifuged at 3000x *g* for 15 min at 4°C. The polysaccharide pellet was visible and the supernatant was decanted into a fresh microcentrifuge tube. To precipitate the RNA, 300 µl of 2-butyloxyethanol was added to the retained supernatant and then incubated on ice for a second period of 30 min. The sample was centrifuged at 3000x *g* at 4°C for 15 min. The pellet was then washed with 1 ml of 40 mM sodium acetate (pH 4.5)/ 2-butoxyethanol (1:1, v/v), left on ice for 5 min and then centrifuged at 3000x *g* for 5 min at 4°C. These wash procedures were repeated with 70% (v/v) ethanol, followed by 100% ethanol. The pellet was air dried then stored in 20 µl of distilled water at -20°C.

2.3.5 Determination of nucleic acid concentration

The concentration and purity of RNA was determined by spectrophotometry measuring the absorbance at 260nm and 280nm. One µl of the RNA sample was diluted 250-fold in RNAse-free water in a quartz cuvette and measured in a UV absorbance

spectrophotometer over the range 200-300nm. The optical density at 260nm of a 1mg/ml solution of single stranded RNA is 25, so therefore the concentration of a diluted aliquot of RNA (in μg/μl) = (1/25) × OD_{260nm} × dilution factor × 2. The measurement at OD_{280nm} is used to determine the level of contaminating protein and the ratio of OD_{260nm}/OD_{280nm} can be used as an indication of the purity of the sample. An ideal ratio is between 1.75 -2.0. A low ratio may indicate protein or phenol contamination, while a higher ratio can indicate polysaccharide contamination and/or degradation of the sample.

The Nanodrop ND-1000 Spectrophotometer (Nanodrop, Wilmington USA) was also used to determine RNA or DNA concentration. One μl of RNA or DNA sample is applied to the Nanodrop and following the manufactures instructions the concentration and purity of sample was determined.

2.4 Extraction of genomic DNA

Two or three leaves were cut from each plant and placed in a microcentrifuge tube and immediately frozen in liquid nitrogen. Samples were then kept at -80°C until ready for genomic DNA extraction. Samples were taken in batches of no larger than six and genomic DNA was extracted using the Dynamite plant genomic kit (Microzone Limited, West Sussex, UK). Leaves of the same sample were ground in the microcentrifuge tube with a mini pestle and 1 ml of solution LA (cell lysis solution) was added. The sample was ground further and then briefly vortexed. 100 μl of solution PA (protein denaturation solution) was then added and briefly vortexed. The samples were centrifuged for 5 min at 2600x *g* and 500 μl of the supernatant was transferred to a fresh microcentrifuge tube containing 500 μl of solution CA (microCLEAN solution), being careful not to transfer any on the plant debris. Samples were then vortexed briefly and left to stand at room temperature for 5 min, followed by a 7 min centrifugation at 3000x *g* to pellet the DNA. The majority of the supernatant was removed using a pipette then re-centrifuged briefly to aid the removal of any remaining liquid. Samples were then re-suspended in 30 μl of RNase free water and left for 30 min in room temperature. Samples were stored at -20°C.

2.5 Reverse Transcription Polymerase Chain Reaction (RT-PCR)

2.5.1 Reverse transcription

First strand complementary DNA (cDNA) was prepared from total RNA extracted from *Arabidopsis thaliana* seedlings. One μg of oligo $(dT)_{12-18}$ (500μg/ml) primer (Invitrogen, Paisley UK) was added to 5 μg of total RNA diluted in a total of 11μl of RNAse-free sterile water and denatured at 70°C for 10 minutes followed by a short chill on ice. Four μl of 5x first strand buffer (Invitrogen), 2 μl of 0.1M DTT (Invitrogen) and 1 μl 10mM dNTP mix (10mM of each dATP, dGTP, dCTP and dTTP at neutral pH) (Promega, Southampton UK) was added and the sample was heated at 42°C for 2 minutes. One μl (two hundred units) of superscript reverse transcriptase (Invitrogen) was added and mixed by gentle pipetting and incubated at 42°C for 50 minutes. The reaction was inactivated by heating at 70°C for 15 minutes. One μl of *E.coli* RNase was added to degrade RNA complementary to the cDNA to allow amplification of the PCR product.

2.5.2 Oligonucleotide primers designed for PCR amplification

Oligonucleotide primers (Sigma-Genosys, Cambridge UK) were designed to amplify specific products based on the sequence of the gene of interest. The primers were designed to be located in the exons of the cDNA, but also to span over at least one intron to allow the use of genomic DNA as a control to eliminate the possibility of primer contamination. All primers were designed to contain at least 45% G or C base pairs, and to be 20 base pairs in length. Primer pairs were also designed to have similar annealing temperatures. The location in the gene to which the primer was designed depends on the experiment. For routine amplification of genes using RT-PCR, primers were designed to amplify any region of the gene and therefore the product length varies with a maximum product size of 1.5 Kb. Primers designed to genes of interest and constitutive housekeeping genes are shown in tables 2.1 and 2.2.

Table 2.1 Oligonucleotide primers designed for RT-PCR. Primer pairs used to verify the FR-light regulation of the candidate transporter genes using RT-PCR. The cDNA product size and the annealing temperature used for each primer pair are shown.

Gene	Primer Sequence	Tm	Product (cDNA)
STP1			
Forward	TTA TCC CGG CAA ACT CAC TC	61°C	1212 bps
Reverse	CGG GAA GAT TTC ACT CGG TA		
Niemann Pick			
Forward	ACT TGT TCT CCG GAT CAG AG	58°C	1173 bps
Reverse	CCA GTG CAG TAG TTG GAT CA		
FRIMP1			
Forward	TAG GAT GGG CAG GTT TAT GG	60°C	1048 bps
Reverse	CAG GAA TCC CCT CAC AGA AA		
PIN4			
Forward	CTC TAT GGG CTA ACC TAA CC	60°C	1175 bps
Reverse	ACC GAT TAG ACT GGA GTA CG		
ANM2			
Forward	TAT TGC CTC TGA GAT CGC CA	61°C	852 bps
Reverse	CTC ACT TAC CAC TTC TCC AC		
ACA2			
Forward	TAT TGC CTC TGA GAT CGC CA	61°C	1293 bps
Reverse	GTG GCT CTG TAG CTA AAG CA		
CAT4			
Forward	CTC CTC TCC GCT TTC TGT TAC A	63°C	883 bps
Reverse	AGA AAA GTG GAG GCG TTG ACT G		
AHA2			
Forward	CTT AGC AAG AAG GTG CTC TCC A	63°C	1053 bps
Reverse	CAA T CA TCA GCA ATG CTC CAG G		
RAN1			
Forward	CTC TTG CAA AGG GGA AAA CCT C	64°C	208 bps
Reverse	GTA ACT TGA ACC CCA CAC C		

Table 2.2 Oligonucleotide primers designed for RT-PCR. Primer pairs used to amplify control genes including *ACTIN2* and *40S*, and the FR-light induced genes *HEMA1* and *Lhcb1.2*. The sequence of the Lbal primer used to confirm plant zygosity is also shown. The cDNA product size and the annealing temperature used for each primer pair are shown.

Gene	Primer Sequence	Tm	Product (cDNA)
ACTIN2			
Forward	GGT AAC ATT GTG CTC AGT GGT GG	60°C	200 bps
Reverse	CTC GGC CTT GGA GAT CCA CAT C		
40S ribosomal protein			
Forward	GGC GAC TCA ACC AGC TAC TGA	60°C	434 bps
Reverse	CGG TAA CTC TTC TGG TAA CGA		
HEMA1			
Forward	CAA GAA CTC TGC AGC TGA TC	63°C	578 bps
Reverse	GAT ACG TTT GAA GAC TGC GGA A		
Lhcb1.2			
Forward	GTG ACC ATG CGT CGT ACC GTC	62°C	245 bps
Reverse	CTC AGG GAA TGT GCA TCC G		
Lbal			
Forward	TTC ACG TAG TGG GCC ATC G	60°C	

2.5.3 PCR amplification of cDNA

PCR reactions were carried out using genomic DNA or cDNA from the reverse transcription reaction. All PCR reactions were performed in a total volume of 12 µl, containing 5 µl RNase-free sterile water, 5µl Bioline Taq (Bioline, London UK), 0.5 µl (10mM) forward amplification primer (Sigma-Genosys), 0.5 µl (10mM) reverse amplification primer (Sigma-Genosys) and 1 µ1 of genomic DNA or cDNA from the reverse transcriptase reaction. The standard protocol used for PCR was 94°C for 5 mins to denature the cDNA, followed by the cycling program of 94°C for 30 s, annealing temperature for 1 min, 72°C for 1 min, for the appropriate number of cycles for amplification before a final elongation step of 72°C for 5 mins using the PCR PTC-200 thermal cycler (MJ research, San Francisco USA).

2.5.4 Optimisation of PCR conditions

The annealing temperature (T_m) of a primer pair in the amplification of a given gene was determined by using the temperature gradient feature of the automated PCR machine. Multiple reactions were set up for each primer pair and the temperature of the primer annealing step was varied over a temperature range of 55°C – 70°C. The annealing temperature with maximal amplification of the chosen gene, without the amplification of secondary products was selected.

To determine the number of PCR cycles required to achieve amplification of the gene in the exponential phase during PCR amplification, multi-cycle PCR reactions were carried out using each primer pair. A typical multi-cycle PCR reaction consisted of 96 µl (8x the volumes of each component), and after an initial run of 20 cycles, 12 µl of the reaction mixture was removed every 2 or 3 cycles and kept on ice until the end of the PCR cycling protocol.

2.6 Real-time PCR

Real-time quantitative RT-PCR was performed using the MJ Opticon 2 thermal cycler (MJ research, San Francisco USA).

2.6.1 Primer design and dilution preparation

Primers were designed as in section 2.5.2, however as the detection of the SYBR green 1 fluorescent dye is optimal at a product size of under 400 bps, primers where designed to meet this criteria (Table 2.3). One µl of the 100 µM forward primer solution was diluted in 83.3 µl of distilled water creating a primer concentration of 1.2 µM. The same was repeated for the gene specific reverse primer and both primer solutions were combined in the same microcentrifuge tube.

2.6.2 Calculation of primer efficiency

To calculate the efficiency of a pair of gene specific primers including those for the putative control genes, a dilution series of the cDNA was carried out. A range of cDNA dilutions were carried out ranging from 1 in 2 to a 1 in 2000 dilution and a series of cycle threshold values were generated. This was repeated three times and the mean cycle threshold value was taken. The mean cycle threshold value was then plotted against the log cDNA concentration and the efficiency of the primer pair could be calculated using the slope of the amplification in the equation:

$$\text{Efficiency (E)} = (10^{(-1/\text{slope})})$$

2.6.3 Real-time PCR amplification

All PCR reactions including a water control and the dilution series for the primer efficiency calculations were composed of 2.5 µl of the diluted primer solution, 2.5 µl of a 1 in 5 diluted cDNA sample and 5 µl of the SYBR green DyNAmo master mix (Finnzymes, GRI, UK) containing the modified *Thermus brockianus* DNA polymerase, nucleotides and the SYBR green 1 fluorescent dye. Each biological sample and treatment was repeated in triplicate to minimise technical errors.

Table 2.3 Oligonucleotide primers designed for Real-time RT-PCR. Primer pairs used to verify the FR-light regulation of the candidate transporter genes using Real-time RT-PCR. The cDNA product size and the annealing temperature used for each primer pair are shown.

Gene	Primer Sequence	Tm	Product (cDNA)
STP1			
Forward	CTT ATC CCG GCA AAC TCA CTC C	61°C	196 bps
Reverse	GCT ATC GTA CTG ACA GTA CTG G		
FRIMP1			
Forward	CTT AGG ATG GGC AGC TTT ATG C	60°C	180 bps
Reverse	CTT CCA GTT TAT CAT CCT TGC C		
PIN4			
Forward	ACA AGG TGC TAA GGA GAT TCG	60°C	213 bps
Reverse	CAT ATG TGT TCC GTT GTT GCC G		
ACA2			
Forward	ATC GTC ACA GTT GCT AAA TGG G	61°C	207 bps
Reverse	GTG GCT CTG TAG CTA AAG CAA G		
CAT4			
Forward	CTC CTC TCC GCT TTC TGT TAC A	63°C	203 bps
Reverse	GGA AGT TGA GAT CCC GAA AGC T		
AHA2			
Forward	GAA TGC TTG CTG ATC CAA AGG A	63°C	197 bps
Reverse	TGG AGA GCA CCT TCT TGC TAA G		
RAN1			
Forward	CTC TTG CAA AGG GGA AAA CCT C	64°C	208 bps
Reverse	GTA ACT TGA ACC CCA CAC C		

The 10 µl samples were loaded on to a 96 well plate (Starlab, Milton Keynes UK) and 0.2 ml flat caps (Starlab, UK) were placed on the plate. The 96 well plate was centrifuged for 1 min at 500x *g* before loading in the Real-time thermal cycler (MJ research). The PCR cycling program composed of an initial denaturation step at 95°C for 10 mins to denature the cDNA and separate the strands. This was followed by the cycling steps composed of a 30 sec denaturation at 95°C, followed by 1 min at the appropriate annealing temperature (dependent on the primer pair), and then a 1 min elongation step at 72°C. Each cycle was followed by a data acquisition step in which the fluorescent data was collected. To prevent errors resulting from primer dimer formation, the fluorescent data collection was carried out at a higher temperature than the 72°C extension temperature. The program was cycled for the appropriate number of cycles, usually around 45 for sufficient amplification, followed by a final 10 min elongation step. Immediately after the cycling protocol a melting curve analysis of the PCR product was carried out to determine possible primer dimers and other unwanted secondary products. This involved taking a fluorescence reading in 0.2°C increments and holding the temperature for 1 sec, from 50 – 92°C. The data is automatically saved after each fluorescence reading and data can be analysed using the data analysis package to determine cycle threshold (C(T)) values.

2.6.4 Real-time PCR analysis

To calculate the relative expression of a gene (target gene), a suitable reference gene was chosen and the C(T) value was determined for both the control treatment (dark seedling) and the appropriate light treatment for all genes. The relative expression was then calculated using the following equation, as shown at http://www.gene-quantification.info.

$$\text{Relative expression} = \frac{(E^{\text{target})\Delta C(T)\text{target (control – sample)}}}{(E_{\text{reference}})^{\Delta C(T)\text{reference (control – sample)}}}$$

The difference in C(T) of the target gene for the treatment is normalised to the difference in C(T) of the target gene in the control. The efficiency of the primers amplifying the target gene is then raised to the power of the difference in the C(T) of the target gene. This is then repeated for the reference gene, and the relative expression of the

target gene is normalised to the reference gene. So this calculation determines the relative expression of the candidate gene firstly by normalisation to the control treatment and secondly to the constitutively expressed control gene.

2.7 Gel electrophoresis

2.7.1 RNA gel electrophoresis

One μg of RNA sample was separated on a 1.3% (w/v) agarose gel containing 0.9M formaldehyde and 10 x MOPS buffer (containing 0.2M MOPS (3-(N-morpholino) propane sulphonic acid), 0.05M sodium acetate and 0.01M sodium EDTA (pH 8.0). Immediately before loading, the RNA was diluted in 11 μl of RNase-free water and was denatured at 65°C for 10 mins. The RNA was then added to a 0.8 x vol of formaldehyde, 2.0 x vol formamide and 0.4 x vol of 10 × MOPS buffer. The RNA mixture was then loaded in a sample buffer containing 50% (v/v) glycerol, 0.1mg/ml bromophenol blue, and 1 μg of ethidium bromide per sample. Electrophoresis was carried out in 1 x MOPS running buffer at 80 V for 1-1.5 h. The RNA was then visualised using the Alpha Imager™ (Flowgen, Shenstone UK).

2.7.2 cDNA gel electrophoresis

Gel electrophoresis of DNA was performed as described by Sambrook *et al.*,1989. DNA was separated on a 1.5% (w/v) agarose gel, containing 1 x TAE buffer (40mM Tris /acetate (pH 8.0), 1mM EDTA). The gel and running buffer contained 1mM ethidium bromide. As the buffer used for the RT-reaction contains loading buffer, no additional loading buffer was added. Electrophoresis was carried out at 100 V for approximately 1 h depending on product size. DNA was visualised under UV light using an Alpha Imager™ (Flowgen, UK) and the fragment size was estimated using a 1Kb DNA ladder (Eurogentec, Southampton UK). For expression experiments the integrated density values were plotted to determine the relative change in gene expression between treatments. The integrated density value relates to the number of pixels a product band is composed of in a given area.

2.7.3 Genomic DNA gel electrophoresis

Two µl of each genomic sample (exact concentration unknown) was separated on a 1.2% (w/v) agarose gel containing 1 x TAE buffer (40mM Tris /acetate (pH 8.0), 1mM EDTA). One µl of ethidium bromide was added per 100ml of TAE buffer. Two µl of genomic sample was diluted in 8 µl of RNase free water and 2 µl of DNA loading buffer (0.25% (w/v) bromophenol blue, 0.25% (w/v) xylene cyanol FF and 15% (w/v) Ficoll 400 in distilled water). 5 µl of a 1 kb DNA ladder (Eurogentec) was used to estimate the product size. Electrophoresis was carried out at 100 V for approximately 1 h. DNA was visualised under UV light using an Alpha Imager^{TM} (Flowgen).

2.8 DNA gel purification

DNA to be used for sequencing or a subsequent reaction was gel extracted using the WIZARD gel extraction kit (Promega) according to manufactures instructions but with the following modification. An additional 5 min spin at 3000x *g* was included to ensure the complete removal of ethanol in the sample. The quantity of DNA was determined using the Nanodrop (section 2.3.5).

2.9 DNA sequencing

One hundred ng of a cleaned gel extracted PCR product was added to a 0.2 ml PCR tube and made up to 8.8 µl with distilled water. To this, 3.2 µl of a 1 µM primer stock and 8.0 µl of quick start mix (stored at -20°C) was added. The sample was mixed thoroughly and then cycled through the following program: 96°C for 20 sec, 50°C for 20 sec, 60°C for 4 mins. After 29 cycles the sample was kept at 4°C. Samples were either stored at -20°C or used immediately for the ethanol precipitation clean-up. For this samples were transferred to 1.5 ml microfuge tubes and 5 µl of stop solution (2 µl 100 mM EDTA, 2 µl NaOAc pH 5.2 and 1 µl glycogen) was added. 60 µl of 95% ethanol chilled to -20°C was added, vortexed and then centrifuged at 3000x *g* for 15 mins at 4°C. The supernatant was removed and 200 µl of 70% ethanol chilled to -20°C was added, vortexed and centrifuged at 3000x *g* for 15 mins at 4°C. The supernatant was removed and the 70% ethanol wash was repeated. The pellet was air dried at room temperature for 20 -30 mins.

For sequencing the pellet was re-suspended in 40 µl of a defrosted sample loading solution by leaving it to stand for 2 mins and then vortexed for 1 min. The samples were then added to a 96 well plate, filling all 8 wells in the lane. If the lanes were not filled with sample they were filled with distilled water. One drop of mineral oil was added to each sample immediately and the samples were run on the Beckman Coulter CEQ 800 DNA sequence analyzer (Beckham Coulter, High Wycombe, UK) according to manufactures instructions.

2.10 Microarray analysis

2.10.1 RNA preparation (Ethanol salt precipitation)

One hundred µg of RNA extracted from three and a half-day-old *Arabidopsis thaliana* seedlings grown in either darkness or exposed to 12 h of FR-light (10 µmol m^{-2} sec^{-1}) was ethanol salt precipitated in 2.0 vol 100% ethanol and 0.1 vol NaOAc (pH 5.2), vortexed well and then stored at -20°C for 2 h. Samples were centrifuged at 3000x *g* at room temperature for 10 mins and then the pellet was air dried for 2-3 hours. Each RNA pellet was re-suspended in 19 µl of RNase-free water and stored at -20°C for subsequent microarray analysis.

2.10.2 Reverse transcription

Two µl of oligo $(dT)_{12-18}$ (500µg/ml) primer was added to the 19 µl of RNA of each sample and incubated at 65°C for 10 mins, then at room temperature for 10 mins followed by two mins on ice. The reverse transcriptase reaction buffer consisted of 8 µl 5 x buffer (Invitrogen), 4 µl DTT (Invitrogen), 0.8 µl dNTP stock (25 mM dATP, 25 mM dGTP, 25 mM dTTP and 10 mM dCTP) (Promega), 1.2 µl Cy3 or Cy5 dye (Amersham Biosciences) and 3.5 µl RNase-free water. This was added to the RNA and incubated at 42°C for 2 min. Cy3 was added to the control (total RNA extracted from dark-grown seedlings), and Cy5 to the treatment (total RNA extracted from FR-light grown seedlings). One and a half µl (300 units) of Reverse transcriptase Superscript 2 (Invitrogen) was added to each RNA sample and incubated for 2 h at 42°C. After 1 h a second aliquot, of Superscript 2 (1 µl) was added. Reactions were terminated by the addition of 10 µl 1M NaOH, incubated at 65°C for 10

min and then neutralised by adding 10 µl 1M HCl and 250 µl TAE buffer (pH 7.5). cDNA was purified following the QIAquick PCR purification kit protocol (Qiagen). A 5 x vol of PB buffer (approx 1305 µl) was added to 1 x vol of cDNA sample and mixed. The sample was applied to a QIAquick column within a 2 ml collection tube and centrifuged at 3000x *g* for 60 s. The flow-through was discarded and 750 µl of PE buffer was added to each column and centrifuged at for 1 min. The flow-through was again discarded and centrifuged for a second period of 1 min at 3000x *g*. An extra centrifuge step of 1 min at 3000x *g* was then added to the protocol to ensure ethanol was not carried over. The column was placed in a clean microcentrifuge tube and the DNA was eluted with 50 µl EB buffer (10mM Tris-Cl, pH 8.5), by pipetting the buffer to the centre of the column membrane, and centrifuged at 3000x *g* for 1 min.

2.10.3 Determination of cDNA synthesis and dye incorporation

cDNA synthesis and dye incorporation was determined spectrophotometrically over the whole range of 200 – 800 nm using the complete 50 µl reaction in a 100 µl cuvette. The spectrophotometer was blanked using 50 µl of the elution buffer both before and after the two samples were analysed, to determine the amount of cDNA synthesis and the level of dye incorporation. The cDNA exhibits a peak at 260nm, while the Cy3 and Cy5 dyes have absorbance maxima at 550nm and 650nm respectively.

2.10.4 Blocking of microarray chip for hybridisation

The spot area of the array was marked on the slide with a diamond knife. The array was located 26 mm from the top (labelled) end of the slide, 4 mm from the left edge of the slide, and was 17.3mm in width and 15.1mm in length. The surface of the microarray was blocked directly before use using a blocking solution. The blocking solution (25 ml 20 x SSC (0.3 M sodium citrate and 3 M NaCl, pH 7), 1 ml 10% (w/v) SDS and 1g BSA (bovine serum albumin) in 100 ml sterile water) was pre-heated to 42°C ensuring that any precipitate had disappeared. The array was immersed in the blocking solution within a 50 ml plastic centrifuge tube for 45 min at 42°C. The array was rinsed five times with RNase-free sterile water at room temperature, and the excess water was drained off by placing the

array vertically on dust free tissue inside a fresh 50ml plastic centrifuge tube (preventing the tissue from touching the front of the array) and centrifuged at 500x *g* for 15 min.

2.10.5 Hybridisation of the microarray chip

The two cDNA samples were combined and re-dissolved in 12 µl of a formamide based hybridisation buffer (provided by MWG) which was pre-incubated at 42°C. This was achieved by adding the hybridisation buffer to the Cy3 labelled cDNA, pipetting up and down, and then transferring the mixture to the Cy5 labelled cDNA and mixing well. The target mixture was heated at 95°C for 3 min then placed on ice for 30 sec (no longer than 3 min). If precipitation appeared the mixture was pre-heated to 42°C until clear. The hybridisation mixture was centrifuged down briefly and then applied to the centre of the array on the blocked microarray chip. The array was covered with a cover slip and any air bubbles were squeezed out by gently pressing the cover slip with a pipette. The array was placed in a wet hybridisation chamber and 20 µl of sterile water was pipetted in to the four corners of the chamber. The chamber was then tightly secured to prevent water leaking into it. The chamber was transferred to a water bath and incubated at 42°C for 16-24 h.

2.10.6 Washing of the microarray chip

All washing buffers were prepared in 50 ml plastic centrifuge tubes and pre-warmed over night at 30°C, and all washing steps were undertaken at room temperature. The array was vertically immersed in washing buffer 1 (2 x SSC, 0.1% (w/v) SDS) allowing the cover slip to slide off under its own weight. The cover slip was removed from the tube to avoid scratching the array and the array was washed for 5 min with gentle agitation on an orbital shaker. This procedure was repeated with washing buffer 2 (1 x SSC) and washing buffer 3 (0.5 x SSC). The excess buffer was drained off by placing the array on dust free tissue in a fresh 50 ml plastic centrifuge and centrifuged at 500x *g* for 2 min. The microarray chip was scanned and stored in a dark, cool dry slide box.

2.11 T-DNA knockout identification and confirmation

2.11.1 T-DNA mutant identification

T-DNA knockout lines for the light-regulated genes were identified by sequence-based searching of insertional mutagenesis web based databases. Seeds of T-DNA lines were ordered from the **N**ottingham *Arabidopsis* **S**tock **C**entre (NASC) (http://nasc.nott.ac.uk).

2.11.2 Segregation analyses

The seeds from each line were grown up to maturity (see 2.1.1) and subsequent seed was collected. Approximately 50 seeds from each potential T-DNA knockout or the Col-8 wild-type were plated individually on MS plates containing 1% (w/v) sucrose and 1 µl per 1 ml agar of a 100 mM stock of the antibiotic kanamycin. The same is repeated on plates not containing kanamycin. Perti dishes were parafilm sealed and stratified at 4°C for 48 h and then transferred to a diurnal program of 16 h daylight at a constant temperature of 23°C (fluence 130 µmol m^2s^{-1}) , and 8 h dark at 18°C. Seeds were grown for 10-14 days before scoring each seed batch to determine wild-type, heterozygous or homozygous plants.

2.11.3 Genotypic analyses

Genomic DNA was extracted from leaves from each of the potential T-DNA knockouts and PCR was undertaken using 3 primer pair combinations for each gene (Tables 2.4 and 2.5). Primers were designed to identify the presence of the T-DNA insert, with gene specific forward and reverse primers spanning the T-DNA insert and a T-DNA left border primer (Lba1) specific to the insert (Table 2.2). Primers were used in three different combinations; the gene specific primers were used in combination and Lba1 was used in conjunction with both of the gene specific primers.

Table 2.4 Primer combinations for genotypic analysis of putative T-DNA mutants.
Three pairs of primers were used for the analysis of mutants in the *STP1*, *ACA2* and *CAT4* genes. Primers were designed to amplify the wild-type gene, any truncated product and a product spanning the predicted insert site. The cDNA/gDNA product sizes and the annealing temperature for each primer pair are shown.

STP1			Tm	Product (cDNA/gDNA)
W/T	Forward (F1)	AGG CTT ATC CCG GCA AAC TCA CTC	63°C	1508/2615 bps
	Reverse (R2)	GGT TAC TGT TCT TGC CCA TCT CA		
Trun	Forward (F1)	AGG CTT ATC CCG GCA AAC TCA CTC	63°C	772/1786 bps
	Reverse (R1)	GTG CTC TAT CGA CTG CGA CTC TTT		
T-DNA	Forward (F2)	AAA GAG TCG CAG TCG ATA GAG CAC	63°C	759/853 bps
	Reverse (R2)	GGT TAC TGT TCT TGC CCA TCT CA		
ACA2			Tm	Product (cDNA/gDNA)
W/T	Forward (F1)	ATG GCG TAA TCT CTG TGG CGT TGT	63°C	2942/3482 bps
	Reverse (R3)	GGC ATA CCC AAG AAA CCT ATG AAG		
Trun	Forward (F1)	ATG GCG TAA TCT CTG TGG CGT TGT	63°C	672/883 bps
	Reverse (R1)	CTG TCT AAA CCC GTT CCT TGT CAC		
T-DNA	Forward (F2)	GTG ACA AGG AAC GGG TTT AGA CAG	63°C	990/990 bps
	Reverse (R2)	CCT CAG GAA GCT CGA TTA CAA CTC		
CAT4			Tm	Product (cDNA/gDNA)
W/T	Forward (F1)	GTG GTC ACT CTT CTT TCT CCA GTC	64°C	1663/3099 bps
	Reverse (R2)	TTC AGC ATC AGA ACT CGC ATG AAC		
Trun	Forward (F1)	GTG GTC ACT CTT CTT TCT CCA GTC	64°C	493/610 bps
	Reverse (R1)	GGA AGT TGA GAT CCC GAA AGC TGT		
T-DNA	Forward (F2)	ACA GCT TTC GGG ATC TCA ACT TCC	64°C	1290/2513 bps
	Reverse (R2)	TTC AGC ATC AGA ACT CGC ATG AAC		

Table 2.5 Primer combinations for genotypic analysis of putative T-DNA mutants. Three pairs of primers were used for the analysis of mutants in the *FRIMP1*, *FRIMP2* and *AHA4* genes. Primers were designed to amplify the wild-type gene, any truncated product and a product spanning the predicted insert site. The cDNA/gDNA product sizes and the annealing temperature for each primer pair are shown. * The truncated primers for N562371 were used as the T-DNA spanning primers for N622010. No truncated product was shown for N622010.

FRIMP1			Tm	Product (cDNA/gDNA)
W/T	Forward (F1)	CGA TAT ACG AAG GCA CGG TGG TGA	63°C	1266/5724 bps
	Reverse (R2)	TCT CCA CCC AAC ACA TCT GTT ATG A		
Trun	Forward (F1)	CGA TAT ACG AAG GCA CGG TGG TGA	63°C	436/1838 bps
	Reverse (R1)	ACT GAC CAG CTG AGG CAT GGT AAA		
T-DNA	Forward (F2)	AGT AGA TGC TGC ACT CCT CTC ACA G	63°C	257/1215 bps
	Reverse (R2)	TCT CCA CCC AAC ACA TCT GTT ATG A		

FRIMP2			Tm	Product (cDNA/gDNA)
W/T	Forward (F1)	GGA ATG TTG GTG ATT GGA TCT CTG	64°C	1117/5632 bps
	Reverse (R2)	CCA ACC CTC GAC ACT GCA AAG AA		
Trun	Forward (F1)	GGA ATG TTG GTG ATT GGA TCT CTG	64°C	805/2143 bps
	Reverse (R1)	TGG CGG AGT TCA TAA ATT TCC		
T-DNA	Forward (F2)	GGA AAT TTA TGA ACT CCG CCA	64°C	332/1474 bps
	Reverse (R2)	CCA ACC CTC GAC ACT GCA AAG AA		

AHA2 (N562371 and N622010)			Tm	Product (cDNA/gDNA)
W/T	Forward (F1)	CAG ATC TTT GGC CCC AAC AAG CTC	64°C	2717/3959 bps
	Reverse (R2)	CAC AGT GTA GTG ACT GGG AGT TTC A		
Trun*	Forward (F1)	CAG ATC TTT GGC CCC AAC AAG CTC	64°C	1042/1242 bps
	Reverse (R1)	CTC CTT TGG ATC AGC AAG CAT CC		
T-DNA	Forward (F2)	CTA CTG GAG TCG TTC TAG GAG GCT A	64°C	712/996 bps
	Reverse (R2)	CAC AGT GTA GTG ACT GGG AGT TTC A		

2.11.4 Analysis of mRNA levels in T-DNA insertion mutants

To determine whether mRNA for the selected gene was absent in the mutant, total RNA was extracted from both wild-type and mutant white light grown seedlings. RT-PCR was undertaken using three combinations of primer pairs specific to the gene of interest (Tables 2.4 and 2.5). The primer pairs were designed to span different sections of the gene, including primers to amplify the wild-type gene, primers at the 5' end to identify a possible truncated product, and primers spanning the T-DNA insert.

2.12 Cloning and over-expression of *FRIMP1*

A *FRIMP1* clone was obtained from RIKEN (Japan), however before it could be transformed into *E.coli* the clone was sequenced (see 2.9). Five forward primers designed specifically to *FRIMP1* and the M13 forward and reverse primers specific to the modified blue-script expression vector were used to sequence the clone (Table 2.6). The sequencing analysis revealed correct sequencing so was transformed into *E.coli*.

2.12.1 Transformation of chemically competent DH5α *E.coli*

A sample of DH5α cells (Invitrogen) were thawed slowly on wet ice and 50 µl of cells were aliquoted into a microcentrifuge tube. To each sample of cells 1-10 ng of the *FRIMP1* clone DNA was directly added to the competent cells and mixed by gentle tapping. Samples were incubated on ice for 30 mins, then heat-shocked for exactly 20 seconds in a 37°C water bath, followed by 2 mins on ice. 950 µl of pre-warmed LB-broth was added to each sample and shaken continuously in an incubator at 225 rpm at 37°C for 1 h. After this incubation samples were diluted with LB-broth to a 1:10 dilution and 30 µl from each transformation was placed on LB plates containing 100µl/ml ampicillin. Plates were wrapped in parafilm, inverted and then incubated at 37°C for 24-48 h to obtain large colonies.

Table 2.6 Oligonucleotide primers designed for sequencing of the *FRIMP1* clone.
Forward primers designed for *FRIMP1* and M13 forward and reverse primers were used to sequence the RIKEN *FRIMP1* clone. The annealing temperature used for each primer is shown.

Gene	Primer Sequence	Tm
FRIMP1		
Forward (F1)	CGA TAT ACG AAG GCA CGG TGG TGA	60°C
Forward (F2)	ACG CAT TCT GGC GTA TGG GAG TTC A	61°C
Forward (F3)	TTT TAC CAT GCC TCA GCT GGT TCA GT	61°C
Forward (F4)	GGA AGT ATA TGA GCT GCG TCA AGC AA	61°C
Forward (F5)	AGT AGA TGC TGC ACT CCT CTC ACA G	60°C
M13		
Forward	TGT AAA ACG ACG GCC AGT	55°C
Reverse	CAT GGT CAT AGC TGT TTC C	56°C

2.12.2 Plasmid preparation

E.coli transformed with the *FRIMP1* cDNA or vector plasmid were plated on LB-broth agar plates containing 100 μg/ml ampicillin (cDNA and DH5α vector) or 100 μg/ml kanamycin (pBIN19 vector), wrapped in parafilm and incubated at 37°C overnight. A small aliquot of transformed cells from a colony that had survived selection was placed in to a steriline tube containing 5 ml liquid LB-broth (100 μl/ml ampicillin), and incubated on a shaking incubator at 225 rpm at 37°C for 1 h. Plasmid DNA was then isolated using the plasmid prep kit (Qiagen) according to manufactures instructions.

2.12.3 Restriction digest of DNA

The amount of DNA was measured using the Nanodrop (section 2.3.5). The following reaction mixture was used for each digest: 0.5-1.0 μg plasmid DNA, 0.25 μl acetylated BSA and 2.5 μl of the appropriate10 x reaction buffer (Promega). 1.0 μl of each restriction enzyme was used, with two enzymes used for a double digest. Water was added to a final volume of 25 μl. The multi-core 10 x buffer (Promega) was used for a single digest. The appropriate 10 x buffer for a double digest was selected according to the restriction enzymes used. A compatible buffer was selected using a web based program available at www.promega.com. Samples were incubated at the appropriate temperature according to the enzyme for 2 h. If restriction enzyme temperatures were incompatible the first digest was carried out, then ethanol precipitated by adding 2 x vol 100% ethanol and 0.5 x vol NaOAC (pH 5.2) and incubated at -20°C for 30 mins. The sample was then centrifuged at 3000x *g* for 10 mins at 4°C. The supernatant was removed and pellet air dried. The second digest was then carried out at the second temperature. The product was separated by electrophoresis using a 1.2% agarose gel (section 2.7.2), loading the sample with 5μl of DNA loading buffer. The bands were the visualised using a UV lamp and the bands of the correct size were gel extracted (section 2.8). The same protocol was used to digest the *FRIMP1* clone from the modified bluescript vector. The *FRIMP1* clone was first digested with the *Xho*I restriction enzyme (Promega). The *Xho*I digested fragment was then blunt ended using the T4 Klenow fragment polymerase (Promega) (section 2.12.4) to permit ligation with the sma1 digested DH5α fragment. The sample was then ethanol precipitated followed by the *Bam*HI (Promega) digestion.

2.12.4 Klenow fragment digestion

Blunt ended DNA fragments were created using the T4 Klenow fragment polymerase (Promega). The product of the *Xho*I digest (section 2.12.3) was diluted in 25 µl of distilled water and to the *Xho*I digest the following was added; 2.5 µl Klenow buffer, 1 unit of Klenow fragment polymerase per µg of DNA and 1.0 µl of a 1 mM dNTP stock. Reaction was incubated at room temperature for 10 mins then stopped by heating at 75°C for a further 10 mins.

2.12.5 DNA ligation

To undertake the ligation of the cDNA fragment to a vector plasmid fragment a 3:1 ratio of vector:insert DNA is required. The quantity of DNA for both the vector and insert DNA was determined using the nanodrop method (section 2.5). The following equation was used to determine the 3:1 ratio:

$$\frac{\text{ng of vector x kb size of insert}}{\text{kb size of vector}} \times \text{molar ratio of } \frac{\text{insert}}{\text{vector}} = \text{ng of insert}$$

One hundred ng of vector DNA was used in each ligation reaction with the appropriate amount of insert DNA. To each ligation reaction 5 µl of the 2x rapid ligation buffer and 2 µl of T4 DNA ligase (Promega) was added and made up to a total volume of 20 µl with nuclease-free water. The reaction was incubated at 22°C for 2-3 h to ligate the sticky end then followed by a 4°C incubation overnight to ligate the blunt end. The ligated DNA was then transformed into the DH5α strain (section 2.12.1).

2.12.6 Vector dephosphorylation

The digested vector was ethanol precipitated and re-suspended in 20 µl of water. One unit of **S**hrimp **A**lkakine **P**hosphatase (SAP) (Promega) was incubated per µg DNA at 37°C for 15 mins in 1x SAP reaction up to 30 µl. The SAP was inactivated by heating to 65°C for 15 mins. The reaction mix was vortexed and 5 µl of the dephosphorylated vector

was added to the appropriate DNA insert in 1x ligation buffer at 4°C overnight for all types of DNA overhangs. The final volume was adjusted to 20 µl with water.

2.12.7 Colony PCR

A pin-prick of each colony was diluted in 25 µl of distilled water and stored at -4°C. One µl of this sample was then diluted in 4 µl of distilled water and heated at 95°C for 5 mins in the PCR thermal cycler (MJ research). To each sample 4 µl of Taq mixture (Bioline) and 0.5 µl of each primer stock (10 mM) was added. The sequencing protocol used for PCR (see 2.8) was generally performed at 94°C for 2 mins to denature the cDNA, followed by the cycling program of 94°C for 30 s, 65°C annealing temperature for 1 min, 72°C for 1 min, and cycled for 36 cycles of amplification before a final elongation step of 72°C for 5 mins. Samples were then separated by electrophoresis on an aragrose gel (see 2.7.3) to check for the presence of the clone in the expression vector.

2.13 Analysis of FRIMP protein function in *C.elegans* using RNAi

The N2 hermaphrodite worms were cultured on standard NGM plates with OP50 *E.coli* prior to use in feeding experiments for three days. The plates were dried for 6-8 days at room temperature prior to the addition of the worms as damp plates would affect the feeding ability of the worms. Five worms at the L4 developmental stage were transferred to 5 ml plates containing NGM agar. These plates had previously been treated by adding 100µl of a 1mM IPTG stock onto the surface of the plate and 20µl of the RNAi feeding vector *E.coli*. The plates were incubated upside down for 4 days at 37°C. The progeny at the L4 stage were transferred to fresh plates with fresh *E.coli* and incubated upside down for a further 4 days. The first generation progeny of these worms at the L4 stage were visually scored for phenotypic differences. This was repeated for a further 2 generations of progeny. The same protocol was repeated with the N2 worms on *E.coli* feed on the vector control as a comparison (Kamath and Ahringer, 2003).

Chapter 3

Identification of transporter genes regulated by Far-red light

3.1 Introduction

3.1.1 Regulation of transporter gene expression by FR-light

To date a number of studies have investigated the effect of FR-light on gene expression patterns of etiolated seedlings exposed to FR-light (Tepperman *et al.*, 2001; Wang *et al.*, 2002; Devlin *et al.*, 2003). The study of FR-light is used as a model system to identify genes that are specifically regulated by phyA, as phyA is thought to be the sole photoreceptor involved in the perception of FR-light (Nagatani *et al.*, 1994). As FR-light grown seedlings do not photosynthesize, any changes in gene expression are more likely to be as a direct consequence of light signalling rather than as a response to photosynthesis. De-etiolation involves major changes in morphology that must be accompanied by a re-distribution of various molecules and compounds, including signalling molecules and photosynthetic metabolites which allow the seedling to follow a different morphological program and develop accordingly. There are likely to be many types of proteins involved in the transport of such compounds during de-etiolation. *The Arabidopsis thaliana* genome contains approximately 25,498 genes located on 5 chromosomes (Arabidopsis genome Initiative 2000), and of these around 1700 have been predicted as transmembrane proteins (Bock *et al.*, 2006)). Of these a significant proportion are believed to function in transport across plasma and intracellular membranes. They are responsible for the acquisition, re-distribution and compartmentalisation of organic nutrients and inorganic ions, as well as for the efflux of toxic compounds and metabolic end products. It is hypothesized that transporters involved in de-etiolation can be identified by looking for light-regulation of transporter gene transcripts. Changes in gene expression can be monitored by examining the expression profiles of membrane transporters and a subsequent change in the expression of a transporter could provide an insight into the movement of compounds around the seedling. Transporter genes identified as being FR-light regulated are candidates for mediating phyA responses or may even be involved in phyA signalling.

3.1.2 DNA microarrays for functional plant genomics

The development of microarray technology has enabled plants researchers to compare simultaneously the transcriptional regulation of thousands of genes. Since microarray technology has become the researchers chosen method to measure global changes in gene expression, it has been used to develop the transcript profiles following a wide variety of experimental variables (Ma *et al.*, 2001). Several important plant processes have been investigated by this chosen route of experimentation (Ma *et al.*, 2001). These include analysis of the female gametophyte transcriptome (Yu *et al.*, 2005), integration of membrane transport with male gametophyte development (Bock *et al.*, 2006) nutrient responses (Wang *et al.*, 2000; Matthius *et al.*, 2003), drought and cold stress responses (Seki *et al.*, 2001; Vogel *et al.*, 2005), toxic metal responses (Weber *et al.*, 2006), regulation of biochemical pathways during photomorphogenesis (Ghassemian *et al.*, 2006), early dark-responses (Kim and von Armin, 2006), shade avoidance responses (Devlin *et al.*, 2003) and regulation of gene expression by blue (Wang *et al.*, 2001, Jiao *et al.*, 2003), far-red (Tepperman *et al.*, 2002) and red (Tepperman *et al.*, 2004) light.

3.1.3 Transcript profiling using DNA microarrays

After the completion of the genomic sequencing of *Arabidopsis* the next key challenge of researchers is to identify the function and expression patterns of all genes. Transcript profiling is playing a substantial role in annotating and determining gene functions, having advanced from methods looking at one gene at a time to new technologies viewing the whole genome simultaneously (Donson *et al.*, 2002). DNA microarray technology is one of these new methods and is a key genomic tool used worldwide. Microarray technology is based on the hybridisation of cDNA and using fluorescent dyes for labelling to examine changes in expression. Labelling uses the combination of two fluorescent dyes each labelling a different sample (control and treatment) in a single competitive hybridisation experiment, leading to the determination of the relative expression of large numbers of genes simultaneously (Aharoni and Vorst 2001). To compare relative mRNA levels in different cells, tissues or physiological states, mRNA extracted from these samples is extracted, reverse transcribed to the corresponding cDNA, labelled with the different fluorescent dyes and hybridised on to the array (Kazan *et*

al., 2001). After hybridisation and washing the slide is imaged using a scanner and fluorescence measurements are made separately for each dye at each spot on the array (Figure 3.1). Dual labelling enables the ratio of transcript levels for each gene on the array to be determined (Schulze and Downward 2001). DNA microarrays are currently being undertaken using two main approaches involving either in situ synthesis of oligonucleotides (oligonucleotide microarrays) or pre-synthesised DNA fragments (cDNA microarrays) on solid surfaces (Aharoni and Vorst 2001). An example of oligonucleotide-based arrays are Affymetrix arrays which have been constructed containing about 8200 different Arabidopsis ESTs (Zhu and Wang 2000). However an almost full transcriptome *Arabidopsis* Genechip from Affymetrix containing probes for 22,000 genes has been created and has been used to study expression profiles of most of the *Arabidopsis* genome (Pylatuik and Fobert 2005). These arrays are produced by the synthesis of oligonucleotides directly onto a solid matrix using photolithographic masks to determine correct sequences (Lockhart *et al.*, 1996). cDNA microarrays use synthesised cDNA probes which are the products of the polymerase chain reaction generated from cDNA libraries or genomic DNA, and are typically in excess of 150 nucleotides in length (Wullschleger and Difazio 2003). On the other hand, oligonucleotides have a maximum length of 80 nucleotides creating a greater specificity among members of gene families allowing the relative expression of individual members of a gene family to be profiled specifically (Kuo *et al.*, 2002). Recently the CATMA (**C**omplete **A**rabidopsis **T**ranscriptome **M**icro**A**rray) array has been used as a novel tool for *Arabidopsis* transcriptome analysis (Allemeersch *et al.*, 2005). Such arrays have been developed to the whole of the *Arabidopsis* genome with gene-specific tags of 150 - 500 base pairs which allows a greater degree of specificity between genes (Allemeersch *et al.*, 2005).

3.1.4 The *Arabidopsis* membrane transporter array

The *Arabidopsis* genome contains nearly 1700 known or genes encoding putative proteins involved in transport, with only 15% of these genes represented on the arrays used in early array studies. Twelve hundred of these transporter genes are included on the custom-made AMT (**A**rabidopsis **M**embrane **T**ransporter) which allows researchers to compare the transcriptional regulation of all transporter genes simultaneously to an experimental variable (Maathius *et al.*, 2003). The AMT array was designed and

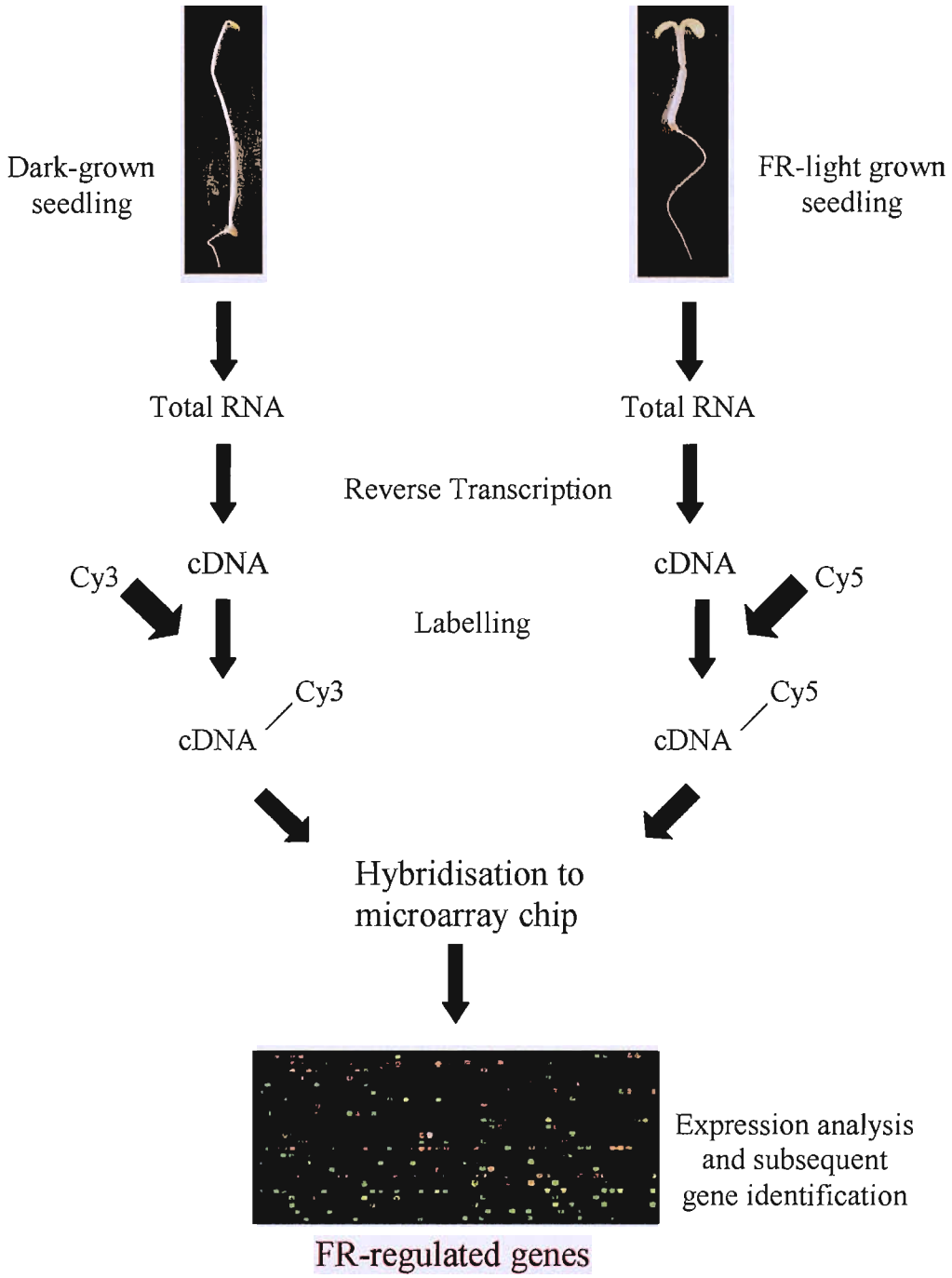

Figure 3.1 Schematic representation of the identification of FR-light regulated transporter genes using microarrays. Total RNA is extracted from etiolated and FR-light grown seedlings and is reversed transcribed to cDNA. cDNA is labelled with a fluorescent dye, etiolated with Cy3 and FR-light with Cy5. Samples are hybridised to the array and FR-light regulated genes are identified.

constructed by a consortium of seven membrane transporter laboratories worldwide all focusing on different aspects of plant membrane transport processes of families of transporters, and was designed to study global changes in gene expression of all known and putative membrane transporters to a given treatment (Maathius *et al.*, 2003). The array is comprised of approximately 1250 oligonucleotide probes as 50-mers generating good signals that are highly responsive, which in total represents 1153 genes. Of these genes 57 are control genes, including genes encoding non-transporter related proteins in both plants and animals (Maathius *et al.*, 2003). The list of transporters was compiled using the **A**rabidopsis **M**embrane **P**rotein **L**ibrary (AMPL), a web-based membrane transporter database produced by John Ward (http://www.cbs.umn.edu/arabidopsis/). Genes are spotted into 8 groups and transporters are placed randomly within these groups. All probes are spotted in replicate on each array, creating 16 gene subgroups in total. Most genes represented on the array have been assigned to transporter families based either on functional characterisation or on the basis of nucleotide sequence homology with characterised transporters (Figure 3.2). The functions of approximately 364 genes on the array are unknown so these genes have been characterised into one of two families. The genes in the group labelled "other transporters" show homology with members of transporter families characterised in non-plant systems, whereas the genes in the group labelled "putative transporters" have a high number of predicted transmembrane spanning domains. Genes predicted to encode proteins which a high number of transmembrane spanning domains were included on the array because these proteins have potential transport functions (Maathius *et al.*, 2003).

3.1.5 RT-PCR – a molecular technique used to study gene expression

The polymerase chain reaction (PCR) has allowed rapid advances in monitoring changes in gene expression at the level of transcription and it is based on *in vivo* gene transcription, and has completely revolutionised the detection of RNA and DNA (Sambrook *et al.*, 1989). The purpose of PCR is to make large numbers of copies of the gene of interest so that changes in expression can be studied. Disadvantages of RT-PCR for quantitative analysis are mainly due the fact that detection is at the end point of the reaction low sensitivity and resolution, ethidium bromide staining is not quantitative and involves post PCR processing (Deprez *et al.*, 2002). However, traditional PCR has advanced from

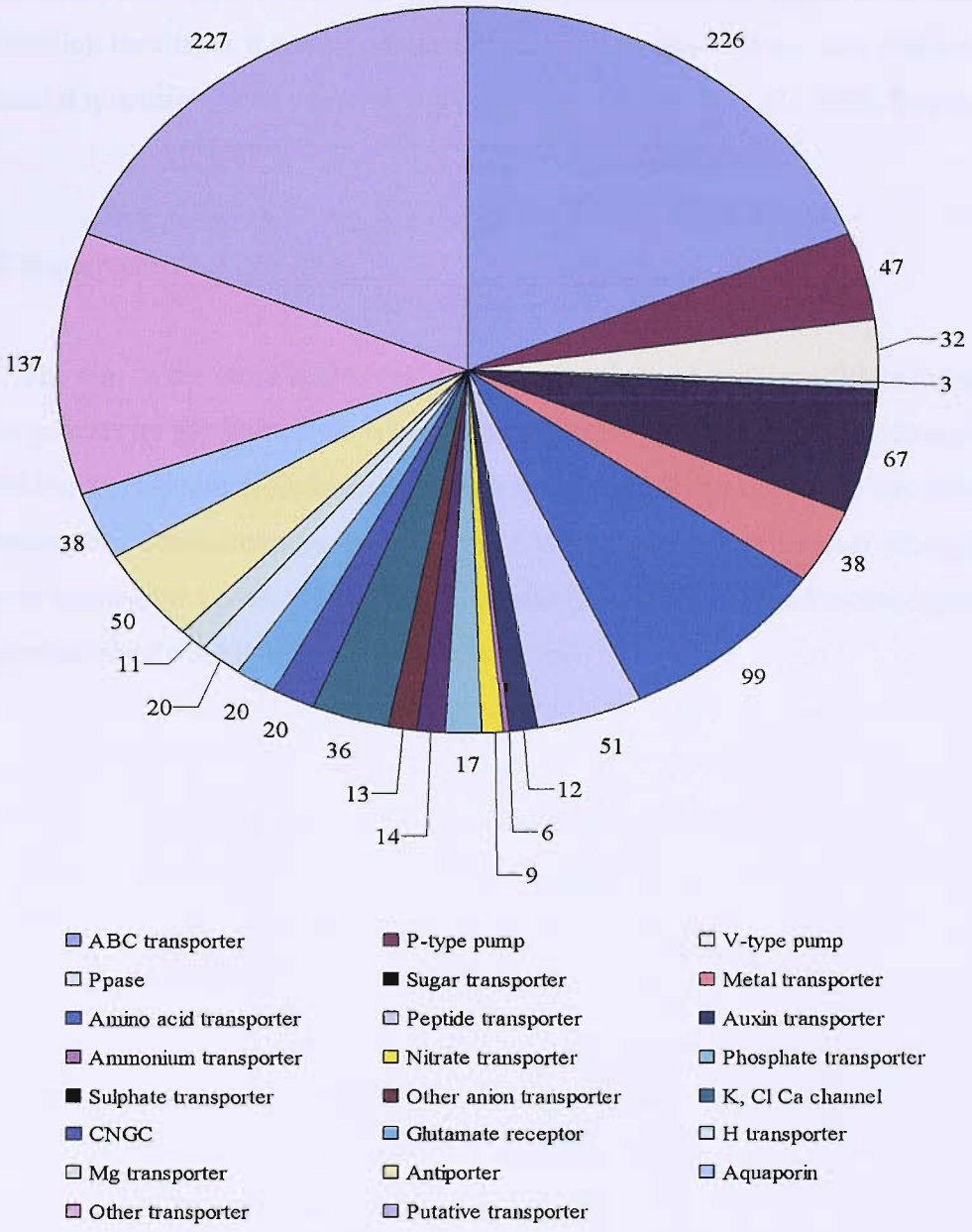

Figure 3.2 The number of transporters represented in each family on the Arabidopsis Membrane Transporter (AMT) array. The AMT array contains all known and putative membrane transporters. Genes are characterised into 23 transporters families based on either functional characterisation or on the basis of sequence homology with characterised transporters. Data taken from Maathius *et al.*, (2003).

detection at the end point of the reaction to detection during amplification. This method is quantitative and is termed Real-time PCR and is becoming a routine tool in molecular biology to study low abundance gene expression (Pfaffl, 2001). It is highly sensitive and allows quantification of rare transcripts and small changes in gene expression. Advantages of this technique include the fact that it is easy to perform and produces reliable and rapid quantification results, as it can be conducted on large numbers of samples and/or many genes and it quantifies gene expression by real-time (Freeman *et al.*, 1999; Deprez *et al.*, 2002).

3.1.6 Chapter aims

The aim of the work described in this chapter is to identify candidate transporter genes regulated by FR-light. Two approaches will be taken to achieve this; firstly by undertaking an in-depth bioinformatical analysis of published microarray datasets for FR-light treatments. Then secondly, by using the AMT array to identify novel FR-light regulated transporter genes. A selection of candidate genes will then be chosen for further characterisation of the FR-light regulation response.

3.2 Results

3.2.1 Identification of light-regulated transporter genes by data mining of published microarray experiments

A bioinformatical analysis process was undertaken on a selection of previously published microarray datasets in the attempt to identify putative FR-light regulated transporter genes. A data mining process was completed using a list of genes encoding all known and putative transmembrane-spanning proteins. The list was made available and published in Maathius *et al.* (2003). A number of microarray datasets were searched with this list of genes and those showing light-regulation were identified. These genes were categorised into a number of families according to the function of the protein (Maathius *et al.*, 2003), as shown in Figure 3.1. This process was undertaken with four datasets: Wang *et al.* (2002), Devlin *et al.* (2003), Tepperman *et al.* (2001) and Tepperman *et al.* (2004). The first three examine FR-light regulation, whereas the latter studied R-light regulation. The experimental design for each of the studies varies and this will be discussed later in the results section. However details of the microarray chip used, the number of genes included on the chip and the cut-off fold to identify light-regulated genes in each experiment will be discussed in turn. The work undertaken by Wang *et al.*, (2002) was conducted using a chip containing 9126 EST clones representing 6126 unique genes, approximately one quarter of the *Arabidopsis* genome. Results were analysed using the Genepix image analysis software using a cut-off point of 1.5-fold. In contrast the work compiled by Tepperman *et al.*, (2001, 2004) uses an oligonucleotides array (Affymetrix) containing probes set for approximately 8200 different *Arabidopsis* genes and identifies light-regulated genes using a two-fold cut-off. The arrays conducted by Devlin *et al.*, (2003) also uses the Affymetric array using a cut-off of 1.5-fold. A summary of the genes identified as being light-regulated is shown in Table 3.1, indicating the number of genes both up and down-regulated in each membrane protein family for each microarray study. The number of genes in each family is shown in brackets in Table 3.1. Of the 1153 genes searched, 69% of the genes have been assigned a known or putative function as a transporter, channel or pump. The function of the other proteins encoded by the remaining 31% of genes is unknown, but these proteins have been predicted to have at least six transmembrane spanning domains (Maathius *et al.*, 2003).

Table 3.1 Summary of light-regulated transporter genes. Transporter genes that are up or down-regulated by light identified from previously published microarray datasets. Genes have been classified into multiple transporter families to identify possible expression patterns between families. The datasets used are Wang *et al.* 2002, Devlin *et al.* 2003, Tepperman *et al.* 2001 and Tepperman *et al.* 2004. The number of genes classified into each transport family is shown in brackets.

	Wang 2002		Devlin 2003		Tepperman 2001		Tepperman 2004		
Transporter Family	Up	Down	Up	Down	Up	Down	Up	Down	Total
(364) Unknown function	14	11	1	2	2		13	3	46
(226) ABC transporter	2	6	2	1	4	3	6	1	25
(99) Amino acid transporter	4	1	2	3	1	1	2	2	16
(38) Aquaporins	1	9		1			2	1	14
(59) Sugar transporter	2	3	1	1	1	1	1	2	12
(47) P-type pump	2	3	1		1				7
(17) Phosphate transporter		4			2			1	7
(13) Other Anion	1				1	1	2	1	6
(36) K, Cl, Ca channel			2		1		2		5
(6) Ammonium transporter					2		2		4
(50) Antiporter		1				1	1	1	4
(8) Invertase	1	1					1		3
(12) Auxin transporter	1		1					1	3
(9) Nitrate transporter					1		2		3
(51) Peptide transporter				1	1		1		3
(20) CNGC	1		1						2
(38) Metal transporter		1				1			2
(32) V-type pump		2							2
(3) PPase	1						1		2
(14) Sulphate transporter		1							1
(11) Magnesium transporter									0
Total	30	43	11	9	17	7	36	13	

The analyses revealed that at least one transporter from almost all families are light-regulated with some families being more highly represented than others (Table 3.1). Due to duplication of genes in the datasets the proportion of the total number of genes regulated in each family can not be calculated due to some of the genes showing light-regulation in more than one study. The largest selection of genes is classified as unknown with a total of 45 genes showing light-regulation. Other families of transporters showing light regulation include ABC transporters, aquaporins, sugar, amino acid and phosphate transporters. Seven P-type pumps are also identified as light regulated. However, in contrast fewer metal, sulphate and V-type pumps show light-regulation. The only transporter family not represented are the magnesium transporters. The major limitation with this process is that not all genes are represented on all the arrays. Individual light-regulated genes for some of the families are shown in Table 3.2; each array will in turn be described.

3.2.1.1 Analysis of microarray data; Wang *et al.* (2002)

This array dataset examined FR-light regulated genome expression of phytochrome A pathway mutants. The light-regulated genes were identified from the first of a number of array studies, looking at the expression profiles of four wild-type ecotypes (COL, Ler, No-0 and RLD) of *Arabidopsis*. Wild-type seedlings were grown in white light for one day to induce germination and then transferred to either FR-light (approximately 160 μmol $m^{-2}s^{-1}$) or darkness for 5 days (Wang *et al.*, 2002). Examination of the expression ratios of the genes in the microarray between FR-light versus dark grown wild-type seedlings revealed that FR-light regulates the expression of a large selection of genes in these four ecotypes. Subsequent analysis revealed 30 transporter genes showed a 1.5-fold or greater induction in gene expression and 43 genes showed a 1.5-fold or greater repression in gene expression in at least two ecotypes in the FR-light grown seedlings compared to the dark grown control seedlings (Table 3.1). Genes from a broad subset of transporters are represented. FR-light induced transporters include two sugar transporters *STP1* and *AZT1*, two amino acid transporters *AAP2* and *AAP5*, two calcium ATPases, *ACA2* and *ACA4* and the auxin transporter *PIN4* (Table 3.2). Genes repressed by FR-light include four phosphate transporters, the amino acid transporter *CAT4*, the proton pump *AHA2* and two sugar transporters *STP13* and *SUGTL12* (Table 3.2).

Table 3.2 Summary of some of the main light-regulated transporter genes. Light up and down-regulated transporter genes have been identified from previously published microarray datasets, showing specific genes from eight transporter families. Light up-regulated genes are shown in bold and down-regulated genes not. Only named genes of known function are shown.

Type of Transporter	Wang 2002	Devlin 2003	Tepperman 2001	Tepperman 2004
ABC Transporter	***WBC2, ATH13*** *PDR7, WBC11 WBC12, MDR1 MDR4, ATH13*	***WBC3, WBC5*** *MRP2*	***ABC1, ATH8, PMP1*** *MDR4, WBC1*	***PMP1, MRP2, MRP4, ABC1,*** *ATH8*
Sugar Transporter	***STP1, AZT1,*** *STP13, SUGTL2*	***ERD6*** *AZT1*	***SUC1*** *PLT6*	***SUC1*** *STP1, STP14*
Amino acid Transporter	***AAP5, AAP2,*** *CAT4*	***AAP6***		***ANT1*** *AAP2, AAP4*
P-type pump	***ACA2, ACA4*** *AHA2, RAN1, ACA12*	***ECA2***	***HMA4***	
Phosphate transporter	*PTR22, PTR26 PTR36, PTR44*		*PHT2.1*	*PHT1*
Auxin Transporter	***PIN4***	***PIN7***		*PIN2*
Ammonium Transporter			***AMT1-2*** *AMT1-3*	***AMT1-2***
Invertase	***FRUCT8*** *FRUCT3*			***FRUCT1***

3.2.1.2 Analysis of microarray data; Devlin *et al.* (2003)

The second array dataset examines a different aspect of light regulation; a genomic analysis of the shade avoidance response to identify light regulated genes. A number of phytochrome mutant seedlings, namely *phyB* and the *phyA phyB* double mutant, alongside the wild-type were exposed to artificial shading conditions over time to identify genes as shade responsive. Seedlings were grown in the dark for three days and then transferred to white light for seven days. Seedlings were then either left in these conditions or transferred to white light supplemented with FR-light for either 1 or 24 hours to mimic the shading response. Genes were characterised into groups with expression patterns corresponding to one of various physiological response modes. These responses are complex and for the simplicity of the identification of light-regulated transporter genes, the genes showing regulation are characterised into shade responsive up and down-regulated only. With 11 and 9 genes showing shade responsive up and down-regulation respectively (Table 3.1). Up-regulated genes include two ABC transporters *WBC3* and *WBC5*, the amino acid transporter *AAP6*, the calcium ATPase *ECA2* and the auxin transporter *PIN7* (Table 3.2). The ABC transporter *MRP2* and the sugar transporter *AZT1* are examples of down-regulated genes.

3.2.1.3 Analysis of microarray data; Tepperman *et al.* (2001)

In this study Tepperman *et al.* (2001) examined the affect of FR-light on the expression profiles during de-etiolation of both wild-type and the *phyA* null-mutant, indicating 10% of the genes on the array were regulated by phyA in response to continuous FR-illumination. Seedlings were exposed to white-light for two hours and then grown in the dark for 4 days. The seedlings were then transferred to continuous FR-light for between 1 and 24 hours. Analysis revealed 25 candidate transporters genes, with 17 showing an induction and 8 genes showing a repression in gene expression of 2-fold or greater during seedling de-etiolation in response to FR-light (Table 3.1). These genes were also grouped according to the time of their response (grouping not shown). Genes which responded within one hour were termed early response genes and late response genes if the response occurred between 3 to 24 hours of FR-light exposure. Seventeen genes including four ABC transporters, two phosphate transporters and the sucrose transporter *SUC1* are induced by

FR-light (Table 3.2). Eight genes showed a down-regulation by FR-light, these included 3 ABC transporters and the heavy metal transporter *AtHMA4* (Table 3.2).

3.2.1.4 Analysis of microarray data; Tepperman *et al.* (2004)

In contrast to the other three microarray datasets this array profiles the phyB mutant, demonstrating a contribution of other phytochromes other than phyB to red-light regulated gene expression during de-etiolation. This had provided an insight into the transporter genes which are regulated by red light. The same experimental design was applied as with the FR-light array undertaken by the same research group with the exception of the seedling were transferred to red-light rather than FR-light. On the array 49 genes encoding transporter genes were shown to be regulated by red-light, with 36 and 13 being induced and repressed respectively (Table 3.1). Examples of red-light induced transporters include 4 ABC transporters and the amino acid transporter *ANT1*. The two sugar transporter *STP1* and *STP14*, the amino acid transporters *AAP2* and *AAP4* and the auxin transporter *PIN2* are examples of red-light repressed genes (Table 3.2). The sucrose transporter *SUC1* and the ammonium transporter *AMT1.2* are induced by both red and FR-light (Table 3.2).

3.2.2 The *Arabidopsis* Membrane Transporter (AMT) array

Analysis of microarray data had provided an insight into genes regulated by far-red and red light. The major limitation with this approach is that full genome chips were not used in any of the studies as they were not available at the time. Therefore only a selection of the transporter genes, (around 15-20%) were present on the array depending on the array used. So to achieve a more global insight into the light regulation of transporter genes the AMT array was used to further identity novel FR-light regulated genes. Whilst following the AMT microarray methodology (Maathius *et al.*, 2003) as shown in section 2.10 many complications arose, so modifications were made and are outlined below.

3.2.2.1 RNA quality and cDNA dye incorporation

Total RNA was extracted from two-and-a-half day old etiolated seedlings and two-day-old etiolated seedlings exposed to a 12 hour FR-light treatment using the

phenol:chloroform extraction protocol. The total RNA was purified and quantified and 100 μg of each total RNA sample was used to synthesize labelled cDNA. RNA extracted from etiolated (control) seedlings was labelled with Cy3 and RNA from FR-light exposed (treatment) seedlings was labelled with the Cy5 dye. The initial cDNA synthesis using RNA extracted from seedlings using the phenol:chloroform extraction methods led to insufficient dye incorporation for hybridisation and was therefore abandoned (Table 3.3). This led to the hypothesis that the RNA samples were not sufficiency pure enough and contaminates could potentially inhibit the incorporation of the fluorescent dyes. For sufficient hybridisation there must be at least a final cDNA amount of 0.5 μg and a dye incorporation of 10 pmol of dye per μg of cDNA. Only 0.5 μg of cDNA is required from the 100 μg of the total RNA as only 1-3% of the RNA is mRNA. The original cDNA synthesis did not meet either of these criteria. The removal of contaminates was shown to improve the quantity of cDNA but not dye incorporation (Table 3.3). One contaminant expected was DNA as the LiCl step may not be 100% efficient at removing DNA so some may be present, so samples were treated with DNase. Subsequently this increased the cDNA synthesis yield but in turn lowered the dye incorporation. Spectrometric analysis revealed high polysaccharide contamination and this was subsequently removed using a butoxyethanol precipitation. Nucleotides absorb at an optimal wavelength of 260 nm, whereas polysaccharides absorb at 230 nm. The 260/230 ratio is used to calculate the level of contaminating polysaccharide. The butoxyethanol precipitation improved both the 260/230 ratio and the purity of the total RNA dramatically, which in turn increased the cDNA yield to 0.3654 and 0.4818 μg for the etiolated and far-red samples respectively. The removal of polysaccharide on DNAse treated RNA using butoxyethanol increased the cDNA by approximately 3-fold compared to untreated RNA in both samples, however the dye incorporation is less than half compared to the untreated sample. The amount of dye incorporated per μg of cDNA was increased, although not to the same extent as untreated RNA when the original starting amount of RNA was halved from 100 μg to 50 μg of total RNA. The two individual cDNA samples of the same treatment were combined to a make a total of 100 μg starting RNA. These changes to the protocol RNA increased the amount of cDNA to sufficient levels; however the level of dye incorporation for hybridisation was still too low. Despite this the samples were used and hybridisation was successful.

Table 3.3 The effect of the removal of contaminants from RNA samples on cDNA synthesis and dye incorporation. The removal of DNA and polysaccharide from the RNA samples affects the levels of cDNA synthesis, the purity of the samples and the level of dye incorporation. The purities of the samples in terms of sugar and proteins for both the Cy3 and Cy5 samples are shown.

Treatment	cDNA synthesis (μg)		Sample purity		Dye incorporation (pmol dye/μg cDNA)	
	Control Cy3	Treatment Cy5	Sugars (260/230)	Proteins (260/280)	Control Cy3	Treatment Cy5
Phenol/chloroform extraction protocol	0.1287	0.1650	(Cy3) 1.63 (Cy5) 1.69	(Cy3) 1.54 (Cy5) 1.43	12.95	7.27
RNA treated with DNase to remove DNA	0.2353	0.2657	(Cy3) 1.54 (Cy5) 1.75	(Cy3) 1.63 (Cy5) 1.68	4.23	5.27
RNA treated with butoxyethanol to remove polysaccharides	0.3465	0.4818	(Cy3) 1.97 (Cy5) 2.06	(Cy3) 1.71 (Cy5) 1.93	5.77	4.28
All treatments above using 50μg of RNA	0.2386 0.3185	0.2056 0.2271	(Cy3) 1.94 (Cy5) 1.90	(Cy3) 1.86 (Cy5) 1.94	7.22 6.14	5.68 5.72

3.2.2.2 Identification of novel FR-light regulated transporter genes

Upon cDNA hybridisation using the RNA samples which were treated to remove DNA and polysaccharide contamination, the AMT array chip was scanned at high resolution. The initial scan from the first successful hybridisation revealed smearing of excess fluorescent dyes on the array surface particularly down the two sides and the middle to the chip. Subsequent additional salt washes using diluted SSC washes resulted in some improvement to the sharpness of the fluorescence reading but this also caused a re-allocation of the dyes. Different salt concentration washes were used but the best result was achieved using a 0.1 x SSC wash leaving the right hand side of the chip smear free (Figure 3.3). The rest of the array even after these washes to improve the chip quality was unusable, so a true representation of transporter genes expression could not be made. Only 50% of the array was usable for interpretation.

Upon scanning of the array a grid was created which was used to circle each spot individually using the software package to produce a comprehensive dataset containing the spot position, spot intensity, and the spot background for each of the spots. The array contained replicate spots for each gene of the same oligo with the exception of the ABC transporters genes which were represented by 3 oligos (Maathius *et al.*, 2003). As the chips showed excessive fluorescence over significant areas of the array due to the incomplete washing of the array, the first process was the elimination of all genes where the signal ratio of the gene was affected by the background signal as these spots were termed as unreliable. The scans show the unsuccessful removal via washing of the Cy5 dye, so this process eliminates all these genes leaving just the genes unaffected by the excess dye. The remaining spots were then analysed to determine FR-light regulated genes using a 1.5-fold cut-off.

The scan revealed 15 novel FR-light regulated transporter genes with 8 up-regulated genes and 7 down-regulated genes (Figure 3.4). Two ABC transporters *ATM1* and *MDR17* were among the genes showing the largest induction by FR-light, however a third ABC transporter *AMT1-3* also showed an up-regulation. The calcium-H^+ antiporter *CAX1*, the cation H^+ antiporter *CHX9* and two genes of unknown function, At5g03080 and At1g30360, also show an induction in FR-light. A number of transporter genes were shown

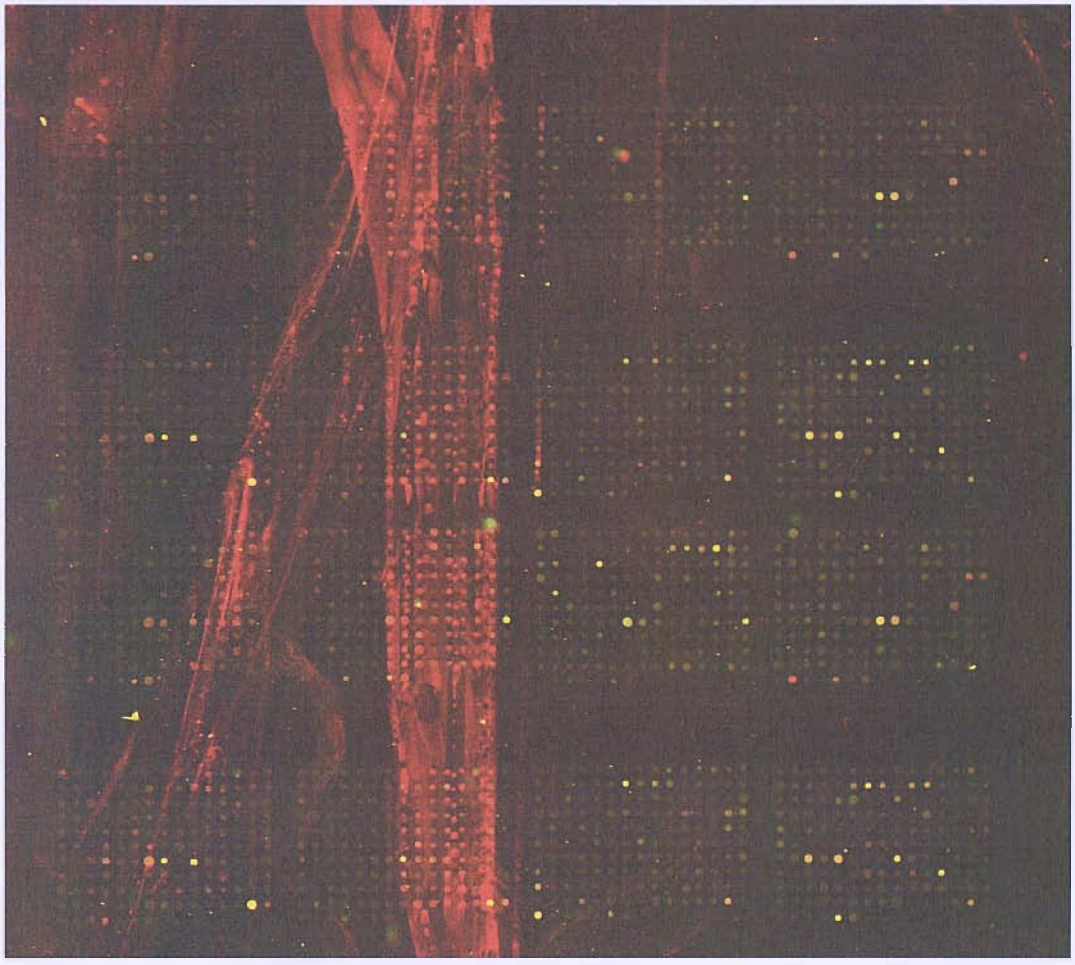

Figure 3.3 Scan of the microarray post hybridisation with the labelled cDNA, following the 0.01 x SSC wash. 100 µg of total RNA from etiolated (Cy3 red dye) and far-red light (Cy5 green dye) treated *Arabidopsis* seedlings was isolated and cDNA and labelled. The labelled cDNAs were hybridised to the array and visualised. Bar = 1mm.

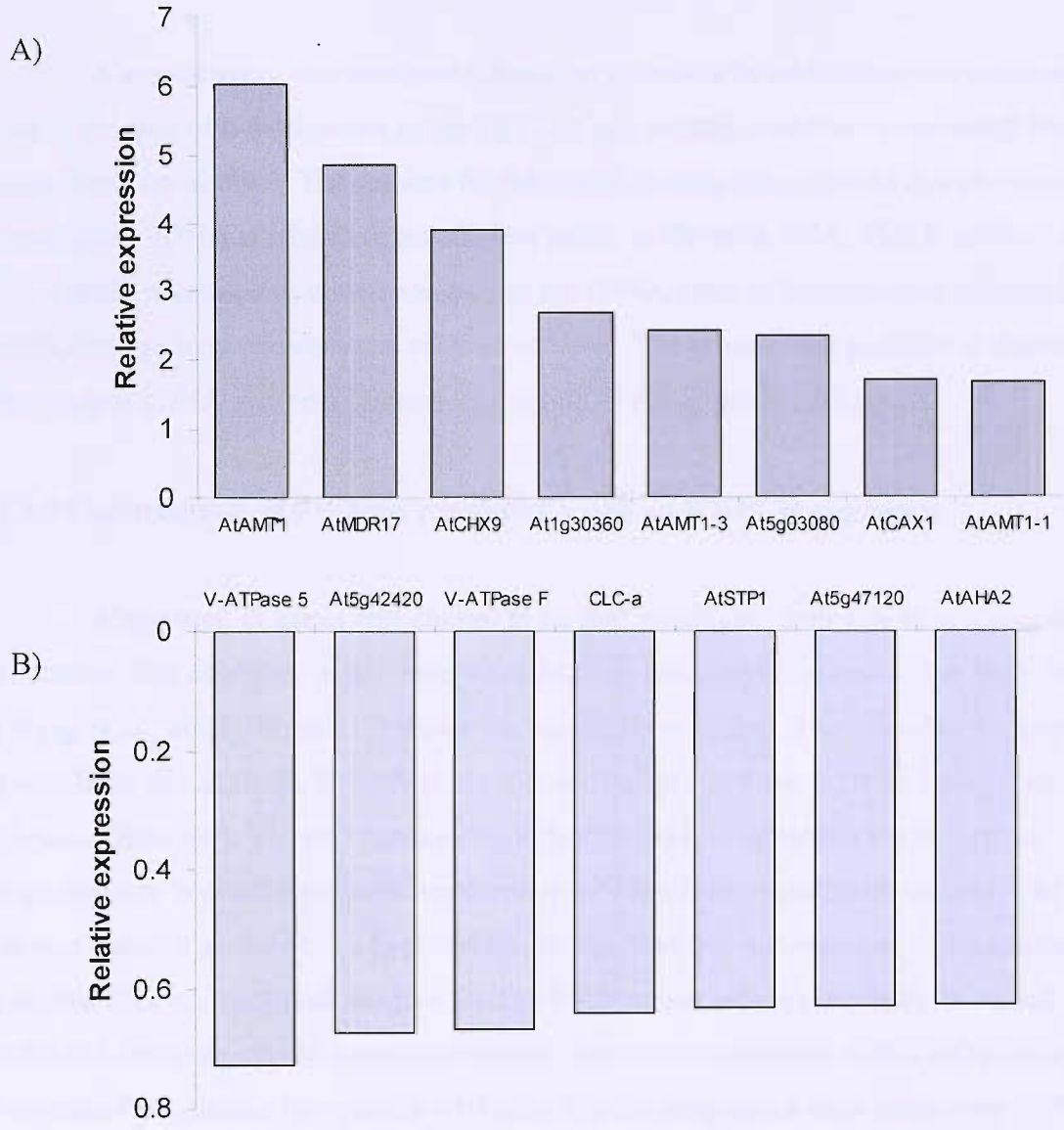

Figure 3.4 Relative expression of transporters identified using the AMT array. Transcriptional response of *Arabidopsis* transporters in response to FR-light using the AMT array. Due to the smearing of the fluorescent dyes on the chip, the array was washed sequentially with a 0.1 x SSC dilution. The relative expression ratios of genes which show at least a 1.5-fold induction (A) or repression (B) are shown.

to be FR-light down-regulated, including two V-type ATPase subunits, two genes of unknown function, the proton ATPase *AHA2*, the chloride channel *CLC-a* and the monosoaccharide transporter *STP1*.

A second array was performed, however complete hybridisation was unsuccessful due to the lack of hybridisation of the Cy3 dye and no data could be extrapolated from this chip (array not shown). The reasons for this could include unsuccessful dye incorporation, insufficient cDNA synthesis or insufficient purity of the total RNA. This is unlikely as the UV-visible spectrophotometric analysis of the cDNA prior to hybridisation indicated sufficient dye incorporation and cDNA synthesis. The cause of the problem is therefore due to post cDNA synthesis procedures including the actual hybridisation.

3.2.3 Confirmation of FR-light regulation using an RT-PCR approach

A selection of genes was chosen to further investigate their role in seedling de-etiolation. The candidate genes were selected from the analysis of one of the array datasets (Wang *et al.*, 2002). Figure 3.5 shows the top ten most up and down-regulated transporter genes from this analysis. From here six induced genes and three repressed genes were chosen. These were chosen because they either showed the greatest change in gene expression or because they were representative of families of particular interest. The chosen induced genes were a hypothetical protein that was annotated as being similar to a putative G-protein coupled receptor (At1g64990) which will subsequently be called *FRIMP1*, the anthocyanin transporter *ANM2*, the auxin transporter *PIN4* (At2g01420), a Niemann Pick disease like protein (At1g42470), the monosaccharide transporter *STP1* and the calcium transporting ATPase *ACA2*. The chosen repressed genes were the proton translocating ATPase *AHA2*, the ATP dependent copper transporter *RAN1*, and the amino acid transporter *CAT4*.

3.2.3.1 Phenotypic analysis of etiolated and FR-light grown seedlings

A series of RT-PCR experiments were set up to confirm the FR-light regulation using the design shown in section 2.1.2. The seedlings used in this particular study were grown in complete darkness for 48 hours, followed by either a 12 hour exposure to FR-

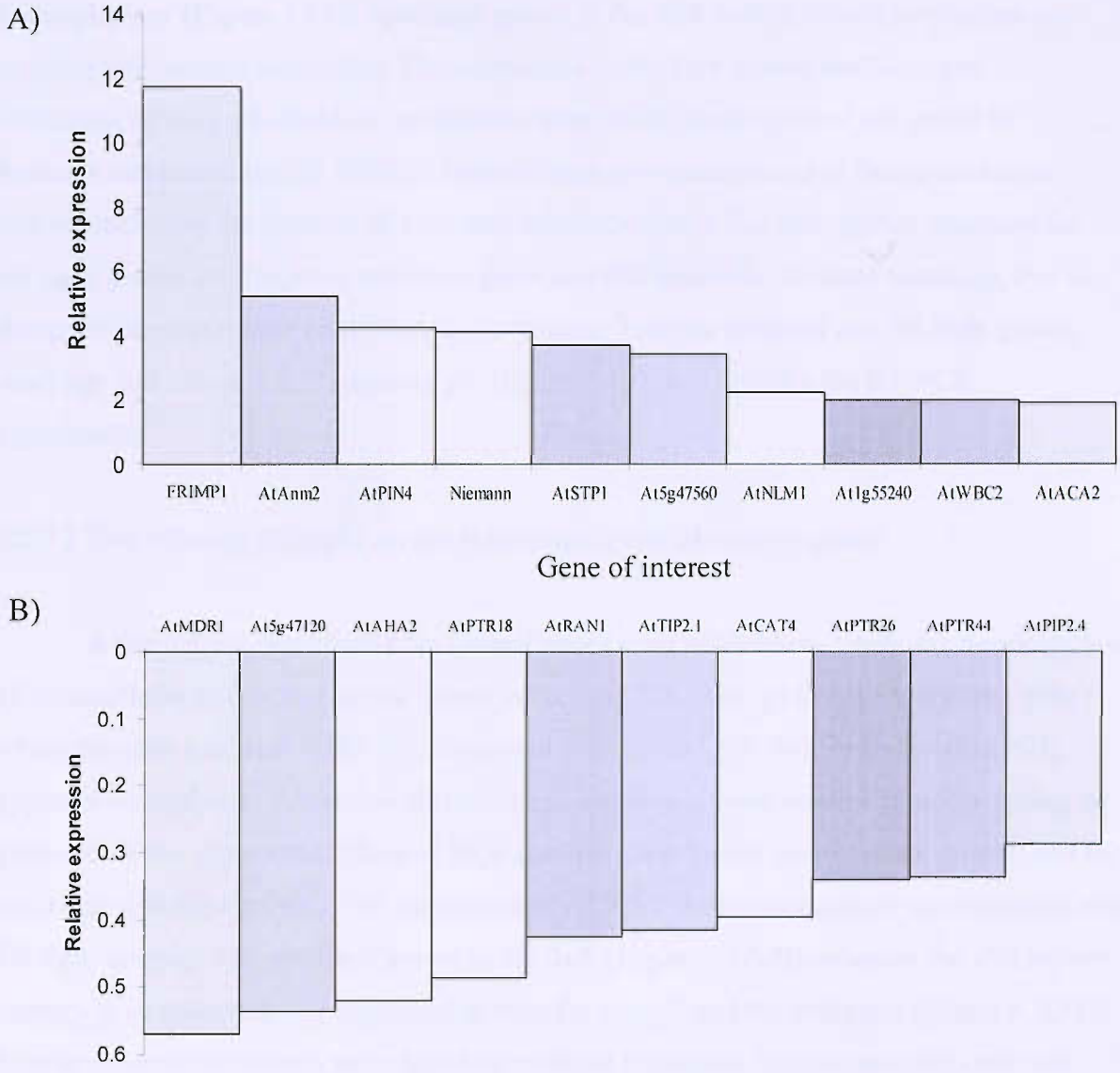

Figure 3.5 Relative expression of putative FR-light up and down-regulated transporter genes, taken from published microarray data, (Wang *et al.*, 2002). Transporter genes which showed an average of 1.5-fold or greater change in relative expression of the four selected wild-type ecotypes, A) up-regulated genes and B) down-regulated genes.

light or remained in darkness for the same period. After just a 12 hour exposure to FR-light the morphologies of both the etiolated seedling and the FR-light grown seedlings are not too dissimilar, as the exposure duration is not significant enough to show dramatic changes in morphology (Figure 3.6A). Seedlings grown in the dark exhibit closed cotyledons and maximum hypocotyl elongation. The cotyledons of the dark-grown seedlings are colourless, as they are unable to synthesize chlorophyll. Seedlings that are grown in darkness and transferred to FR-light begin to undergo some aspects of the de-etiolation process including the opening of their cotyledons, however like dark-grown seedlings the FR-light grown seedlings are unable to green and still resemble etiolated seedlings. For the design of the experiment total RNA was extracted from the etiolated and FR-light grown seedlings and run on a 1.3% agarose gel (Figure 3.6B) and used for the RT-PCR experiments.

3.2.3.2 The effect of FR-light on the transcript levels of control genes

A limited number of putative control genes were available to verify the transcript levels of the candidate transporter genes. These include *ACTIN2* (At5g18380) and the *40S* gene which encodes a subunit of the S16 ribosomal protein (At3g18780). A multi-cycle PCR approach was taken to determine the relative expression of these control genes by taking the gradients of the exponential phase of PCR amplification for the control (dark grown) and the treatment (FR-light grown). The expression of *ACTIN2* shows an apparent up-regulation under FR-light compared to seedlings grown in the dark (Figure 3.7A-B), whereas the *40S* subunit appears to be constitutively expressed in both the control and the treatment (Figure 3.7C-D). Similar expression patterns were found on multiple biological replications with only one shown here. This indicates that *40S* is the preferred choice as a control gene over *ACTIN2* (Table 3.4) and will be used in subsequent control genes in later chapters.

3.2.3.3 The effect of FR-light on the transcript levels of transporter genes

Six up-regulated and three down-regulated genes were selected for further investigation of the microarray analyses. The FR-light regulation has been confirmed using an identical multi-cycle RT-PCR approach to that used to calculate the relative expression of the putative control genes. The monosaccharide transporter *STP1* and the *FRIMP1* gene

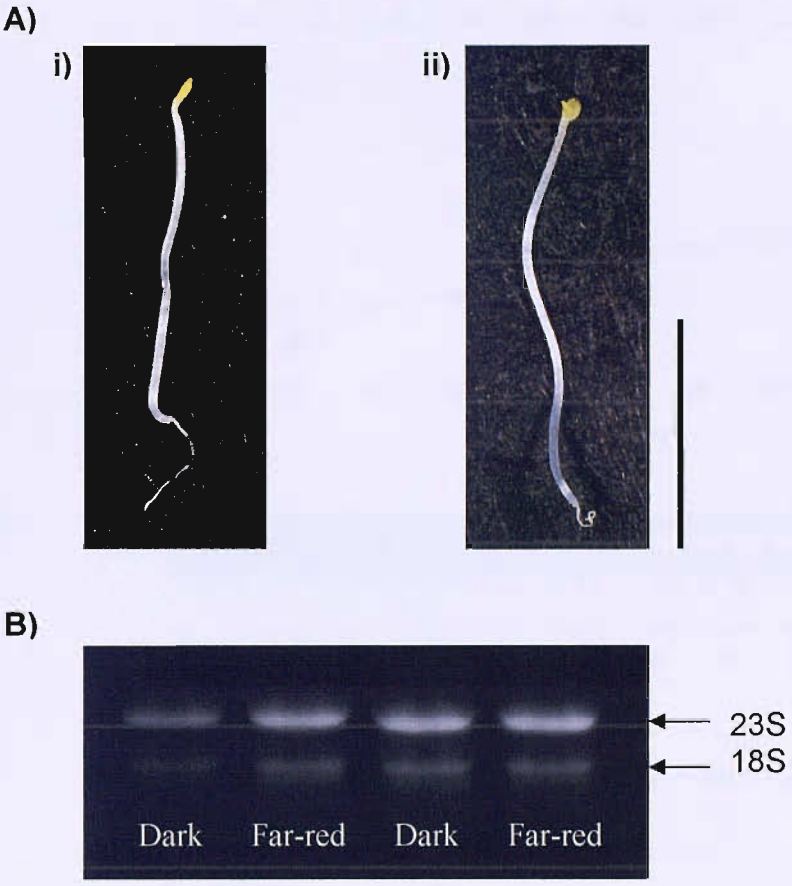

Figure 3.6 Seedling morphology under different light treatments in *Arabidopsis* and total RNA extracted from these seedlings. A) Phenotypic differences of wild-type seedlings as a consequence of the light environment. Seedlings were stratified for 48 h at 4°C then placed under white light to induce germination. All seedlings were transferred to complete darkness for 48 h, then either continued in darkness (i), or were transferred to the FR-light (ii) for 12 h. Bar = 5 mm. B) Agarose gel or total RNA extracted from wild-type (Col-0) grown in darkness of FR-light following the growth conditions above.

A) *ACTIN2*

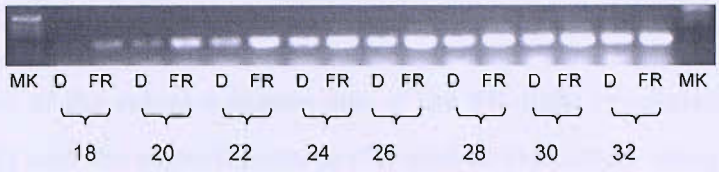

B)

C) *40S*

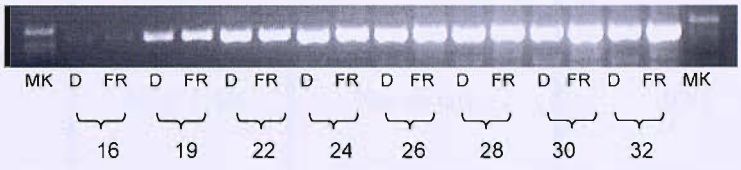

D)

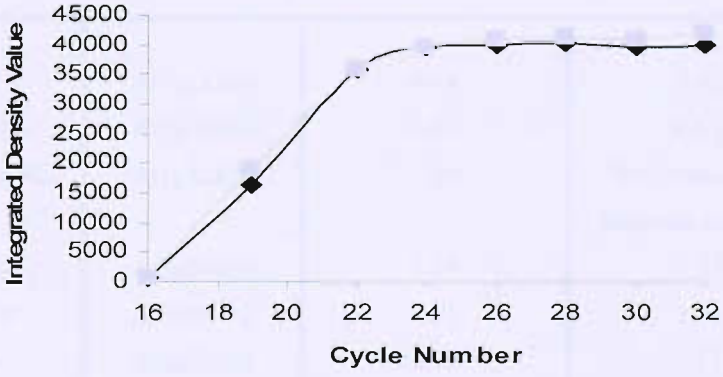

Figure 3.7 Expression of *ACTIN2* and *40S*, two putative constitutively expressed control genes in etiolated and FR-light grown seedlings. Multi-cycle RT-PCR and integrated density values (IDVs) were used to determine transcript levels of two putative control genes in etiolated (♦) and FR-light illuminated ( ) seedlings. A) Multi-cycle RT-PCR analysis of *ACTIN2*. B) IDVs of *ACTIN2* multi-cycle RT-PCR analysis. C) Multi-cycle RT-PCR analysis of *40S*, a subunit of the S16 ribosome. D) IDVs of *40S*. An annealing temperature of 60°C was used for both primer pairs, (MK represents 1Kb DNA ladder marker). IDVs shown are the mean of two biological repetitions.

Table 3.4 A comparison of the relative expression of the FR-light regulated genes from Wang *et al.* (2002) and the experiments performed in this study using RT-PCR. The relative expression ratios of the control genes and the candidate FR-light regulated genes. A comparison is made of the relative expression ratios of the original microarray data (Wang *et al.*, 2002) and the relative expression verification of the RT-PCR using the multi-cycle approach. Both expression studies used the Col-0 wild-type. The final relative expression is the mean of two biological samples.

Gene	Gene	MATDB code	Relative expression (Wang et al., 2002)	Relative expression (RT-PCR)
Control genes	*ACTIN2*	At5g18380	Not on array	2.03
	40S	At3g18780	Not on array	0.92
FR-light up-regulated genes	*STP1*	At1g11260	5.28	2.82
	FRIMP1	At1g64990	6.45	6.01
	Niemann Pick	At1g42470	7.30	Not expressed in etiolated seedlings
	PIN4	At2g01420	3.19	1.62
	ANM2	At3g59320	6.25	3.97
	ACA2	At4g57640	2.12	1.71
FR-light down-regulated genes	*CAT4*	At5g04770	0.464	1.18
	AHA2	At4g30190	0.613	0.53
	RAN1	At5g44790	0.664	0.900

(At1g64990) both showed a marked up-regulation in FR-light grown seedlings compared to etiolated seedlings (Figure 3.8). This is also true for *ACA2*, a calcium ATPase (Figure 3.10A), as does the auxin transporter *PIN4* (Figure 3.9B). Although expressed in the dark on the array, the Niemann Pick C disease-like protein (At1g42470) was not expressed in etiolated seedlings using RT-PCR but shows a marked up-regulation in FR-illuminated seedlings (Figure 3.9A). The anthocyanin transporter *ANM2* shows a very weak expression in etiolated seedlings. However, the transcript levels are up-regulated in seedlings grown in FR-light (Figure 3.9C). This multi-cycle PCR approach has indicated that all six transporters are up-regulated after just 12 hours of FR-light illumination.

Of the three FR-light down-regulated transporter genes from the array, only one gene showed the appropriate down-regulation. The ATP-dependent copper transporter *RAN1* showed no significant down-regulation (Figure 3.10C), whereas the amino acid transporter *CAT4* showed an up-regulation in FR-light (Figure 3.11A). However, the proton pump *AHA2* showed a down-regulation in FR-light (Figure 3.11C). All graphs show the average of the change in expression in two biological samples, with the gel representing one biological sample. A comparison of the relative expression obtained using the RT-PCR approach was made to the relative expression from the original microarray data (Table 3.4). Overall this shows that seven of the transporter genes show the same change in FR-light expression in both methods, with *CAT4* and *RAN1* being the exceptions. As the majority of genes showed the expected expression profile it is an indication that the original microarray data is reliable and more importantly these genes are indeed regulated by FR-light.

3.2.4 Further analysis of FR-light regulated transporters identified by microarray experiments

To date few software applications have been developed to query large microarray gene expression databases. The development of the GENEVESTIGATOR program has integrated multiple array databases, to enable data mining experiments to study expression profiles of particular genes of interest during selected growth stages, stresses or in particular organs (Zimmermann *et al.*, 2004). The database and analysis toolbox is available as a scientific resource at https://www.genevestigator.ethz.ch. The nine selected

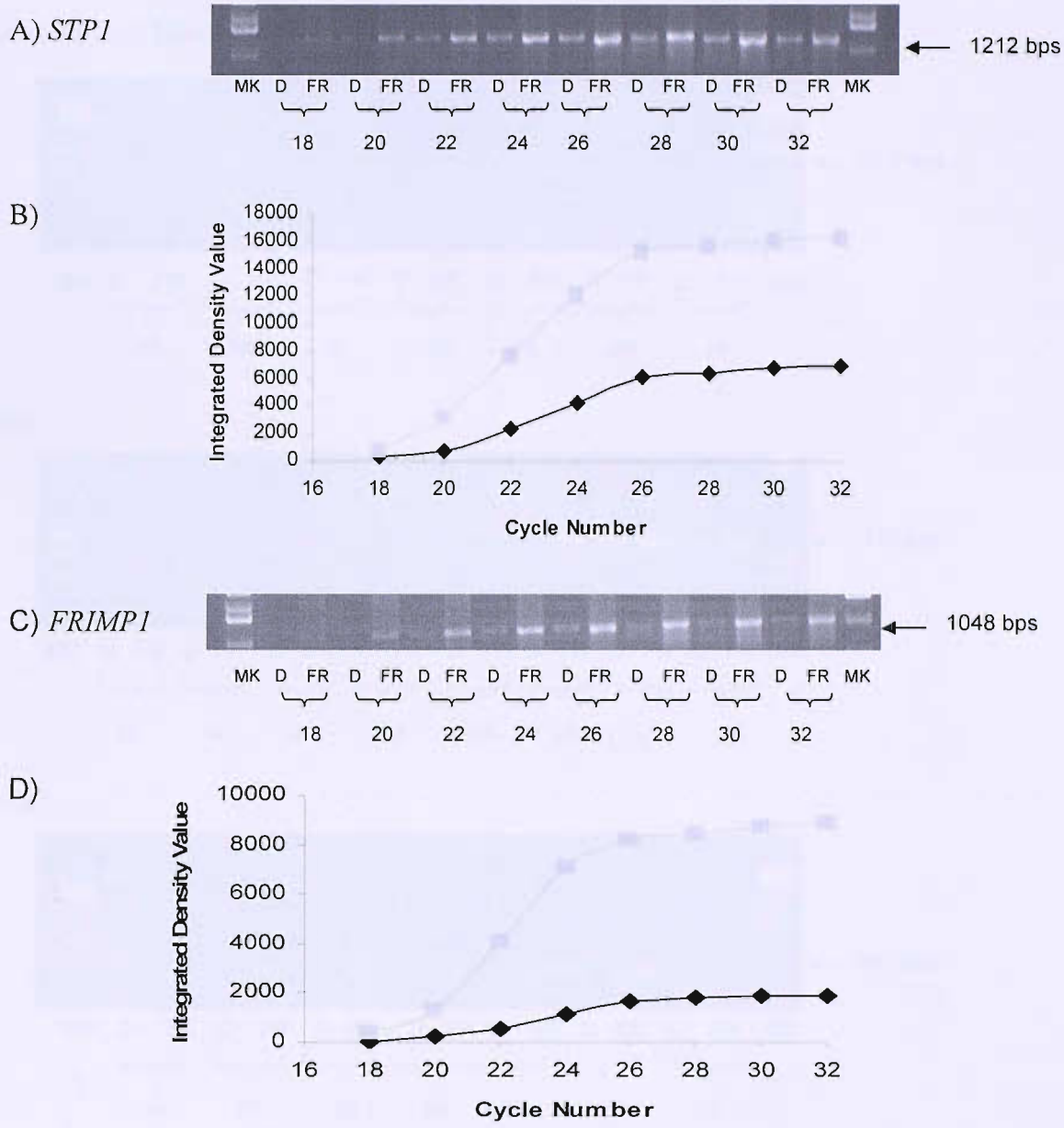

Figure 3.8 Expression of *STP1* and *FRIMP1*, two candidate FR-light induced genes in etiolated and FR-light grown seedlings. Multi-cycle RT-PCR and integrated density values (IDVs) were used to determine transcript levels of up-regulated transporter genes in etiolated (♦) and FR-light illuminated ( ) seedlings. A) Multi-cycle RT-PCR analysis of *STP1* using an annealing temperature of 60°C. B) IDVs of *STP1* multi-cycle RT-PCR analysis. C) Multi-cycle RT-PCR analysis of *FRIMP1* using an annealing temperature of 63°C. D) IDVs of *FRIMP1*. (MK represents 1Kb DNA ladder marker). IDVs shown are the mean of two biological repetitions.

A) Niemann Pick Disease-like Protein

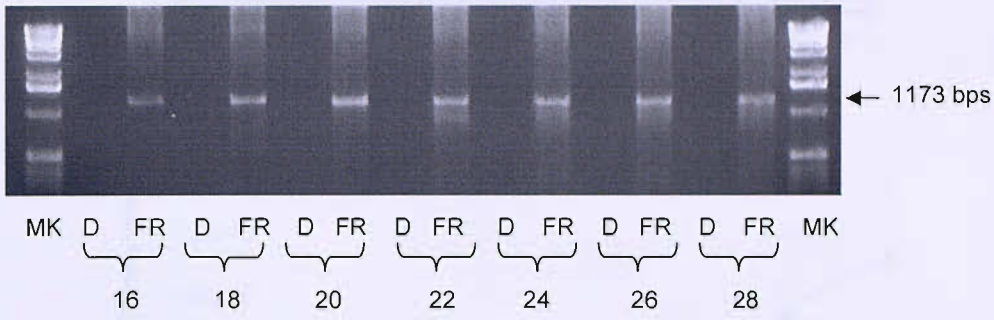

B) *PIN4*

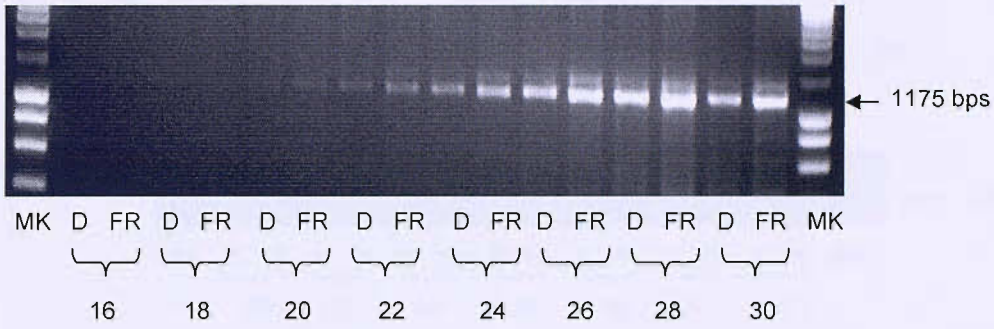

C) *ANM2*

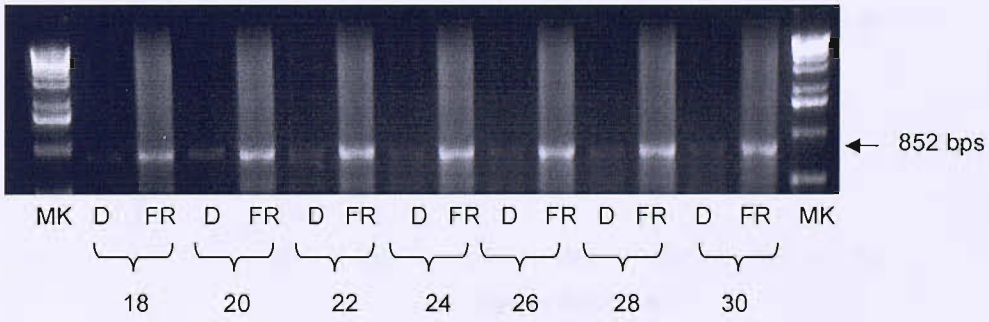

Figure 3.9 Expression of three candidate FR-light induced genes in etiolated and FR-light grown seedlings. Multicycle RT-PCR and integrated density values (not shown) were used to determine transcript levels of three FR-light up-regulated transporter genes in etiolated and FR-light illuminated seedlings. A) The Niemann Pick C disease like protein using an annealing temperature of 58°C, B) the auxin transporter *PIN4* using an annealing temperature of 60°C and C) the anthocyanin transporter *ANM2* using an annealing temperature of 61°C. MK represents a 1Kb DNA ladder marker.

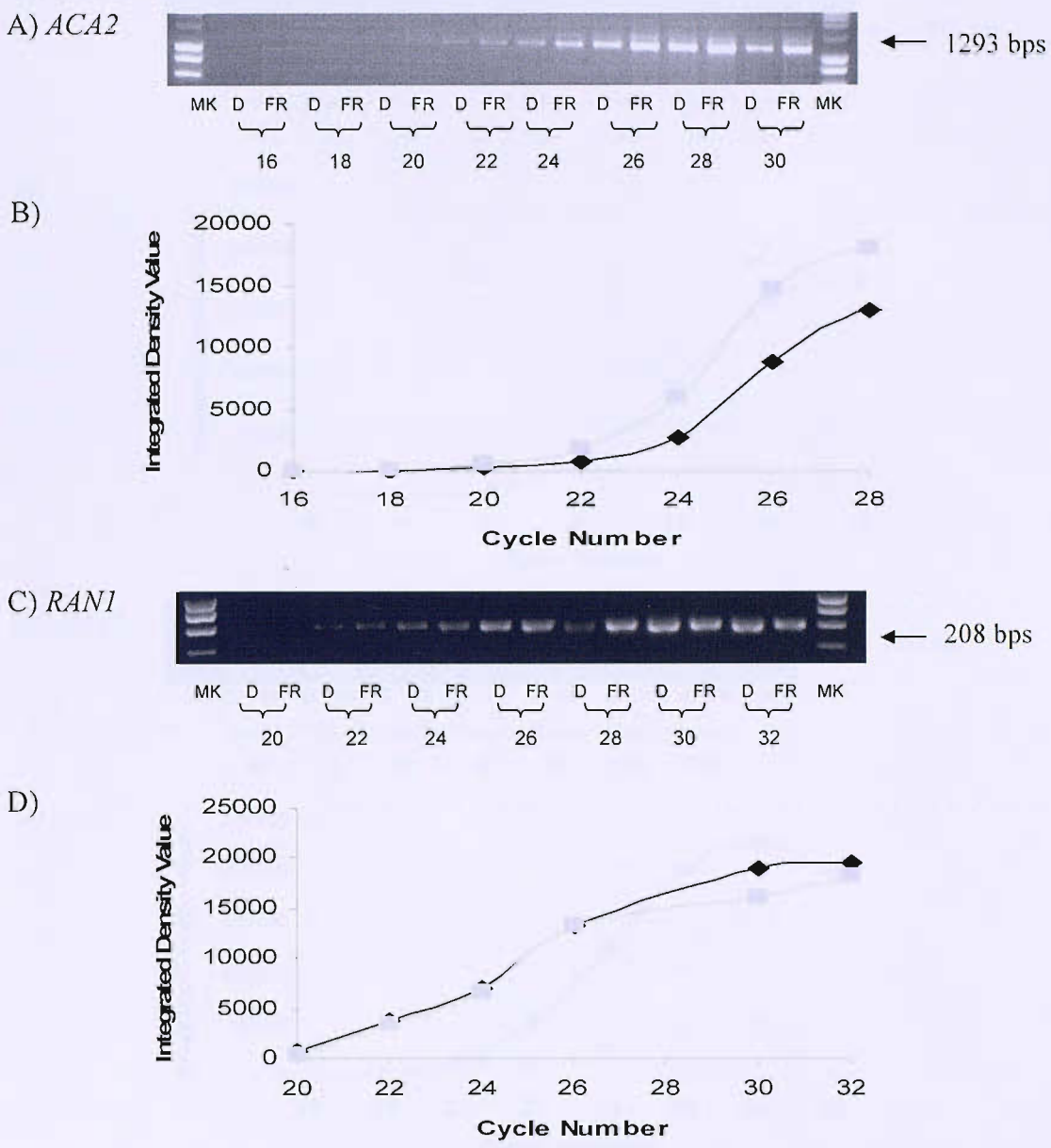

Figure 3.10 Expression of *ACA2* a FR-light induced gene and *RAN1* a FR-light repressed gene in etiolated and FR-light grown seedlings. Multi-cycle RT-PCR and integrated density values (IDVs) were used to determine transcript levels FR-light regulated transporter genes in etiolated (♦) and FR-light illuminated ( ) seedlings. A) Multi-cycle RT-PCR analysis of *ACA2* using an annealing temperature of 65°C. B) IDVs of *ACA2* multi-cycle RT-PCR analysis. C) Multi-cycle RT-PCR analysis of *RAN1* using an annealing temperature of 58°C. D) IDVs of *RAN1*. (MK represents 1Kb DNA ladder marker). IDVs shown are the mean of two biological repetitions.

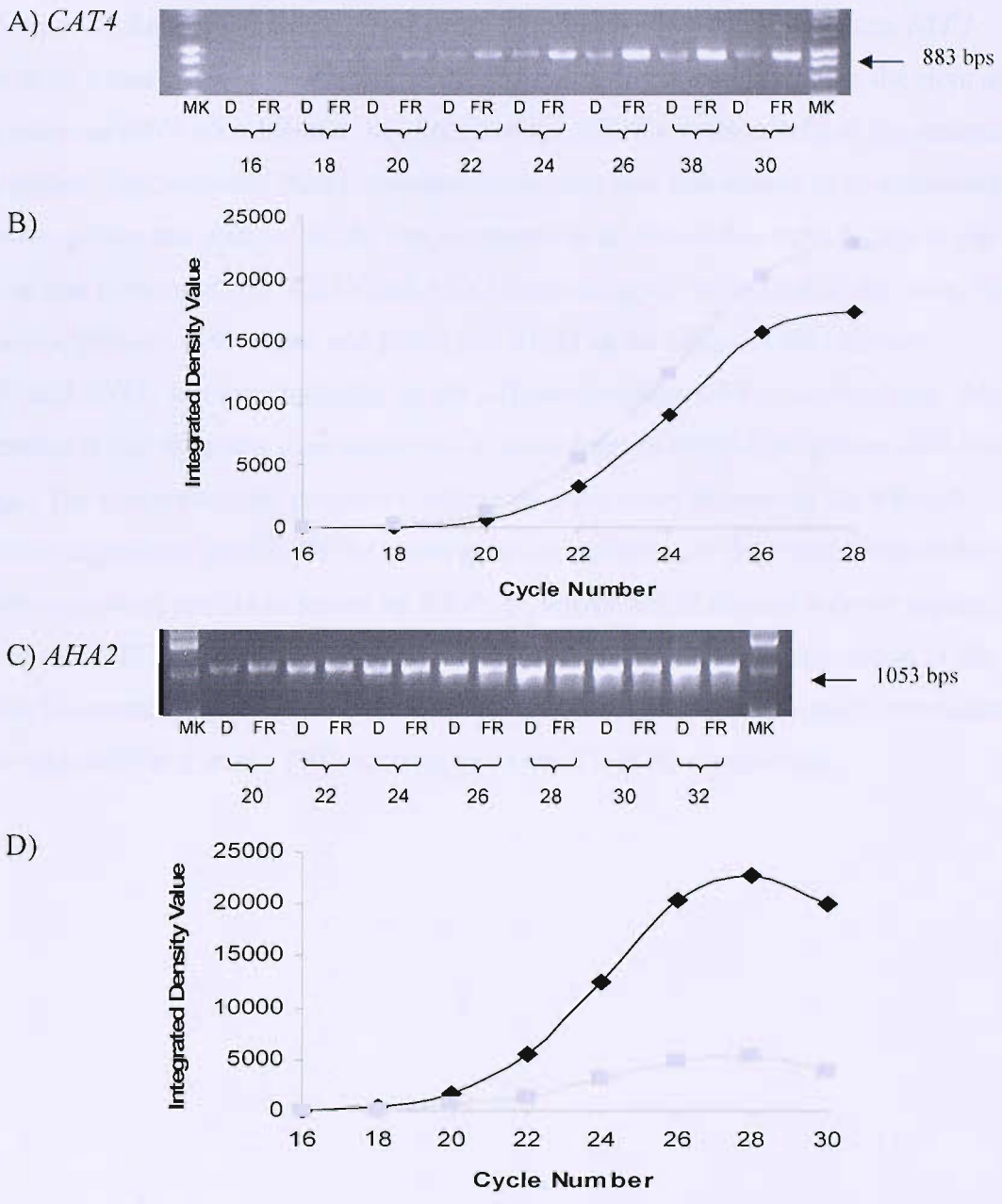

Figure 3.11 Expression of *CAT4* and *AHA2*, two candidate FR-light repressed genes in etiolated and FR-light grown seedlings. Multi-cycle RT-PCR and integrated density values (IDVs) were used to determine transcript levels of down-regulated transporter genes in etiolated (♦) and FR-light illuminated ( ) seedlings. A) Multi-cycle RT-PCR analysis of *CAT4* using an annealing temperature of 63°C. B) IDVs of *CAT4* multi-cycle RT-PCR analysis. C) Multi-cycle RT-PCR analysis of *AHA2* using an annealing temperature of 65°C. D) IDVs of *AHA2*. (MK represents 1Kb DNA ladder marker). IDVs shown are the mean of two biological repetitions.

FR-light light regulated candidate transporter genes were examined using Genevestigator. Table 3.5 shows the tissue distribution of seven of the genes in particular organs. *STP1* appears in all tissue types but was most highly expressed in cotyledons, roots, the stem and rosette, whereas *PIN4* was shown to be expressed specifically in the seedling, the stamen and the pollen. The Niemann Pick C disease-like protein was also shown to be expressed in the flowers, pollen and stamen. *ACA2* was expressed in all tissues but most highly in the roots, leaf and flowers. *RAN1*, *CAT4* and *AHA2* were all highly expressed in the roots, with *RAN1* also expressed in the sepal and petals and *AHA2* in the silique. Unfortunately *FRIMP1* and *ANM2* were not included on the Affymetrix chips used in the database. What is interesting is that all genes were expressed at some level in white-light grown wild-type seedlings. The Genevestigator program contains an array study examining the FR-light light grown expression profile. Of the seven genes examined only three genes shows the predicted expression profile as shown by RT-PCR, where *AHA2* showed a down-regulation and *PIN4* and *CAT4* although originally down-regulated, showed an up-regulation in FR-light. The Genevestigator program therefore does not show a particularly good correlation with the original Wang *et al.*, 2002 microarray or the RT-PCR experiments.

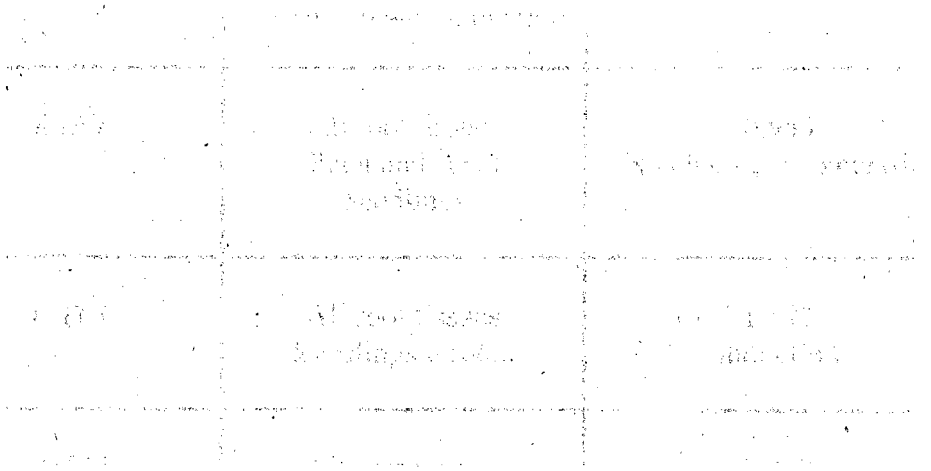

Table 3.5 Tissue localisation and FR-light relative expression profiles for the candidate transporters genes using the Genevestigation Program. The Genevestigator program contains multiple microarray datasets looking at tissue localisation and stress response treatments. Some of the FR-light regulated candidate genes were selected looking at both tissue localisation and the change in relative expression in the FR-light dataset.

Gene	Tissue Localisation	Relative Expression of candidate gene in FR-light
STP1	Stem All root tissues Rosette Seedlings – cotyledons	0.608 repression
Niemann Pick Protein	Flower Stamen and pollen Seedlings	0.733 repression
PIN4	Stamen and pollen Seedlings	2.109 induction
ACA2	All root tissues Leaf Flowers Stamen Seedlings - cotyledon and hypocotyl	0.967 No change in expression
RAN1	All root tissues Petal and sepal Seedlings	0.953 No change in expression
CAT4	All root tissues Seedlings – roots	1.123 induction
AHA2	All root tissues Silique	0.759 repression

3.3 Discussion

3.3.1 Identification of FR-light regulated genes through data-mining of previously published microarray datasets

Microarrays have proven to be a powerful molecular tool to investigate expression profiles of whole genomes under a range of external conditions. The identification of FR-light regulated genes is the first key step in providing an insight into the developmental pathway of seedlings undergoing de-etiolation in response to FR-light. Analysis of multiple previously published microarray datasets has provided such an insight and a number of light-regulated transporter genes from different transporter families have been identified. This indicates a complex signalling pathway is involved during the partial de-etiolation of seedlings exposed to FR-light. The analysis has revealed transporters from almost all of the major transporter families are regulated by FR-light. The functions of many of the proteins encoded by the genes are unknown. However, ABC transporters, aquaporins, P-type pumps and transporters involved in the transport of sugars, amino acids and phosphate are amongst the genes showing FR-light regulation. Of the major groups of transporters only those involved in the transport of magnesium show no FR-light regulation. Some classes of transport families are highly represented. For example, of the 8 known PIN auxin transporters, three of them show some light regulation, with *PIN4* (Wang *et al.*, 2002) and *PIN7* (Devlin *et al.*, 2003) showing an up-regulation in FR-light and *PIN2* (Tepperman *et al.*, 2004) an up-regulation in red-light. Also of the 10 ACA calcium pumps, three of them show an up-regulation in FR-light (Wang *et al.*, 2002). It is interesting that some family members show the same expression patterns and this gives some degree of confidence in the microarray and the role of particular groups of transporters in seedling de-etiolation.

There is also some correlation between transporters showing FR-light regulation in more than one of the four microarray datasets examined. For example the ammonium transporter *AMT1-2* and the sucrose transporter *SUC1* show an up-regulation in both FR-light (Tepperman *et al.*, 2001) and R-light (Tepperman *et al.*, 2004) indicating potential identical pathways for both light treatments. It has been suggested by comparison of the observed expression patterns from wild-type and *phyA* seedlings exposed to FR-light and wild-type and *phyB* seedlings exposed to red light, that an early convergence of the far-red

and red photosensory pathways control a largely common transcriptional network (Tepperman *et al.*, 2004). This indicates than a percentage of transporter genes may be involved in both the red and FR-light signalling pathways and the pathways may even overlap. This is not surprising as many of the morphological changes, including cotyledon opening and inhibition of hypocotyl elongation are similar under both light treatments. Some transporters also show opposing regulation in FR-light and R-light induced de-etiolation. For example the monosaccharide transporter *STP1* and the amino acid transporter *AAP2* both show an up-regulation in FR-light (Wang *et al.*, 2002) but they show a down-regulation in R-light (Tepperman *et al.*, 2004).

3.3.2 Identification of novel FR-light regulated genes using the AMT array

The use of custom-made microarrays such as the *Arabidopsis* membrane transporter array has allowed the investigation of transcript levels of specific groups of genes to the chosen environmental stimulus. The AMT array has been used here to study the transcript levels of genes encoding proteins involved in transport across membranes in response to FR-light during seedling de-etiolation. This would hopefully allow an insight into the re-allocation of various plant compounds mediated specifically by phyA and FR-light.

The quality of the isolated RNA is of most importance for the synthesis of cDNA for hybridisation and microarray analysis, as contaminants could inhibit the synthesis of cDNA and the subsequent incorporation of the dyes. To improve the quantity of cDNA synthesis, additional procedures were undertaken to remove possible contaminants affecting the activity of the polymerase. Possible contaminates included DNA and polysaccharides and a number of methods were used to eliminate these in order to improve RNA quality. The removal of DNA and polysaccharide increased the purity of the samples making them sufficient enough for hybridisation. When sufficient labelled cDNA was generated it was hybridised to the array which was then scanned at high resolution using the Genetix microchip scanner. However, the scan revealed the array was unusable for analysis using the Array-Pro analyser software package due to excess smearing of the dyes over the array area. Some of the excess fluorescence was removed using SSC salt washes, allowing a section of the array to be analysed. The array protocol clearly requires further development, for example using a post labelling protocol rather than the simultaneous

cDNA synthesis and fluorescence labelling step. However the AMT array was successful in identifying a number of FR-light regulated transporter genes.

The subsequent analyses revealed 8 putative FR-light up-regulated and 7 down-regulated transporter genes. The most interesting result is the up-regulation of two ammonium transporters, *AMT1-1* and *AMT1-3*, as ammonium and nitrate are important nitrogen sources for the growth and development of plants. Both transporters have been localised to the roots of *Arabidopsis* and are involved in the uptake of exogenous ammonium from the environment (Grossman and Takahashi 2001). Ammonium acquisition by plant roots involves six members of the ammonium transport family, and AMT1-1 is considered to be the prime ammonium transporter in the roots where mRNA for this gene is highly abundant (Kaiser *et al.*, 2002). It has been shown that ammonium influx into roots and *AMT1-3* mRNA expression are highly diurnally regulated and respond strongly when nitrogen status is varied (Kaiser *et al.*, 2002). *AMT1-3* transcript levels peaked with an ammonium uptake at the end of the day, suggesting AMT1-3 provides a link between nitrogen assimilation and carbon provision in the roots (Gazzarrini *et al.*, 1999). At the end of the day FR-light increases, resulting in a low R/FR-light ratio. The up-regulation of *AMT1-3* during this FR-light rich (Gazzarrini *et al.*, 1999) period correlates with the up-regulation shown by this AMT array and supports a role in ammonium transport during FR-light induced seedling de-etiolation.

Another interesting FR-light induced transporter is *CAX1* (**ca**tion e**x**changer 1), an H^+/cation exchanger, showing an approximate 2-fold up-regulation. Cytosolic Ca^{2+} levels are maintained by two opposing fluxes, Ca^{2+} influx via channels and efflux via calcium pumps and antiporters including CAX1, which are driven by a proton electrochemical gradient (Shigaki *et al.*, 2001). CAX1 has been localised to the tonoplast (Cheng *et al.*, 2003). The *cax1* mutant exhibits alteration in growth, stress responses and hormone perception (Cheng *et al.*, 2003), but has not previously been shown to be involved in light responses. The strong role of Ca^{2+} in photomorphogenic responses could indicate the involvement of CAX1 in the light signalling pathway during FR-light induced seedling de-etiolation.

Seven transporters have shown a down-regulation by FR-light during de-etiolation, these include the gene encoding the chloride channel CLC-a. In plants, voltage-dependent chloride channels of the CLC family contribute to a variety of plant specific functions, including stomatal movement, nutrient transport and metal tolerance (Hechenberger *et al.*, 1996). They also play a role in basic cellular functions such as epithelial transport, plasma membrane excitability, and the control of pH and membrane potential (Geelen *et al.*, 2000). *CLC-a* mRNA was found to be expressed in roots and shoots and levels increased rapidly in both tissues upon the addition of nitrate suggesting it plays a role in controlling the intracellular nitrate status (Geelen *et al.*, 2000). During FR-light induced seedling de-etiolation there could be changes in the demand for nitrogen, so the regulation of *CLC-a* by FR-light could play a vital role in the re-distribution and the control of intracellular concentration.

3.3.3 Correlation between different microarray datasets

Even though only a limited number of genes were identified using the AMT array, it is interesting to see that there is some correlation between the AMT array and the microarray experiment carried out by Wang *et al.*, 2002. Three genes appear in both datasets; the monosaccharide transporter *STP1*, the proton pump *AHA2* and a gene of unknown function (At5g47120). *AHA2* shows a down-regulation by FR-light in both microarrays, with a relative expression of 0.614 in the original Wang *et al.* (2002) array and a relative expression of 0.635 on the AMT array. This implicates a role for *AHA2* in seedling de-etiolation and will be discussed later. In contrast, *STP1* shows an up-regulation in the original dataset, but a down-regulation in the AMT array. RT-PCR has been used to validate the expression of *STP1* by FR-light and this will also be discussed later.

The novel FR-light genes identified by the AMT array add to the idea that certain transporter classes are well-represented, for example the ammonium transporters *AMT1-1* and *AMT1-3* show an up-regulation in FR-light as shown by the AMT array and so does *AMT1-2* in the microarray dataset of Tepperman *et al.*, (2001).

3.3.4 Regulation of transporter gene expression by FR-light

3.3.4.1 Identification of constitutively expressed control genes

A selection of the identified FR-light regulated transporter genes were chosen to validate the FR-light regulation using semi-quantitative RT-PCR. This cycling procedure was firstly undertaken using two putative constitutively expressed housekeeping genes to indicate equal levels of RNA in each sample. The two putative control genes used were identified as, At3g18780 encoding the gene *ACTIN2*, a cytoskeletal protein and At5g18380, encoding the 40S subunit of the S16 ribosome. The *ACTIN2* gene belongs to a family of 8 actin genes in *Arabidopsis thaliana* and actin microfilaments constitute a fundamental part of the cytoskeleton of all eukaryotes (Gilliland *et al.*, 2003). In plants, actin functions in essential processes such as cytoplasmic streaming, organelle orientation and tip growth of the pollen tube and root hairs. Actin is also involved in several developmental processes including the establishment of cell polarity, cell division plane determination, cell wall deposition and cell elongation (Meagher *et al.*, 2004). The actin genes are sub-divided into two groups according to their direct function in either vegetative or reproductive structures (Meagher *et al.*, 1999). The vegetative actins include ACT7, ACT8 and ACT2 and are expressed strongly in roots, stems and leaves of germinating seedlings, young and mature plants (McDowell *et al.*, 1996). In particular it has been shown that ACT2 is important throughout root hair formation (Ringli *et al.*, 2002). The core function of ACTIN2 in plant development could implicate it is constitutively expressed under various treatments. RT-PCR has shown that the *ACTIN2* gene is regulated by FR-light and shows a 2-fold induction in FR-light grown seedlings compared to etiolated seedlings, and is therefore not a suitable control gene. The up-regulation of *ACTIN2* by FR-light was shown in three biological repeats. In contrast the 40S ribosomal protein appears to be constitutively expressed in both the control and the FR-light treated seedlings. The 40S ribosomal subunit protein belongs to the S9P family of ribosomal proteins. Such ribosomes have a basic role in protein synthesis so it is not surprising it is constitutively expressed. Suitable primers for the amplification of this gene were taken from Bovet *et al.* (2003), who had already shown that the *40S* gene remained constant under different cadmium treatments. As this gene appears to be constitutively expressed in both tissues it can therefore be applied as a

suitable control gene. The identification of a constitutively expressed control gene allows the verification of the putative FR-light regulated transporter genes.

3.3.4.2 Confirmation of the FR-light regulation of the induced candidate transporter genes

STP1 is a high-affinity monosaccharide/proton symporter and belongs to the **M**ajor **F**acilitator **S**uperfamily (MFS). STP1 is also a member of the **S**ugar **T**ransport **P**rotein family (STP), of which there are 14 members (Sherson *et al.*, 2000). STP1 shows at least 50% identity to all other members of the STP family at the nucleotide level, showing the highest degree of homology, around 80% identity to STP2. These genes encoding the monosaccharide transporters show temporal and spatial expression patterns.

RT-PCR indicated that *STP1* showed a marked up-regulation of 2.8-fold in FR-light grown seedlings compared to etiolated seedlings. *STP1* mRNA was reported to be most abundant in leaves but was also found in other organs including stem, roots, siliques and flowers (Sauer *et al.*, 1990), but no specific function for this protein had been proposed. STP1 is active during seed germination and is responsible for approximately 60% of glucose uptake activity in *Arabidopsis* seedlings, but its activity is markedly repressed by treatment with exogenous sugars (Sherson *et al.*, 2000). It was also shown that active transport by STP1 plays a major role at very high concentrations of exogenous sugar (Sherson *et al.*, 2000). Such findings provide vital insights into the function of STP1, clearly establishing its importance in the uptake of extracellular sugars by the embryo and seedlings (Sherson *et al.*, 2000). The expression of *STP1* has recently been shown in guard cells and additional RNase protection analyses revealed a strong increase of *STP1* expression in the dark and a diurnally regulated increase during the photoperiod around midday (Stadler *et al.*, 2003). This increase in expression correlates in time with the guard cell-specific accumulation of sucrose, with monosaccharide import into guard cells during the night and a possible role in osmoregulation during the day (Stadler *et al.*, 2003). As *STP1* has shown to be expressed in the roots of seedlings and has been shown to be involved in the uptake of exogenous sugar it is likely that this gene could be regulated by FR-light. When the etiolated seedling is transferred to FR-light and undergoes partial de-etiolation the seedling could require an additional source of sugar. As the seedling is still

unable to photosynthesize it could potentially result in the uptake of exogenous sugar via the increase in *STP1* indicating the up-regulation of this gene by FR-light. Also this indicates STP1 is one of the principle sugar transporters involved in the transport of sugars throughout the developing seedling.

An unknown gene (At1g64990) showed the most significant induction in gene expression in FR-light grown seedlings. A 6.3-fold up-regulation was shown in the Col-0 wild-type in FR-light grown seedlings in the array analyses, and subsequent RT-PCR has shown that this gene indeed does show an induction by FR-light, showing a 6-fold induction. As the function of the protein is unknown and as it shows a up-regulation in FR-light it has subsequently been named FRIMP1 (**F**ar-**r**ed light **I**nduced **M**embrane **P**rotein). The light regulation of this gene and the generation of a knockout mutant for this gene provide an insight into the function of this gene and will be discussed in chapter 5.

ACA2, a calcium ATPase is another of the FR-light up-regulated transporter genes and belongs to the ACA family of which there are 10 members. RT-PCR has confirmed that *ACA2* indeed shows an up-regulation in FR-light grown seedlings compared to etiolated seedlings, with a 1.7-fold induction. The *ACA* gene family of P-type pumps function in ATP driven Ca^{2+} efflux pumping at plasma and endomembranes to maintain low cytoplasmic Ca^{2+} concentrations (Geisker *et al.*, 2000). Calcium is essential for many aspects of plant growth, development and signalling (Sze *et al.*, 2000). One of the most significant roles of Ca^{2+} is as a signal transduction element, and the concentration of cytosolic free Ca^{2+} is critically important in controlling many cellular responses (Sze *et al.*, 2000). An astonishing variety of physiological stimuli elevate cytosolic Ca^{2+} in plant cells, including cold, drought, nod factors, gibberellins, abscisic acid and red light (Sanders *et al.*,1999). An elevation in Ca^{2+} causes changes in proteins modulated by Ca^{2+} and their targets that elicit downstream events in such signalling pathways. Changes in the plants environment signal an elevation in the cytoplasmic concentration of calcium. After the initial response calcium levels must return to the basal level, so therefore an increase in the ACA2 protein may be involved in the efflux of calcium from the cytoplasm to the endoplasmic reticulum during de-etiolation. The partial de-etiolation by FR-light represents the change in environment, so could therefore up-regulate *ACA2* transcription to aid the return of basal calcium concentrations. As calcium plays a vital role in the growth and

development of plants, it is viable that *ACA2* is indeed regulated by light and involved in responding to physiological changes.

The function of another candidate FR-light has also yet to be identified but the protein sequence does show significant homology to a Niemann Pick C disease like protein in *Homo sapiens*. A number of *Arabidopsis* databases refer to this gene as the Niemann Pick C disease-like protein. In humans, Niemann-Pick type C (NPC) disease is a recessive inherited lysosomal storage disorder resulting in the accumulation of cholesterol and shingolipids with a progressive and eventually fatal neurodegenerative course (Patterson *et al.*, 2001). Usually, cellular cholesterol is imported into lysosomes of the cell that is processing it. Cells taken from NPC patients have been shown to be defective in releasing cholesterol from lysosomes. This leads to a build-up of cholesterol inside lysosomes causing processing errors. The *NPC1* gene was found to have known sterol sensing regions similar to other proteins, suggesting it plays a role in regulating cholesterol trafficking (Carstea *et al.*, 1997). The importance of NPC as a model for subcellular imbalance is now being studied in more common diseases, such as Alzheimer's and cardiovascular disease (Ikonen and Holtta-Vuori 2004).

The Arabidopsis At1g42470 Niemann-Pick C disease-like protein is comprised of 1248 amino acids and has a molecular mass of 137,129 Da. The Arabidopsis membrane protein library has categorised this gene together with a second gene (At4g38350) also of unknown function, into a putative metal exporter family and also the resistance nodulation cell division (RND) family. Proteins in this family probably catalyse substrate efflux via an H^+ antiport mechanism. Transmembrane prediction programs have predicted 11 transmembrane spanning domains; however, there is some variation in the exact location of these domains. It appears that the gene encoding the Niemann-Pick C disease like protein is not expressed in etiolated seedlings, however there is a marked induction after 12 hours of FR-light exposure suggesting that it may be important in seedling responses to FR-light. This protein could perhaps be required for metal transport or mobilisation of lipid-based compounds.

RT-PCR indicates an up-regulation of *PIN4* by 1.6-fold in FR-light grown seedlings compared to etiolated seedlings. Many links have been made between light-

regulation and the plant phytohormone auxin. Auxin has a central role in the establishment and elaboration of the root meristem, and regulation of root development by auxin begins early during embryogenesis and persists throughout the lifetime of the root (Jiang and Feldman, 2002). So PIN transporter proteins, including PIN4 must play a crucial role in the distribution of auxin. *pin4* mutants are defective in establishment and maintenance of endogenous auxin gradients, fail to utilise externally applied auxin and display patterning effects in both embryogenic and seedling roots (Friml *et al.*, 2002). It has been demonstrated that *PIN4* is expressed just below the PIN1 domain in both developing and mature root meristems, and is essential for the correct establishment of an auxin gradient that is important for formation of the root (Friml *et al.*, 2002). So the role of PIN4 is in generating a sink for auxin below the quiescent centre of the root meristem that is essential for auxin distribution (Friml *et al.*, 2002). It has been shown that plants perceive stimuli, such as light and change the subcellular position of auxin-transport components accordingly, perhaps even auxin transporters. These changes modulate auxin fluxes, and the newly established auxin distribution triggers the corresponding developmental response (Friml., 2003). As auxin and light have been shown to be involved in hypocotyl elongation it is likely that at least one auxin transporter is indeed regulated by light, however as *PIN4* has been shown to be located in roots it cannot be this auxin transporter, but it could still play a vital role in the roots during de-etiolation. However other members of the PIN family also show light regulation, with *PIN7* also showing an up-regulation in FR-light (Devlin *et al.*, 2003) and *PIN2* shows an up-regulation in red light (Tepperman *et al.*, 2004). These could also function in changes in morphology during seedling de-etiolation.

Until recently the function of the protein encoded by At3g59320 was unknown, however, it is now thought that it has a role in the transporter of the pigment anthocyanin. It is believed that the *Arabidopsis* genome contains two anthocyanin related transporter proteins, and this protein is referred to as the anthocyanin-related transport protein 2 (ANM2). This protein has a molecular weight of 37,495 Da, consists of 339 amino acids and shows the highest degree of sequence identity, around 74% to *ANM1* (At3g59340), the other anthocyanin-related transporter.

The RT-PCR experiment indicated *ANM2* is indeed up-regulated by FR-light, as this gene showed a 3.97-fold induction in FR-light grown seedlings. It is well established

that anthocyanin accumulates in light-grown seedlings alongside other morphological changes such as inhibition of hypocotyl growth and cotyledon expansion (Duek and Fankhauser, 2003) so it is likely that the expression of such transporter genes are regulated by light. The synthesis and accumulation of anthocyanin has previously been shown to be induced by FR-light even via short monochromatic light treatments (Cho *et al.*, 2003). It is therefore possible that an anthocyanin transporter is FR-light induced to co-inside with the increase in anthocyanin synthesis. The up-regulation of this anthocyanin transporter by FR-light indicates that the anthocyanin pigment could be important for de-etiolation and the gene is involved in the light signalling pathway.

3.3.4.3 Confirmation of the FR-light regulation of the repressed candidate transporter genes

The only candidate FR-light reduced gene which showed a down-regulation using RT-PCR was *AHA2*. AHA2 is an H^+-ATPase, which like ACA2, is a member of the P-type pump superfamily. P-type ATPases encoded by the *AHA* gene family, of which there are 12 members are located at the plasma membrane and establish a proton motive force which energises the uptake of nutrients including K^+ via the symport of H^+ (Maathius and Sanders 1994) and the extrusion of Ca^{2+} via H^+ antiport (Kasai and Muto 1990). *AHA2* is mainly expressed in the root epidermis (Palmgren, 2001) and is believed to play a crucial role in energising Na^+ extrusion at the root-soil boundary by providing the necessary proton motive force to drive Na^+/H^+ antiport (Maathius *et al.*, 2003). The expression of *AHA2* in the roots has also been shown by the microarray within Genevestigator. As AHA2 plays a vital role in the establishment of a proton motive force which energises the activity of many secondary transporters, it is likely that this protein is involved in maintaining the proton motive force during the morphological changes during de-etiolation. During FR-light induced de-etiolation there could potentially be changes in the demand of the seedling for external nutrients via the roots, hence the down-regulation of *AHA2*.

RAN1 shows one of the smallest changes in expression of the genes identified from the Wang *et al.* (2002) microarray and unlike *AHA2* the FR-light repression was not confirmed as only a small 0.90-fold repression was shown by RT-PCR. *RAN1*, previously known as *HMA7* is a member of the P-type pump superfamily. Recently RAN1 as been

classified as an ATP-dependent copper transporter, along with 3 other genes. RAN1 is 49% identical to HMA5 another heavy metal transporter and is a 1001 amino acid polypeptide with a molecular weight of 107295 Da. Little is known about the localisation of RAN1, however Genevestigator microarrays indicates is it expressed in all seedling tissues, the roots and the sepals and petals. The *ran1-3* mutant results in the constitutive activation of ethylene responses in seedlings and adults. Analysis of the interaction with other mutants affected in ethylene action indicates that dominant, ethylene-insensitive receptor mutants are epistatic to *ran1-3*, indicating that the *RAN1* gene product acts very early in signalling (Woeste and Kieber 2000). In addition to its role in ethylene signalling, RAN1 function has been shown to be required for cell elongation in an ethylene-independent manner (Woeste and Kieber 2000). When the etiolated seedling is transferred to FR-light there is a decrease in hypocotyl cell elongation, so as a consequence, transcript levels of this gene may also decrease. Ethylene controls multiple physiological processes in plants and has shown to be circadian clock regulated in wild-type *Arabidopsis* seedlings (Thain *et al.*, 2004). It has been shown in tobacco that there are interactions between phytochrome signalling and ethylene action in shade avoidance responses whilst also interacting with Gibberellins (Poerik *et al.*, 2004). Low R/FR ratios have been shown to enhance ethylene production in wild-type tobacco, resulting in the shade avoidance responses, whereas the ethylene-insensitive plants showed reduced shade avoidance responses. With the evidence of the cross talk between phytochromes and ethylene it is possible that RAN1 is involved during the morphological changes of FR-light induced de-etiolation and both ethylene and light act in parallel in inhibiting hypocotyl elongation.

CAT4 encodes an amino acid transporter and belongs to the putative cationic amino acid family of transporters of which there are 9 members The MIPS database classifies this protein as a member of the amino acid, polyamine and choline transporter (APC) superfamily. RT-PCR indicated that *CAT4* is not down-regulated in FR-light but instead shows a small up-regulation of 1.18-fold in FR-light grown seedling compared to etiolated seedlings. Compared to other transporter families little is known about amino acid transporters, including CAT4, however *CAT4* has been shown to be localised in a variety of tissues, including roots, stem, leaves and flowers (Su *et al.*, 2004). However it would be assumed that the movement of amino acids during the changes in morphology of a seedling developing in light would be extremely vital. It is plausible that after just 12 hours of FR-

light exposure, the inhibition of hypocotyl elongation requires a change in the demand of amino acids resulting in the up-regulation of *CAT4*.

The RT-PCR approach taken to validate the FR-light regulation has confirmed that seven of the nine genes showed the expected FR-light regulation with *CAT4* and *RAN1* being the exception. As the majority of the genes show the expected expression profile using RT-PCR it validates the original microarray indicating the genes are indeed FR-light regulated. These genes may be relevant during the morphological changes of FR-light induced seedling de-etiolation.

Chapter 4

Transporters in *Arabidopsis* Seedling Development

4.1 Introduction

4.1.1 Transporter proteins in *Arabidopsis*

Complete sequencing of the *Arabidopsis thaliana* genome has provided an insight into functional genomics which has broadened and accelerated plant biology research (Arabidopsis Genome Initiative 2000). With the availability of complete genome sequences, the focus now is on functional genomics and to assign functions to newly identified DNA sequences (Radhamony *et al.*, 2005). When a new sequence has been identified, a comparison with sequences in the databases is the simplest way to obtain functional information about the protein. The functions of approximately 69% of the genes were classified according to sequence similarity to proteins of known functions in a variety of organisms (Arabidopsis Genome Initiative 2000). Information about the hypothesized function of an unknown gene may be deduced from its sequence using already known functions of similar genes as the basis for comparison (Holtorf *et al.*, 2002). The functions of only a few thousand genes of the *Arabidopsis* genome have been identified with a high degree of confidence (Bouche and Bouchez; 2001). An essential tool for functional analyses is the ability to create loss-of-function mutants for all the genes (Alonso *et al.*, 2003). Reverse genetics via random insertional mutagenesis allows the isolation of mutated genes. Foreign DNA, either a piece of T-DNA (Krysan *et al.*, 1999) or a transposon (Martienssen., 1998) is introduced into the plant and used to disrupt genes by random integration. This creates loss-of function mutants which are tagged by the interrupting piece of DNA. The potential of these mutants can be fully exploited when using such lines for reverse genetics (Parinov and Sandaresan, 2000) and can be used to confirm physiological function. A large proportion of proteins in *Arabidopsis* are involved in the transport of many compounds including phytohormones, photoassimilates and signalling molecules. Membrane transport processes in *Arabidopsis* have been compared to those of fungi, animals and prokaryotes and over 1700 predicted membrane transport proteins have

been identified in *Arabidopsis* (Maathius *et al.*, 2003). The structure of the transporter proteins studied in this chapter will be discussed along side examples of T-DNA mutants isolated to examine transport protein function.

4.1.2 Amino acid transporters

Amino acids are the currency of nitrogen exchange in plants, so amino acid transport is a fundamental activity in plant growth. The majority of amino acid transporters in plants are proton-amino acid symporters (Bush, 1993). These transporters couple amino acid uptake to the proton electrochemical potential difference that is maintained across the plasma membrane of plant cells by a P-type proton pumping ATPase (Bush, 1993). Molecular cloning of amino acid transporters by functional complementation in yeast has revealed that there are multiple gene families that encode different classes of amino acid transporters in plants (Bush *et al.*, 1996). Recent studies have shown there are more than 50 amino acid transporter genes in the *Arabidopsis* genome (Liu and Bush, 2006). Two superfamilies of amino acid transporters have been defined; the amino acid, polyamine and choline transporters superfamily (APC) and amino acid transporter family (ATF) superfamily (Fischer *et al.*, 1995). There are 14 APC transporters in the *Arabidopsis* genome, among these nine members are cationic amino acid transporters (CAT1-9) (Liu and Bush, 2006). CATs contain 14 putative transmembrane spanning domains and they are high-affinity basic amino acid transporters (Liu and Bush, 2006). The ATF superfamily has at least five sub-classes of transporters, including the amino acid permeases (AAPs), the lysine, histidine transporters (LHTs), the proline transporters (ProTs), the putative auxin transporters (AUXs) and the aromatic and neutral amino acid transporter (ANT) family (Ortiz-Lopez *et al.*, 2000). Given the large number of amino acid transporters in plants with overlapping substrate specificity, it is clear that they must be distinguished from one another by tissue expression patterns and by their responses to environmental signals, including light. The use of T-DNA and transposon mutants has yet to be very successful for amino acid transporters due to redundancy. For example homozygous *aap3* mutants showed no difference from wild-type grown under various growth conditions (Okumoto *et al.*, 2004).

4.1.3 Calcium ATPases

Arabidopsis thaliana has been shown to have 14 Ca^{2+} ATPases and these calcium ATPases form two distinct groups, type P_{2A} (or ECA for ER-type Ca^{2+} ATPases) and type P_{2B} (or ACA for autoinhibited Ca^{2+} ATPase). ACA2 is an example of a calmodulin-regulated Ca^{2+} ATPase and has been localised to the endoplasmic reticulum using a GFP fusion protein (Hong *et al.*, 1999). In comparison to animal homologs the distinct feature of ACA2 and the other ACA ATPases is the absence of a long C-terminal regulatory domain. Instead there is a unique, relatively long N-terminal domain of 160 residues (Harper *et al.*, 1999). The catalytic activity of ACA2 can be modulated by cytoplasmic concentration either through activation upon binding calmodulin or by inhibition following phosphorylation by Ca^{2+}-dependent protein kinases (Hwang *et al.*, 2000). ACA2 has been shown to contain a autoinhibitory domain sequence located between amino acids 20 and 44, and it is thought that an interaction between this sequence and a site in the Ca^{2+} pump core keeps the pump un-activated (Curran *et al.*, 2000).

The N-terminal domain also contains a calmodulin-binding sequence, as shown by calmodulin binding assays (Harper *et al.*, 1999). The calmodulin/Ca^{2+} ATPase interaction at the plasma membrane was shown to be dependent on calmodulin isoforms showing isoform-specific Ca^{2+} dependencies (Luoni *et al.*, 2006). In the absence of calmodulin the regulatory domain interacts with the sites in the cytoplasmic loops hampering the enzymes catalytic activity. This may provide a Ca^{2+} regulated feedback system to control Ca^{2+} levels in the cytoplasm. The activation of ACA2 occurs as a result of calmodulin binding to a site overlapping or immediately adjacent to the autoinhibitory domain, and thereby displacing its inhibitory interactions (Hwang *et al.*, 2000). Calcium ATPase specificity and function has been studied using the generation of insertional mutants. For example ACA9 has been shown to be required for normal pollen tube growth and fertilization as disruption of *ACA9* resulted in partial male sterility (Schiott *et al.*, 2004).

4.1.4 Sugar transporters

The cloning of monosaccharide transporter cDNAs identified closely related integral membrane proteins with 12 transmembrane helices, showing homology to monosaccharide transporters from yeast, bacteria and mammals (Buttner and Sauer, 2000). The kinetic mechanism of monosaccharide H^+ symport has been studied in detail for STP1. Patch clamp techniques have suggested a sequential mechanism for sugar uptake by STP1, *i.e.* protons and sugar molecules are imported in two ordered sequential steps (Buttner and Sauer 2000). There is considerable sequence similarity between the amino-terminal and carboxyl-terminal halves of monosaccharide transporters indicating that they may have evolved from gene duplication of an ancestral gene coding for a six transmembrane helix transporter (Marger *et al.*, 1998).

The function of sugar transporters has also been examined using insertional mutants, however due to protein redundancy such mutants have not been that successful in establishing specific function for these proteins. For example STP6 has shown to be a pollen specific H^+-monosaccharide symporter, however there were no phenotypic differences between *stp6* and wild-type plants (Scholz-Starke *et al.*, 2003)

4.1.5 H^+-ATPases

The P_{3A} ATPases are a subfamily of plasma membrane H^+-ATPases found only in fungi and plants, and consist of 11 closely related members with at least 66% homology. AHA1 and AHA2 are five to eight times more abundant than other AHAs (Palmgren, 2001). H^+-ATPases play a role in many aspects of plant development, including phloem loading, movement of stomatal guard cells, energization of nutrient uptake into the roots, and for the growth of pollen tubes and root hairs (Songergaard *et al.*, 2004).

Plasma membrane H^+-ATPases are primary cellular motors behind the generation of the electrochemical gradient present across the plasma membranes of plant cells (Buch-Pedersen and Palmgren 2003). As a primary transporter, it mediates ATP-dependent H^+ extrusion to the extracellular space, thus creating pH and potential differences across the plasma membrane that activates a large set of secondary transporters (Arango *et al.*, 2003).

They are characterised by forming a phosphorylated intermediate during catalysis and consist of just a single catalytic unit which is responsible for both ATP hydrolysis and cation transport. The C-terminal extension of plasma membrane H^+ ATPases is cytoplasmically located and has a regulatory function in plant H^+-ATPases (Eraso and Portillo, 1994). This regulatory domain (R-domain) functions as an autoinhibitory domain, keeping the enzyme in a low activity state (Eraso and Portillo, 1994). Removal of the C-terminus leads to an activation of H^+-ATPases activity, and it was hypothesised that the C terminal is a target for physiological factors activating or inactivating proton pumps (Palmgren and Harper 1999). This includes a group of regulatory proteins, called 14-3-3 proteins

The use of T-DNA mutants has provided an insight in to the function of specific AHA family members. For example the isolation of the *aha3* mutant has revealed the proton pump is essential for pollen development (Robertson *et al.*, 2004). The *aha3* mutant showed male gametophytic lethality and the pollen grains had a uniformly shape and size and could not develop a functional pollen tube (Robertson *et al.*, 2004). This indicated a specific function for AHA3 in pollen development.

4.1.6 Chapter Aims

The aim of this chapter is to identify and confirm homozygous T-DNA mutants for the candidate transporter genes outlined in chapter 3. Phenotypic characteristics of these mutants will aid in identifying the role of these proteins in light-regulated plant and seedling development.

4.2 Results

4.2.1 Isolation of homozygous knockout mutants

Seed stocks from T-DNA insertion mutants originating from the genome wide insertional mutagenesis program conducted by the SALK institute (Alsonso *et al.*, 2003) were obtained. The T-DNA lines are available through NASC (http://arabidopsis.info) as seed stocks. A preliminary assignment of the location of the T-DNA insert within the gene was initially performed by the SALK Institute. Most seed provided by stock centres is only putatively mutagenised in the advertised location. The seed stock may be provided as a mixture of wild-type (Col-8), heterozygotes (heterozygous for the T-DNA insert) or possible homozygotes (homozygous for the T-DNA insert). The T-DNA insert contains a dominant kanamycin resistance gene *NPTII* (**N**eomycin **P**hosphot**t**ransferase) (Alsonso *et al.*, 2003). This resistance in combination with PCR was used to determine the zygosity of the plants. This process was undertaken with the following mutants *Atstp1*, *Ataca2*, *Ataha2* and *Atcat4.* Putative T-DNA mutants for these genes from two mutagenesis programs, SALK and GABI-KAT (http://www.gabi-kat.de/) are outlined in Table 4.1. The ordered seed stock is labelled with an asterix*. The advantage of the seed stock provided by the GABI-KAT institute is that the homozygosity of the seed has been proven allowing instant phenotypic analysis of the mutant. While stocks from the SALK institute require the determination of the zygosity of the seed stock line. This process was undertaken with all the four genes of interest. However for the purpose of this chapter only the confirmation of *cat4* will be discussed in detail as an example of the analysis performed.

Seed stocks from three separate T-DNA insertions in *CAT4* were ordered from the SALK institute; these were N567045, N576909 and N576917. The kanamycin resistance gene *NPTII* can be used as a selection method to determine the zygosity of the plants from the three lines. The original seed sent by the NASC were grown to maturation and the zygosity of the progeny was tested. Approximately 50 seeds from each plant were plated on MS plates, with and without kanamycin selection. This was also repeated with wild-type seed, in this case Col-8, to test for positive selection. The survival:death ratios for the plants from the three *CAT4* lines were calculated. Of the three lines only progeny from line N567045 survived selection, indicating the progeny from lines N576909 and N576917 do

Table 4.1 Summary of potential T-DNA mutants for the candidate far-red light regulated genes. Potential T-DNA insertional mutants were identified by screening a number of web-based *Arabidopsis* mutant databases, including the Gabi-Kat (http://www.gabi-kat.de/) and Salk Lines (http://www.signal.salk.edu/). The mutants marked by a asterix* were ordered for screening. The lines confirmed as containing the insert and homozygous for the gene of interest are indicated by a †.

Gene code and name	T-DNA line	Line ID	Putative insert Position
At1g11260 *STP1*	Gabi-Kat	030C12	5' UTR
		224F11	3' UTR
		492C04	Second of four exons
		757D05	Second of four exons
		876B02	5' UTR
	Salk line	N639194	Second of three exons
		N548818* †	Third of Four exons
At4g37640 *ACA2*	Gabi-Kat	262E01	Fourth of seven exons
		457B03	Third of seven exons
		683B03	First of seven exons
	Salk line	N584865	5' UTR
		N582624* †	Third of seven exons
At4g30190 *AHA2*	Gabi-Kat	219D04	Seventh of fifteen exons
		294G08	Last of fifteen exons
		760F11	First of fifteen exons
	Salk line	N573730	3' UTR
		N621432	3' UTR
		N562371* †	Thirteen of fifteen exons
		N582786	Last of fifteen exons
		N622010* †	Fourth of fifteen exons
At5g04770 *CAT4*	Gabi-Kat	137A07	5' UTR
		275G04	5' UTR
		335E10	Second of three introns
		418A05	Third of three introns
		896D10	Third of three introns
	Salk line	N567045* †	Third of four exons
		N628133	5' UTR
		N576909*	Third of four exons
		N576917*	Third of four exons
		N523654	Last of three introns
		N582408	Last of four exons

not have kanamycin resistance and are therefore likely to be wild-type or the kanamycin gene may have been silenced. The survival:death ratios for six putative N567045 mutants and the wild-type plant are shown in Table 4.2. A 100% survival on selection indicates a putative homozygote, a 75% survival indicates a putative heterozygote and a 0% seedling survival indicates a wild-type. Of these plants 2, 3 and 5 showed a 100% seedling survival when plated on kanamycin indicating all the seedlings have kanamycin resistance and therefore contain the T-DNA insert. Plants 1 and 4 showed a segregating population with approximately 75% of the seedlings surviving the selection. This indicates that the seedlings showed a 1:2:1 ratio of wild-type, heterozygote and homozygote seedlings respectively, with only the heterozygote and homozygote seedlings surviving selection. Plant 6 like the wild-type seedlings showed a 0% survival indicating the absence of the T-DNA insert and therefore is a wild-type plant. The wild-type (Col-8) also shows a 0% seedling survival on kanamycin indicating selection was successful. The presence of multiple insertions at different sites affects the survival rate of the seedlings. An approximate 97% seedling survival rate on selection indicates two insertions and these seeds cannot be used for further analysis, without undertaking a backcross with a wild-type plant to remove the second insertion. Segregation analysis cannot be solely relied on to determine the zygosity of a plant and it is therefore used in combination with PCR on genomic DNA extracted from each putative mutant. PCR was undertaken on the genomic DNA using three combinations of primers. Gene specific forward (F) and reverse (R) primers were designed spanning the predicted T-DNA insertion site. These individual primers were also used in combination with a T-DNA left border primer (L) which is located within the insert. PCR using these primers revealed that the seed stocks N576909 and N576917 contained no insert and only amplified a band using the gene-specific forward and reverse primers proving the parent to be wild-type. However PCR on genomic DNA extracted from ten plants from the N567045 seed stock showed a combination of wild-type, heterozygote and homozygote plants (Figure 4.1A). Figure 4.1A shows PCR on genomic DNA extracted from both wild type and three mutant plants using the three primer combinations. Figure 4.2 is a representation of the genomic sequence of the gene *CAT4*, showing the predicted location of the T-DNA insert, which is predicted to be inserted in the reverse orientation to the gene sequence in the third of four exons. Using the forward primer (F2) and the reverse primer (R2) which span the predicted T-DNA insert site, from wild-type genomic DNA a band of 1194 bps was amplified (Figure 4.1A lane 2).

Table 4.2 Predicted parent plant zygosity of *cat4* N567045 T-DNA mutant using antibiotic selection. The survival rate of progeny of six putative *cat4* T-DNA mutants and wild-type (Col-8) visually assessed by percentage survival on MS agar plates with and without kanamycin (100 µg/ml) at 10 days post germination. The predicted zygosity of the parent plant is given.

	Number and Percentage survival		Predicted Zygosity of parent plant
	(Kan +)	(Kan -)	
Plant 1	38/50 (76%)	50/50 (100%)	Heterozygote
Plant 2	51/51 (100%)	50/50 (100%)	Homozygote
Plant 3	49/49 (100%)	52/52 (100%)	Homozygote
Plant 4	39/51 (76%)	51/51 (100%)	Heterozygote
Plant 5	51/51 (100%)	50/50 (100%)	Homozygote
Plant 6	0/51 (0%)	49/49 (100%)	Wild-type
Col-8	0/50 (0%)	51/51 (100%)	Wild-type

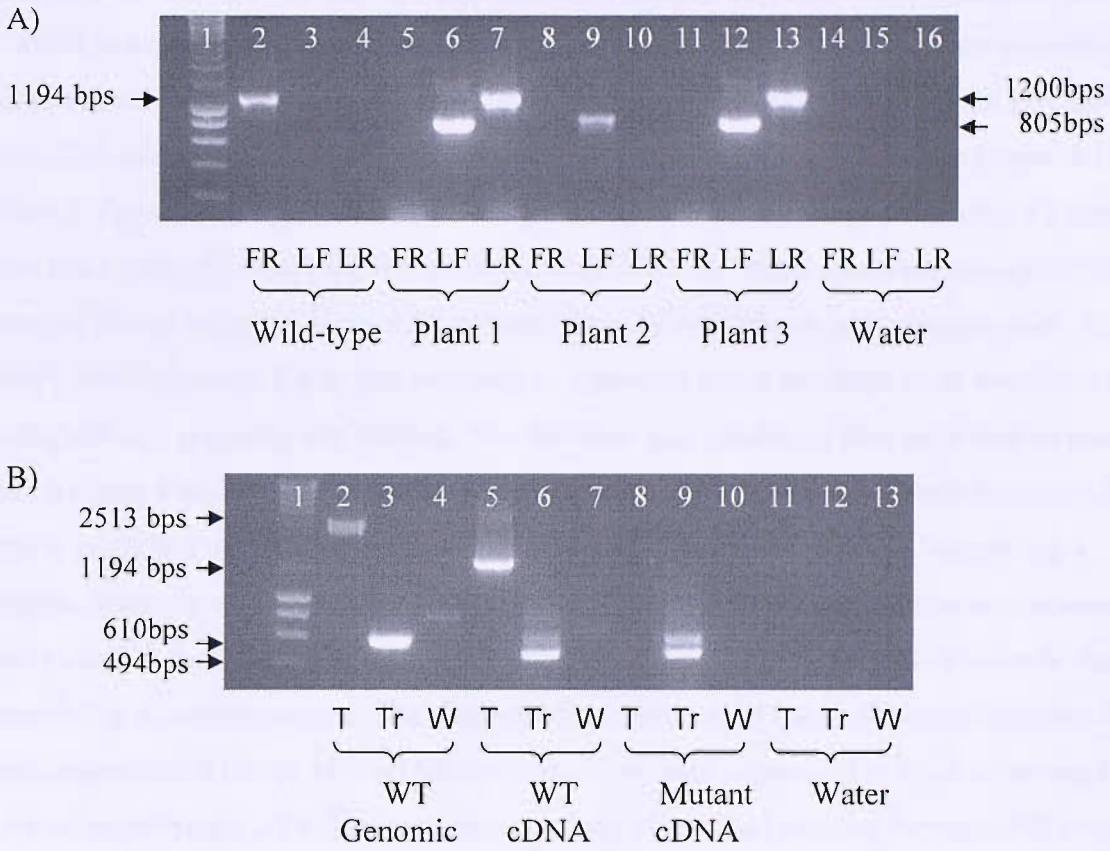

Figure 4.1 Identification of a homozygous *cat4* mutant. A) PCR on genomic DNA extracted from wild-type (Col-0) and three potential *cat4* T-DNA mutants (N567045). Three primer pair combinations were used to identify the genotype of the mutant, gene specific forward primer F2 (F), gene specific reverse primer R2 (R) and T-DNA left border primer Lba1 (L). Refer to Figure 4.2 for the location of the primers. B) PCR on wild-type genomic DNA and cDNA from the wild-type and *cat4* identified from genotypic analyses. Three primer pair combinations were used to confirm the absence of mRNA for the gene of interest, spanning different sections of the gene. Primers F1 and R2 were used to amplify the wild-type gene (W), primers F1 and R1 were used to amplify a truncated gene (Tr) and primers F2 and R2 to the T-DNA flanking region (T). Refer to Figure 4.2 for location of primers. Lane 1 on both gels represents the molecular marker.

However, when the F2 primer is used in conjunction with the left border primer, Lba1 (L) no product is amplified on wild-type material (lane 3). The same is true when the R2 primer is used with Lba1 on wild-type material (lane 4). The absence of a product in lanes 3 and 4 is expected as there should be not insert in the wild-type plant. When the same three primer combinations were used on the genomic DNA extracted from the putative N567045 mutants, a range of bands are seen, examples of this are shown in Figure 4.1. In Plant 2 a product of approximately 805 bps is amplified using the gene specific F2 primer and Lba1 (lane 9), indicating the presence of the T-DNA insert. However, no wild-type band is shown using the F2 and R2 primers (lane 8) indicating a homozygous plant. The T-DNA itself is several Kb in size resulting in a product that is too large to be amplified when using primers spanning the T-DNA. The 805 base pair product is also amplified in plants 1 and 3 (lanes 6 and 12). However in plants 1 and 3 a second product of approximately 1200 bps is amplified using the reverse primer R2 and Lba1 (lanes 7 and 13), suggesting a double insertion or rearrangement of the insert. The same three combinations of primers were used on samples containing water rather than the cDNA template to eliminate the possibility of contamination. The absence of products using water shows the samples were not contaminated (lanes 14-16). All three products were sequenced to confirm primers are indeed amplifying *CAT4*. The sequence obtained using Lba1 and the forward (F2) primers are shown in Figure 4.3. The T-DNA can be clearly seen to be located within the *CAT4* sequence.

4.2.2 Confirmation of Knockout Status

A RT-PCR approach was used to monitor mRNA levels in the N567045 *cat4* knockout mutant (Figure 4.1B). Primers were designed to amplify different sections of the gene, the wild-type gene (W), a truncated product (Tr), and primers spanning the T-DNA (T). These primers were used on genomic DNA from the wild-type (Col-8) plant and cDNA from both wild-type and the *cat4* mutant. Refer to Figure 4.2 for the locations of all primers used and Table 2.4 for primer sequences. Primers designed to span the T-DNA (F2 and R2) amplify products of 2513 and 1194 bps from wild-type genomic DNA (lane 2) and cDNA (lane 5) respectively. This band is not present in the *cat4* mutant (lane 8) indicating *CAT4* mRNA spanning the insertion site is not present. Primers designed to amplify the

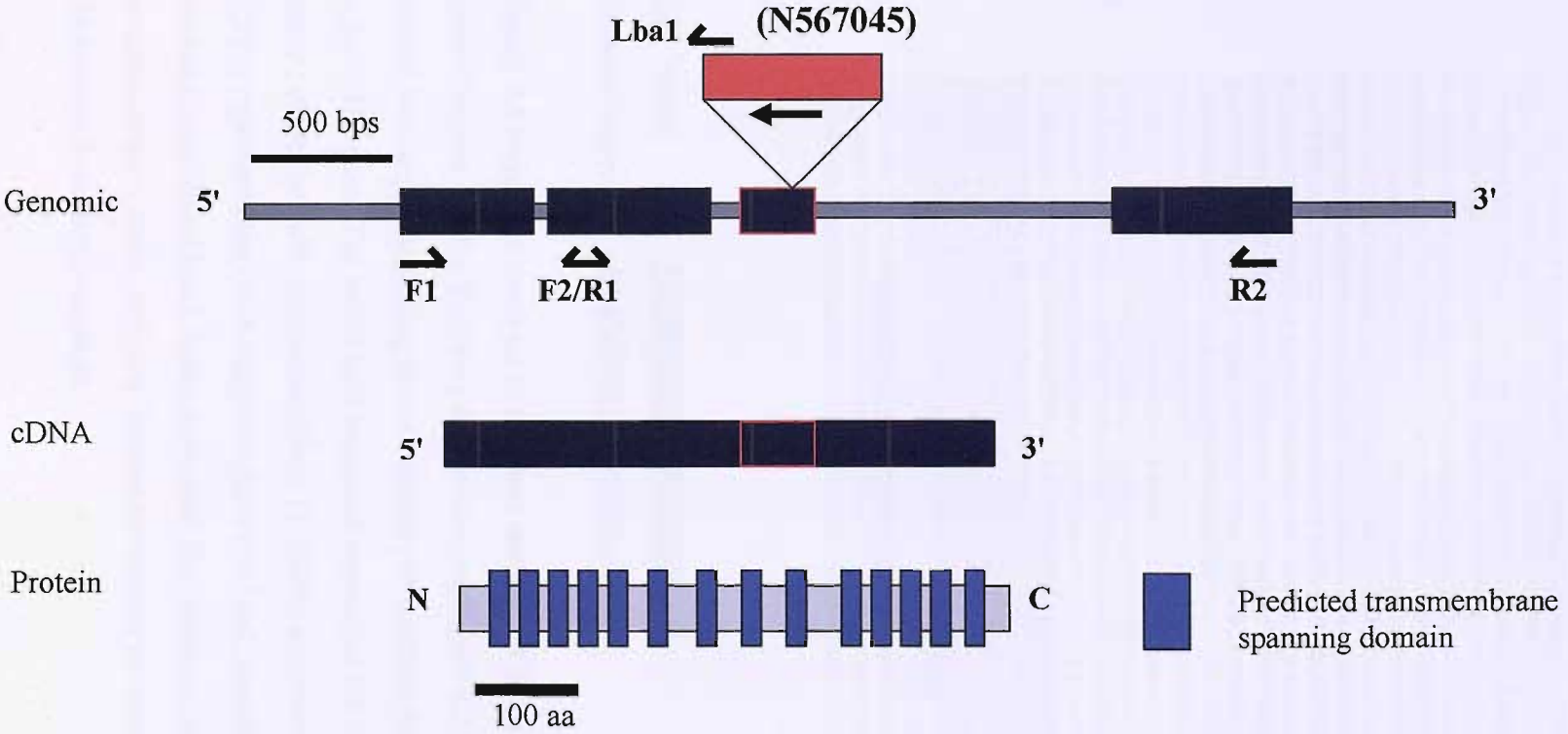

Figure 4.2 Schematic representation of the genomic, cDNA and protein sequences of CAT4, indicating the location of the T-DNA insertion. The T-DNA insertion of the mutant (N567045) is located in the third of four exons, which is in between the eighth and ninth of fourteen predicted transmembrane spanning domains (TMS). Locations of TMS were predicted using hydrophobicity plots. The T-DNA sequence is inserted in the reverse complementation to the gene. Arrows shown indicate the location of gene specific forward and reverse primers designed to confirm the presence of the T-DNA insert and the absence of mRNA in the mutant. The Lba1 primer is designed within the T-DNA insert and is used to identify the presence of the insert. T-DNA insert not to scale.

ATGGAGGTCCAAAGCAGCAGCAACAATGGTGGTCACTCTTCTTTCTCCAGTCTCCGCGTC
TACCTCAACTCTCTTTCCGCGACGCCTTCTCGCTTATCCCGCCGCGCTATTTCCGTCTCC
ACCTCTTCCGACGAGATGAGTCGCGTCCGCGCCGTCTCCGGCGAACAGATGCGCCGTACT
CTCCGGTGGTACGATCTCATTGGACTCGGAATCGGGGGAATGGACGGCGCCGGTGTCTTT
GTCACCACCGGCCGTGCTATTGCTCTCGACGCCGGTCCTTCAATTGTCGCCTCTTACGCC
ATCGCCGGGCTCTGCGCTCTCCTCTCCGCTTTCTGTTACACCGAATTTCGCCGTCCATTC
CCGGTCGCCGGCGGTGCCTTCAGCTACATCCGTATCACATTCGgttagtctcccgcgaaa
atcatcactactcctccgatctgttcacggttttctgaaaattttaatttcaaaatcaaa
aaccgtaactgatttcttttctgttacatttccgttcagGTGAATTTCCAGCATTTTTCA
CCGGAGCAAATCTTGTAATGGATTACGTAATGTCAAACGCGGCCGTTTCGAGAAGCTTCA
CCGCTTATTTAGGAACAGCTTTCGGGATCTCAACTTCCAAGTGGCGATTCGTCGTCTCCG
GTTTACCGAAAGGATTCAAACGAGATTGATCCAGTCGCAGTTCTCGTCGTCCTCGTAATC
CAGTCATCATCTGTTCTAGTACAAGAGAGAGTTCCAAAGTGAACATGATAATGACTGCAT
TTCACATTCCATTCATATTCTTCGTGATCGTTATGGGATTCATAAAAGGAGATTCAAAGA
ATCTATCCTCACCGGCGAATCCAGAGCACCCCTCGGGATTTTTTCCGTTCGGCGCGGCGG
GAGTTTTCAACGGAGCTGCCATTGGTTACTTAAGCTACATAGGATACGACGCCGTTTCAA
CCATGGCGGAAGAAGTTGAAAATCCGGTCAAAGATATCCCCGTCGGTGTTTCCGGCTCCG
TCGCAATCGTCACCGTTCTTTACTGTCTCATGGCAGTCTCTATGTCAATGCTTCTGCCAT
ACGATCTGgtccgtacttcaaatttattattttcttattgtatatttccgttttcataaa
gacggcactgagtctgagtctaaagctgaaaacggcggggcatgtgttgttgtaacgcag
ATAGATCCGGAGGCGCCGTTTTCCGCGGCGTTCAGAGGATCGAACGGCTGGAATGGGTGG
ACGAAAGTGGTGGGGATAGGAGCAAGCTTTGGGATATTAACATCACTTTTGGTGGCAATG
TTAGGTCAGGCTCGCTACATGTGTGTCATCTTTGGAATATATATTGTGGTGTAAACAAAA
TTGACGCTTGACAACTTAATAACACATTGCGGACGTTTTTAATGTACTGGGGTGGTTTTT
CTTTTCACCAGTGAGACGGGCAACAGCTGATTGCCCTTCACCGCCTGGCCCTGAGAGAGT
TGCAGCAAGCGGTCCACGCTGGTTTGCCCCAGCAGGCGAAAATCCTGTTTGATGGTGGTT
CCGAAATCGGCAAAATCCCTTATAAATCAAAAGAATAGCCCGAGATAGGGTTGAGTGTTG
TTCCAGTTTGGAACAAGAGTCCACTATAAAGAACGTGGACTCCAACGTCAAAGGGCGAAA
AAACCGTCTATCAGGGCGATGGCCCACTACGTCAACCATCACCCAAATCAAGTTTTTTGG
GGTCGAGGTGCCGTAAAGCACTAAATCGGAACCCTAAAGGGAGCCCCCGATTTAGAGCTT
GACGGGGAAAGCGGCGAACGTGGCGAGAAAGGAAGGGAAGAAAGCG

Key

Lba1 Primer	GCGATGGCCCACTACGTCAACCA
Forward Primer	ACAGCTTTCGGGATCTCAACTTCC

Figure 4.3 Sequence analysis of the *cat4* mutant. PCR on genomic DNA using the *cat4* forward primer and the T-DNA Lba1 primer (see figure 4.2 for primer locations). The product was sequenced using the two primers to confirm the presence of the T-DNA insert in the *CAT4* gene. The bold black sequence represents the DNA sequence from the forward primer, while the bold under-lined black (T-DNA) sequence, and the grey sequence (*CAT4*) represents the DNA sequence from the Lba1 sequence. The join between the grey and bold under-lined black bases represents the insertion site of the T-DNA confirming the presence of the T-DNA in *CAT4*. Introns are shown in lower case, while the exons and T-DNA insert is shown in capitals.

wild-type gene (F1 and R2) with products of 3099 and 1664 bps from genomic DNA (lane 4) and cDNA respectively were unsuccessful therefore the lanes show no product in both wild-type (lane 7) and mutant material (lane 10). A third set of primers (F1 and R1) were used to check for the presence of a truncated mRNA, producing 610 and 494 bps products from genomic DNA (lane 3) and cDNA (lane 6) respectively. The *cat4* mutant shows a truncated mRNA upstream of the T-DNA insertion (lane 10), indicating that a possible truncated protein could be produced. The template was replaced with water using all three primer combinations to eliminate the possibility of sample contamination (lanes 11-13). A control *ACTIN2* product was amplified from all cDNA samples (result not shown).

4.2.3 Phenotypic characterization of the *cat4* mutant

Once the parent plant had been confirmed as homozygote, progeny were grown under different light treatments and their phenotype was recorded. Wild-type (Col-8) and *cat4* seedlings were grown under the following light treatments: dark, white, red, blue and FR-light. Hypocotyl length was measured in all light treatments and cotyledon area for white, blue and red light-grown seedlings. The apical hook angle of dark grown seedlings was also measured. *cat4* seedlings grown in continuous darkness show a significant ($P<0.005$) increase in apical hook angle and also a small decrease in the hypocotyl length ($P<0.005$) compared to Col-8 (Figure 4.4A). FR-light grown *cat4* seedlings show no difference to wild-type in hypocotyl length (Figure 4.4B). The *cat4* mutant also shows no significant difference to wild-type in either hypocotyl length or cotyledon area in either white, red or blue light (Figure 4.5).

The phenotype of the *cat4* mutant was also monitored and recorded throughout the whole development of the mutant to the onset of senescence. The mutant showed no significant difference compared to wild-type in rosette diameter (Figure 4.6A and D) but did show a small decrease in height over its developmental program (Figure 4.6B and E). Compared to wild-type, *cat4* also showed no significant difference regarding timing of the first bolt, flower or silique (Figure 4.6C), or in the number of leaves at first bolt, the number of bolts at senescence and the total number of leaves (results not shown).

A) Dark

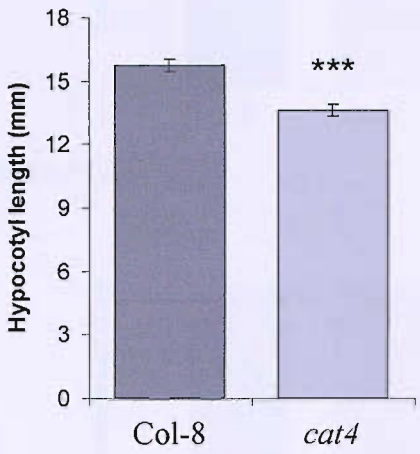

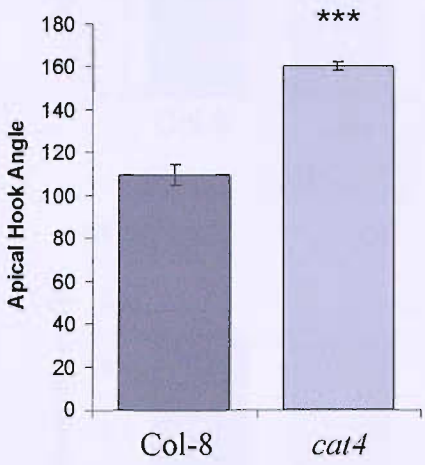

B) FR-light

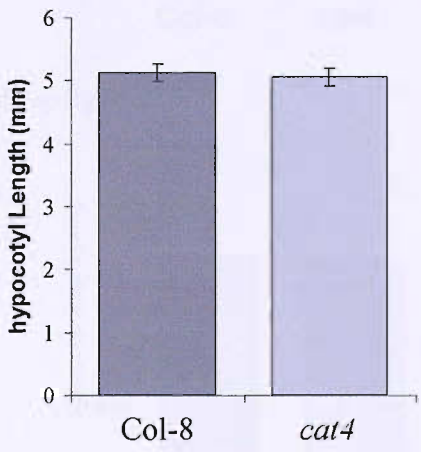

Figure 4.4 Analysis of the *cat4* mutant seedlings grown in the dark and FR-light.
A) Hypocotyl length and apical hook angle comparing wild-type (Col-8) to *cat4* (N567045) in the dark. The hypocotyl length of the dark grown seedling is significantly shorter than wild-type and the apical hook angle is significantly less hooked than wild-type. B) Hypocotyl length comparing Col-0 and *cat4* in FR-light. All graphs show the mean ± standard error, n = 30. Data shown represents one biological repeat. Identical results were shown in a second repeat. Scale bar of the photographs = 5mm. Significant levels are shown with *** ($P<0.005$).

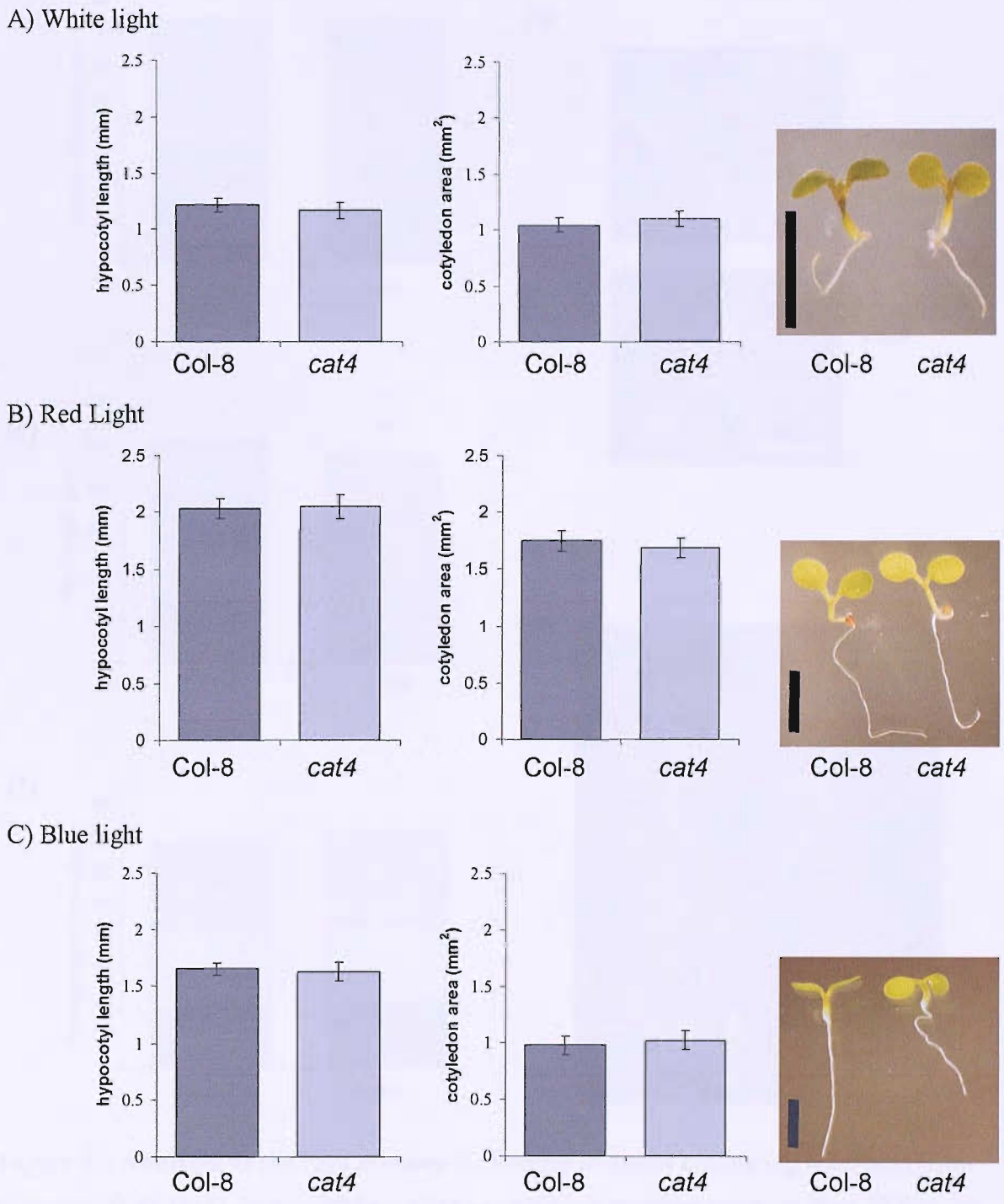

Figure 4.5 Analysis of the *cat4* mutant seedlings grown in white, red and blue-light. Hypocotyl length and cotyledon area comparing wild-type (Col-8) to *cat4* (N567045) in, A) white light, B) red light and C) blue light. All graphs show the mean ± standard error, n = 30. Data shown represents one biological repeat. Identical results were shown in a second repeat. Scale bar of the photographs = 2mm.

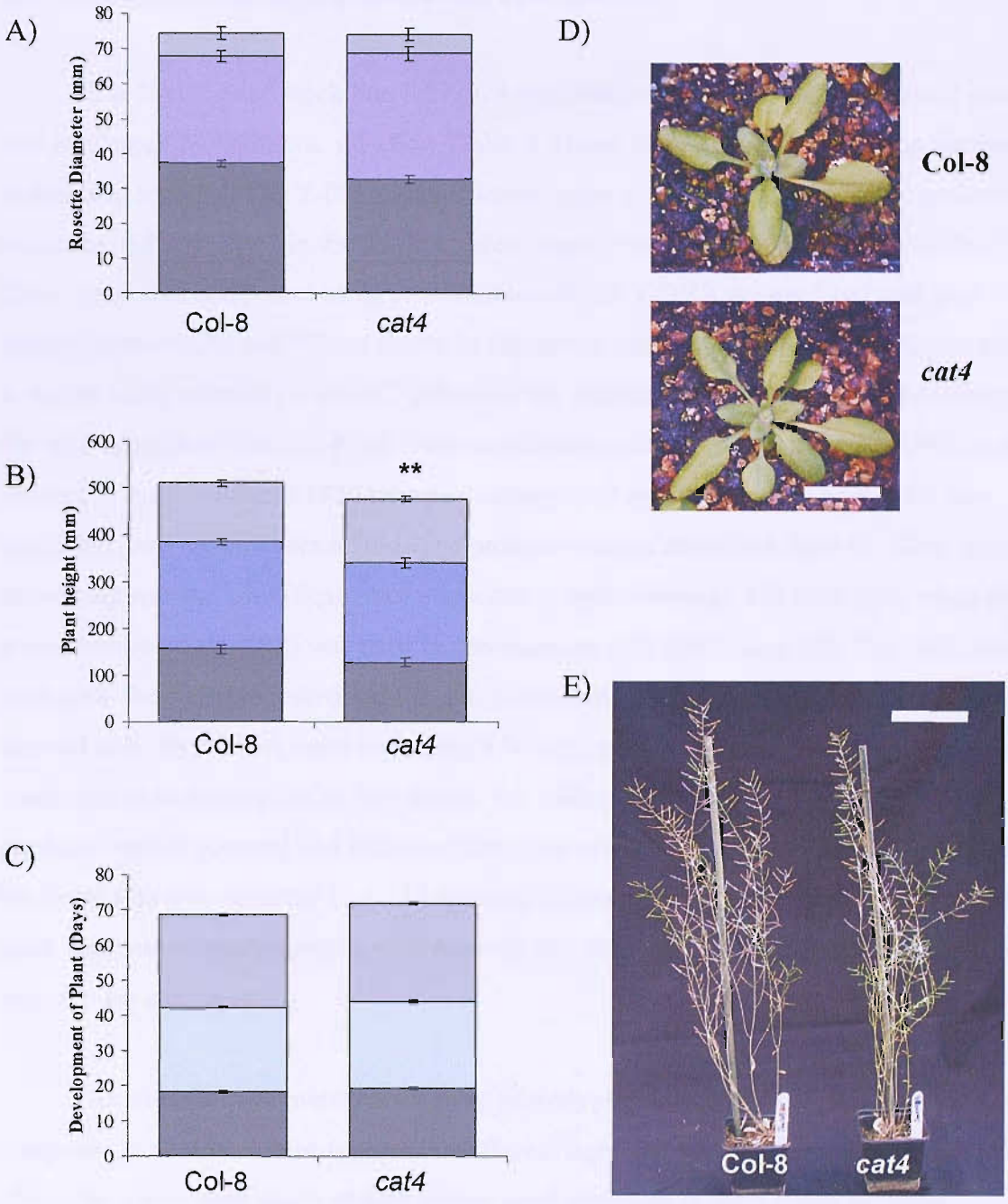

Figure 4.6 Analyses of the *cat4* mutant. A) Rosette diameter comparing wild-type (Col-8) to *cat4* (N567045), at days 17 (■), 25 (■) and 32 (■). B) Plant height at days 25 (■), 32 (■) and 50 (■). *cat4* is significantly shorter than wild-type at all three time points. C) Development of plant, showing day of first bolt (■), flower (■) and silique (■). All graphs show mean ± standard error of n = 20, of one biological repeat. D) Photographs of Col-8 and *cat4* at day 17, scale bar of photographs = 10 mm and E) day 50, scale = 10 cm. Significant levels are shown with **($P<0.01$).

4.2.4 Phenotypic characterization of the *aca2* mutant

The SALK seed stock line N572624 was obtained and a homozygous *aca2* mutant was confirmed by antibiotic selection (Table 4.3) and PCR (Figure 4.7A) using the same methods as for *cat4*. The T-DNA is positioned in the reverse orientation to the genomic sequence and is situated in the third of seven exons (Figure 4.8). The location of the T-DNA insert was confirmed using combinations of the T-DNA primer Lba1 and gene specific primers (F2 and R2) as shown in Figure 4.8 and Table 2.4. A 990 base pair product is shown using primers F2 and R2 indicating the presence of a wild-type band as shown by the wild-type plant (lane 2). Plant 3 was confirmed as homozygous for the T-DNA as a product of approximately 1020 base pairs using Lba1 and the forward primer F2 was amplified (lane 9), however a wild-type product was not amplified (lane 8). What was interesting was the amplification of a product of approximately 475 base pairs when the gene-specific primer (R2) was used in combination with Lba1 (lane 10). This indicates as with *cat4*, the multiple insertion of inserts at the same position within the genome. Plant 3 showed only the T-DNA band indicating a homozygous plant, whereas plants 5 and 6 were confirmed as heterozygous as they shown the wild-type band and the insert band. The three products were sequenced and indicated that these primers were specific to *ACA2* and that the insert was truly inserted in *ACA2* resulting in loss-of-function. The zygosity of each plant was determined by segregation analysis and PCR and both methods predict the same zygosity for each plant.

As with the *cat4* mutant a seedling phenotypic analyses was undertaken with *aca2* compared to the Col-8 wild-type under different light treatments. The analyses showed no change in apical hook angle of dark grown *aca2* seedlings (Figure 4.9A) or in the hypocotyl lengths of dark or FR-grown seedlings (Figure 4.9A and B) compared to Col-8. However, white light grown *aca2* seedlings appeared significantly smaller than with-type in regards to hypocotyl length and cotyledon area ($P< 0.005$), (Figure 4.10A). A similar phenotype was shown for blue light-grown *aca2* seedlings ($P<0.005$), (Figure 4.10C). In addition the cotyledons of the *aca2* mutant grown under blue-light appeared folded downwards and the roots showed a curling phenotype around the hypocotyl. A wild-type phenotype was shown for the *aca2* mutant grown under red light (Figure 4.10B).

Table 4.3 Predicted parent plant zygosity of the *aca2* (N582624) and *stp1* (N548818) T-DNA mutants using antiobiotic selection. The survival rate of progeny of 10 putative *ACA2* and *STP1* T-DNA mutants and wild-type (Col-8) visually assessed by percentage survival on MS agar plates with and without kanamycin (100 μg/ml) at 10 days post germination. The predicted zygosity of the parent plant is given.

ACA2	Number and Percentage survival (Kan +)	(Kan -)	Predicted Zygosity of parent plant
Plant 1	39/51 (76%)	51/51 (100%)	Heterozygote
Plant 2	39/50 (76%)	50/50 (100%)	Heterozygote
Plant 3	52/52 (100%)	52/52 (100%)	Homozygote
Plant 4	0/53 (0%)	53/53 (100%)	Wild-type
Plant 5	38/50 (77%)	49/49 (100%)	Heterozygote
Plant 6	37/48 (77%)	49/50 (98)	Heterozygote
Plant 7	39/52 (75%)	53/53 (100%)	Heterozygote
Plant 8	39/54 (72%)	50/50 (100%)	Heterozygote
Plant 9	52/52 (100%)	49/49 (100%)	Homozygote
Plant 10	37/51(73%)	52/52 (100%)	Heterozygote
Col-8	0/50 (100%)	50/50 (100%)	Wild-type

STP1	Number and Percentage survival (Kan +)	(Kan -)	Predicted Zygosity of parent plant
Plant 1	50/50 (76%)	50/50 (100%)	Homozygous plant
Plant 2	50/50 (100%)	51/51 (100%)	Homozygous plant
Plant 3	38/50 (76%)	56/56 (100%)	Heterozygous plant
Plant 4	51/51 (100%)	55/55 (100%)	Homozygous plant
Plant 5	38/51 (77%)	51/51 (100%)	Heterozygous plant
Plant 6	57/57 (100%)	52/52 (100%)	Homozygous plant
Plant 7	54/54 (100%)	51/51 (100%)	Homozygous plant
Plant 8	53/53 (100%)	50/50 (100%)	Homozygous plant
Plant 9	50/52 (96%)	49/49 (100%)	(Unknown genotype)
Plant 10	54/54 (0%)	51/51 (100%)	Homozygous plant
Col-8	0/53 (0%)	51/51 (100%)	Wild-type

A) *aca2*

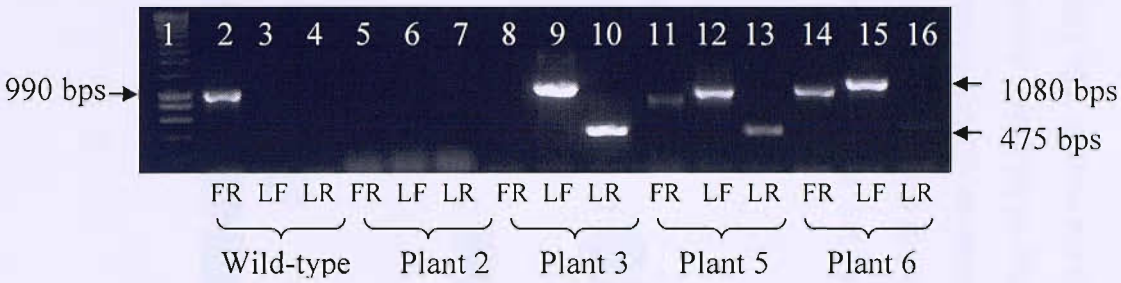

B) *stp1*

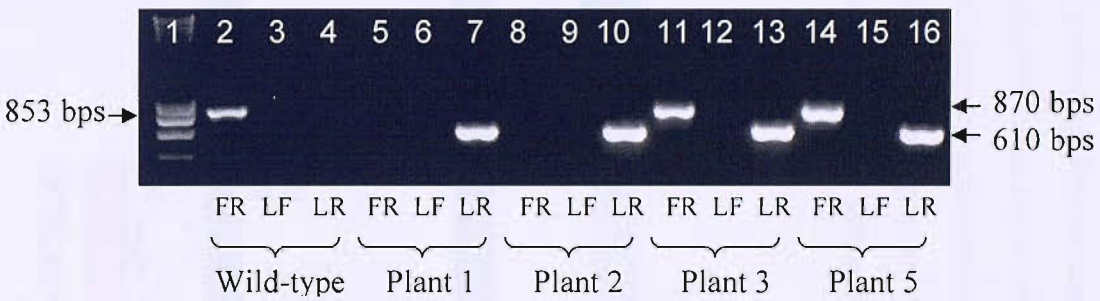

Figure 4.7 Identification of homozygous *aca2* and *stp1* mutants. PCR on genomic DNA extracted from wild-type (Col-0) and 4 potential T-DNA mutants for A) *ACA2*, Three primer pair combinations were used to identify the genotype of each putative *aca2* mutant, gene specific forward primer (F2), gene specific reverse primer (R2) and a T-DNA left border primer (L). Refer to Figure 4.8 for the location of the primers. B) STP1, the following combinations of primers were used to genotype each *stp1* mutant, gene specific forward primer (F2), gene specific reverse primer (R2) and a T-DNA left border primer (L). Refer to Figure 4.12 for the location of the primers. Lane 1 on both gels represents the molecular marker.

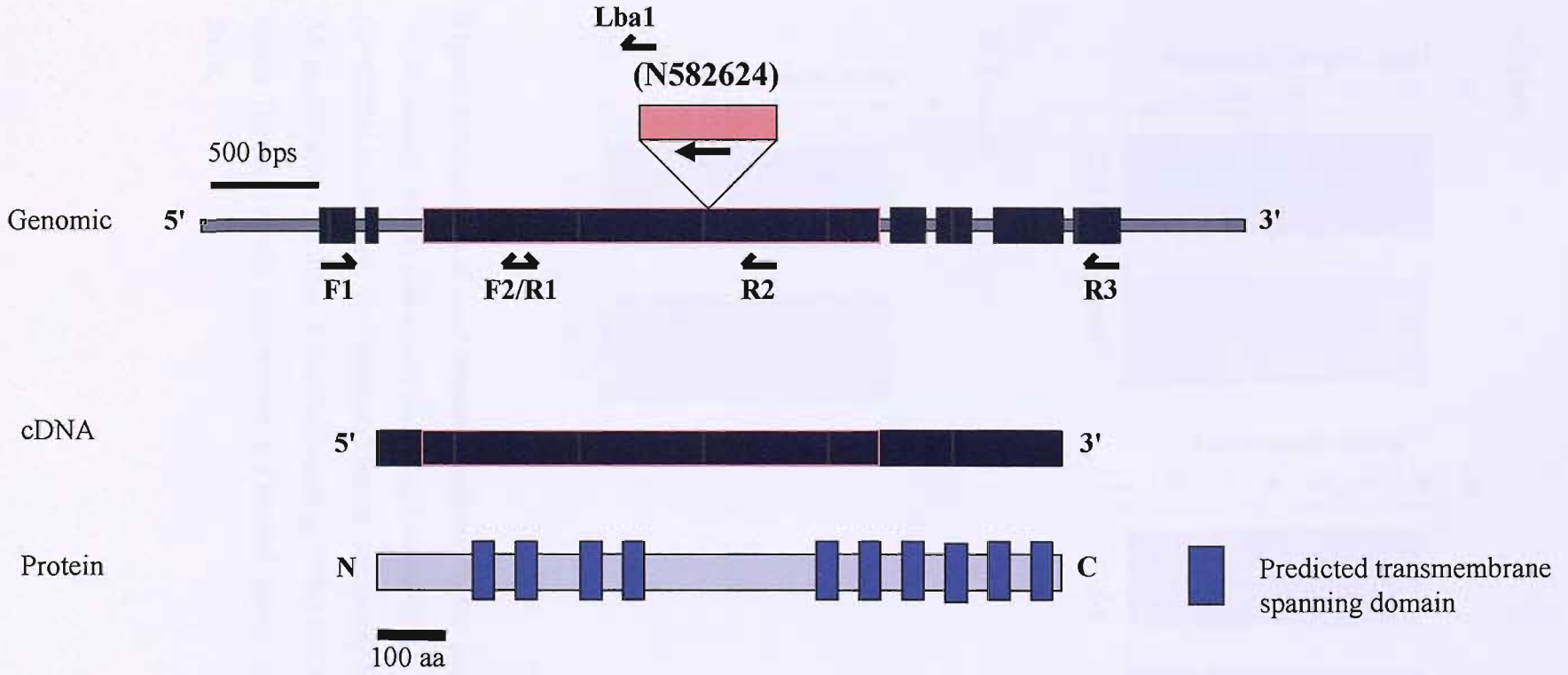

Figure 4.8 Schematic representation of the genomic, cDNA and protein sequences of ACA2, indicating the location of the T-DNA insertion. The T-DNA insertion of the mutant (N582624) is located in the centre of the third of seven exons, which is in the large cytoplasmic loop of the protein between the fourth and fifth of ten predicted transmembrane spanning domains (TMS). Locations of TMS were predicted using hydrophobicity plots. The T-DNA sequence is inserted in the reverse complementation to the gene. Arrows shown indicate the location of primers designed to confirm the presence of the T-DNA insert and the absence of mRNA in the mutant. The Lba1 primer is designed within the T-DNA insert and is used to identify the presence of the insert. T-DNA insert not to scale.

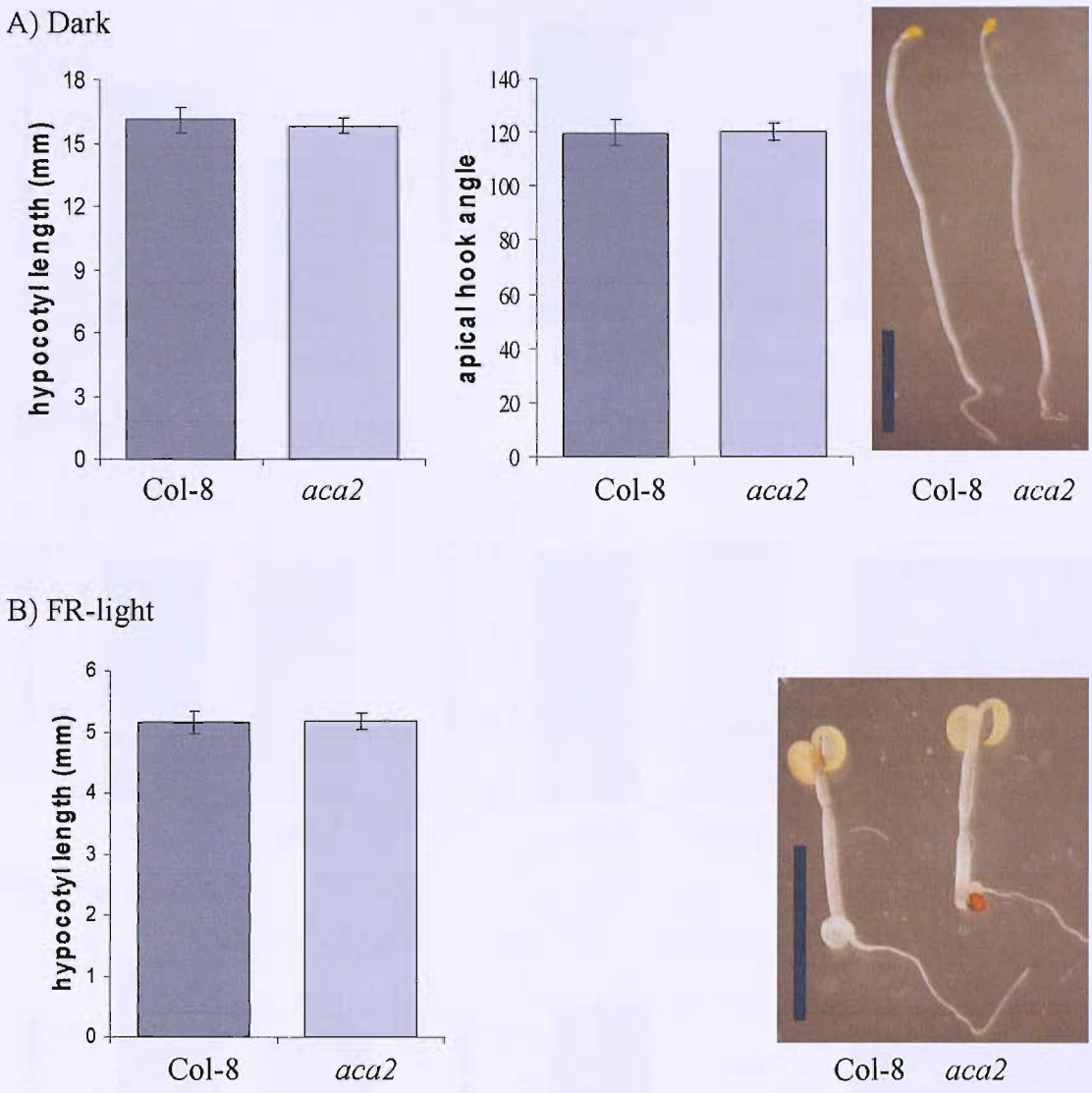

Figure 4.9 Analysis of *aca2* mutant seedlings in the dark and FR-light.

A) Hypocotyl length and apical hook angle comparing wild-type (Col-8) to *aca2* (N582624) in the dark. B) Hypocotyl length comparing Col-0 and *aca2* in far-red light. All graphs show the mean ± standard error, n = 30. Data shown represents one biological repeat. Identical results were shown in a second repeat. Scale bar of the photographs = 5mm.

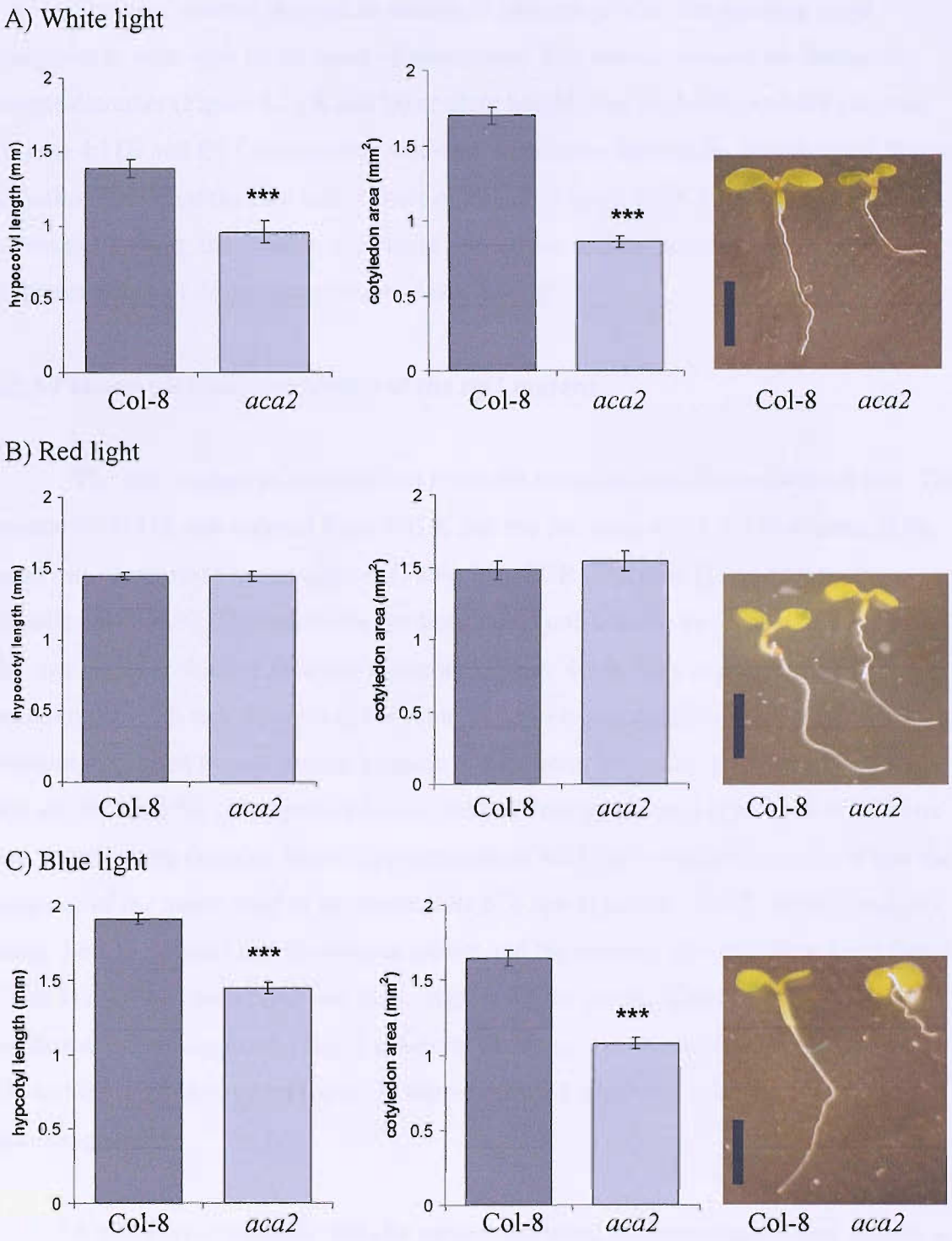

Figure 4.10 Analysis of the *aca2* mutant seedling in white, red and blue-light.
Hypocotyl length and cotyledon area comparing wild-type (Col-8) to *aca2* (N582624) in, A) white light, B) red light and C) blue light. The hypocotyl length and cotyledon area of *aca2* was significantly smaller than wild-type All graphs show the mean ± standard error, n = 30. Data shown represents one biological repeat. Scale bar of the photographs = 2mm. Significance levels are shown with ***(P< 0.005).

The *aca2* mutant showed no change in phenotype after the seedling stage compared to wild-type to the onset of senescence. The mutant showed no change in rosette diameter (Figure 4.11A and D) or plant height over its developmental program (Figure 4.11B and E). Compared to wild-type, *aca2* also showed no significant difference regarding timing of the first bolt, flower or silique (Figure 4.11C), or in the number of leaves at first bolt, the number of bolts at senescence and the number of leaves at different stages of development (results not shown).

4.2.5 Phenotypic characterization of the *stp1* mutant

The next mutant to be identified is for the monosaccharide transporter STP1. The mutant N548818 was ordered from SALK and the presence of the T-DNA insert in the gene was confirmed via segregation (Table 4.3), PCR (Figure 4.7) and sequencing (results not shown). The insert was predicted and confirmed to be located in the third of the four exons within the genomic sequence (Figure 4.12). This is predicted to be between the tenth and eleventh of the proteins twelve transmembrane spanning domains. Primers were used to confirm the location of the insert, including gene specific primers (F2 and R2) and the insert primer Lba1. The presence of the wild-type band of 853 bps was shown using the gene specific primers with a wild-type template (lane 2). While the presence of the insert band of approximately 610 bps in plants 1 and 2 (lanes 7 and 10) using the Lba1 primer and the reverse primer and the absence of a wild-type band (lanes 5 and 8) indicated both plants are homozygous for the insert. While plants 1 and 2 were confirmed as homozygous, plant 3 is heterozygous as both the wild-type product (lane 11) and the T-DNA product (lane 13) were amplified. Plant 5 was also shown to be heterozygous.

A phenotypic analysis was also carried out using the homozygous *stp1* mutant at both the seedling and mature plant level and compared to the Col-8 wild-type. The seedling phenotypic analysis showed no change in apical hook angle or hypocotyl length of the etiolated seedling or in hypocotyl length of the FR-light grown *stp1* seedling compared to wild-type (Figure 4.13). A wild-type phenotype was shown in regard to hypocotyl length and cotyledon area of white, red or blue light grown *stp1* seedlings (Figure 4.14).

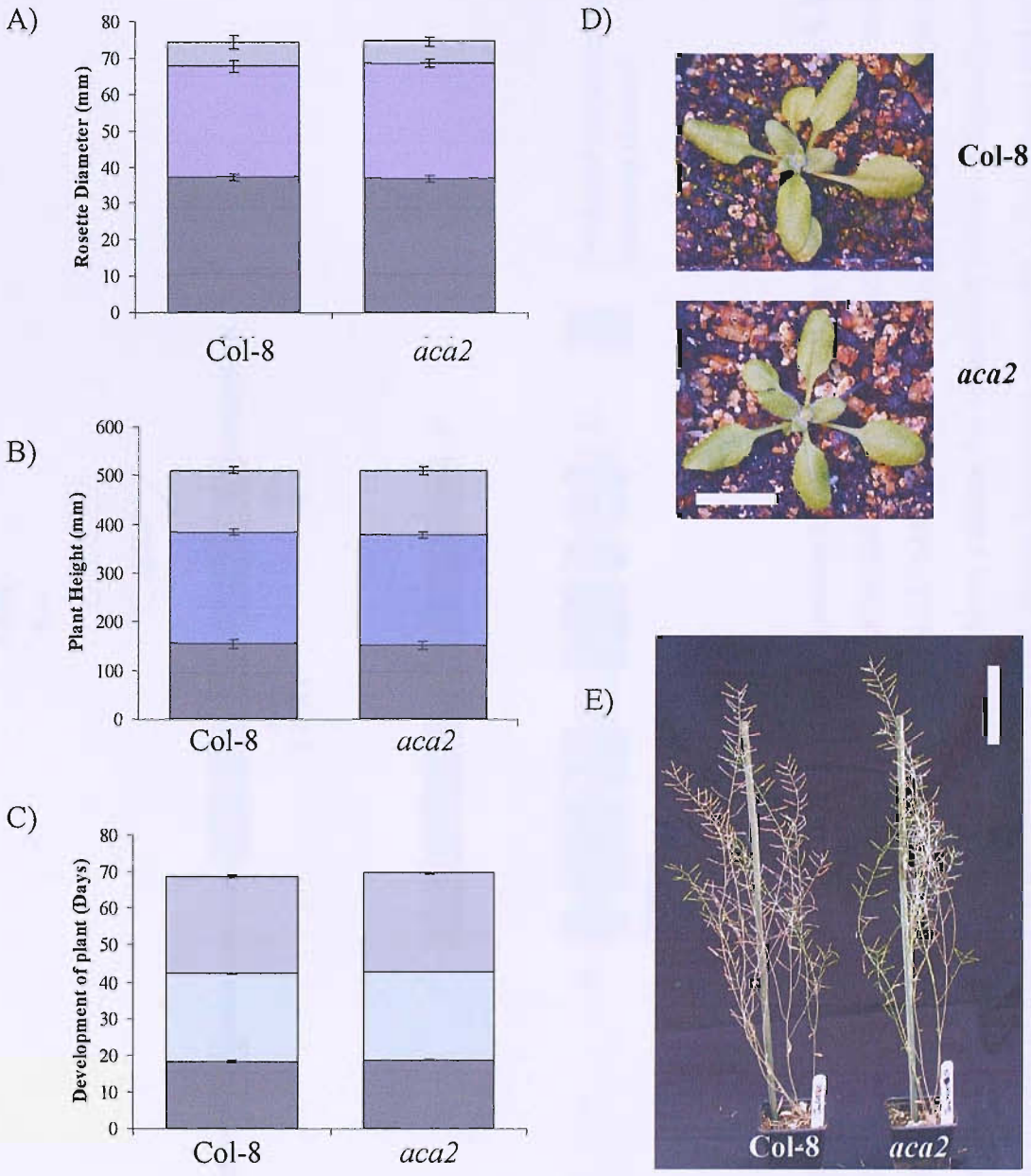

Figure 4.11 Analyses of *aca2* mutant. A) Rosette diameter comparing wild-type (Col-8) to *aca2* (N582624), at days 17 (■), 25 (■) and 32 (■). B) Plant height at days 25 (■), 32 (■) and 50 (■). C) Development of plant, showing day of first bolt (■), flower (■) and silique (■).All graphs show mean ± standard error of n = 20, of one biological repeat. D) Photographs of Col-8 and *aca2* at day 17, scale = 10 mm and E) day 50, scale = 10 cm.

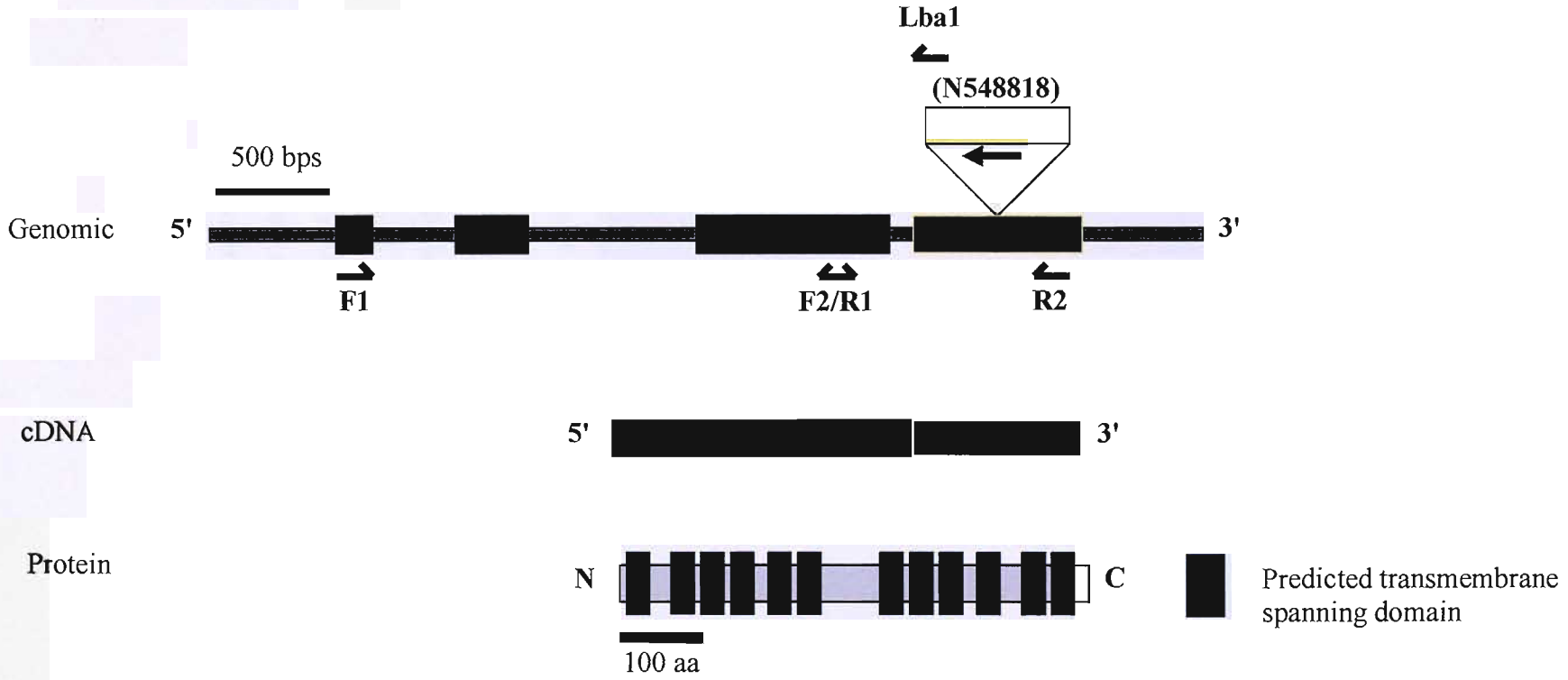

Figure 4.12 Schematic representation of the genomic, cDNA and protein sequences of STP1, indicating the location of the T-DNA insertion. The T-DNA insertion of the mutant (N548818) is located in the start of the last of four exons, which is in between the tenth and eleventh of twelve predicted transmembrane spanning domains (TMS). Locations of TMS were predicted using hydrophobicity plots. The T-DNA sequence is inserted in the reverse complementation to the gene. Arrows shown indicate the location of primers designed to confirm the presence of the T-DNA insert and the absence of mRNA in the mutant. The Lba1 primer is designed within the T-DNA insert and is used to identify the presence of the insert. T-DNA insert not to scale.

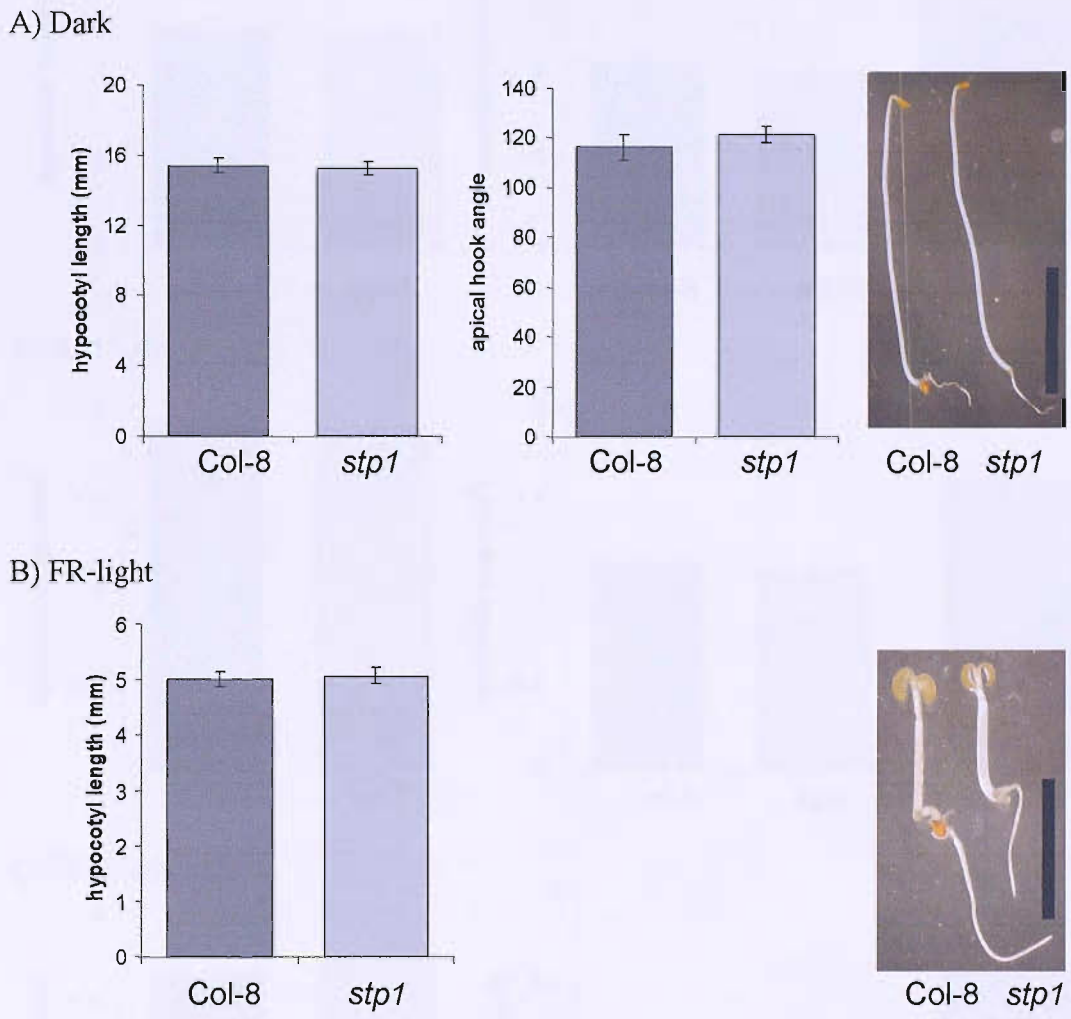

Figure 4.13 Analysis of the *stp1* mutant seedling in the dark and FR-light.

A) Hypocotyl length and apical hook angle comparing wild-type (Col-8) to *stp1* (N548818) in the dark. B) Hypocotyl length comparing Col-0 and *stp1* in FR-light. All graphs show the mean ± standard error, n = 30. Data shown represents one biological repeat. Identical results were shown in a second repeat. Scale bar of the photographs = 5mm.

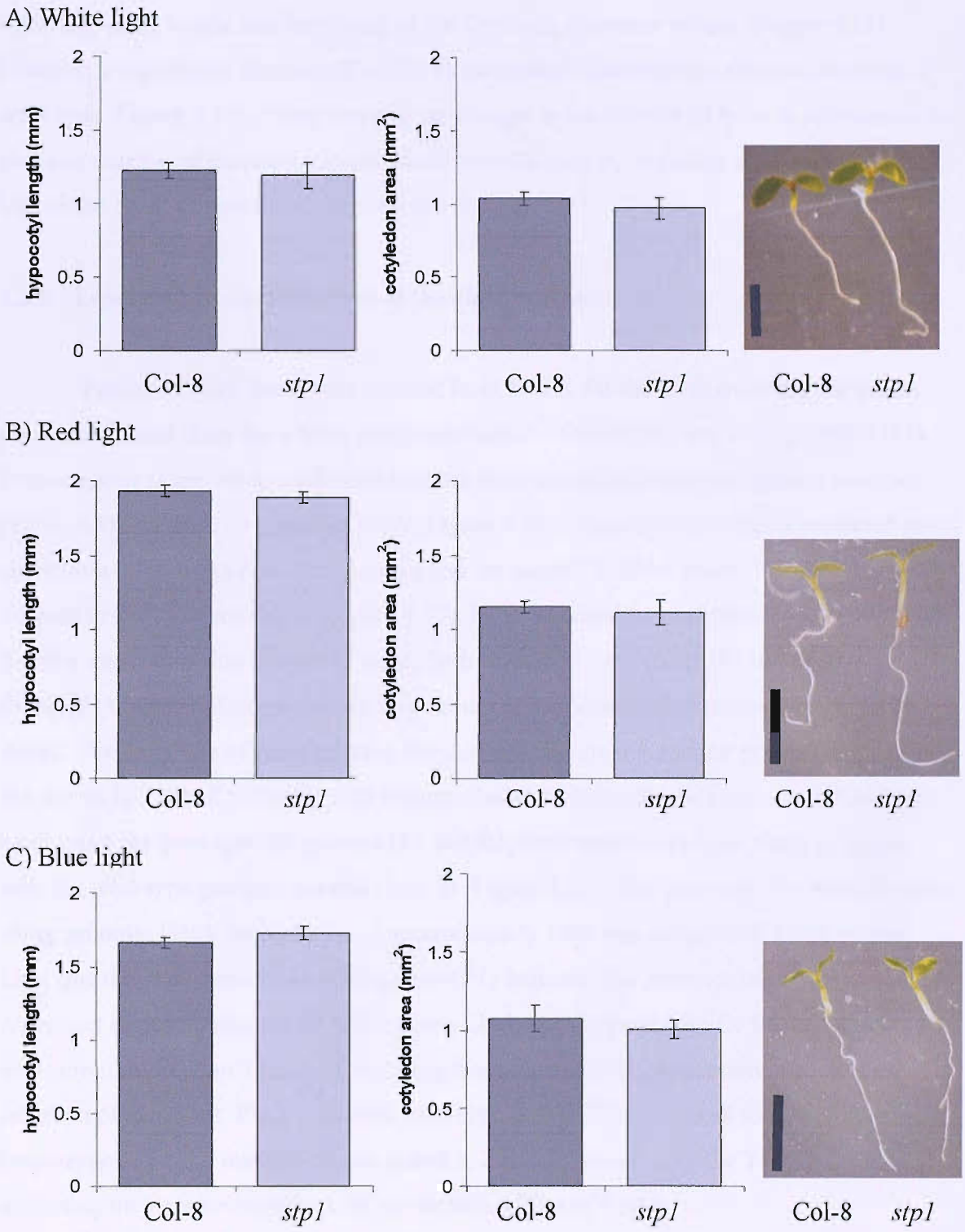

Figure 4.14 Analysis of the *stp1* mutant seedling in white, red and blue-light.
Hypocotyl length and cotyledon area comparing wild-type (Col-8) to *stp1* (N548818) in, A) white light, B) red light and C) blue light. All graphs show the mean ± standard error, n = 30. Data shown represents one biological repeat. Scale bar of the photographs = 2mm.

The *stp1* mutant showed a wild-type phenotype in most developmental aspects including plant height and the timing of the first bolt, flower or silique (Figure 4.15). However a significant decrease ($P<0.05$) in the rosette diameter was shown compared to wild-type (Figure 4.15). There was also no change in the number of bolts at senescence or the total number of leaves at various developmental stages, including at the time of first bolt or the onset of senescence (results not shown).

4.2.6 Phenotypic characterization of the *aha2* mutants

Two seed stock lines were ordered from SALK for the gene encoding the proton pump *AHA2* and these have been designated, *aha2-1* (N622010) and *aha2-2* (N562371). Homozygous plants were confirmed for both lines using antibiotic segregation analyses (Table 4.4) and PCR on genomic DNA (Figure 4.16). Line N622010 had a predicted insert site within the fourth of its fifteen exons and the second T-DNA insert (N562371) is situated in the thirteenth exon (Figure 4.17). PCR was used to confirm the location of both T-DNA mutants within the *AHA2* gene. Both lines, *aha2-1* (N622010) and *aha2-1* (N562371) were confirmed as homozygous using combinations of primers designed to *AHA2*. The locations of these primers are shown in Figure 4.7 and the primers sequences are shown in Table 2.5. Firstly with mutant *aha2-1* (N622010), the presence of 1242 bp band using the gene specific primers (F1 and R1) indicates a wild-type plant, as shown with the wild-type genomic sample (lane 2) (Figure 4.17). The presence of a weak product using genomic DNA from plant 1 of approximately 1000 bps using the T-DNA primer Lba1 and the gene specific forward primer (F1) indicates the presence of the insert (lane 6). A product of approximately 1020 bps using Lba1 and the gene specific forward primer was also amplified in plant 1 (lane 7), resulting from the possible duplication or multiple insertion of the insert. Plant 3 showed wild-type and T-DNA products so is therefore heterozygous for the insert, whereas plants 1, 2 and 5 showed only the T-DNA band indicating they are homozygous for the mutation (Figure 4.6A).

Due to the location of the second insert (N562371) a different set of gene specific primers were used to confirm the zygosity of the plant. The F2 and R2 primers located towards the 3' of the gene were used as shown in Figure 4.16 and Table 2.5. A wild-type product of 996 bps was shown using the gene specific F2 and R2 primers in the wild-type

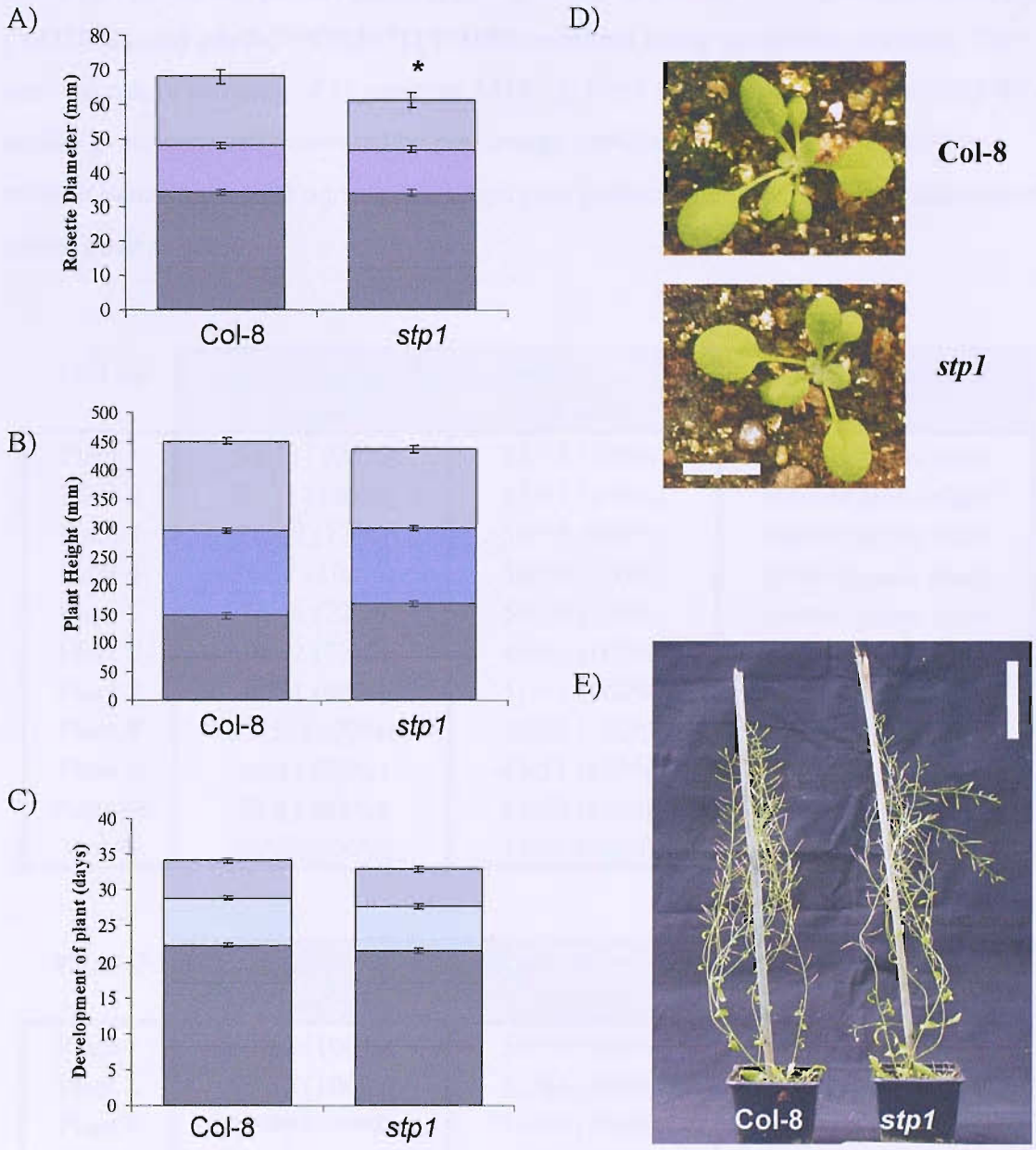

Figure 4.15 Analyses of *stp1* mutant. A) Rosette diameter comparing wild-type (Col-8) to *stp1* (N548818), at days 20 (■), 28 (■) and 35 (■). The rosette diameter of *stp1* is significantly smaller than wild-type by 35 days (P = <0.05). B) Plant height at days 32 (■), 42 (■) and 60 (■). C) Development of plant, showing day of first bolt (■), flower (■) and silique (■).All graphs show mean ± standard error of n = 20 of one biological repeat D) Photographs of Col-8 and *stp1* at day 20, scale = 10 mm and E) day 60, scale = 10 cm.

Table 4.4 Predicted parent plant zygosity of the two *aha2* T-DNA mutants *aha2-1* (N622010) and *aha2-2* (N562371) T-DNA mutants using antibiotic selection. The survival rate of progeny of 10 putative AHA2 T-DNA mutants and wild-type (Col-8) seedlings were visually assessed by percentage survival on MS agar plates with and without kanamycin (100 μg/ml) at 10 days post germination. The predicted zygosity of the parent plant is given.

AHA2-1	Number and Percentage survival (Kan +)	(Kan -)	Predicted Zygosity
Plant 1	50/50 (100%)	54/54 (100%)	Homozygous plant
Plant 2	51/51 (100%)	51/51 (100%)	Homozygous plant
Plant 3	36/49 (77%)	50/50 (100%)	Heterozygous plant
Plant 4	51/51 (100%)	50/50 (100%)	Homozygous plant
Plant 5	37/48 (77%)	50/50 (100%)	Heterozygous plant
Plant 6	39/52 (75%)	49/49 (100%)	Heterozygous plant
Plant 7	46/51 (90%)	51/51 (100%)	Unknown
Plant 8	53/53 (100%)	50/50 (100%)	Homozygous plant
Plant 9	39/51 (77%)	51/51 (100%)	Heterozygous plant
Plant 10	32/51 (63%)	53/53 (100%)	Unknown
Col-8	55/55 (100%)	51/51 (100%)	Wild-type

AHA2-2	Number and Percentage survival (Kan +)	(Kan -)	Predicted Zygosity
Plant 1	52/52 (100%)	50/50 (100%)	Homozygous plant
Plant 2	50/50 (100%)	52/52 (100%)	Homozygous plant
Plant 3	49/49 (100%)	53/53 (100%)	Homozygous plant
Plant 4	51/51 (100%)	51/51 (100%)	Homozygous plant
Plant 5	37/48 (77%)	49/49 (100%)	Heterozygous plant
Plant 6	39/52 (75%)	49/50 (98)	Heterozygous plant
Plant 7	37/51(73%)	51/51 (100%)	Heterozygous plant
Plant 8	50 (100%)	50/50 (100%)	Homozygous plant
Plant 9	37/48 (77%)	49/50 (98)	Heterozygous plant
Plant 10	37/51(73%)	50/50 (100%)	Heterozygous plant
Col-8	52/52 (100%)	50 (100%)	Wild-type

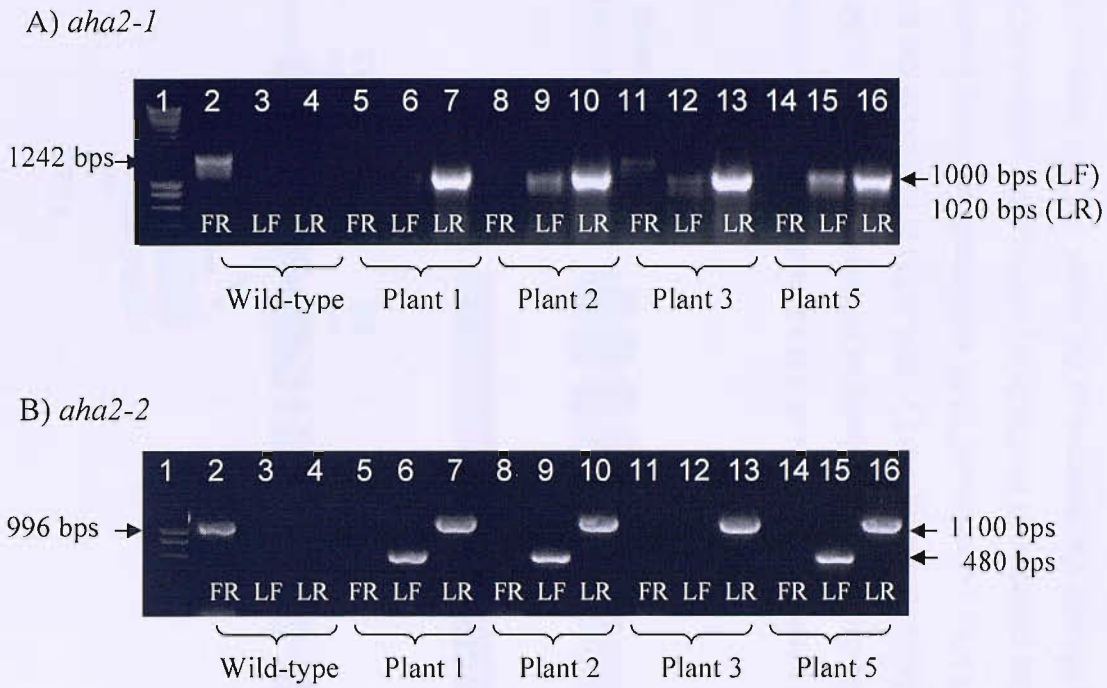

Figure 4.16 Identification of two homozygous *aha2* mutants. PCR on genomic DNA extracted from wild-type (Col-0) and 4 potential T-DNA mutants for two different AHA2 lines for A) *aha2-1* (N622010) and B) *aha2-2* (N562371).Three primer pair combinations were used to identify the genotype of each putative *aha2* mutant. In the case of mutant N622010 the gene specific forward primer (F1), gene specific reverse primer (R1) and a T-DNA left border primer (L). Whereas for mutant N562371 situated further towards the 3' of the gene different gene specific primers (F2 and R2) were used with Lba1. Refer to figure 4.7 for the location of the primers. B) STP1, the following combinations of primers were used to genotype each *stp1* mutant, gene specific forward primer (F2), gene specific reverse primer (R2) and a T-DNA left border primer (L). Refer to Figure 4.17 for the location of the primers. Lane 1 on both gels represents the molecular marker.

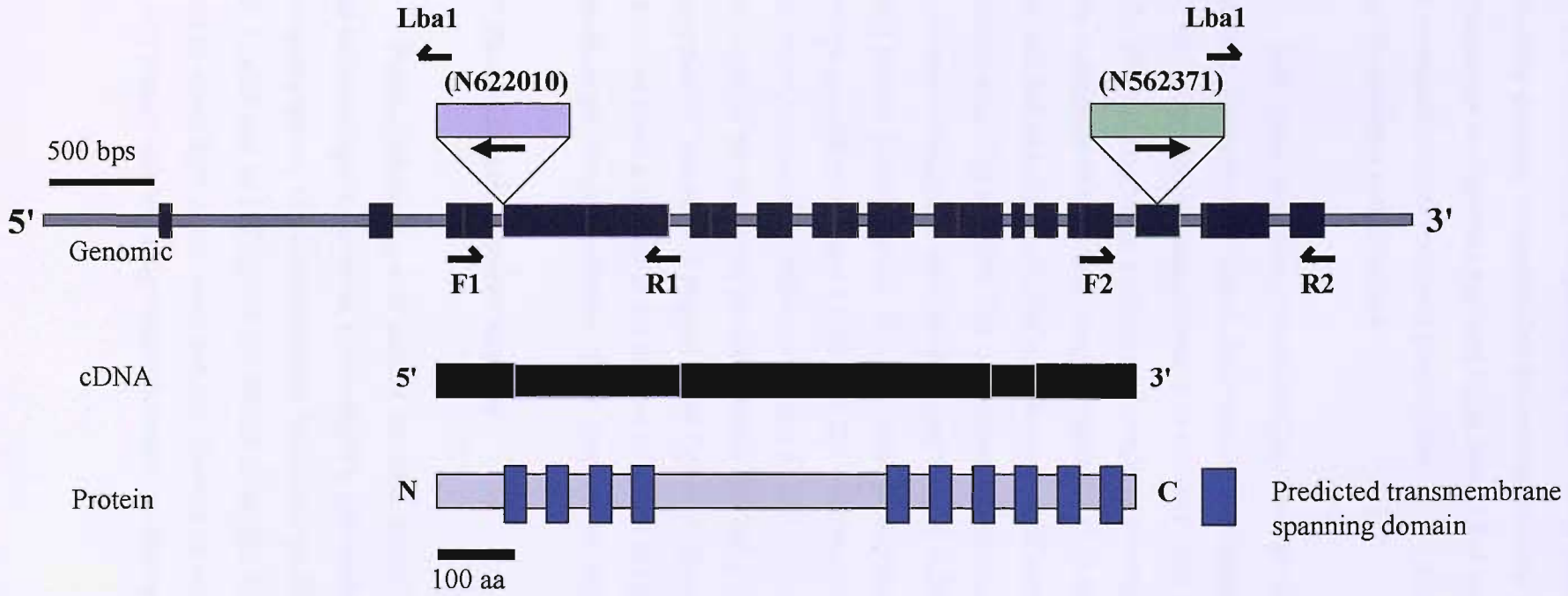

Figure 4.17 Schematic representation of the genomic, cDNA and protein sequences of AHA2, indicating the location of the two T-DNA insertions. The first T-DNA insertion, *aha2.1* (N622010) is located at the start of the fourth of fifteen exons, which is therefore before the first of the 8 predicted transmembrane spanning domains. The second T-DNA insertion, *aha2.2* (N562371) is located in the thirteenth exon, which is predicted to be between transmembrane spanning domains 5 and 6 (TMS). Locations of TMS were predicted using hydrophobicity plots. Arrows shown indicate the location of primers designed to confirm the presence of the T-DNA insert and the absence of mRNA in the mutant. The Lba1 primer is designed within the T-DNA insert and is used to identify the presence of the insert. T-DNA inserts not to scale.

plant (lane 1) (Figure 4.6B). A presence of a product of approximately 1100 bps using Lba1 and R2 confirmed the presence of the T-DNA insert in plant 1 (lane 7). As with some of the other mutants, it appears that this mutant also had a double insertion or rearrangement as a product was amplified using Lba1 and the F2 reverse primer (lane 6). PCR revealed both heterozygous plants (plant 3) and homozygous plants (plants 1, 2 and 5) using these primer combinations.

Both *aha2* lines were plated with Col-8 and grown under the different light treatments. There was no change in the apical hook angle or hypocotyl length of either *aha2* line grown in darkness compared to Col-8 (Figure 4.18). When grown under FR-light *aha2-1* showed no change in hypocotyl length compared to wild-type, however *aha2-2* shows a decrease in hypocotyl length (Figure 4.18). Both *aha2* lines were also grown under white, red and blue light, all of which showed no difference in hypocotyl length or cotyledon area (Figure 4.19). The phenotype of both *aha2* lines, N622010 and N562371 was recorded throughout their development (Figure 4.20). *aha2-2* showed a slightly smaller rosette diameter at 20, 28 and 35 days post germination, whereas *aha2-1* showed a wild-type phenotype (Figure 4.20A and D). Both mutant lines also showed an increase in plant height compared to wild-type at days 32 and 42, but by day 60 both mutants had the same height as the wild-type plant (Figure 4.20B and E). There is no change in the development of the plant in respect to the first bolt, flower or silique (Figure 4.20C). Neither was there a change in the number of leaves at the first bolt, the number of leaves at senescence, and the total number of bolt (results not shown).

4.2.7 Photosynthetic Pigment Analysis

Photosynthetic pigment content was also determined in the mutant seedlings grown under different light treatments. Chlorophyll a, chlorophyll b, total chlorophyll and total carotenoid pigment was determined per individual seedling in the different mutants, *cat4*, *aha2-1*, *aca2* and *stp1* (Figure 4.21). When these four homozygous mutant lines were grown in white light, *aha2*, *aca2* and *stp1* showed no change in pigment content, whereas the *cat4* mutant showed a significant decrease in chlorophyll and carotenoid content

A) Dark

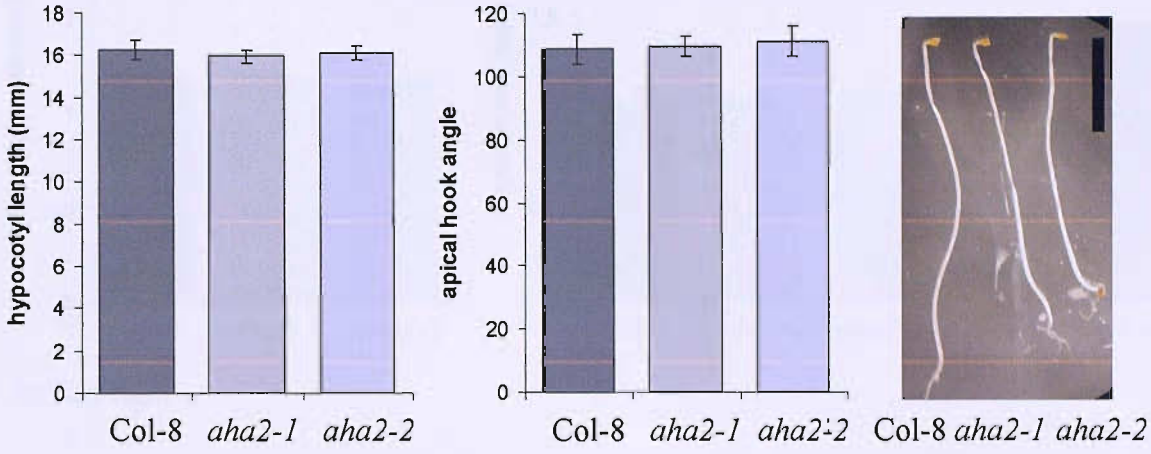

B) FR-light

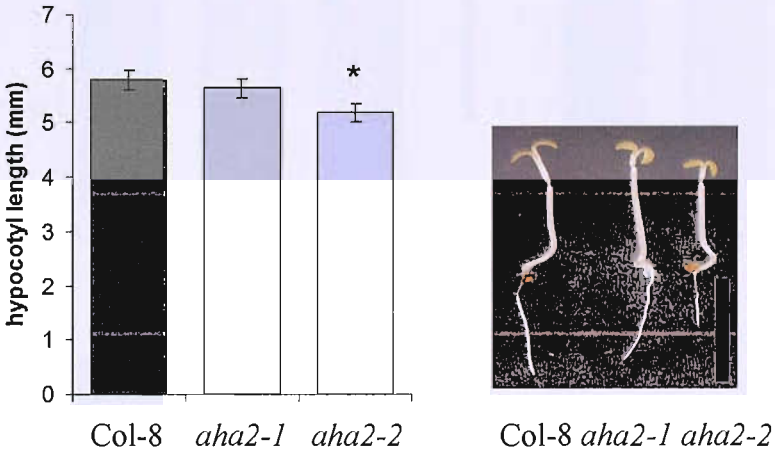

Figure 4.18 Analysis of two *aha2* mutant seedlings in dark and FR-light. A) Hypocotyl length and apical hook angle comparing wild-type (Col-8) to *aha2-1* (N622010) and *aha2-2* (N562371) in the dark. B) Hypocotyl length comparing Col-0 to *aha2-1* and *aha2-2* in FR-light. All graphs show the mean ± standard error, n = 30. Data shown represents one biological repeat. Identical results were shown in a second repeat. Scale bar of the photographs = 5mm. Significance levels are shown with *($P<0.05$).

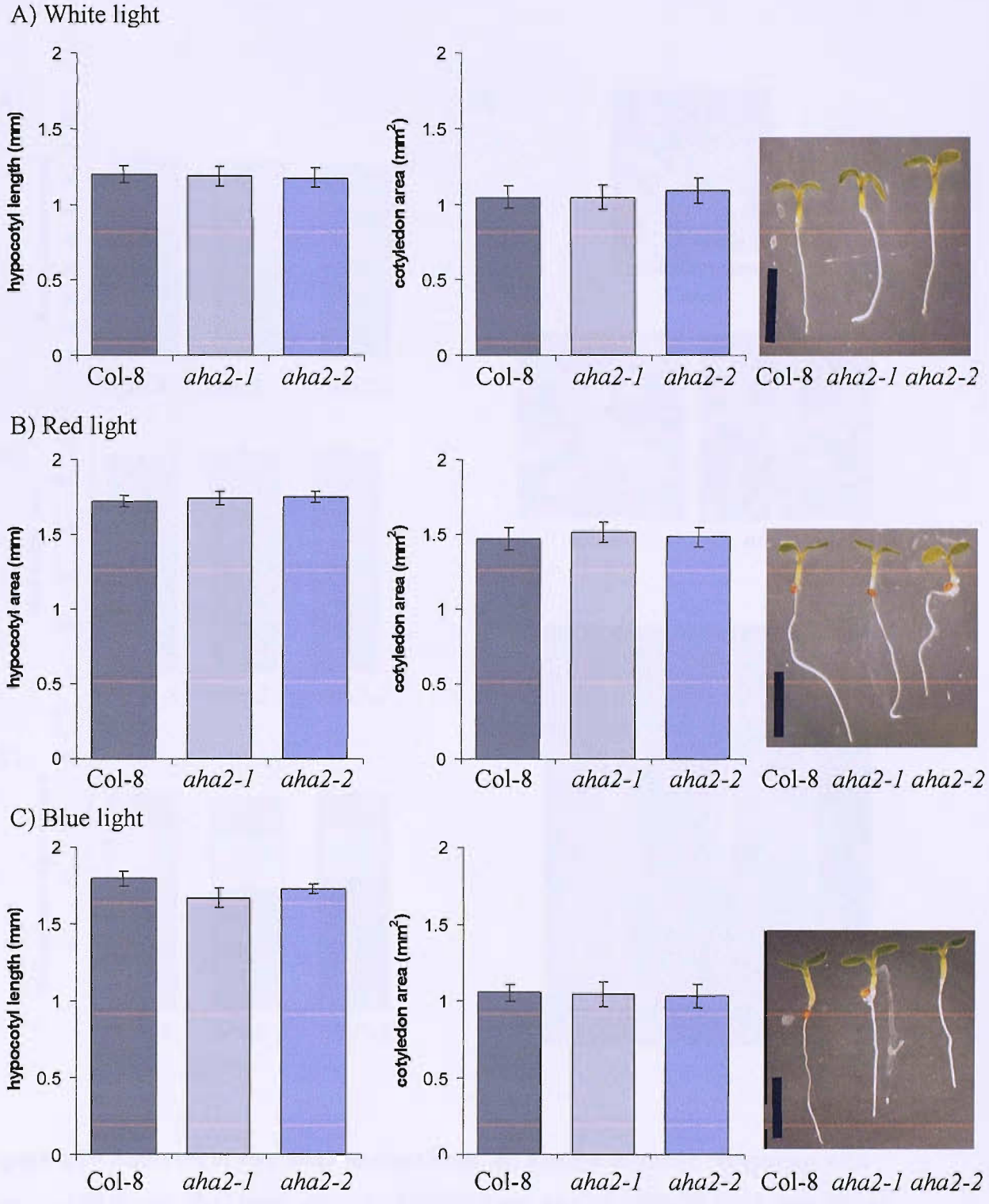

Figure 4.19 Analysis of two *aha2* mutant seedling in white, red and blue light.
Hypocotyl length and cotyledon area comparing wild-type (Col-8) to *aha2-1* (N622010) and *aha2-2* (N562371) in, A) white light, B) red light and C) blue light. All graphs show the mean ± standard error, n = 30. Data shown represents one biological repeat. Scale bar of the photographs = 2mm.

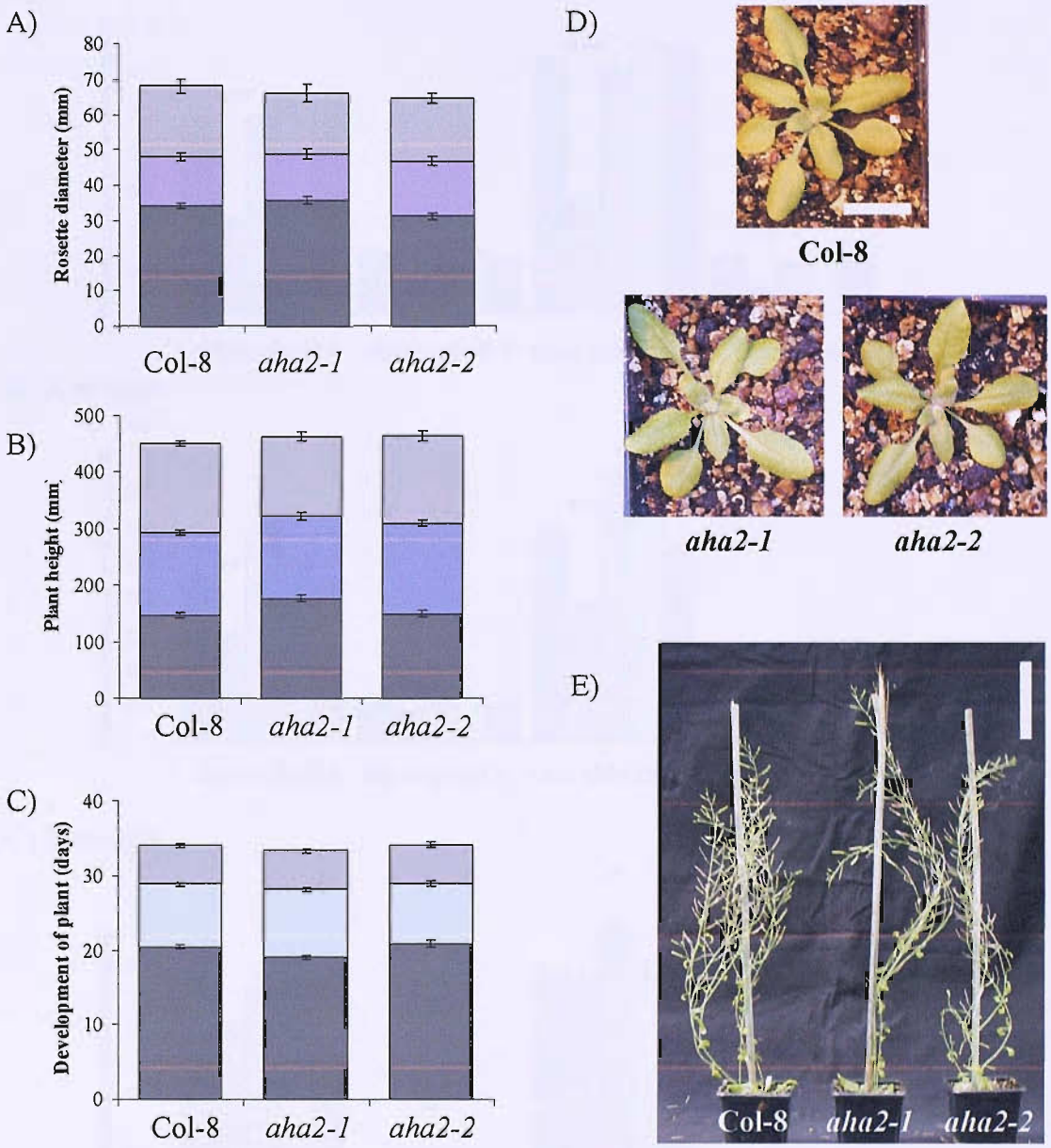

Figure 4.20 Analyses of two *aha2* mutant lines. A) Rosette diameter comparing wild-type (Col-8) to two *aha2* lines, *aha2-1* (N522010) and *aha2-2* (N562371), at days 20 (■), 28 (■) and 35 (■). B) Plant height at days 32 (■), 42 (■) and 60 (■). C) Development of plant, showing day of first bolt (■), flower (■) and silique (■).All graphs show mean ± standard error of n = 20, of one biological repeat. D) Photographs of Col-8, *aha2-1* and *aha2-2* at day 20, scale = 10 mm and E) day 60, scale = 10 cm.

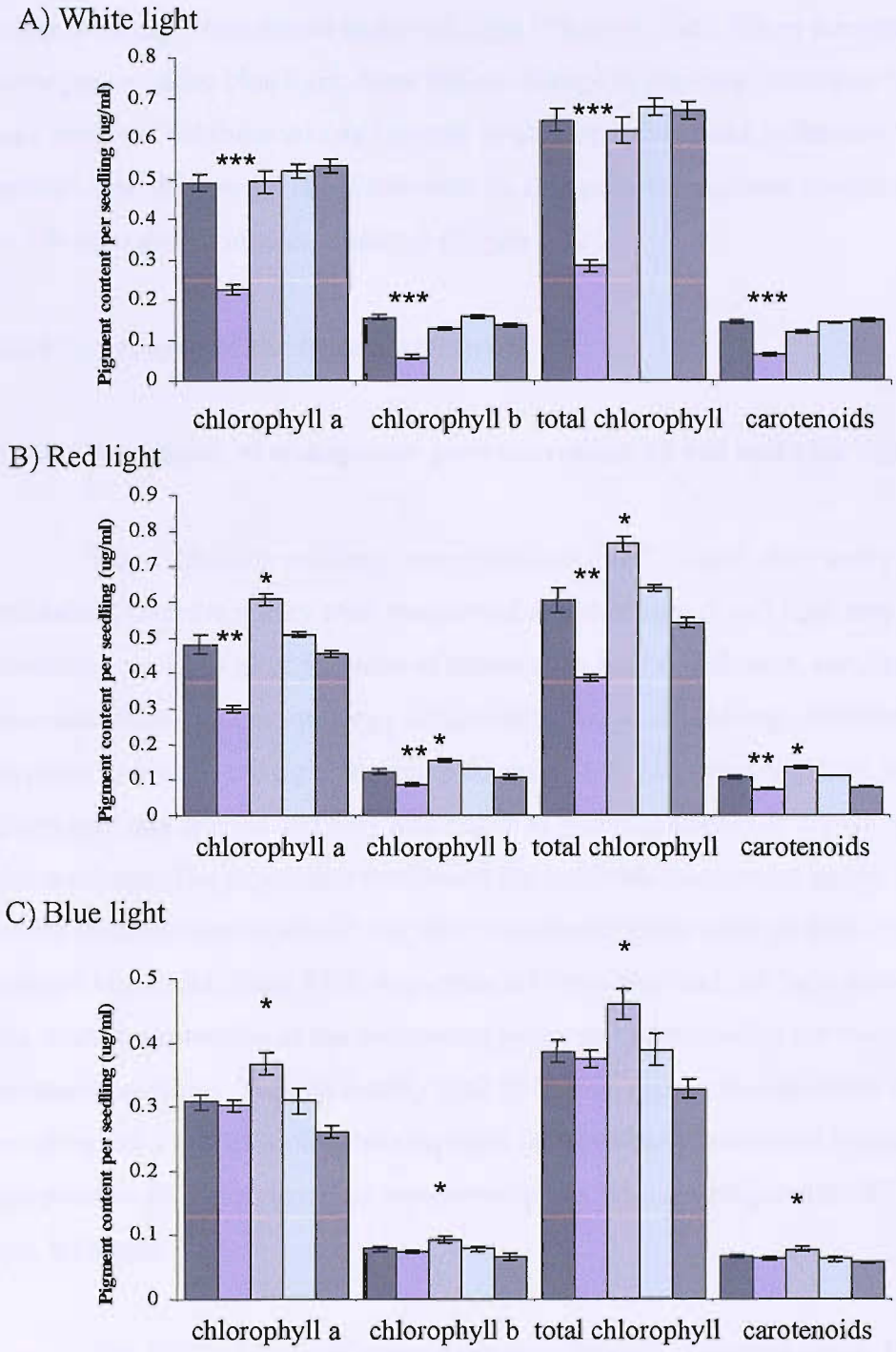

Figure 4.21 Pigment content of T-DNA knockout mutant seedlings. Comparison of chlorophyll a and b, total chlorophyll and total carotenoid concentrations per seedling of (■) wild-type (Col-8) to (■) *cat4* (N567045), (■) *aha2* (N622010), (■) *aca2* (N582624), (■) *stp1* (N548818). Seedlings were grown under A) white light, B) red light and C) blue light. Seedlings were pooled in six groups of 10, therefore n = 6, using two biological repeats. Significant levels are shown with *(P<0.05), **(P<0.01) and ***(P<0.005).

compared to wild-type (Figure 4.21). The same pattern of pigment content was also shown when seedlings were grown under red light (Figure 4.21B). When the mutant seedlings were grown under blue light, there was no change in pigment content of the *cat4, aca2* or *stp1* mutants, but there was an increase in chlorophyll content in the *aha2* mutant compared to wild-type (Figure 4.21C). There was no change in the pigment concentration in etiolated or FR-light grown mutant seedlings (Figure 4.22).

4.2.8 Expression of the transporter genes

4.2.8.1 Regulation of transporter gene expression by red and blue light

When etiolated seedlings were transferred to FR-light, they under went partial de-etiolation, whereas if they were transferred to either blue or red-light they under went full de-etiolation. Even after 12 hours of exposure to blue or red-light, seedlings begin to show dramatic changes in morphology compared to etiolated seedlings. Seedlings that were exposed to blue or red light showed a decrease in hypocotyl elongation, their cotyledons developed and opened and they also began to photosynthesize as shown by the colouring of the seedlings. The expression profiles of the candidate transporter genes, including genes in which mutants were obtained and other transporter genes such as *RAN1* were examined in red and blue-light. Total RNA was extracted from blue and red-light grown seedlings and the relative expression of the transporter genes was compared to the transcript levels in etiolated seedlings. Simultaneously total RNA was again extracted from FR-light grown seedlings as a further biological repetition of previous experiments. Expression levels of the putative FR-light regulated transporter genes were investigated by RT-PCR and by qPCR (Figure 4.23).

The *ACTIN2* and *40S* genes were initially used as control genes. However *ACTIN2* gene shows a small up-regulation under blue and FR-light compared to etiolated seedlings (result not shown), whereas the 40S ribosomal protein shows to be constitutively expressed in all light treatments (Figure 4.23G). So the *40S* gene was used as a control gene. Examination of the transporter genes under other light conditions has indicated that some may be regulated by other light wavelengths. The qPCR expression levels of the transporter genes were normalised in a two step process. Firstly each sample was

A) Dark

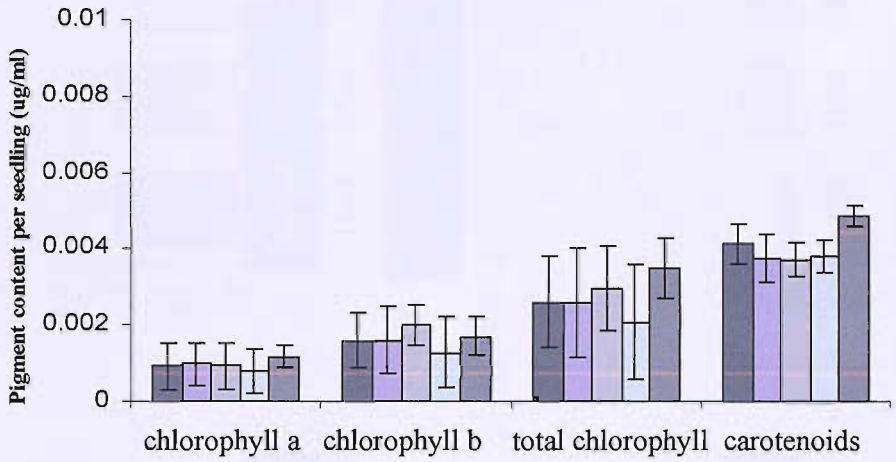

B) FR-light

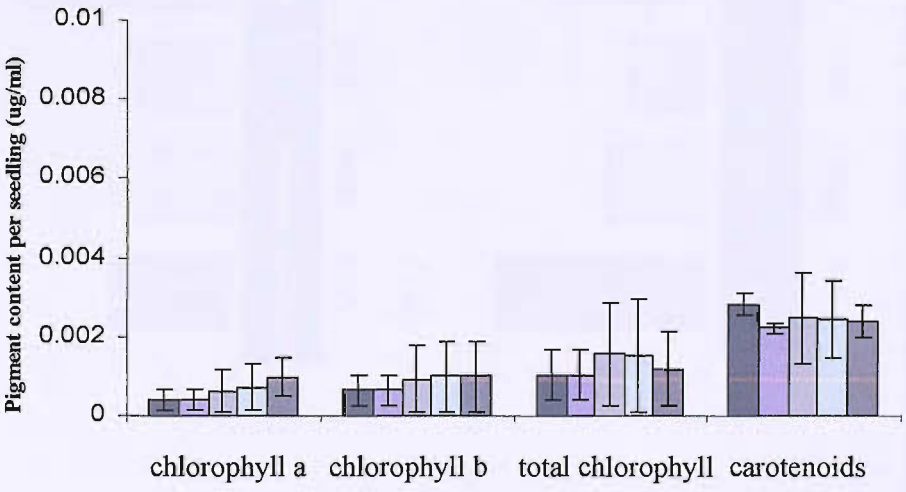

Figure 4.22 Pigment content of T-DNA knockout mutant seedlings. Comparison of chlorophyll a and b, total chlorophyll and total carotenoid concentrations per seedling of (■) wild-type (Col-8) to (■) *cat4* (N567045), (■) *aha2* (N622010), ( ) *aca2* (N582624), (■) *stp1* (N548818). Seedlings were grown under A) etiolated and B) far-red light. Seedlings were pooled in six groups of 10, therefore n = 6, using two biological repeats.

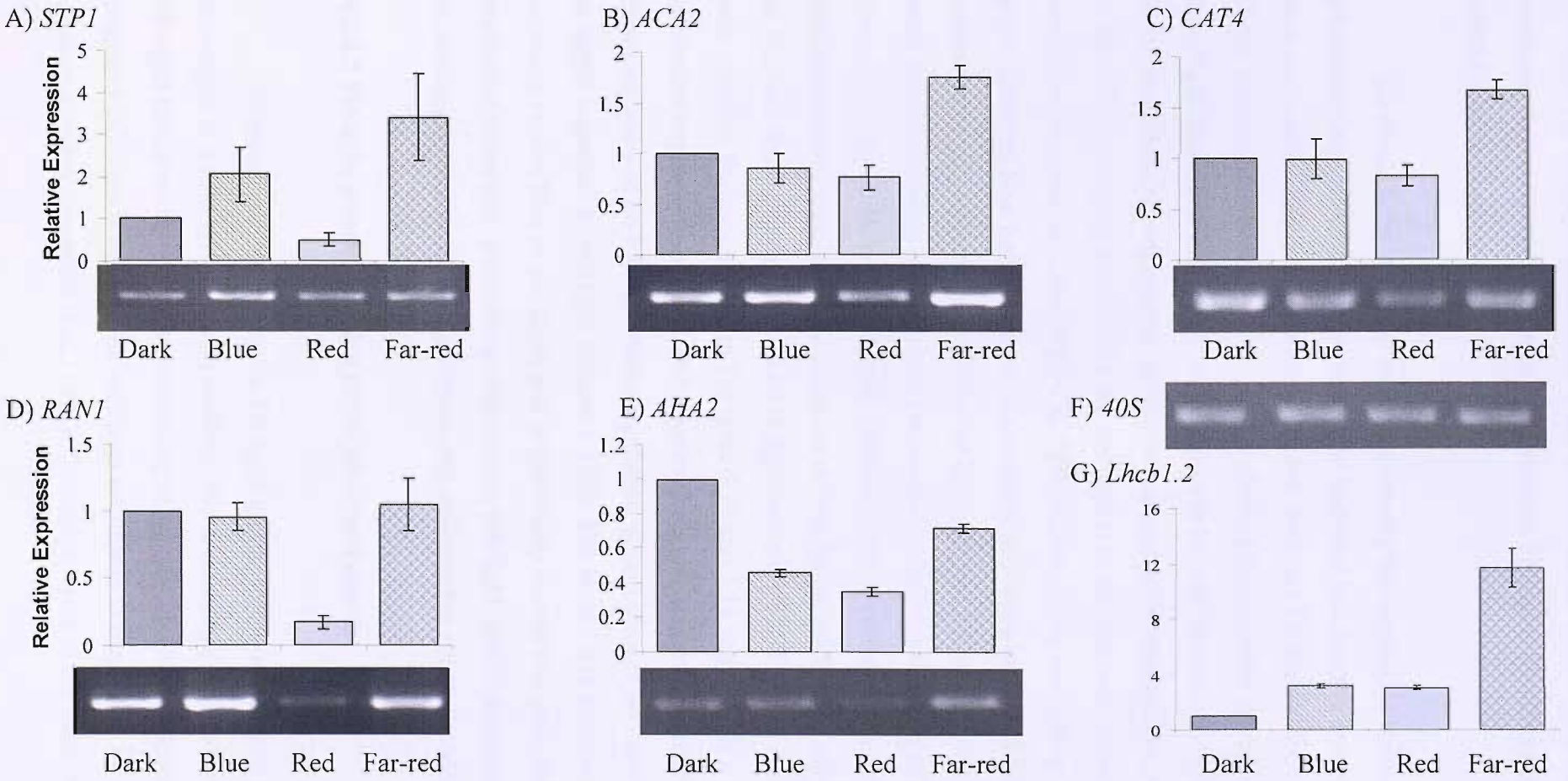

Figure 4.23 Relative expression of candidate genes normalised to 40S in etiolated, blue, red and far-red light grown seedlings. Semi-quantitative RT-PCR and quantitative real-time PCR was used to determine transcript levels of the candidate genes in seedlings grown under different light treatments. A) *STP1*, B) *ACA2*, C) *CAT4*, D) *RAN1*, E) *AHA2*, F) *40S* and G) *Lhcb1-2*. Real-time n = 3 ± standard error. Each sample was normalised to the 40S control gene and then to the dark grown Col-0 seedling.

normalised to the expression levels of the *40S* ribosomal subunit gene for each specific treatment. Secondly each treatment (red, blue and FR-light) was then normalised to the control sample (dark).

To check the system was working correctly the expression levels of the chlorophyll a/b binding protein *Lhcb1.2* were examined and used as a positive control. *Lhcb1.2* has been well established as being induced by red, blue and FR-light (McCormac and Terry 2002). As shown in Figure 4.23G *Lhcb1.2* showed the expected up-regulation under all three light treatments indicating the samples can be used to examine the transporter genes. When examining the transporter genes some appear to be regulated by other wavelengths of light. The transcript levels *STP1* did not appear to be consistent between the two amplification methods. Using RT-PCR, *STP1* showed an up-regulation by FR-light and to a greater extent blue light, but there is no change in expression in red-light grown seedlings compared to etiolated seedlings. However this expression pattern is not consistent for the same gene when using qPCR, which shows up-regulation under blue and FR-light but shows a down-regulation by red light. However, most genes do show consistency using both expression methods. *ACA2* shows an up-regulation in FR-light but did not appear to be blue and red-light regulated. The FR-light induction of STP1 and ACA2 is consistent with previous findings in chapter 3 (Figure 3.10 and 3.11 respectively). The ATP-dependent copper transporter *RAN1*, as previously shown using the multi-cycle RT-PCR approach, showed no FR-light down-regulation. It also showed no blue light regulation but is highly repressed by red light (Figure 4.23D). The amino acid transporter *CAT4* showed no change under blue or red-light, and as previously shown this gene shows an up-regulation rather than a down-regulation under FR-light. *AHA2* showed a down-regulation in seedlings grown under all light treatments compared to etiolated seedlings.

4.2.8.2 FR-light gene expression in the *phyA* null mutant

As mentioned previously the FR-light grown wild-type seedling shows a different phenotype to a wild-type etiolated seedling. However a *phyA* null mutant seedling grown in FR-light has an etiolated wild-type seedling phenotype and the cotyledons do not open (Figure 4.24). This is because the seedlings are unable to respond to FR-light, due to the absence of phyA (Nagatani *et al.*, 1993). Transcript levels of the putative FR-light

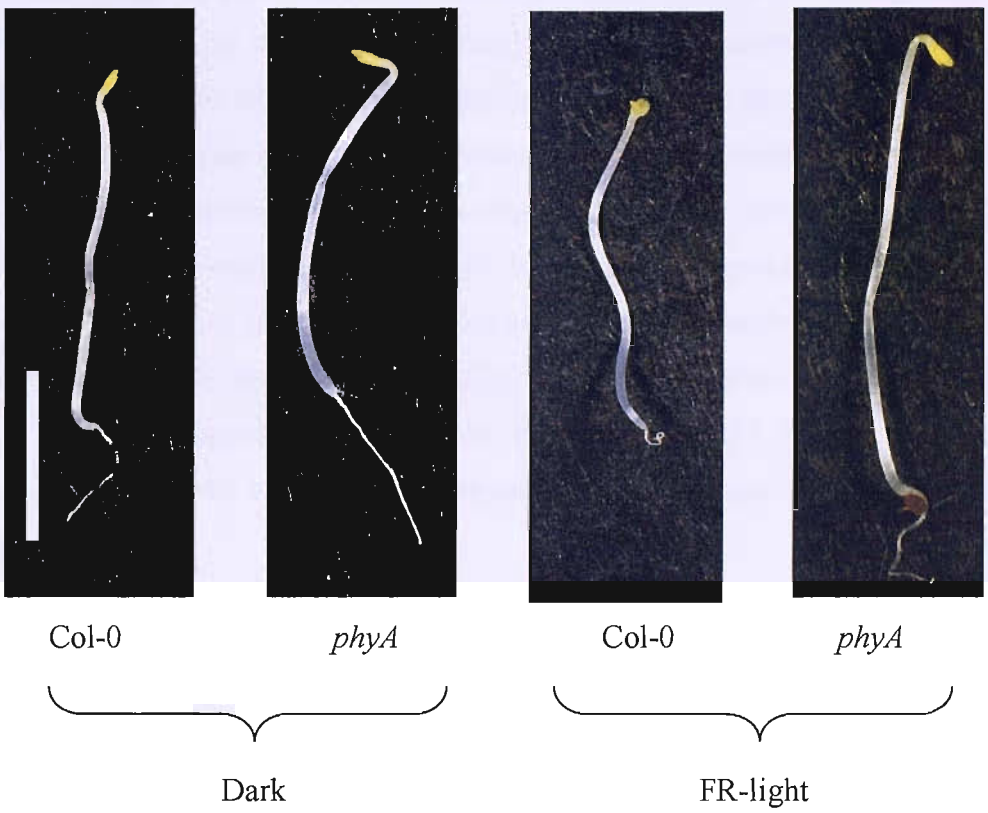

Figure 4.24 Wild-type and *phyA* null mutant seedling development under different light treatments in *Arabidopsis*. Phenotypic differences of wild-type and the *phyA* null mutant seedlings as a consequence of the light environment. Seedlings were stratified for 48 h at 4°C and then placed under white light to induce germination. All seedlings were transferred to complete darkness or FR-light for 120 h. Bar = 5 mm

regulated transporter genes were studied in etiolated and FR-light grown *phyA* seedlings and compared to the expression levels in the wild-type seedlings (Figure 4.25). In advance of looking at the candidate genes, two genes *Lhcb1-2* and *HEMA1* were examined. These genes are established as being FR-induced, and this was confirmed by qPCR (Figure 4.25A-B). However these genes show no induction in the *phyA* seedling grown in FR-light. As these genes show the established expression pattern in both wild-type and *phyA* seedlings the RNA can be used to examine the expression profiles of the candidate transporter genes. As mentioned previously the treatment samples were normalised to the expression levels of *40S* and then to expression level of the specific gene in the control wild-type dark-grown seedling. The ribosomal subunit as previously shown appears to be constitutively expressed after all treatments. As previously shown the genes *STP1* and *ACA2* show an up-regulation in FR-light, however, both genes showed no up-regulation in the *phyA* null mutant under FR-light when normalised to the ribosomal subunit (Figure 4.25). The FR-light up-regulated gene *CAT4* showed a reduced FR-light induction in the *phyA* mutant compared to wild-type. The repression of *AHA2* was also not retained in the *phyA* seedling grown in FR-light, as expression levels are equal to that of the etiolated *phyA* seedling.

4.2.9 Summary

A summary of observed phenotypes shown by the mutants, changes in photosynthetic pigment levels in the mutants and changes in expression levels of the candidate genes in the wild-type seedling grown under different light treatments are shown in Table 4.5. The mutants identified as homozygous for the T-DNA insert for each gene are also highlighted.

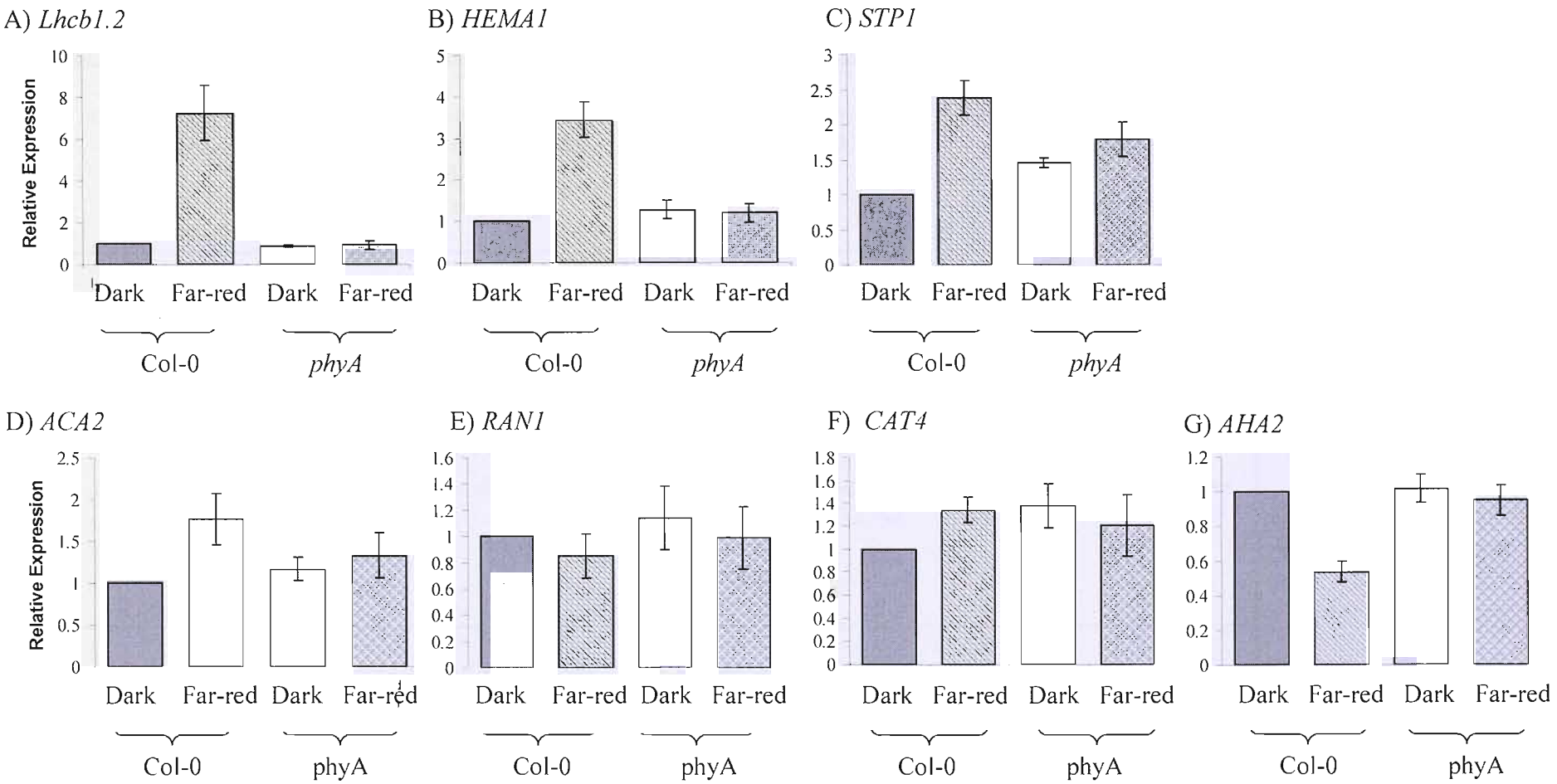

Figure 4.25 Relative expression of control and candidate genes normalised to *40S* in dark and far-red light grown Col-0 and phyA seedlings. Quantitative Real-time PCR was used to determine transcript levels of the control genes A) *Lhcb1.2* and B) *HEMA1*, and the candidate genes C) *STP1*, D) *ACA2*, E) *RAN1*, F) *CAT4*, G) *AHA2*, in wild-type (Col-0) and *phyA* mutant seedlings grown in dark and far-red light. Real-time n = 3 ± standard error. Each sample was normalised to the *40S* control gene and then to the dark grown Col-0 seedling.

Mutant	Seedling Phenotype	Mature Plant Phenotype	Pigment Concentration	Gene Expression
***cat4* (N567045)**	Increase in apical hook angle and decrease in hypocotyl length of etiolated seedlings.	Decrease in plant height at days 25, 32 and 50	Decrease in chlorophyll and carotenoid concentration in white and red-light grown seedlings.	*CAT4* is induced in FR-light, but no change in blue or red-light grown seedlings.
***aca2* (N582624)**	Decrease in hypocotyl length and cotyledon area in white and blue-light grown seedlings.	No significant differences.	No significant differences.	*ACA2* is induced in FR-light, no change in blue and red-light grown seedlings
***stp1* (N548818)**	No significant differences.	Decrease in rosette diameter at days 32, 42 and 50.	No significant differences.	*STP1* is induced in blue and FR-light, but repressed in red-light grown seedlings.
***aha2.1* (N622010)**	No significant differences.	No significant differences.	No significant differences.	*AHA2* is repressed in blue, red and FR-light grown seedlings.
***aha2.2* (N562371)**	No significant differences.	No significant differences.	No significant differences.	

Table 4.5 Summary of gene expression and the phenotypes observed from the transporter mutants. Changes in gene expression of the candidate genes in blue, red and FR-light grown seedling and significant changes in the phenotype of the mutant seedlings and plants are summerised. Changes in photosynthetic pigment levels of etiolated, white, blue, red and FR-light grown mutant seedlings are also shown.

4.3 Discussion

4.3.1 Confirmation of homozygous knockout status

An essential tool for functional analyses is the ability to create loss-of-function mutants for any given gene (Alonso *et al.*, 2003). Homozygote mutants have been generated and confirmed for a selection of the FR-light regulated genes as identified in chapter 3. Database searches allowed the identification of putative null T-DNA mutants for these genes and a number were ordered from the NASC collection. SALK mutants were chosen specifically and the zygosity of each plant was determined through a combination of segregation analysis and PCR methods. For the purpose of this discussion only the identification of *cat4* homozygous mutants will be discussed, although an identical approach was used for all lines.

Of the three putative mutant lines for *CAT4*, only one, line N567045, proved to contain the T-DNA insert, while the other two were wild-type (Table 4.1). The zygosity of the knockout was originally shown by segregation analysis. As the original seed contains an average 1.5 T-DNA insertions per line (Alonso *et al.*, 2003), it was important that only plants showing 100% or 75% seedlings survival were used for homozygous and heterozygous mutants respectively. The zygosity of each plant predicted by segregation was confirmed by PCR. There was a high degree of correlation between the results shown by segregation and PCR. PCR was also used to confirm the orientation of the T-DNA and that it is located in the correct gene, resulting in the loss-of-function of the gene of interest. Sequencing of the band generated by PCR using the combination of gene-specific forward and reverse primers with the T-DNA primer Lba1 revealed the T-DNA is located in *CAT4*. It also indicated the possibility of multiple insertions at the same site or a rearrangement of the T-DNA insert. There is growing awareness that major, sometimes multiple chromosomal rearrangements can accompany integration events (Nacry *et al.*, 1998), and it is likely that this is indeed occurring here. Ideally two mutant lines for the same gene should be isolated and the phenotype scored for both mutants and compared to wild-type. This would eliminate the possibility of a phenotype resulting from multiple insertions in different genes. Two different mutants showing similar or identical phenotypic traits would confirm that the phenotype shown results from the knockout of the gene of interest and not from an additional mutant. The

isolation of two mutants was not possible for all of the candidate genes, so the mutant would ideally be backcrossed with a wild-type plant resulting in a heterozygous mutant. The loss of a phenotypic trait by backcrossing is a good indication that the phenotype was due to the loss of the gene of interest or if the gene dominant. It is important to show that the phenotypic trait shown segregates with the insert. This approach would be vital in confirming any phenotype shown by the mutants in this study.

The purpose of the knockout mutant is to eliminate or vastly reduce the amount of functional protein which is expressed within the plant. Occasionally truncation of the protein may occur which may also have some residual functionality which must always be considered in the analysis of any mutant (Alonso *et al* 2003). The total elimination or reduction in the level of protein is achieved by the elimination/reduction of the mRNA corresponding to the gene. In a total null knockout it is possible to be confident that there is no functional protein. However, if a truncated mRNA is produced it is possible but unlikely that a truncated protein may also be produced (Alonso *et al* 2003). It was therefore necessary to check for mRNA levels of the knockout gene in putative knockout plants before further studies.

The T-DNA insert positioned in *CAT4* was shown to be located in the third of the genes four exons (Figure 4.2), and in terms of the protein sequence is in the ninth of fifteen putative transmembrane spanning domains. As the insert is inserted towards the end of the gene, there was a possibility of a truncated mRNA, which could result in a partially functional truncated protein. To test for the presence of a truncated mRNA, total RNA was extracted from both wild-type tissue and the *cat4* mutant as identified by both segregation and genomic PCR. Three combinations of primers were used to test for the presence of *CAT4* mRNA. RT-PCR shows that although the full gene or the section of the gene spanning the T-DNA is not present, a truncated gene is indeed present. This means that a truncated protein of up to the first nine transmembrane spanning domains maybe present, and must be considered when undertaking a phenotypic analysis of the mutant.

4.3.2 Analysis of the *cat4* mutant

The homozygous *cat4* mutant was visually assessed and a number of phenotypic traits were measured and compared to the Col-8 wild-type. The Col-8 wild-type was used as opposed to Col-0 line as used in the gene expression analysis because the SALK lines are in the Col-8 background. The *cat4* mutant showed no phenotypic differences compared to the wild-type when grown under white, red, blue or FR-light. However the phenotype shown by the dark-grown *cat4* seedling indicates an important role of CAT4 in the development of the etiolated seedling. This is shown by the straightening of the apical hook and a reduction in hypocotyl elongation in *cat4*. In a wild-type seedling the apical hook is clearly bent over, however in the *cat4* mutant the apical hook angle is straighter and the hook appears absent. It appears that CAT4 is important in retaining the apical hook, and its absence results in straightening of the hook. The apical hook is vital in aiding the etiolated seedling to push through the soil and its loss could cause physiological problems for the seedling in attempting to reach a light source when under the soil. Apical hook development is governed by the combined activities of cell division and cell elongation which control the growth of a tissue (Raz and Koornneef 2001). A fast change in growth is exhibited at the apical hypocotyl of etiolated seedlings where cells grow at different rates to form the hook-shaped structure (Raz and Koornneef 2001). In Arabidopsis the apical hook is formed 24 hours after germination and maintained for 4 days by differential growth (Ecker, 1995). The development of the apical hook has been shown to be regulated by plant hormones including auxin and ethylene. Treatment of wild-type seedlings with auxin results in a reduced hook curvature, whereas ethylene enhances the curvature of the hook (Ecker., 1995; Lehman *et al.*, 1996). The hookless phenotype shown by the *cat4* mutant resembles the treatment of wild-type seedlings treated with auxins and the hookless mutants *HLS1* and *COP2* (Raz and Ecker 1999). The analyses of the hookless mutants have shown they are involved in an early aspect of hook formation. The amino acid transporter CAT4 maybe involved in the developmental pathway of hook formation and linked to LSH1 and COP2 and possibly to auxin. In addition to cell elongation in the apical hook, CAT4 also appears to play a role in cell elongation in the hypocotyl of the etiolated seedling possibly by providing amino acids. Ethylene has also been shown to reduce cell elongation in the dark grown seeding (Vandenbussche *et al.*, 2005). It would be interesting to see if the curvature of the apical hook and increase in hypocotyl elongation is rescued in the *cat4* mutant supplemented with ethylene in the dark to see if

CAT4 is possibly linked to the hormone transduction cascade in addition to the etiolated developmental pathway. The *cat4* mutant also showed a decrease in photosynthetic pigment levels compared to the wild-type seedling when grown in white and red-light. This indicates a putative direct role of the transporter in the photosynthetic light-regulated pathways mediated by the phytochromes.

The wild-type phenotype shown by the *cat4* mutant growth in the light could be due to redundancy of the various amino acid transporters within the *Arabidopsis* genome. To date, over 50 amino transporters including 8 members of the cationic amino acids transporters (CAT) have been identified and thought to be involved in the transport of different amino acids (Su *et al.*, 2004). Although much is known of the amino acid transporter (ATF) superfamily, regarding localisation and regulation, little is known about the second class of amino acid transporters, the amino acid polyamine choline (APC) superfamily. The CAT family of amino acid transporters is included in the APC superfamily. The method of regulation of the CAT amino acid transporters is unknown, but recently their localisation has been determined. CAT4, like all the other members of the CAT family have been shown to be expressed in many tissues, including in the roots, stem, leaves and flowers (Su *et al.*, 2004). The global expression of these genes could simply imply that none of the family members have individual roles in plant development, rather they are simultaneously involved in amino acid transport. However, it is more likely is that the different family members are located at different membranes in the cell and would have distinct physiological roles and transport distinct amino acids. It would be interesting to see if these transporters have roles in transporting specific amino acids and to locate the expression of the amino acid transporters to specific membranes in the cell. The isolation of double or triple mutants in genes encoding proteins transporting the same amino acids or transporters expressed on the same membrane could result in an interesting phenotype.

4.3.3 Analyses of the *aca2* mutant

One T-DNA insertional mutant (N582624) was obtained for *ACA2*, and using PCR the insert was shown to be located in the large third exon of the seven exons in ACA2. The *aca2* mutant, when grown under white light appeared much smaller than wild-type in regards to hypocotyl length and cotyledon area. A similar phenotype was shown when the seedling

was grown under blue light. The mutant also appears to have a curled root that is spiralled around the hypocotyl, in contrast the root of the wild-type seedling that grows downwards and is longer in length. However, when grown under red or FR-light and in the etiolated seedling, the *aca2* seedling shows a wild-type phenotype, indicating this response is specific to white and blue light. This could be linked to the cryptochromes and phototropins, the blue light specific photoreceptors, and indicating ACA2 maybe be linked to the blue-light signalling pathways that control seedling development. However, when the wild-type seedling is grown under blue light the expression levels of *ACA2* decrease. This would be the opposite of what could be expected if ACA2 plays a role in blue-light mediated seedling development. However this is not necessarily true as phyA is reduced in the light. No noticeable phenotype was observed when the *aca2* mutant was grown to maturity and compared to wild-type, with regards to rosette diameter, plant height, leaf number and timing of first bolt, silique and flower.

Unlike the *cat4* mutant, the absence of *ACA2* mRNA was not confirmed using RT-PCR. To determine if the *aca2* mutant is a null mutant or if a truncated product is generated, RT-PCR is required before further phenotypic analysis. The predicted location of the T-DNA insert is approximately 513 amino acids into the protein sequence, which in terms of the protein structure is in the large cytoplasmic loop situated between the fourth and fifth of 10 transmembrane spanning domains. Due to the location of the inserted T-DNA, a truncated protein would contain the N-terminal autoinhibitory domain and the calmodulin binding domain, but the catalytic domain would be absent resulting in de-activation of the protein. Ten members of the type IIB Ca^{2+}-ATPases have been identified in the *Arabidopsis* genome (Axelsen and Palmgren 2001), residing on various cellular membranes. The lack of any phenotype can again be linked back to redundancy with the ACA family members, and any phenotype could be shown when double and triple mutants are created and observed. As the *Arabidopsis* genome also contains the type IIA Ca^{2+}-ATPases of which there are four members this could also give rise to calcium pump redundancy and the lack of a visible phenotype in the *ACA2* mutant. ECA1 was also shown to be localised to the endoplasmic reticulum endomembranes (Axelsen and Palmgren 2001), so it would be interesting to study the phenotype of the *ACA2/ECA1* double mutant.

4.3.4 Analyses of the *stp1* mutant

The next mutant to be isolated was *stp1*, one of the 14 putative monosaccharide transporters in the *Arabidopsis* genome (Buttner and Sauer 2000). The T-DNA insert was located in the last of the four exons of the gene towards the C-terminal of the protein sequence. The T-DNA insert has been localised to amino acid 423, approximately two thirds through the protein sequence, in between the tenth and eleventh of the proteins twelve transmembrane spanning domains. A truncated protein potentially formed from the presence of the T-DNA, would result in the absence of the carboxy-terminal half, resulting in an inactivation of the protein. However due to the location of the insert it is possible that a truncated product is synthesised, and this needs to be taken into consideration during phenotypic analysis. As with *aca2* the absence of a truncated product should be confirmed before further analysis is undertaken. The *stp1* mutant exhibited a wild-type phenotype when seedlings were grown under all light treatments and during the adult developmental program of the plant. To date, 14 monosaccharide transporters, along side many other sugar transporters have been identified in the *Arabidopsis* genome, and again redundancy could play a role in the absence of a visible phenotype in the *stp1* mutant.

The *stp1* mutant has previously been studied and the plant was shown to grow and develop normally and *STP1* was found to be expressed in germinating seeds and seedlings, with the STP1 activity found mainly in the roots of the seedling (Sherson *et al.*, 2000). The transport of D-galactose and D-mannose is up to 60% less in the *stp1* mutant compared to be respective wild-type, but the transport of sucrose is not reduced. The *stp1* mutant seedlings grow effectively on concentrations of D-galactose that would inhibit wild-type growth, even at 100mM D-galactose. This indicates that active transport by STP1 plays a major role at very high concentrations of exogenous sugar (Sherson *et al.*, 2000). These findings provided vital insight into the function of STP1, clearly establishing its importance in the uptake of extracellular sugars by the embryo and in seedlings (Sherson *et al.*, 2000). It would be interesting to examine the root phenotype of *stp1* seedlings grown in different light treatments supplemented with different sugars to see if there is any correlation between sugar uptake and light signalling.

4.3.5 Analyses of the *aha2* mutants

Two different homozygote T-DNA mutants were obtained for *AHA2*. The T-DNA insert of the first mutant (N622010) is located towards the 5' end of the gene, in the fourth of the fifteen exons, and in terms of the protein is positioned before the first of proteins ten predicted transmembrane spanning domains. In contrast the second insert (N562371) was confirmed to be located in the thirteenth exon, which is predicted to be between the fifth and sixth of the ten transmembrane spanning domains. It is therefore possible that a truncated protein is produced in the second mutant line *aha2-2*, and any differences in the phenotypes of the two mutant lines may result from the location of the T-DNA insert. This was not the case as both mutants had a wild-type seedling phenotype in all light treatments with the exception of the seedlings grown in FR-light. Previous studies using *aha2* showed the mutant to have a wild-type phenotype (Palmgren *et al.*, 2001), however the seedling phenotype of *aha2* under different light conditions has not been examined. A small decrease in hypocotyl length was apparent in the *aha2-2* seedlings grown under continuous FR-light. The FR-light grown *aha2-1* seedling showed a wild-type phenotype. As the insert in *aha2-2* is located more towards the 3' of the gene compared to the insert in *aha2.1* it is more likely that a truncated protein is produced in *aha2-2*. The decrease in hypocotyl elongation shown by *aha2-2* in FR-light is an unexpected phenotype as functional protein activity is more likely in *aha2.2*. This is not necessarily true as a truncated protein could have an inhibitory affect. The decrease in hypocotyl elongation may result from some other factor rather than a truncated product. For example the *aha2-2* seedlings when grown in FR-light may not have germinated simultaneously with the wild-type and *aha2.1* lines. The location of the two different T-DNA insert results in significant loss of protein function even if a truncated protein is formed in the N562371 line. In both mutants the C-terminus of the protein is lost, including the 14-3-3 protein binding site, the phosphorylated thr-947, the whole of the autoinhibitory R-domain and also the proton acceptor amino acid Asp684.

Several candidate H^+-ATPases have emerged as being involved in the energization of nutrient uptake into the roots. It has been shown that AHA2 accumulates in the roots and promoter-GUS fusions in *Arabidopsis* has suggested that AHA2 is expressed predominately but not exclusively in the root epidermis (Arango *et al.*, 2003). Phenotypic analysis of the roots of seedlings under different light could prove important in understanding the role of

AHA2 is seedling development. The *aha2* mutant line *aha2.1* also showed an increase in pigment content in seedlings grown in white and blue light, possibly linking the transporter to the blue-light photoreceptors and signalling pathways. The second AHA2 mutant *aha2.2* (N562371) showed wild-type levels of the photosynthetic pigments; this should not be the case due to presence of the insert towards the C-terminal of the protein, resulting in a truncated protein as the autoinhibitory domain of the protein is still absent.

No phenotype was observed in either *aha2* line throughout the development of the plants, including rosette diameter, plant height, leaf number and the timing of first bolt, flower or silique. The tissue-specific localization of only a few H^+-ATPase isoforms has been determined and their physiological roles have proven difficult to analyze, as no phenotypes of H^+-ATPase knockouts have been reported so far (Cutler and McCourt 2004). The analysis of the intron number and position within the H^+-ATPase genes in *Arabidopsis* identified five groups, and *AHA2* belongs with *AHA1*, *AHA3* and *AHA5* in subfamily II (Arango *et al.*, 2003). As mentioned previously *AHA2* is expressed in the root epidermis, and the reason for the wild-type phenotype in *aha2* could be the presence of other ATPases in the root, including AHA1, AHA3 and AHA4 (Arango *et al.*, 2003). These other ATPases could be working in conjunction with AHA2 in the roots resulting in redundancy. Several mutant alleles have been identified for a number of the isoforms (Cutler and McCourt 2004). The analysis of these knockout lines also showed a wild-type phenotype, therefore single gene mutations may not result in a visible phenotype due to possible redundancy. However, knockouts in more than a single H^+-ATPase can be generated by crossing mutant lines, creating double or triple mutant resulting in a phenotype and this may be more informative (Young *et al.*, 2001).

4.3.6 Light-regulation of transporter gene expression

RT-PCR and quantitative PCR reveals that some of these genes are not solely regulated by FR-light. Experimental analyses have revealed these genes are regulated by other light wavelengths, namely red and blue light. *STP1* shows a marked up-regulation under blue light, to a greater extent than FR-light, but there is a down-regulation in relative expression under red light using RT-PCR and qPCR. As explained previously, an explanation for the up-regulation of *STP1* in FR-light could be to uptake exogenous sugars during partial

de-etiolation, however the gene is down-regulated by red-light. When the etiolated seedling is transferred to red-light it begins to photosynthesize and can produce its own source of carbohydrate, which in turn could result in a decrease in the requirement for exogenous sugar and hence the down-regulation of *STP1*.

STP1 is up-regulated by blue light indicating other photoreceptors such as the cryptochromes are involved in the light mediated response. This implies the regulation of STP1 is more complex than being regulated by just phyA and indicates the role of multiple photoreceptors in the light-regulation of this gene. Multiple photoreceptors have previously been shown to regulated the same genes, as the *phyB* mutant seedlings have been shown to retain a high level of responsiveness to red-light for the majority of red-light regulated genes on the microarray indicating than one or more other phytochromes have a major role in regulating their expression (Tepperman *et al.*, 2004).

Some of the other transporters are specifically regulated by FR-light, as *ACA2* showed no regulation in either red and blue light indicating *ACA2* is mediated specifically by phyA. *RAN1* and *AHA2* also show down-regulation in red-light and both blue and red-light respectively. *RAN1* shows a significant down-regulation in red-light in comparison to FR-light; this could be due to the rapid decrease in hypocotyl cell elongation, as *RAN1* has shown to be required for cell elongation in an ethylene-independent manner (Woeste and Kieber 2000). As elongation is strongly inhibited under FR-light it is more likely to result from photosynthesis and sugar availability.

It is interesting that many genes show opposing changes in expression in red and FR-light grown seedlings. In some putative FR-light induced genes where the up-regulation has been confirmed, the genes show a down regulation in the red light. This could be perhaps seen as a strange phenomenon but a number of genes from the original microarrays show an identical expression profile under these light treatments (Tepperman *et al.*, 2001; Teppperman *et al.*, 2004). For example the monosaccharide transporter *STP1* and the amino acid transporter *AAP2* both show an up-regulation in FR-light (Wang *et al.*, 2002) but they show a down-regulation in red light (Tepperman *et al.*, 2004). Changes in transcript levels of all the candidate transporter genes under different light treatments indicate the involvement of

multiple photoreceptors in regulating gene expression and a complex and overlapping signalling network.

To date only a small number of genes encoding proteins involved in transport have been shown to be regulated by the light environment. For example previously an unknown maltose transporter has shown up-regulation in the dark and was shown to be essential for the degradation of starch to sucrose in *Arabidopsis* leaves (Niittyka *et al.*, 2004). This transporter was identified using two mutants containing high starch and very high maltose levels, an intermediate of the degradation of starch. The mutations affect the regulation of the maltose transporter MEX1. The *mex1* phenotype is severe and the *mex1* plants are significantly smaller than wild-type thus demonstrating that MEX1 is the predominant route of carbohydrate export from chloroplasts at night (Niittyka *et al.*, 2004).

A second transporter, an auxin-induced voltage-gated rectifying K^+ channel, has been shown to be regulated in the coleoptile of maize by blue light and is involved in phototropic curvature of the coleoptile (Fuchs *et al.*, 2003). The K^+ channel gene *ZMK1* follows the re-distribution of auxin, which was shown by illuminating the coleoptile with unilateral blue light to stimulate phototropic bending. When the *ZMK1* mRNA transcript levels were measured in the illuminated and shaded halves of the coleoptile during prolonged stimulation, *ZMK1* transcripts decreased in the light-exposed half, which is growth restricted and auxin depleted, whereas they remained constant in the growing half of the coleoptile (Fuchs *et al.*, 2003). This indicated that differential expression of the K^+ channel *ZMK1* is involved in phototropic curvature and is regulated by blue light (Fuchs *et al.*, 2003).

To identify if the candidate genes are truly regulated by FR-light and acting down stream of phytochrome A (phyA) during de-etiolation, the expression levels of these genes were examined in the *phyA* null mutant.

HEMA1 and *Lhcb1.2* genes are considered to play key role during chloroplast development and encodes glutamyl-tRNA reductase and chlorophyll a/b-binding proteins respectively (McCormac and Terry 2002). Both *HEMA1* and *Lhcb1.2* are significantly induced in wild-type seedlings grown in FR-light as well as blue and red light (McCormac *et al.*, 2001; McCormac and Terry 2002). *HEMA* and *Lhcb1.2* expression in photoreceptor-

deficient mutants showed that induction by FR-light required phyA, but not phyB or the blue light photoreceptors cry1 and cry2 (McCormac and Terry 2002).

Both *HEMA1* and *Lhcb1.2* transcript levels were induced in the wild-type FR-light grown seedlings, but this up-regulation was not upheld in the FR-light grown phyA seedling. This expression profile is a positive indication of FR-light regulation and RNA can be used to examine the regulation of the transporter genes by FR-light in the phyA mutant. The majority of the candidate transporter genes showed this example profile. For example the FR-induction of *STP1* transcript levels in the wild-type is significantly reduced in the *phyA* mutant.

Chapter 5

FRIMP1 and FRIMP2: novel membrane proteins required for light-regulated development of *Arabidopsis*

5.1 Introduction

For light-controlled development of plants, photoreceptors perceive and interpret light and transduce the signals to modulate light-responsive nuclear genes, which in turn direct appropriate growth and developmental responses. At present intense efforts are focussed on identifying the components of the intracellular signalling networks of phytochrome signalling at the cell biology level. Many approaches have been used to identify signalling components downstream of phytochrome. These include physiological, molecular, pharmacological and genetic approaches. The combination of such approaches has led to the identification of a large number of putative genes involved in mediating phytochrome-dependent signal transduction (Nagy and Schafer, 2002). Recently considerable progress has been made in the identification of the mechanism of phytochrome signalling (Moller *et al.*, 2002) and it has become evident that phytochrome signalling consists of a highly ordered network of signalling events.

The discovery that some phytochromes and light-signalling intermediates show a light-dependent cytoplasmic to nuclear translocation has led to the idea that early signalling events take place in the nucleus (Moller *et al.*, 2002). Upon activation by light phytochrome has been shown to be imported into the nucleus (Nagatani *et al.*, 2004). This nuclear localization is due to the carboxy-terminal of phytochrome and this activity is suppressed in the dark by the amino-terminal domain and retains phytochrome in the cytoplasm (Nagatani *et al.*, 2004). In the nucleus phytochrome is able to directly affect transcription of light-regulated genes. However phytochrome signalling components have also been identified in the cytoplasm demonstrating that the nucleus is not the only place for phytochrome action (Moller *et al.*, 2002). This indicates that phytochrome responses must also be mediated by cytoplasmic events and these could include a direct effect on a number of proteins including membrane proteins (Nagy and Schafer, 2002). Cytoplasmic

events are likely as the nuclear import of some phytochrome isoforms takes hours and their nuclear actions could not explain more rapid phytochrome responses such as changes in hypocotyl growth rate (Nagy *et al.*, 2000). Also studies have revealed cytoplasmic proteins such as FIN219 are signalling intermediates for phyA signalling (Hsieh *et al.*, 2000). More interestingly phytochrome has shown to interact with a number of cytoplasmic proteins including PSK1 and NDPK2 (Fankhauser *et al.*, 1999; Choi *et al.*, 1999). To date there has been little evidence for membrane proteins that are involved directly with phytochrome signalling. However the identification here of two proteins, termed FRIMP1 and FRIMP2 could provide the first insight into membrane proteins being implicated in phytochrome signalling.

5.1.1 Chapter Aims

Although much is known about the cytoplasmic to nuclear translocation of phytochromes in light signalling and the identification of light-regulated transcription factors, little is known about the cytoplasmic events and the involvement of effector proteins further downstream the light-signalling pathway. The aim of this chapter is to obtain and characterise homozygous mutants for FRIMP1 and FRIMP2, two proteins of unknown function. The phenotypic analysis of these mutants will aid in identifying a putative function for these proteins and their role in seedling de-etiolation and plant photomorphogenesis.

5.2 Results

5.2.1 FRIMP1 sequence alignments

As shown in chapter 3 the function of the protein encoding the FR-light regulated gene At1g64990 is currently unknown. The FR-light up-regulation was confirmed using RT-PCR and semi-quantitative real-time PCR. To date the protein is unnamed but as the protein is up-regulated by FR-light the protein will be named FRIMP1 (**F**ar-**r**ed **I**nduced **M**embrane **P**rotein **1**). To help identify a putative function for FRIMP1, BLAST analysis using the amino acid sequence of FRIMP1 was undertaken to identify proteins with high sequence identity. BLAST analyses revealed a homolog to FRIMP1 in the *Arabidopsis thaliana* genome showing 92% protein sequence identity which has been named FRIMP2. As shown in Figure 5.1 the proteins are almost identical throughout the sequence. As with FRIMP1, the function of the FRIMP2 protein is unknown. Sequence analysis has also revealed that FRIMP1 shows high sequence identity to a number of proteins in a range of other organisms with at least 35 % sequence identity to FRIMP1 (Figure 5.2). These proteins include those from other plant species such as rice, showing 78% sequence identity to FRIMP1. Homologues from non-plant systems include the mouse (38% identity), drosophila (35% identity) and xenopus (36% identity) and two proteins from *C.elegans*, Y75B8A, and C11H1.2, both showing 35% sequence identity to FRIMP1. There was also a human homolog to FRIMP1 showing 40% sequence identity. When the protein sequences from the different organisms are aligned, they show 27% sequence identity in all sequences (Figure 5.2). The degree of identity is enhanced further when looking at the functional identity of each amino acid, where individual amino acids are substituted by another with a similar functional activity, where the sequences now show 49% sequence identity. The function of all of these proteins have to date not been identified. The human protein was predicted to contain seven transmembrane spanning domains, identical to human G-protein coupled receptors (GPCR). All proteins including the FRIMP proteins are termed as putative GPCR's in the computer based databases as they are predicted to contain between 7 and 9 putative transmembrane spanning domains. This is because it is well established that GPCR's contain 7 transmembrane spanning domains.

Figure 5.1 Sequence alignment of AtFRIMP1 and AtFRIMP2. Sequence alignment of two putative membrane proteins in *Arabidopsis*, AtFRIMP1 and AtFRIMP2. The protein sequences show 92% sequence identity, with identical amino acids shown in red (*) and non-identical amino acids with a conserved substitution shown in blue (:).

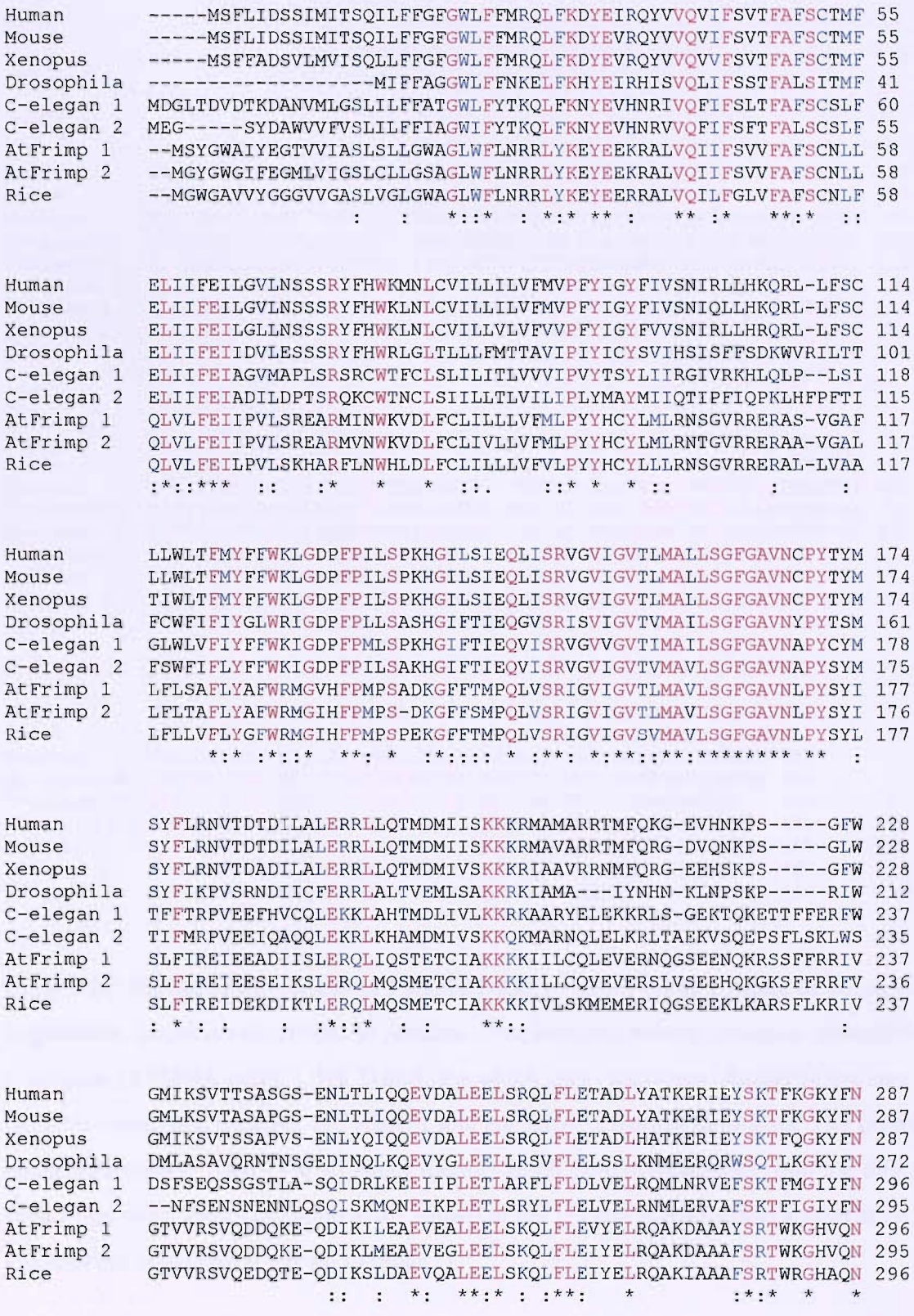
Human -----MSFLIDSSIMITSQILFFGFGWLFFMRQLFKDYEIRQYVVQVIFSVTFAFSCTMF 55
Mouse -----MSFLIDSSIMITSQILFFGFGWLFFMRQLFKDYEVRQYVVQVIFSVTFAFSCTMF 55
Xenopus -----MSFFADSVLMVISQLLFFGFGWLFFMRQLFKDYEVRQYVVQVVFSVTFAFSCTMF 55
Drosophila ------------------MIFFAGGWLFFNKELFKHYEIRHISVQLIFSSTFALSITMF 41
C-elegan 1 MDGLTDVDTKDANVMLGSLILFFATGWLFYTKQLFKNYEVHNRIVQFIFSLTFAFSCSLF 60
C-elegan 2 MEG-----SYDAWVVFVSLILFFIAGWIFYTKQLFKNYEVHNRVVQFIFSFTFALSCSLF 55
AtFrimp 1 --MSYGWAIYEGTVVIASLSLLGWAGLWFLNRRLYKEYEEKRALVQIIFSVVFAFSCNLL 58
AtFrimp 2 --MGYGWGIFEGMLVIGSLCLLGSAGLWFLNRRLYKEYEEKRALVQIIFSVVFAFSCNLL 58
Rice --MGWGAVVYGGGVVGASLVGLGWAGLWFLNRRLYKEYEERRALVQILFGLVFAFSCNLF 58
ELIIFEILGVLNSSSRYFHWKMNLCVILLILVFMVPFYIGYFIVSNIRLLHKQRL-LFSC 114
ELIIFEILGVLNSSSRYFHWKLNLCVILLILVFMVPFYIGYFIVSNIQLLHKQRL-LFSC 114
ELIIFEILGLLNSSSRYFHWKLNLCVILLVLVFVVPFYIGYFVVSNIRLLHRQRL-LFSC 114
ELIIFEIIDVLESSSRYFHWRLGLTLLLFMTTAVIPIYICYSVIHSISFFSDKWVRILTT 101
ELIIFEIAGVMAPLSRSRCWTFCLSLILITLVVVIPVYTSYLIIRGIVRKHLQLP--LSI 118
ELIIFEIADILDPTSRQKCWTNCLSIILLTLVILIPLYMAYMIIQTIPFIQPKLHFPFTI 115
QLVLFEIIPVLSREARMINWKVDLFCLILLLVFMLPYYHCYLMLRNSGVRRERAS-VGAF 117
QLVLFEIIPVLSREARMVNWKVDLFCLIVLLVFMLPYYHCYLMLRNTGVRRERAA-VGAL 117
QLVLFEILPVLSKHARFLNWHLDLFCLILLLVFVLPYYHCYLLLRNSGVRRERAL-LVAA 117
LLWLTFMYFFWKLGDPFPILSPKHGILSIEQLISRVGVIGVTLMALLSGFGAVNCPYTYM 174
LLWLTFMYFFWKLGDPFPILSPKHGILSIEQLISRVGVIGVTLMALLSGFGAVNCPYTYM 174
TIWLTFMYFFWKLGDPFPILSPKHGILSIEQLISRVGVIGVTLMALLSGFGAVNCPYTYM 174
FCWFIFIYGLWRIGDPFPLLSASHGIFTIEQGVSRISVIGVTVMAILSGFGAVNYPYTSM 161
GLWLVFIYFFWKIGDPFPMLSPKHGIFTIEQVISRVGVVGVTIMAILSGFGAVNAPYCYM 178
FSWFIFLYFFWKIGDPFPILSAKHGIFTIEQVISRVGVIGVTVMAVLSGFGAVNAPYSYM 175
LFLSAFLYAFWRMGVHFPMPSADKGFFTMPQLVSRIGVIGVTLMAVLSGFGAVNLPYSYI 177
LFLTAFLYAFWRMGIHFPMPS-DKGFFSMPQLVSRIGVIGVTLMAVLSGFGAVNLPYSYI 176
LFLLVFLYGFWRMGIHFPMPSPEKGFFTMPQLVSRIGVIGVSVMAVLSGFGAVNLPYSYL 177
SYFLRNVTDTDILALERRLLQTMDMIISKKKRMAMARRTMFQKG-EVHNKPS-----GFW 228
SYFLRNVTDTDILALERRLLQTMDMIISKKKRMAVARRTMFQRG-DVQNKPS-----GLW 228
SYFLRNVTDADILALERRLLQTMDMIVSKKKRIAAVRRNMFQRG-EEHSKPS-----GFW 228
SYFIKPVSRNDIICFERRLALTVEMLSAKKRKIAMA---IYNHN-KLNPSKP-----RIW 212
TFFTRPVEEFHVCQLEKKLAHTMDLIVLKKRKAARYELEKKRLS-GEKTQKETTFFERFW 237
TIFMRPVEEIQAQQLEKRLKHAMDMIVSKKQKMARNQLELKRLTAEKVSQEPSFLSKLWS 235
SLFIREIEEADIISLERQLIQSTETCIAKKKKIILCQLEVERNQGSEENQKRSSFFRRIV 237
SLFIREIEESEIKSLERQLMQSMETCIAKKKKILLCQVEVERSLVSEEHQKGKSFFRRFV 236
SLFIREIDEKDIKTLERQLMQSMETCIAKKKKIVLSKMEMERIQGSEEKLKARSFLKRIV 237
GMIKSVTTSASGS-ENLTLIQQEVDALEELSRQLFLETADLYATKERIEYSKTFKGKYFN 287
GMLKSVTASAPGS-ENLTLIQQEVDALEELSRQLFLETADLYATKERIEYSKTFKGKYFN 287
GMIKSVTSSAPVS-ENLYQIQQEVDALEELSRQLFLETADLHATKERIEYSKTFQGKYFN 287
DMLASAVQRNTNSGEDINQLKQEVYGLEELLRSVFLELSSLKNMEERQRWSQTLKGKYFN 272
DSFSEQSSGSTLA-SQIDRLKEEIIPLETLARFLFLDLVELRQMLNRVEFSKTFMGIYFN 296
--NFSENSNENNLQSQISKMQNEIKPLETLSRYLFLELVELRNMLERVAFSKTFIGIYFN 295
GTVVRSVQDDQKE-QDIKILEAEVEALEELSKQLFLEVYELRQAKDAAAYSRTWKGHVQN 296
GTVVRSVQDDQKE-QDIKLMEAEVEGLEELSKQLFLEIYELRQAKDAAAFSRTWKGHVQN 295
GTVVRSVQEDQTE-QDIKSLDAEVQALEELSKQLFLEIYELRQAKIAAAFSRTWRGHAQN 296

```
Human         FLGYFFSIYCVWKIFMATINIVFDRVGKTDPVTRGIEITVNYLGIQFDVKFWSQHISFIL 347
Mouse         FLGYFFSIYCVWKIFMATINIVLDRVGKTDPVTRGIEITVNYLGIQFDVKFWSQHISFIL 347
Xenopus       FLGYFFSIYCVWKIFMATINIVFDRVGKTDPVTRGIEITVNYLGIQFDVKFWSQHISFIL 347
Drosophila    VLGHFFSVYCVYKIFMCCINIIFDRVGRKDPVTRGLEIAIHWCGFNIDFAFWNQHISFLL 332
C-elegan 1    ILGHFFSIYCIWKIFISFINIVFDRVGKVDPVTKTIEIGVHWMGIPLDISFWSQYISFFL 356
C-elegan 2    VLGHFFSLYCVWKIFISLVNILFDRVGKVDPVTRLIEISVNYVGIDMDVRYWSQYISFFL 355
AtFrimp 1     LLGYACSIYCVYKMLKSLQSVVFKEAGTKDPVTTMISIFLRLFDIGVDAALLSQYISLLF 356
AtFrimp 2     FLGYACSIYCVYKMLKSLQSVVFKEAGTKDPVTMMISIFLQFFDIGVDAALLSQYISLLF 355
Rice          LLGYALSVYCVYKMLKSLQSVVFKEAGSVDPVTMTITIFLRHFDIGIDVTLLSQYISLIF 356
               **:  *:**::*::    .:::   *  ****  : * :    :  *  :  *:**:::

Human         VGIIIVTSIRGLLITLTKFFYAISSSKS--SNVIVLLLAQIMGMYFVSSVLLIRMSMPLE 405
Mouse         VGIIIVTSIRGLLITLTKFFYAISSSKS--SNVIVLLLAQIMGMYFVSSVLLIRMSMPPE 405
Xenopus       VGIIIVTSIRGLLITLTKFFYAISSSKS--SNVIVLLLAQIMGMYFVSSVLLIRMSMPLE 405
Drosophila    VGCIVITSIRGLLLTLTKFFYRISSSKS--SNIIVLILGQIMGMYFCSSVLLMRMNMPAE 390
C-elegan 1    VGVIAVTSVRGLLITMTKFFVSISNATSSLSNIIALLMAQIMGMYFVSSVLLMRMNVPEE 416
C-elegan 2    VGVIAITSVRGLLITMAKFFVSISNVRS--SNIIVLGFAQIMGMYFVSSVLLMRMNVPPE 413
AtFrimp 1     IGMLIVISVRGFLTNLMKFFFAVSRVGSGSSSNVVLFLSEIMGMYFLSSILLIRKSLRNE 416
AtFrimp 2     IGMLIVISVRGFLTNLMKFFFAVSRVGSGSSSNVVLFLSEIMGMYFLSSILLIRKSLRNE 415
Rice          IGMLVVISVRGFLANVMKFFFAVSRVGSGSTTNVVLFLSEIMGMYFISSILLIRKSLANE 416
              :* : : *:**:*  : ***  :*   *  :  : *::.:****** **:**:*  :  *

Human         YRTIITEVLG-ELQFNFYHRWFDVIFLVSALSSILFLYLAHKQAPEKQMAP- 455
Mouse         YRTIITEVLG-ELQFNFYHRWFDVIFLVSALSSILFLYLAHKQAPEKHMAP- 455
Xenopus       YRTIITEVLG-ELQFNFYHRWFDVIFLVSALSSILFLYLAHKQAPEKHMAL- 455
Drosophila    YRVIITEVLG-NLHFNFYHRWFDVIFLVSALTTIIVLYLSRKPVRVDDSDLN 441
C-elegan 1    YRTILTRILG-DLKFNFYHRWFDVIFLISAVSSIVFLTLIHKSGSSMFRA   465
C-elegan 2    YRKILTRILGDLLQFNFYHRWFDVIFLISAVTSIAVFSLIRKSGDTRFKH   460
AtFrimp 1     YRGIITDVLGGDIQFDFYHRWFDAIFVASAFLSLVLLSAHYTSRQSDKHAIE 468
AtFrimp 2     YRGIITDVLGGDIQFDFYHRWFDAIFVASAFLSLLLLSAHYTSRQIDKHPID 467
Rice          YRVIITDVLGGDIQFDFYHRWFDAIFVASAFLSLLLISAQYTSRQTDKHPID 468
              ** *:* :** :::*:******* **: **  ::: :
```

Figure 5.2 Sequence alignment of FRIMP1-like proteins from a range of eukaryotic organisms. Sequence alignment of proteins from humans, mouse, xenopus, drosophila, *C.elegans* (Y75B8A and C11H1.2) and rice which show sequence identity to the two putative membrane proteins, AtFRIMP1 and AtFRIMP2 from *Arabidopsis*. The protein sequences show at least 27% sequence identity in all protein sequences from the different organisms, with identical amino acids shown in red (*) and non-identical amino acids with a conserved substitution shown in blue (:).

Figure 5.3 shows a phylogenetic tree constructed using the protein sequences identified from the BLAST searches. The protein sequence from rice, termed OsFRIMP1 shows the highest degree of sequence identity to AtFRIMP1 and forms a cluster with the AtFRIMP proteins. The human, mouse, drosophila and xenopus proteins also show a high degree of sequence identity and form a separate cluster, along with the two proteins from *C.elegans*. Whereas the protein identified in neurophora show the smallest degree of identity and form its own cluster. What is interesting is that FRIMP-like proteins appear to be present in many multicellular eukaryotes, but are absent in unicellular organisms such as yeast and algae.

5.2.2 Isolation of *frimp1* and *frimp2* homozygous knockout mutants

Seed stocks for T-DNA mutants for both FRIMP1 and FRIMP2 originating from the genome wide insertional mutagenesis program conducted by the SALK institute (http://signal.salk.edu/) were obtained. The seed stocks were available through NASC (http://arabidopsis.info). A number of putative T-DNA lines for both genes were available from both SALK and GABI-KAT (Table 5.1). SALK lines were requested initially rather than the GABI-KAT lines and the lines ordered are highlighted with an asterix (*). Two T-DNA lines (N628150 and N585678) were ordered for FRIMP1 and one line (N555330) was ordered for FRIMP2. A disadvantage of the SALK lines compared to the GABI-KAT lines is that the zygosity of the seed stock was not determined. The location of the T-DNA insert within the gene was initially performed by the SALK institute and the seed stock provided was only putatively mutagenised in the advertised location. The location of the T-DNA was subsequently determined using a combination of antibiotic selection and PCR based methods as discussed below. As the T-DNA insert contains the dominant kanamycin resistant gene *NPTII*, it is used as a selection marker to identify the presence of the insert. The seed progeny of the seed stock lines provided by the NASC were sown alongside wild-type seed (Col-8) on plates with and without the antibiotic kanamycin and survival rates were calculated (Table 5.2). This was repeated with the two *frimp1* lines and the *frimp2* line. All the mutant seeds of the *frimp1* line N585678 showed 100% death on kanamycin as did the wild-type, indicating the absence of the T-DNA insert in line N585678 (results not shown).

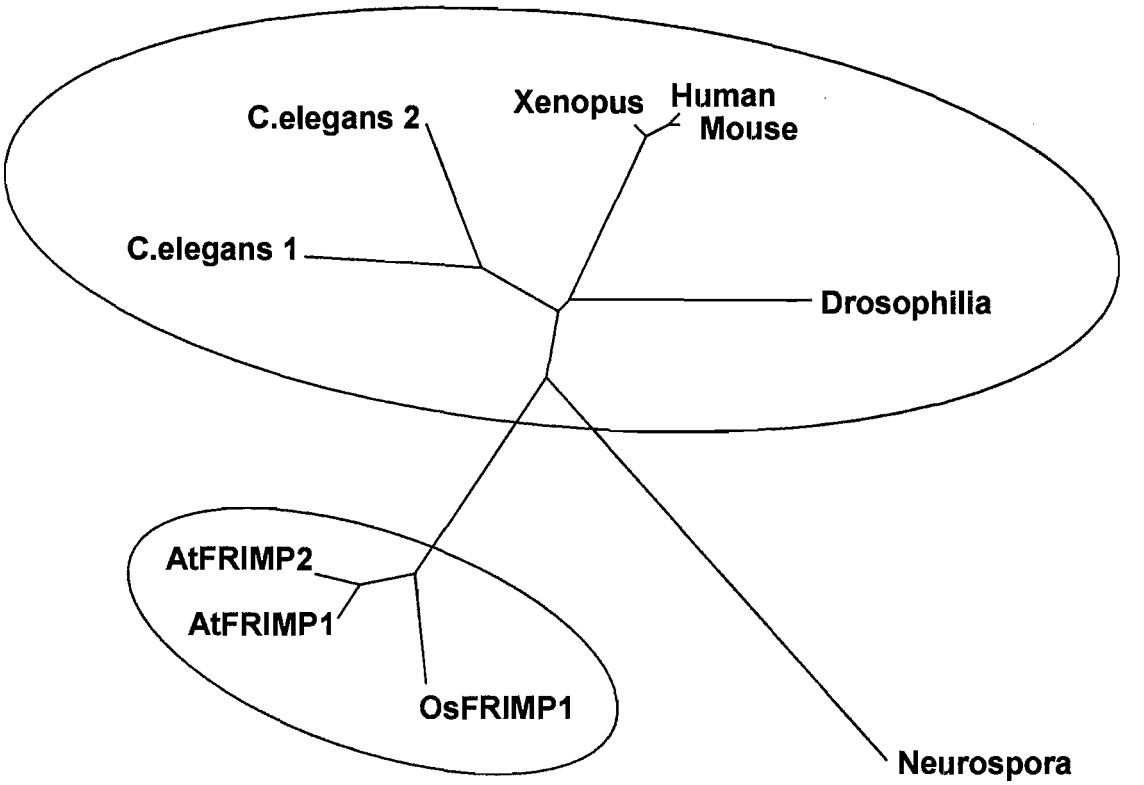

Figure 5.3 Phylogenetic tree of AtFRIMP1-like proteins from a range of eukaryotic organisms. The phylogenetic tree shows a number of proteins from other organisms including rice (OsFRIMP1), *C.elegans* and humans which show sequence identity to the Arabidopsis membrane proteins FRIMP1 and FRIMP2.

Table 5.1 Summary of potential T-DNA mutants for *FRIMP1* and *FRIMP2*. Potential T-DNA insertional mutants were identified by screening a number of web-based *Arabidopsis* mutant databases, including the Gabi-Kat (http://www.gabi-kat.de/) and Salk Lines (http://www.signal.salk.edu/).

Gene Name	T-DNA line	Line ID	Insert Position
At1g64990 *FRIMP1*	Gabi-kat	202B01	3' UTR
		202D03	5' UTR
	Salk line	N585678*	Seven of thirteen exons
		N526083	5' UTR
		N628150*†	Last of thirteen exons
At4g27630 *FRIMP2*	Gabi-kat	188H04	Ninth of twelve introns
		309F09	First of thirteen exons
		565B04	5' UTR
		790H01	5' UTR
	Salk line	N606630	3'UTR
		N555330*†	Tenth of thirteen exons
		N561749	5' UTR

* These mutants were selected and ordered for screening to investigate the phenotype of the T-DNA mutant.

† The lines confirmed as containing the insert and are homozygous for the gene of interest.

The absent of a band using PCR undertaken on genomic DNA extracted from these plants using the *NPTII* primers eliminated the possibility of gene silencing. This line was ordered three times from NASC and the T-DNA insert was absent each time. In contrast the second *frimp1* line N628150 did show selection, with almost every plant showing 100% survival on kanamycin indicating the presence of the T-DNA and the parent plant being homozygous for the T-DNA (Table 5.2).

The progeny of the original seed stock of the 10 *frimp2* mutant plants revealed a selection of wild-type, heterozygote and homozygote mutants (Table 5.2). Plants 1, 2, 4-7 and 9 showed approximately 75% survival indicating these plants were heterozygous for the T-DNA insert, while plants 3 and 8 showed a 100% survival indicating these plants were homozygous for the insert. A 0% seedling survival was shown for plant 10 indicating it was a wild-type plant. The wild-type seeds for each mutant line also gave a 0% seedling survival rate indicating successful selection. Although selection methods reveal the absence or presence of the T-DNA insert, such methods cannot be solely relied on as this does not indicate if the T-DNA insert is located in the gene of interest.

Genomic DNA was extracted from the leaf tissue of 10 plants for both *frimp1* and *frimp2* lines and combinations of primers were used to determine the zygosity of each plant. The T-DNA insert of the *frimp1* line N628150 was predicted to be inserted in the penultimate of the 13 exons, which is predicted to be between transmembrane spanning domains eight and nine within the protein (Figure 5.4). Gene specific forward (F2) and reverse (R2) primers were used in combination with a primer located in the T-DNA (Lba1). A band amplified using the F2 and R2 primers, indicated the presence of a wild-type band (Figure 5.5A). This is the case for the wild-type plant where a genomic band of 1215 bps was amplified (lane 2). A genomic band of approximately 1300 bps was amplified using the Lbal primer and the forward (F2) primer indicating the presence of the T-DNA within the *FRIMP1* gene. This is the case for plants 1-4 indicating they are all homozygous (Figure 5.5A, lanes 6, 9, 12 and 15), which matches the segregation analyses (Table 5.2). No wild-type product was amplified using the F2 and R2 primers in all plants examined (Figure 5.5A, lanes 5, 8, 11 and 14) indicating no heterozygous *frimp1* plants were identified.

Table 5.2 Predicted parent plant zygosity of the *frimp1* and *frimp2* T-DNA mutants using antibiotic selection. The survival rate of the progeny of 10 putative *frimp1* (N628150) and *frimp2* (N555330) T-DNA mutants with wild-type (Col-8) was visually assessed by percentage survival on MS agar plates with and without kanamycin (100 μg/ml) at 10 days post germination. The predicted zygosity of the parent plant is given.

frimp1	Number and Percentage survival (Kan +)	(Kan -)	Predicted Zygosity
Plant 1	52/52 (100%)	53/53 (100%)	Homozygote
Plant 2	47/50 (94%)	48/48 (100%)	Homozygote ?
Plant 3	55/55 (100%)	51/51 (100%)	Homozygote
Plant 4	50/50 (100%)	58/58 (100%)	Homozygote
Plant 5	51/51 (100%)	50/50 (100%)	Homozygote
Plant 6	57/57 (100%)	59/59 (1005)	Homozygote
Plant 7	52/52 (100%)	57/57 (100%)	Homozygote
Plant 8	58/58 (100%)	52/52 (100%)	Homozygote
Plant 9	50/52 (96%)	55/55 (100%)	Homozygote ?
Plant 10	51/51 (0%)	49/49 (100%)	Homozygote
Col-8	0/53 (0%)	51/51 (100%)	Wild-type

frimp2	Number and Percentage survival (Kan +)	(Kan -)	Predicted Zygosity
Plant 1	39/51 (76%)	55/55 (100%)	Heterozygote
Plant 2	39/52 (75%)	52/52 (100%)	Heterozygote
Plant 3	52/52 (100%)	50/50 (100%)	Homozygote
Plant 4	39/51 (76%)	52/52 (100%)	Heterozygote
Plant 5	37/51 (73%)	49/49 (100%)	Heterozygote
Plant 6	39/51(76%)	52/52 (100%)	Heterozygote
Plant 7	38/50 (76%)	53/53 (100%)	Heterozygote
Plant 8	52/52 (100%)	52/52 (100%)	Homozygote
Plant 9	38/50 (76%)	50/50 (100%)	Heterozygote
Plant 10	51/51 (0%)	55/55 (100%)	Wild-type
Col-8	0/53 (0%)	52/52 (100%)	Wild-type

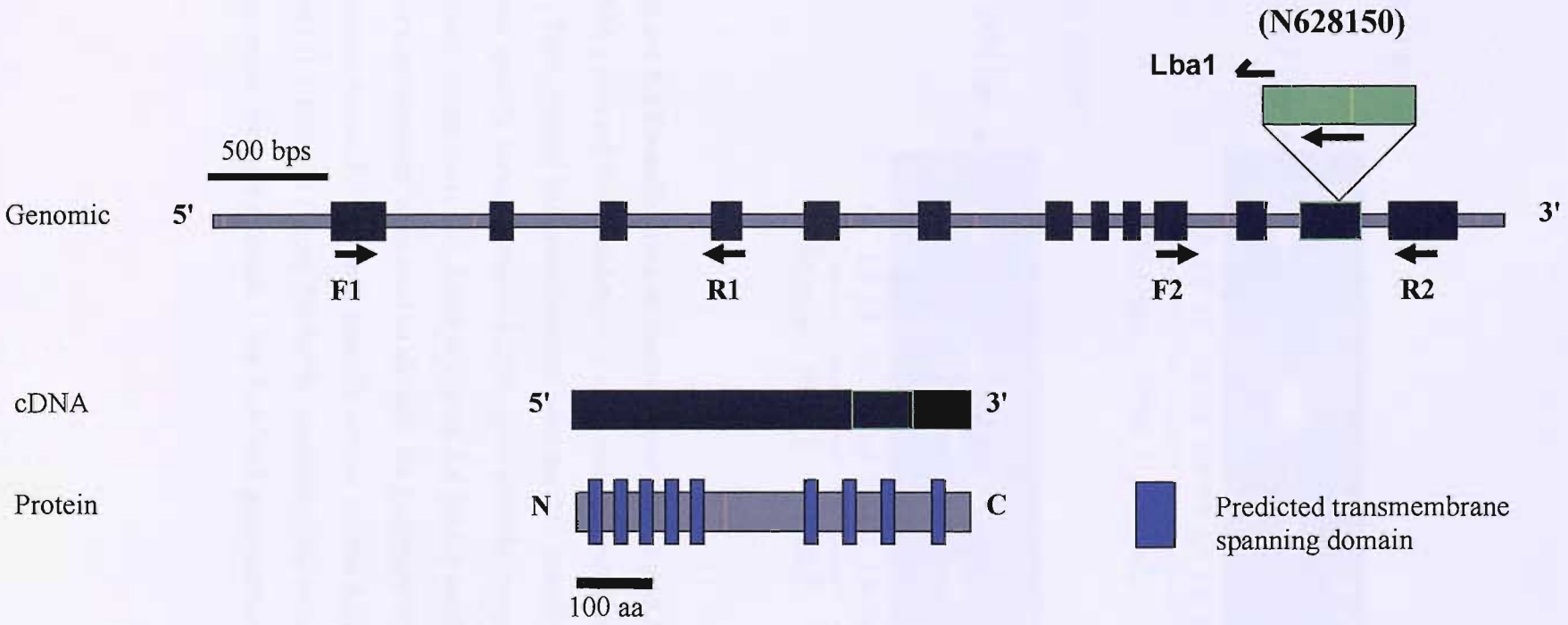

Figure 5.4 Schematic representation of the protein and genomic sequences of At1g64990 (FRIMP1), indicating the location of the T-DNA insertion. The T-DNA insertion, mutant (N628150) is located in the twelfth of thirteen exons, which is in the eighth of nine predicted transmembrane spanning domains. Locations of TMS were predicted using hydrophobicity plots. The T-DNA sequence is inserted in the reverse complementation to the gene. Arrows shown indicate the location of primers designed to confirm the presence of the T-DNA insert and the absence of mRNA in the mutant. The Lba1 primer is designed within the T-DNA insert and is used to identify the presence of the insert. T-DNA insert not to scale.

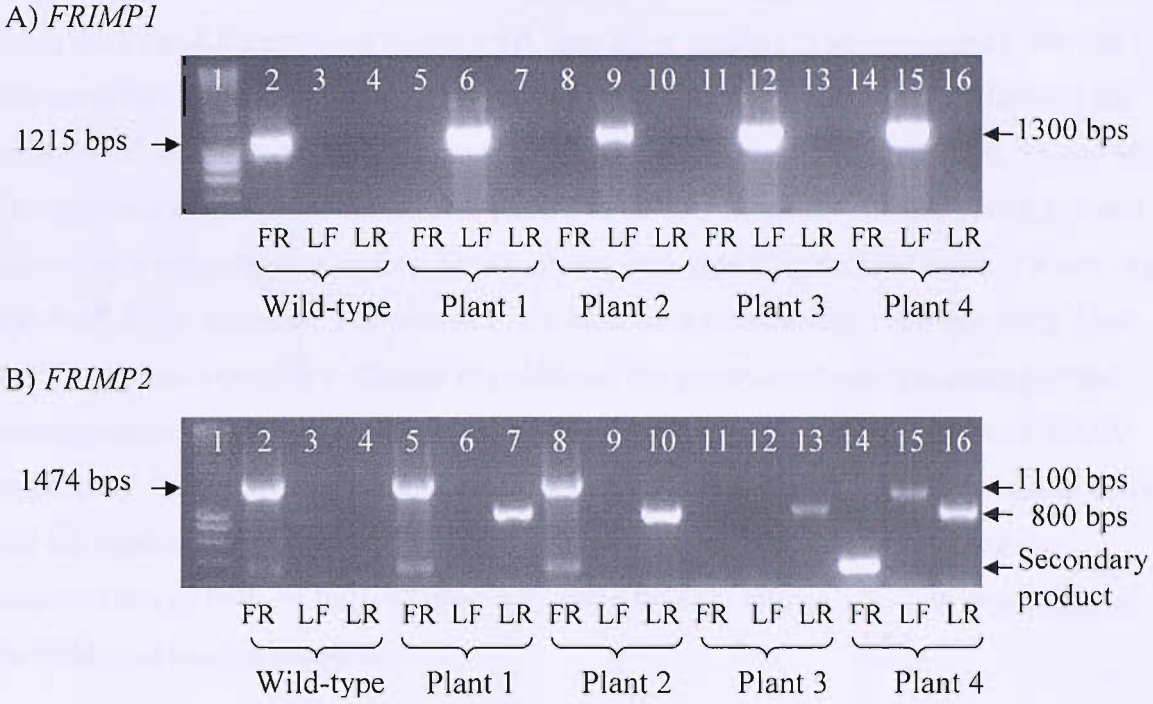

Figure 5.5 Identification of homozygous *frimp1* and *frimp2* mutants. PCR on genomic DNA extracted from wild-type (Col-0) and potential *frimp1* and *frimp2* T-DNA mutants. A) Three primer pair combinations were used to identify the genotype of the *frimp1* mutant, gene specific forward primer F2 (F), gene specific reverse primer R2 (R) and T-DNA left border primer Lba1 (L). Refer to Figure 5.4 for the location of the primers. B) Three primer pair combinations were used to identify the genotype of the *frimp2* mutant, gene specific forward primer F2 (F), gene specific reverse primer R2 (R) and T-DNA left border primer Lba1 (L). Refer to Figure 5.6 for the location of the primers. See Table 2.5 for primer sequences for both mutants. Lane 1 on both gels contains the molecular weight marker.

The same process was repeated with the *frimp2* line N555330, where the T-DNA insert is predicted to be located in the tenth of thirteen exons. In terms of protein sequence, the insert is predicted to be in the seventh of nine transmembrane spanning domains (Figure 5.6). As with *FRIMP1*, gene specific forward (F2) and reverse (R2) primers were used in combination with the Lba1 primer. A wild-type genomic band of 1474 bps was amplified using the F2 and R2 primers (Figure 5.5B, lane 2). A product of approximately 800 bps was amplified when using the Lba1 primer in combination the R2 primer, indicating the presence of the T-DNA insert as shown in plants 1-4 (Figure 5.5B, lanes 7, 10, 13 and 16). The presence of this product indicates plant 3 to be homozygous, whereas plants 1, 2 and 4 appear to be heterozygous as they have both the wild-type (Figure 5.5B lanes 5, 8 and 14) and the T-DNA products. The presence of a band of approximately 1100 bps using Lbal and F2 in plant 4 (Figure 5.5B lane 15) indicates the presence of multiple inserts or the rearrangement of the T-DNA insert. To confirm that the amplified product was *FRIMP1* and *FRIMP2* respectively, both the products using F2 and R2, and the product using Lba1 and the appropriate gene specific primer were sequenced. Sequencing revealed the amplification of both *FRIMP1* (Figure 5.7) and *FRIMP2* (Figure 5.8). The sequencing of the wild-type band is not shown.

5.2.3 Molecular analysis of the *frimp1* and *frimp2* mutants

To confirm the zygosity of the selected homozygous mutants, RNA was extracted from both the putative *frimp1* and *frimp2* mutants. RNA was extracted from leaf tissue from the progeny of plant 1 for *frimp1* and plant 3 for *frimp2*. Primers were designed to amplify different sections of the genes to check for the presence of the wild-type gene (W) and a truncated product (Tr) (Table 2.5). Primers were also used spanning the T-DNA (T) as confirmed via PCR on genomic DNA (Figure 5.9). Firstly these three combinations of primers were used on mRNA extracted from *frimp1*. A cDNA product of 1266 bps was amplified using the F1 and R2 primers designed to amplify the whole gene from a wild-type plant (Figure 5.9A, lane 5), but not in the *frimp1* mutant (lane 8). Due to the size of the product no genomic band was amplified using these primers (lane 2). The same was true using the T-DNA primers (F2 and R2), where a cDNA product of 257 bps was amplified in the wild-type (lane 7) but not in the *frimp1* mutant (lane 10). However when primers were used to check for the presence of a truncated product (F2 and R2), a 436 bp product was

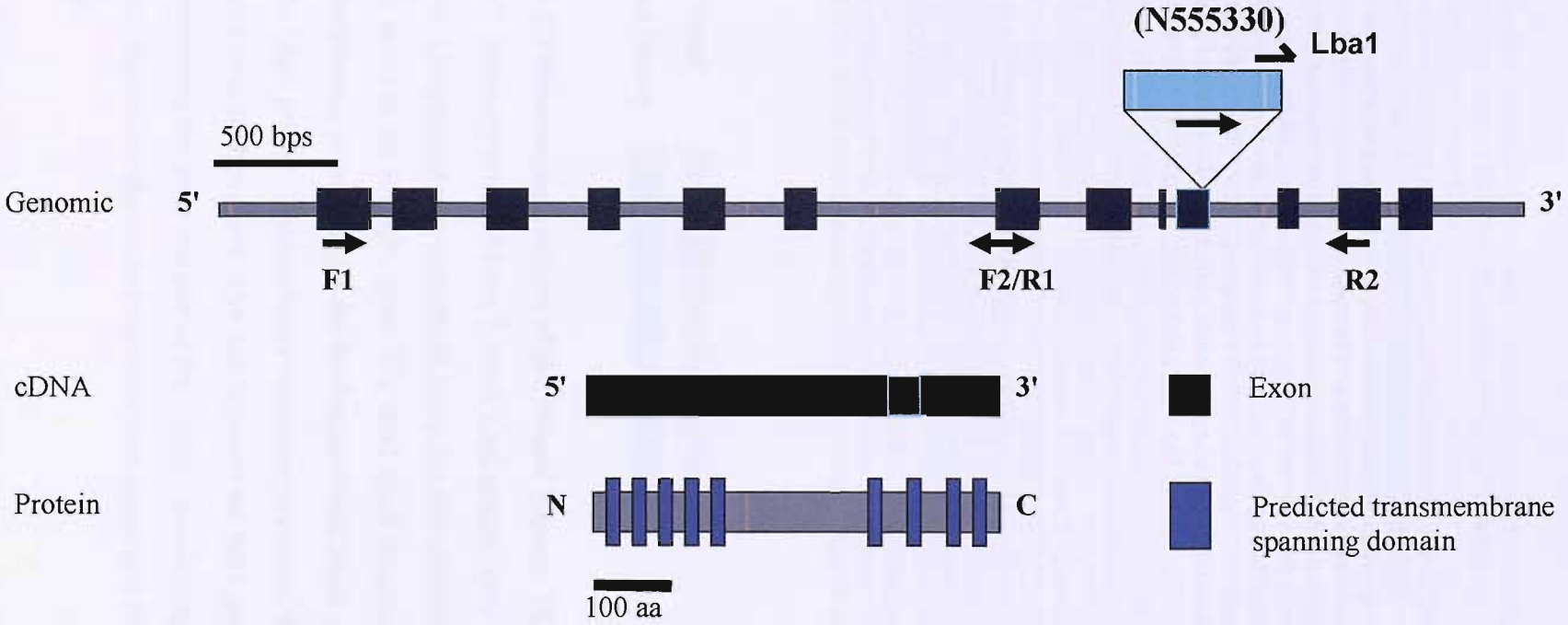

Figure 5.6 Schematic representation of the protein and genomic sequences of At4g27630 (FRIMP2), indicating the location of the T-DNA insertion. The T-DNA insertion, mutant (N555330) is located in the tenth of thirteen exons, which is in the seventh of nine predicted transmembrane spanning domains. Locations of TMS were predicted using hydrophobicity plots. The T-DNA sequence is inserted in the forward complementation to the gene. Arrows shown indicate the location of primers designed to confirm the presence of the T-DNA insert and the absence of mRNA in the mutant. The Lba1 primer is designed within the T-DNA insert and is used to identify the presence of the insert. T-DNA insert not to scale.

tgatctagcttaaaagtcttctcactattgtcgttttgaacatgagtaactcttgttctccttttt
ttgtgctctatttttgCAGTCTCTTCAAAGTGTTGTCTTCAAAgaggtacccacatgcgctatttt
ttttgttaacttatgtatcactaccgttctttaatgggttatatgtgcacctcttactacttgaaa
ttgttagtaatcagcttgtttaCAGGCCGGTACAAAAGATCCTGTCACGACGATGATCAGCATATTC
TTGCGGTTGTTTGATATAGGAGTAGATGCTGCACTCCTCTCAcaggtttgcgttaccttacgttgct
atctctaatgatagagtaattaagctaaagaaatccaatctggacgtttttttcttctagacttgaaa
gtatttctagacttgaaagcctaaagcatttatttcttcaatattaagtcactatctctaagccttt
gatgggatggaaagttagatggttaaagagatcagagctgtcctagggcctagttatattccaaact
atttatcattataaagtaaaacatatgctgaattctctcaacttttctgcgtctggtttgctagatt
gtgagacttatctctaattctgtttctttctttcttgttcgCAGTATATATCCCTGCTGTTCATTGG
GATGTTGATTGTGATTTCTGTGAGGGGATTCCTGACGAACCTGATGaaggtgaattatgattctcgt
ttttcgatttttttcattggtgtgcctctaaactgtcatctattcaacaaagactcttctggatcctt
tgaatttgtgcataaacacattcacatgattactcatacagtccttgatttagtttcaatcttgtat
ccccaccatttaatcaagctacttcttagaggcaatcatgttttaaatagaagaatcctttcactat
ttaagctgcgtatactagactgctagtcacagatgagtattgtggttgtagtgaaaacataacaaac
tgcacgctgaatttttggttaatttgaatgctgtagttttagttaatgagttggagtttgtggatgg
tgCAGTTTTTCTTTGCTGTCTCAAGAGTGGGAAGTGGGTCTTCAAGCAATGTTGTACTTTTCCTATC
TGAAATCATGGGAATGTACTTTTTGTCTTCATTTGGGAATATATATTGTGGTGTAAACAAATTGACG
CTTGACAACTTAATAACACATTGCGGACGTTTTTAATGTACTGGGGTGGTTTTTCTTTTCACCAGTG
AGACGGGCAACAGCTGATTGCCCTTCACCGCCTGGCCCTGAGAGAGTTGCAGCAAGCGGTCCACGCT
GGTTTGCCCCAGCAGGCGAAAATCCTGTTTGATGGTGGTTCCGAAATCGGCAAAATCCCTTATAAAT
CAAAAGAATAGCCCGAGATAGGGTTGAGTGTTGTTCCAGTTTGGAACAAGAGTCCACTATTAAAGAA
CGTGGACTCCAACGTCAAAGGGCGAAAAACCGTCTATCAGGGCGATGGCCCACTACGTGAACCATCA
CCCAAATCAAGTTTTTTGGGGTCGAGGTGCCGTAAAGCACTAAATCGGAACCCTAAAGGGAGCCCCC
GATTTAGAGCTTGACGGGGAAAGCCGGCGAACGTGGCGAGAAAGGAAGGGAAGAAAGCG

Key

Lba1 Primer	TGGTTCACGTAGTGGGCCATCG
Forward Primer	TTCTTTGCAGTGTCGAGGGTTGG

Figure 5.7 Sequencing analysis of the *frimp1* mutant. PCR on genomic DNA using *FRIMP1* forward primer and the T-DNA Lbal primer. (see Figure 5.4 for location of primers). The product was sequenced using the two primers to confirm the presence of the T-DNA insert in the *FRIMP1* gene. The bold black sequence represents the DNA sequence from the forward primer, while the bold under-lined black represents the T-DNA sequence from the Lba1 primer. The bold grey sequence represents the overlapping sequence generated from both primers. The join between the bold grey and bold under-lined black bases represents the insertion site of the T-DNA confirming the presence of the T-DNA in *FRIMP1*. Introns are shown in lower case and exons and the T-DNA insert are shown in capitals.

GCAGCACATCCCCCTTTCGCCAGCTGGCGTAATAGCGAAGAGGCCCGCACCGATCGCCCTTCCCAACAGTTGC
GCAGCCTGAATGGCGCCCGCTCCTTTCGCTTTCTTCCCTTCCTTTCTCGCCACGTTCGCCGGCTTTCCCCGTC
AAGCTCTAAATCGGGGGCTCCCTTTAGGGTTCCGATTTAGTGCTTTACGGCACCTCGACCCCAAAAAACTTGA
TTTGGGTGATGGTTCACGTAGTGGGCCATCGCCCTGATAGACGGTTTTTCGCCCTTTGACGTTGGAGTCCACG
TTCTTTAATAGTGGACTCTTGTTCCAAACTGGAACAACACTCAACCCTATCTCGGGCTATTCTTTTGATTTAT
AAGGGATTTTGCCGATTTCGGAACCACCATCAAACAGGATTTTCGCCTGCTGGGGCAAACCAGCGTGGACCGC
TTGCTGCAACTCTCTCAGGGCCAGGCGGTGAAGGGCAATCAGCTGTTGCCCGTCTCACTGGTGAAAAGAAAAA
CCACCCCAGTACATTAAAAACGTCCGCAATGTGTTAGACCTTGTTACACTAGATGGCTTTTTATCTTGATGCT
TATATGGTTCTCAACTTACCTTATGTAGGTCTGATGCTCTCTCTTTGTTTATTATTTTCAGTATATTTCCCTG
TTATTTATTGGGATGTTGATCGTGGATATCAGTGAGGGGGAATTCTTGACAAATCTGATGAAGGTGAGTTCTG
ATTTCAGCTTTTAAATTTCCCCTTTCGTTCTTTTNCNATCTTGGTTTTGTTTTCCCTTTGTTTTGGGACCTTT
TTGTGTNTGGNTTGGNTTTGGGCTTNTCTTGTTTagtgtcaatggaaaacttgctctggcattatcatgttta
aatattagacggaggctttcacttcttttagctggtgctaactttccttgtgacagtcacatagttacttaag
caaagtatatatgatgtatatcctaagagtggaagatgtagagtgattgaattaacgtatttgttgcagtagc
attacagaacaactcaatgtaatttcagtctgatcataaaaacagaggctactttcttggttggcattagtat
agtgattttacatctaagtaattgtaactcgcaatatactgaaagcttttgttttgaatactgttaaacgttt
tggtgattgaattggggagtttttttcaattcgcttgtacagTTCTTCTTTGCAGTGTCGAGGGTTGGAAGT
GGATCTTCAAGCAATGTTGTGCTCTTCCTATCAGAAATCATGGGAATGTACTTTTTGTCTTCCATTCTTCTTA
TAAGAAAAAGCTTGAGAAATGAGTACAGgtacgtaagataatactataacaataattacaacc

Key

Lba1 Primer	TGGTTCACGTAGTGGGCCATCG
Reverse Primer	TTCTTTGCAGTGTCGAGGGTTGG

Figure 5.8 Sequencing analysis of the *frimp2* mutant. PCR on genomic DNA using *FRIMP2* reverse primer and the T-DNA Lbal primer (see figure 5.6 for location of primers). The product was sequenced using the two primers to confirm the presence of the T-DNA insert in the *FRIMP2* gene. The bold black sequence represents the DNA sequence from the reverse primer, while the bold under-lined black (T-DNA) sequence, and the bold grey sequence (*FRIMP2*) represents the DNA sequence from the Lba1 sequence. The join between the bold under-lined black and bold grey bases represents the insertion site of the T-DNA confirming the presence of the T-DNA in *FRIMP2*.

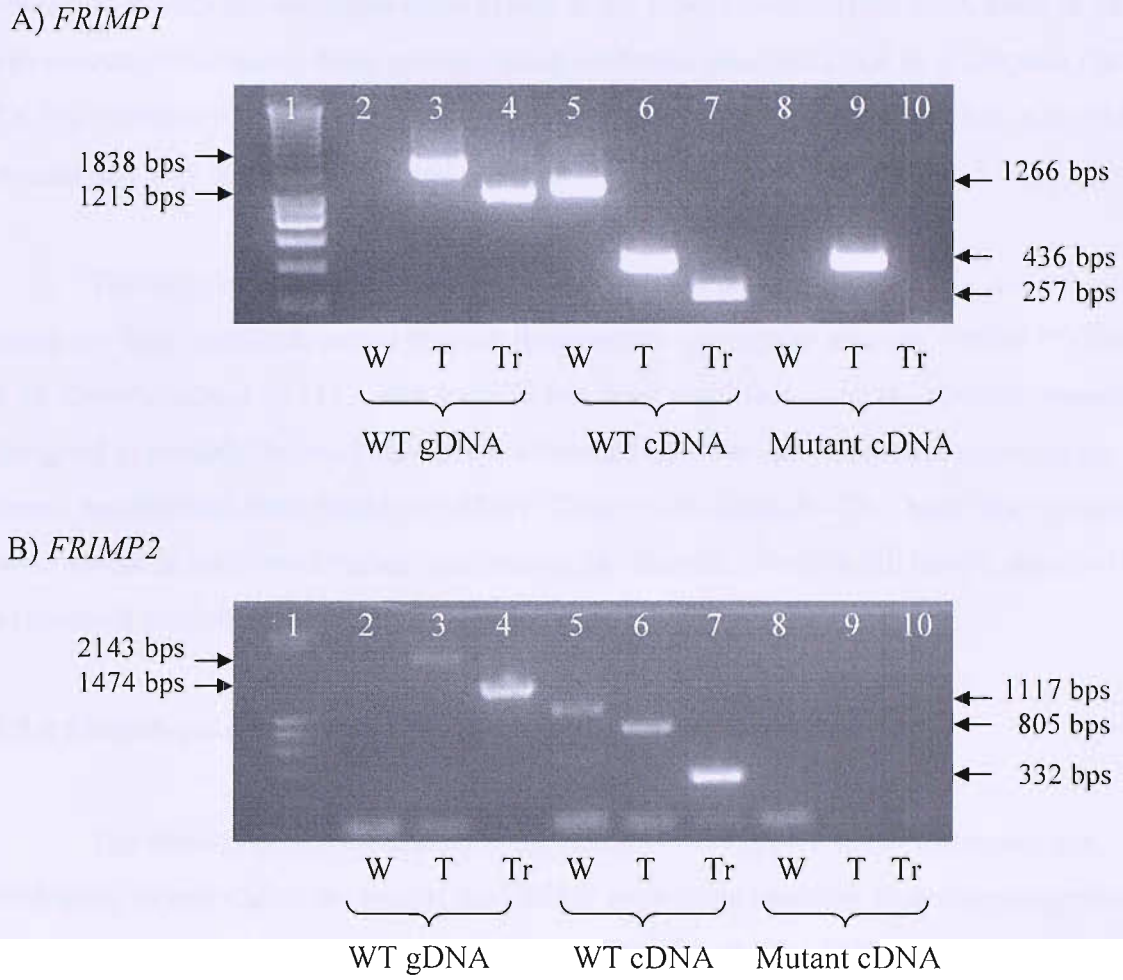

Figure 5.9 Confirmation of homozygous *frimp1* and *frimp2* mutants. A) PCR on wild-type genomic DNA and cDNA from the wild-type and *frimp1* identified from genotypic analyses. Three primer pair combinations were used to confirm the absence of mRNA for the gene of interest, spanning different sections of the gene. Primers F1 and R2 were used to amplify the wild-type gene (W), primers F1 and R1 were used to amplify a truncated gene (Tr) and primers F2 and R2 to the T-DNA flanking region (T). Refer to Figure 5.4 for location of primers. B) PCR on wild-type genomic DNA and cDNA from the wild-type and *frimp2* identified from genotypic analyses. Three primer pair combinations were used to confirm the absence of mRNA for the gene of interest, spanning different sections of the gene. Primers F1 and R2 were used to amplify the wild-type gene (W), primers F1 and R1 were used to amplify a truncated gene (Tr) and primers F2 and R2 to the T-DNA flanking region (T). Refer to Figure 5.6 for location of primers. Lane 1 on both gels contains the molecular weight marker.

amplified in both the wild-type (lane 6) and in the *frimp1* mutant (lane 9). A band of 1838 bps was amplified using these primers using wild-type genomic DNA as a template (lane 3). The presence of a truncated product in the *frimp1* mutant indicates that it is not a null mutant and may contain a truncated protein.

The same methodology was used to confirm the homozygosity of the *frimp2* mutant using the three combinations of primers designed to specifically amplify *FRIMP2* (Table 2.5). Three products of 1117, 805 and 332 bps were amplified using the specific primers designed to amplify the wild-type gene, a truncated product and a product spanning the insert, respectively from wild-type cDNA (Figure 5.9B, lanes 5 – 7). These three products were absent in the *frimp2* mutant confirming the absence of both a full length gene and also a truncated product (Figure 5.9B, lanes 8 – 10).

5.2.4 Phenotypic characterisation of *frimp1* and *frimp2* seedlings

The homozygous *frimp1* and *frimp2* mutants were grown under different light treatments to investigate the role of the FRIMP proteins in seedling photomorphogenesis. Wild-type, *frimp1* and *frimp2* seedlings were grown for one day in the dark and the under the following light treatments, white, red, blue, FR-light or remained in the dark for four days. The etiolated *frimp1* and *frimp2* seedlings showed no difference in hypocotyl length or apical hook angle compared to wild-type (Figure 5.10A). A significant increase in hypocotyl elongation was observed in the *frimp1* seedling grown in FR-light but *frimp2* resembled the wild-type phenotype (Figure 5.10B). No change in hypocotyl length or cotyledon area was seen in either the *frimp1* or *frimp2* mutant grown in white or blue light (Figure 5.11A and C). However when grown under red light, *frimp1* showed a significant increase in both hypocotyl length and cotyledon area, whereas *frimp2* showed a significant decrease in hypocotyl length and cotyledon area (Figure 5.11B).

Variation was seen in the length of the hypocotyl of the FR-light grown *frimp1* seedlings between replicates so this experiment was repeated on multiple occasions. It was noted that a greater difference between the hypocotyl length of the wild-type and *frimp1* was when the wild-type seedlings was at their longest (Figure 5.12). This suggests that FRIMP1 may be most important at lower FR-light fluences. Although the *frimp1* mutant

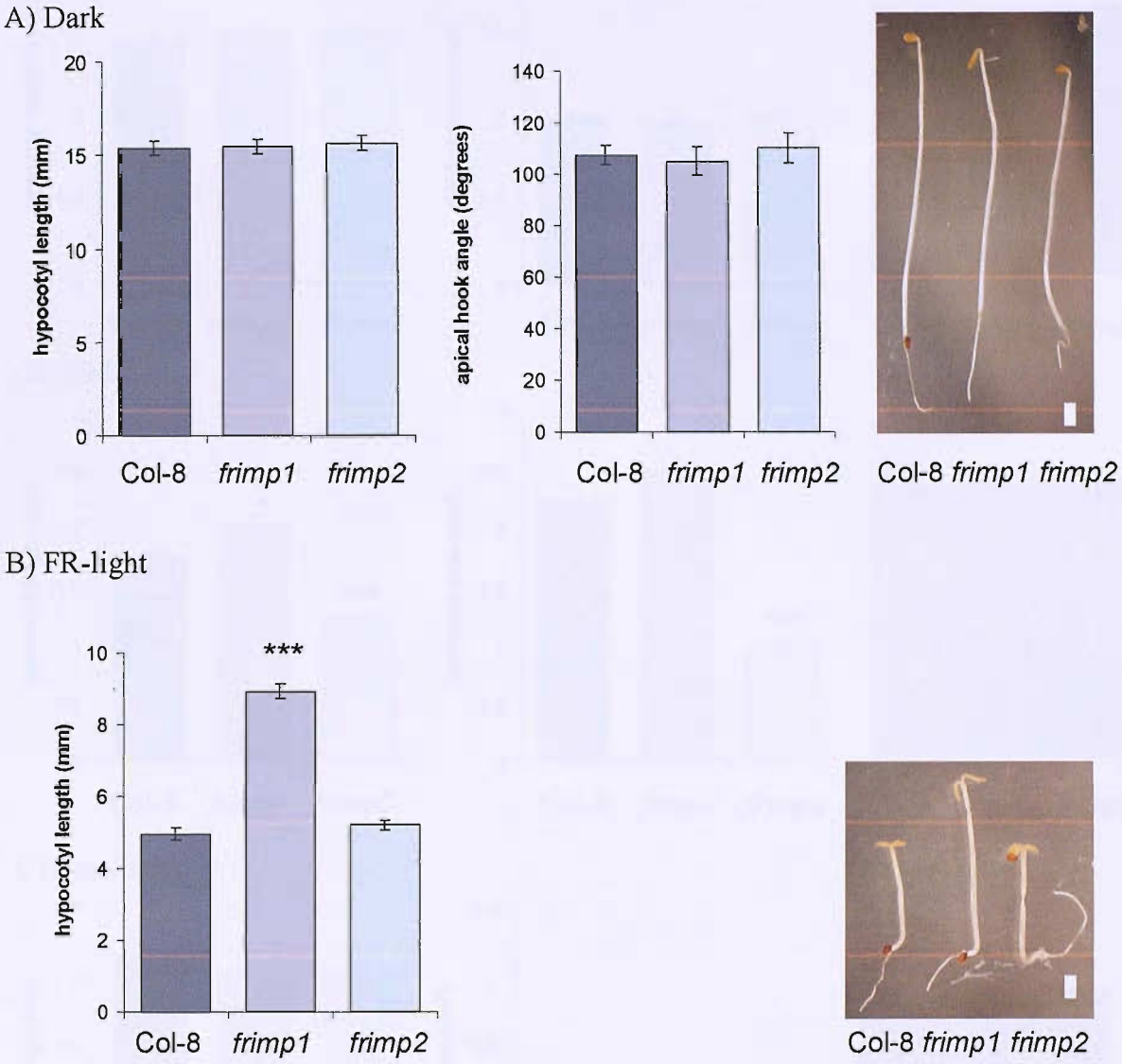

Figure 5.10 Seedling phenotypic analyses of the *frimp1* and *frimp2* mutants. A) Hypocotyl length and apical hook angle of wild-type (Col-8), *frimp1* (N628150) and *frimp2* (N555330) mutants in the dark. B) Hypocotyl length of Col-8, *frimp1* and *frimp2* mutants grown in FR-light. All graphs show the mean ± standard error, n = 30 from one biological repeat. Scale bar of the photographs = 1 mm. Significance levels are shown with *** ($P<0.005$).

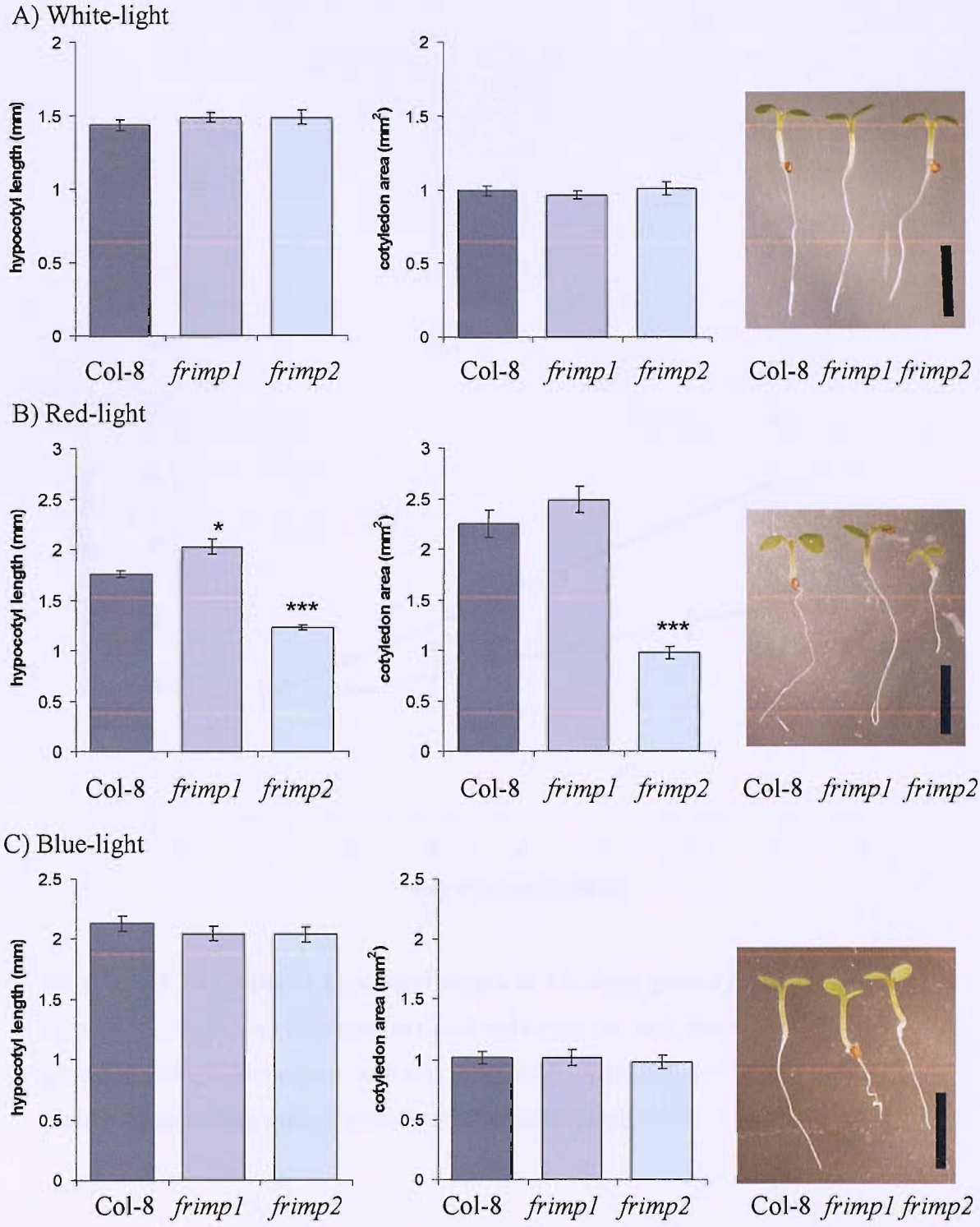

Figure 5.11 Phenotypic analysis of *frimp1* and *frimp2* seedlings. Hypocotyl length and cotyledon area of wild-type (Col-8), *frimp1* (N628250) and *frimp2* (N555330) mutants in, A) white light, B) red light and C) Blue light. All graphs show the mean ± standard error, n = 30. Data shown represents one biological repeat. Similar results were shown on a second biological repeat. Scale bar of the photographs = 2mm. Significant levels are shown with *($P<0.05$) and ***($P<0.005$).

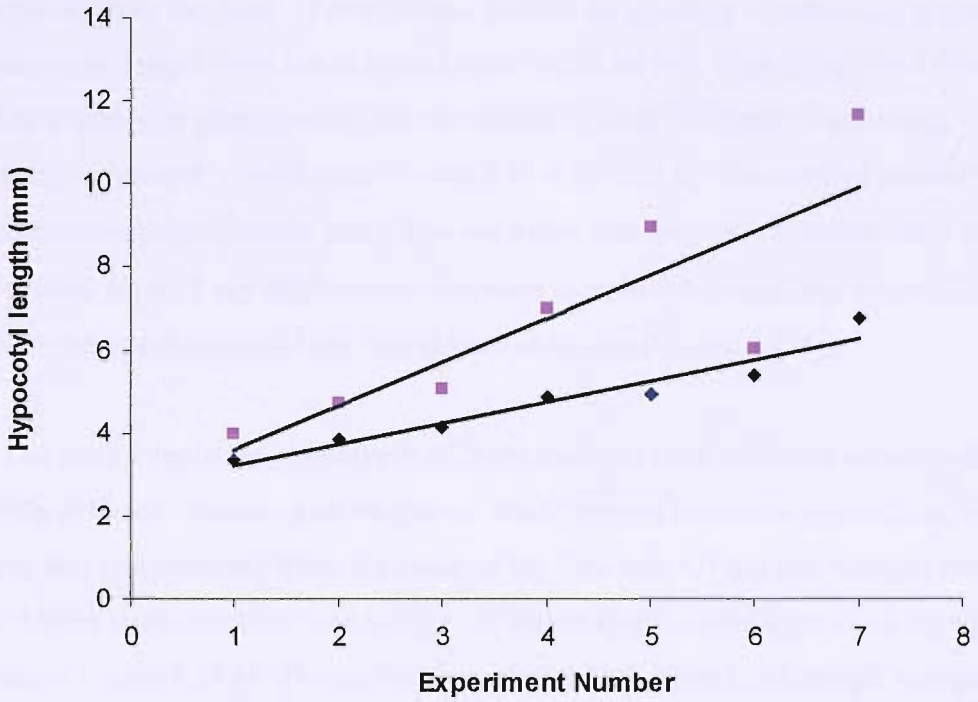

Figure 5.12 Variation of hypocotyl length in FR-light grown *frimp1* seedlings. Hypocotyl length was measured in Col-8 wild-type (■) and *frimp1* (■) FR-light grown seedlings. The experiment was repeated 8 times with n = 30 and the data plotted in ascending rank of wild-type hypocotyl length.

showed 100% germination, the germination rate of the *frimp2* mutant was some what irregular, with a germination rate ranging from 70% upwards using multiple seed batches when plated on agar when grown under red and FR-light (results not shown).

5.2.5 *frimp1* and *frimp2* phenotypic analysis

The *frimp1* and *frimp2* mutants were analysed throughout their development from seed germination to the onset of senescence. Unlike the seedling experiments germination difficulties with *frimp2* were not observed when sown on soil. Both *frimp1* and *frimp2* showed an increase in plant height when measured at three different times during its development compared to wild-type (Figure 5.13A and B). By the onset of senescence, the *frimp1* mutant was significantly taller than wild-type and the *frimp2* mutant taller still. Neither mutant showed any differences compared to wild-type regarding the onset of the first bolt or the development of the first flower or silique (Figure 5.13C).

The most interesting phenotypes of these mutants were observed when looking specifically at the development of the leaves. Both mutants had more leaves than wild-type plants and this was observed from the onset of the first bolt. Of the two mutants *frimp1* had the most leaves with over twice the number of leaves that the wild-type at 30 days post germination (Figure 5.14A). The rosette diameter of both *frimp1* and *frimp2* was greater than wild-type (Figure 5.14B). This difference was noticeable from approximately 15 days post germination before the first bolt, with *frimp2* having a wider rosette than *frimp1* (Figure 5.14B). *frimp1* and *frimp2* also appeared to have more leaves at the development of the first bolt although this was only statistically significant for *frimp1* (Figure 5.15A). The increase in rosette diameter most probably results from the observed increase in the average length of the petioles of *frimp1* (Figure 5.15B). This can be seen in the adaxial and abaxial views of the leaves (Figure 5.15C), and results in a larger petiole to whole leaf length ratio. The wild-type leaf has a petiole:whole leaf length ratio of approximately 0.25 where the petiole makes up one quarter of the length of the total leaf. The *frimp1* mutant has a petiole:whole leaf length ratio of approximately 0.35 resulting from the longer petiole (Figure 5.15B). The *frimp2* mutant appears to be similar to wild-type in terms of the petiole:whole leaf length ratio, and the increase in the rosette diameter is therefore a result of a longer leaf than wild-type (Figure 5.15D).

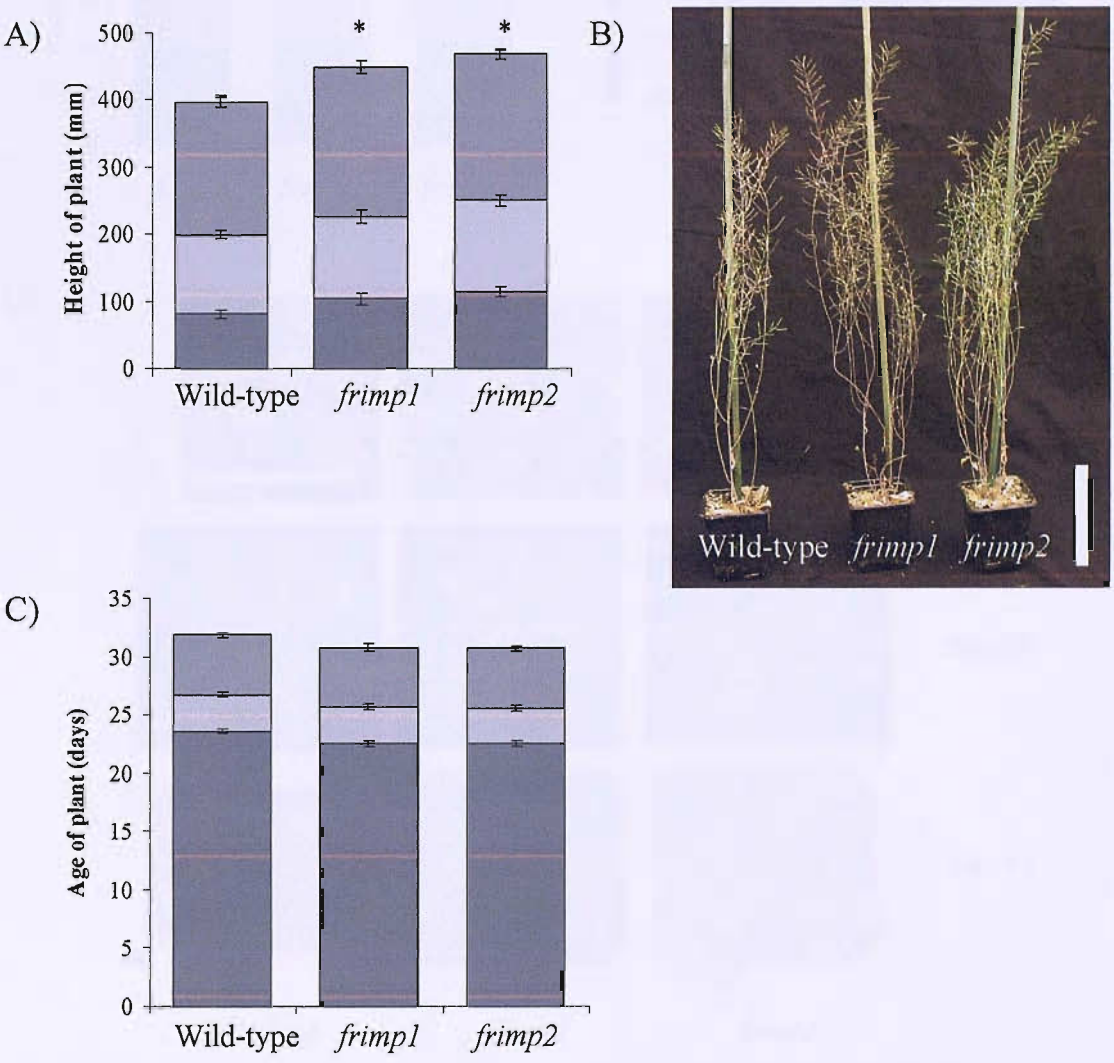

Figure 5.13 Phenotypic analysis of *frimp1* and *frimp2* plants. A) Plant height of wild-type (Col-8), *frimp1* and *frimp2* mutant plants at days 20 (■), 33 (■) and 55 (■). B) Photographs of Col-8, *frimp1* and *frimp2* mutant plants at day 55, scale bar = 10cm. C) The age at which wild-type, *frimp1* and *frimp2* mutant plants showed first bolt (■), flower (■) and silique (■). Both graphs show mean ± standard error (n = 20) of one biological repeat. Significance levels are shown as *($P<0.05$).

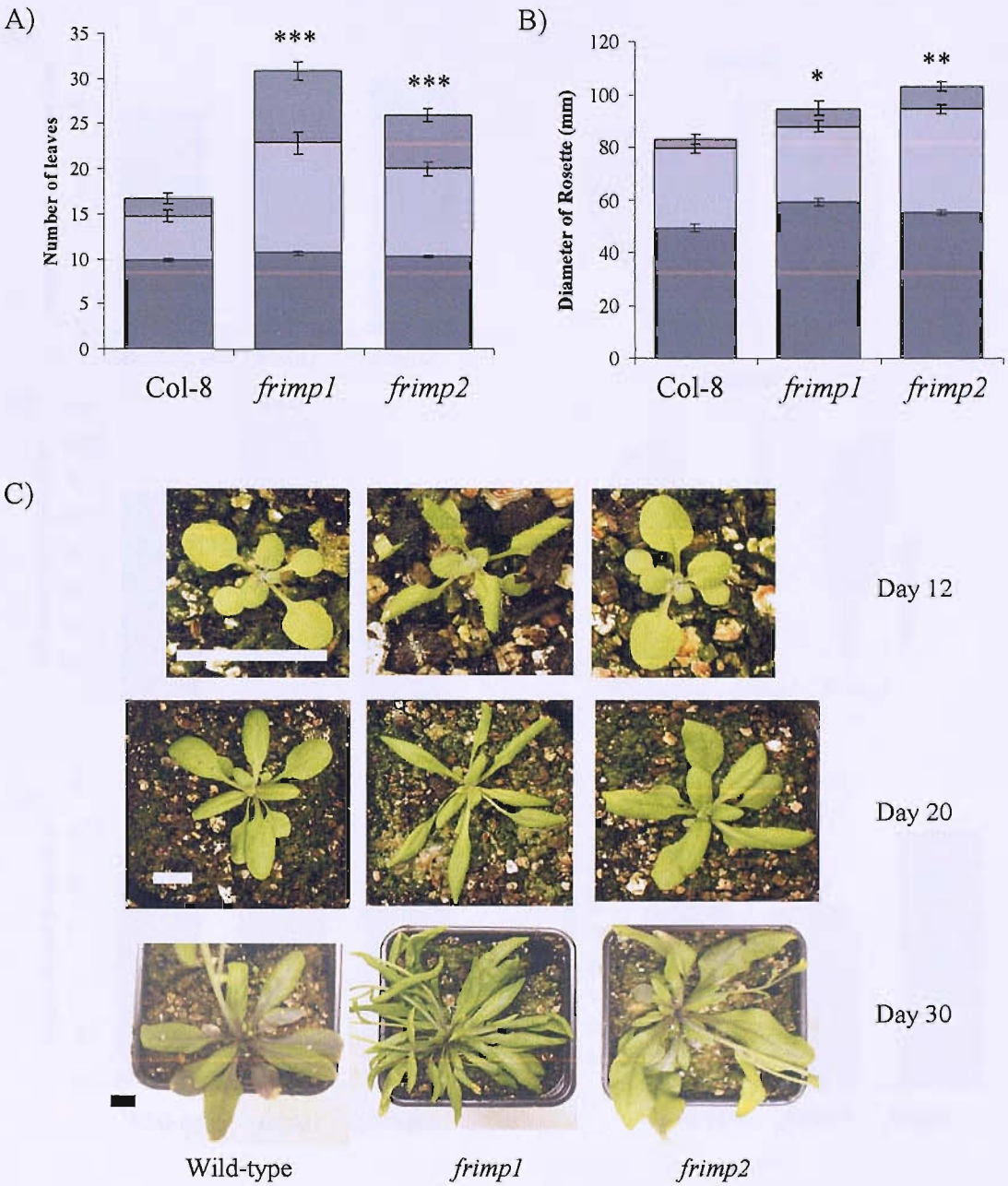

Figure 5.14 Phenotypic analyses of the *frimp1* and *frimp2* plants. A) Number of leaves of wild-type (Col-8), *frimp1* and *frimp2* mutants, at days 20 (■), 27 (■) and 33 (■) post germination. B) Diameter of plant rosette of wild-type (Col-8), *frimp1* and *frimp2* mutants at days 20 (■), 27 (■) and 33 (■) post germination. Mean ± standard error (n = 20) of one biological repeat. C) Photographs of plant rosette of wild-type (Col-8), *frimp1* and *frimp2* mutants at 12, 20 and 30 days post germination. Scale bar = 10 mm. Significance levels shown are *(P<0.05), **(P<0.01) and ***(P<0.005).

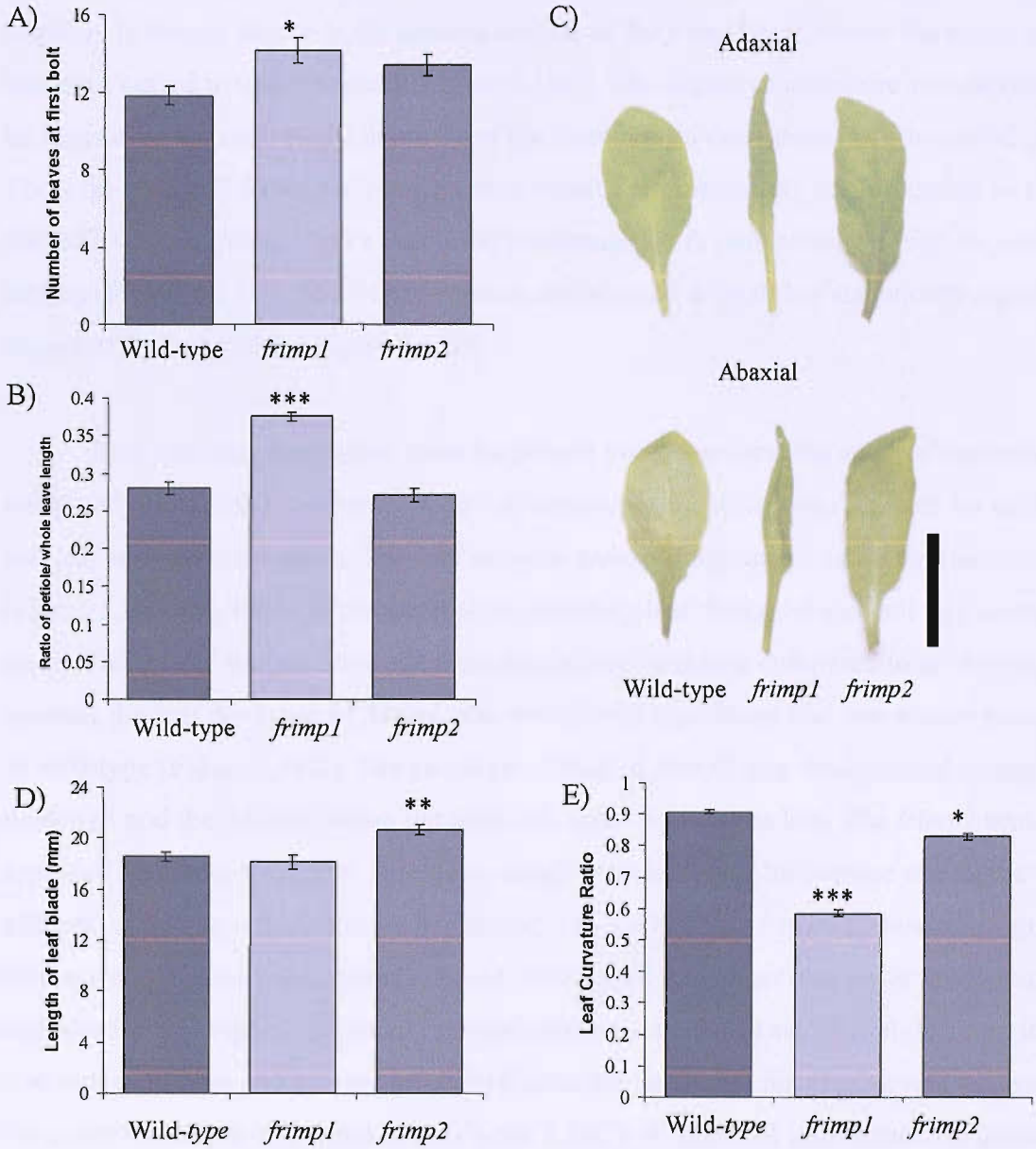

Figure 5.15 Phenotypic analyses of the *frimp1* and *frimp2* mutants. A) Number of leaves at first bolt of Col-0, *frimp1* and *frimp2* plants, mean ± standard error of n = 20. B) Ratio of petiole length to the whole leaf length at day 20. C) Photographs of adaxial and abaxial views of wild-type and the *frimp1* and *frimp2* mutants at 20 days post germination. Scale bar = 10 mm. D) length of leaf blade. E) leaf curvature ratio at day 25. Figures B, D and E show mean ± standard error of n = 20 with the mean of two leaves per plant. Experiment of one biological repeat. Significance levels shown are *($P<0.05$), **($P<0.01$) and ***($P<0.005$).

The most striking phenotype of *frimp1* is the epinastic response of the leaves, where after approximately 10 days post germination the leaves begin to curl (Figure 5.15E). This response is clearly shown in the abaxial section of the *frimp1* leaf, where the edges of the leaf have curled in under the leaf (Figure 5.15C). The degree of curvature was calculated by measuring the ratio of the diameter of the open leaf to the diameter of the curled leaf. The wild-type leaf showed a leaf curvature ratio of approximately 0.9 indicating an almost flat leaf, whereas *frimp1* had a ratio of approximately 0.6, representing a high degree of curling (Figure 5.15D). The *frimp2* mutant also showed a small but statistically significant degree of leaf curvature (Figure 5.15D).

Leaf samples were taken from the *frimp1* and *frimp2* mutant and leaf sections were compared to the Col-8 wild-type. Two leaf samples were taken from 3 plants for each line and leaf sections were taken. The leaf sections were photographed under the microscope (Figure 5.16A). A series of measurements including leaf thickness and cell size areas were taken. The *frimp2* mutant showed no change in leaf thickness compared to wild-type, whereas the leaf thickness of *frimp1* was statistically significant and was almost twice that of wild-type (Figure 5.16B). The cell organisation of *frimp1* was disorganised compared to wild-type and the differentiation between cell types was almost lost. The *frimp2* mutant appeared similar to wild-type in regards to cell organisation. The average size of the different cell types was determined (Figure 5.16C). The *frimp1* mutant showed a significant increase in the size of the palisade, spongy mesophyll and upper and lower epidermal cells compared to wild-type. The *frimp2* mutant showed a small but significant decrease in the size of the palisade and spongy mesophyll cells but no significant change was noticed in the upper and lower epidermal cells (Figure 5.16C). Analysis of photosynthetic pigment concentrations, including chlorophyll a, chlorophyll b and total carotenoids in leaves of 25-day-old *frimp1* and *frimp2* mutants revealed no change in pigment content compared to wild-type (Figure 5.17).

The roots of the *frimp1* and *frimp2* mutants were also studied in terms of root length and weight. The roots of both *frimp1* and *frimp2* were similar to wild-type in terms of root length (Figure 5.18A-B) and number of lateral roots (results not shown) when grown in the presence and absence of sucrose. No change in the weight of the whole seedling, aerial tissues or roots of the *frimp1* or *frimp2* mutant compared to wild-type plants was observed when grown in the presence or absence of sucrose (Figure 5.18C).

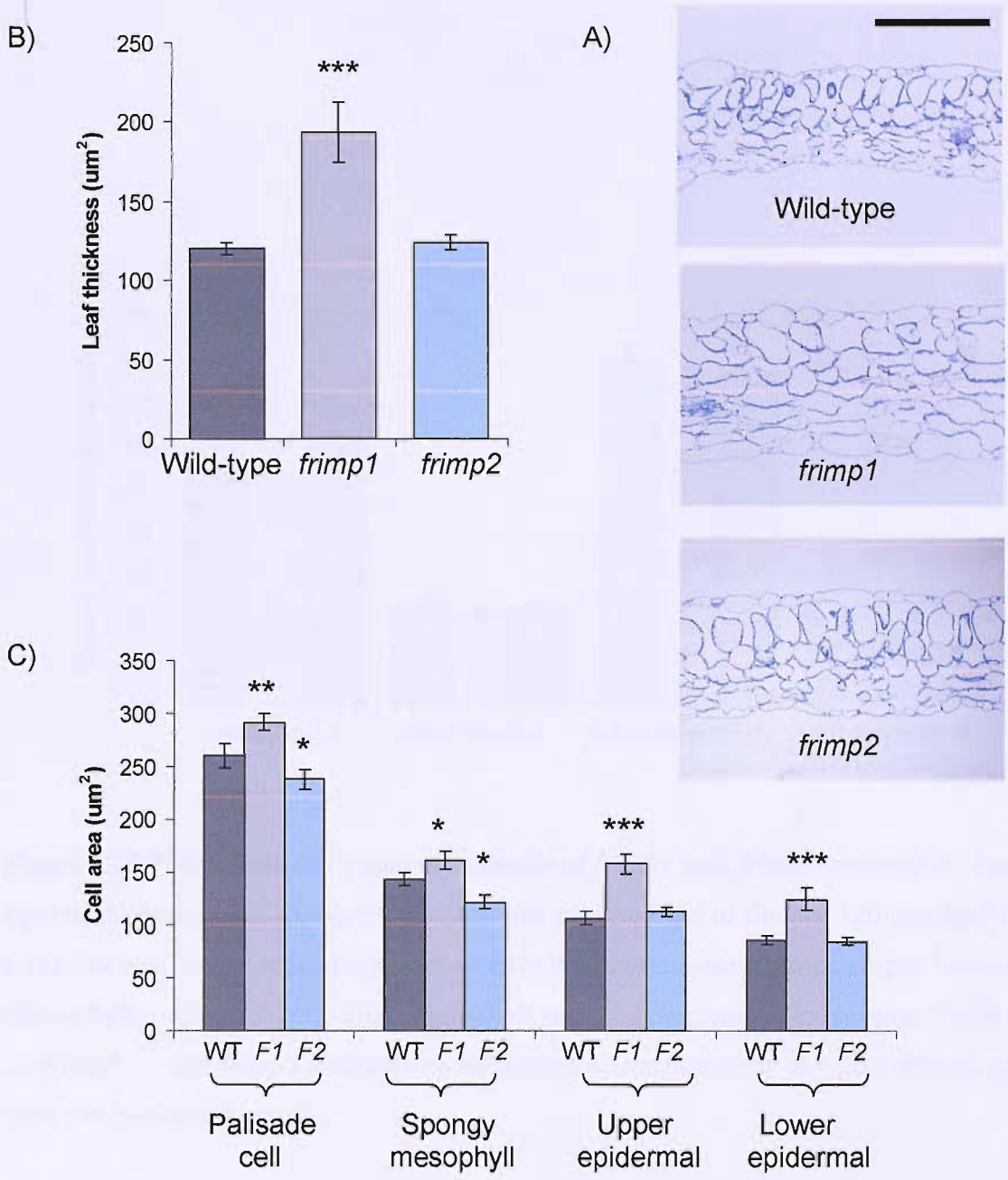

Figure 5.16 Leaf cell sections of the *frimp1* and *frimp2* mutants. A) Leaf cell images of Col-8 and the *frimp1* and *frimp2* mutants. Scale = 120 µm. B) Leaf thickness of wild-type (Col-8), *frimp1* and *frimp2* mutants. Measurements were taken from 3 sections per leaf using 2 leaves from three different plants. C) Palisade, spongy mesophyll, upper and lower epidermal cell measurements in wild-type (WT), *frimp1* (*F1*) and *frimp2* (*F2*), where n = 9 of one biological repeat. Three cells of each type were measured of 3 sections per leaf using 2 leaves from three different plants. Significance levels shown are *($P<0.05$), **($P<0.01$) and ***($P<0.005$).

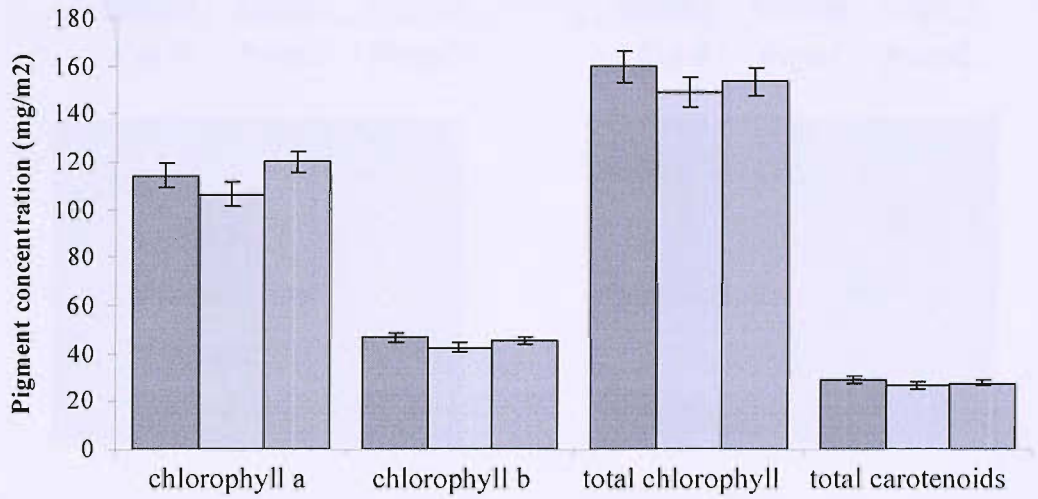

Figure 5.17 Photosynthetic pigments content of *frimp1* and *frimp2* mutants A) Leaves were taken from plants grown for 25 days with a white-light of fluence 120 µmol $m^{-2}s^{-1}$ in a 16h day and 8h night diurnal growth pattern. Pigment measurements in mg/m^2, measuring chlorophyll a, chlorophyll b, total chlorophyll and total carotenoids in leaves of Col-8 (■), the *frimp1* ( ) and *frimp2* mutants (■), with mean ± standard error (n = 20), with 10 plants from two biological repeats.

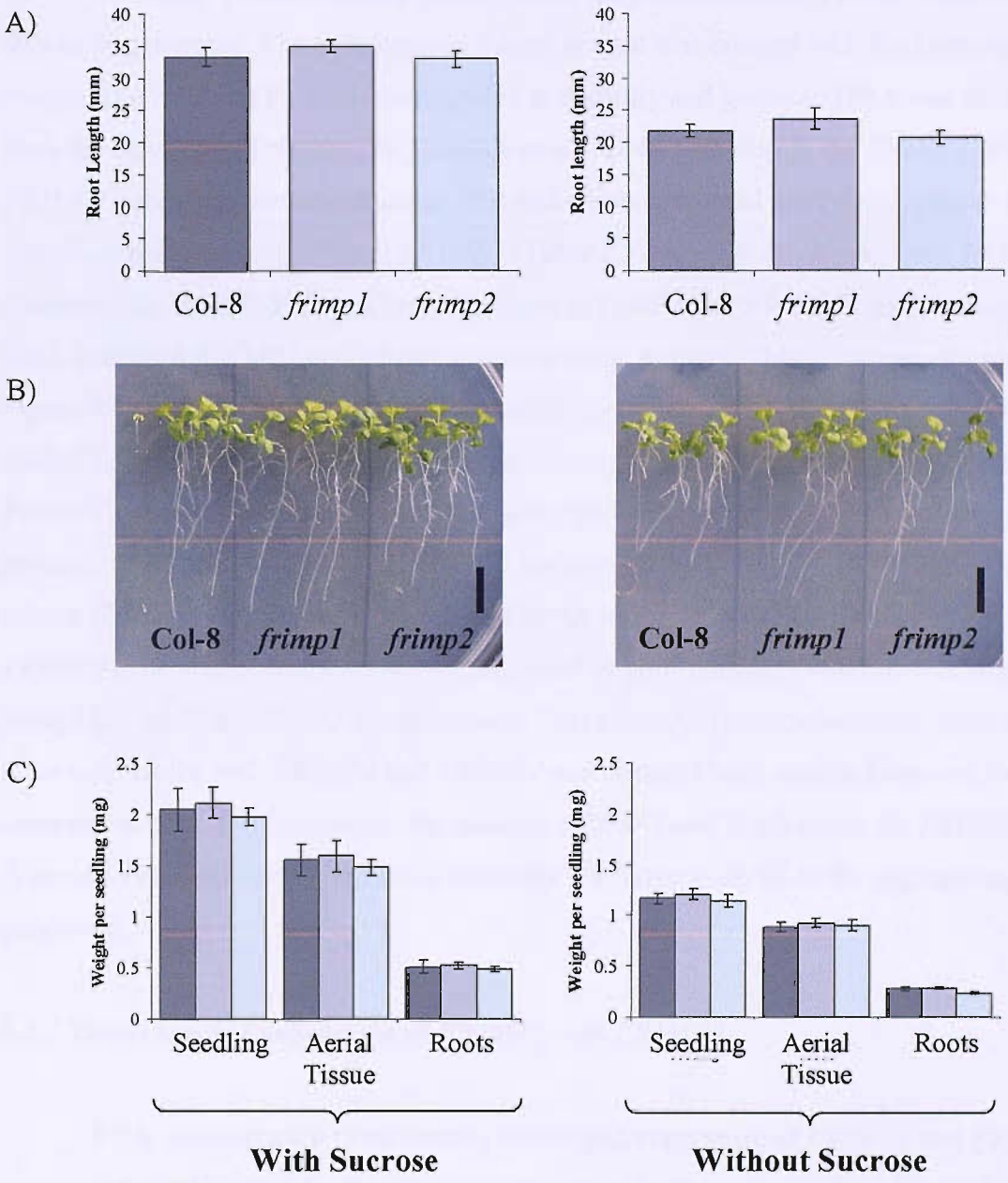

Figure 5.18 Phenotypic analysis of *frimp1* and *frimp2* mutants. A comparison of wild-type (Col-8) to *frimp1* and *frimp2* mutant seedlings grown in the presence and the absence of sucrose. A) Root length comparing Col-8 (■), *frimp1* (■) and *frimp2* (■), B) Photographs of seedlings, scale bar = 5 mm. C) Weight of seedling, aerial tissue and roots. N = 30 seedlings of one biological repeat.

5.2.6 Isolation of a *frimp/frimp2* double mutant

To further characterise the phenotype of the *frimp* mutants, a *frimp1frimp2* mutant should be generated. The homozygous *frimp1* mutant was crossed with the homozygous *frimp2*. The resulting F1 seeds were grown to maturity and genomic DNA was extracted from the leaves of all plants. The presence of a T-DNA insertion in the *FRIMP1* and *FRIMP2* genes was confirmed using PCR and combinations of the T-DNA primer and gene specific primers to *FRIMP1* and *FRIMP2* (Table 2.5). A plant containing both T-DNA inserts would amplify both wild-type products (*FRIMP1* and *FRIMP2*) and products using Lba1 with both *FRIMP1* and *FRIMP2* gene specific primers. This is the case for plant 1 in Figure 5.19. A 1215 bp product was amplified using the F2 and R2 primers specific to *FRIMP1* (lane 2) and also a 1474 bp product using the F2 and R2 primers specific to *FRIMP2* (lane 5), indicating that at least one copy of each wild-type gene is present. The presence of a band 0f approximately 1300 bps using Lba1 with the *FRIMP1* gene specific primer (F2) indicates the presence of the T-DNA in *FRIMP1* (lane 3). One copy of the *FRIMP2* gene also contains a T-DNA, as a band of approximately 800 bps was amplified using Lba1 and the *FRIMP2* reverse primer (R2) (lane 7). This confirms that plant one is heterozygous for both *FRIMP1* and *FRIMP2* and contains both inserts. However for comparison plant 2 contains only the insert in *FRIMP1* and is wild-type for *FRIMP2* (Figure 5.19). Seed from plant 1 was collected for future analysis of the segregating F2 generation.

5.2.7 Tissue specific expression of *FRIMP1* and *FRIMP2*

RNA was extracted from various tissues and expression of *FRIMP1* and *FRIMP2* was investigated (Figure 5.20). Strong expression of both genes was found in leaf and stem tissues and weak expression was observed in silique and flower tissue (Figure 5.20). The intensity of *FRIMP1* was greater than *FRIMP2* suggesting the possibility of higher levels of gene expression. The relative expression of *FRIMP1* was much greater in leaf tissue. The control gene *40S* was constitutively expressed in all tissues (Figure 5.20).

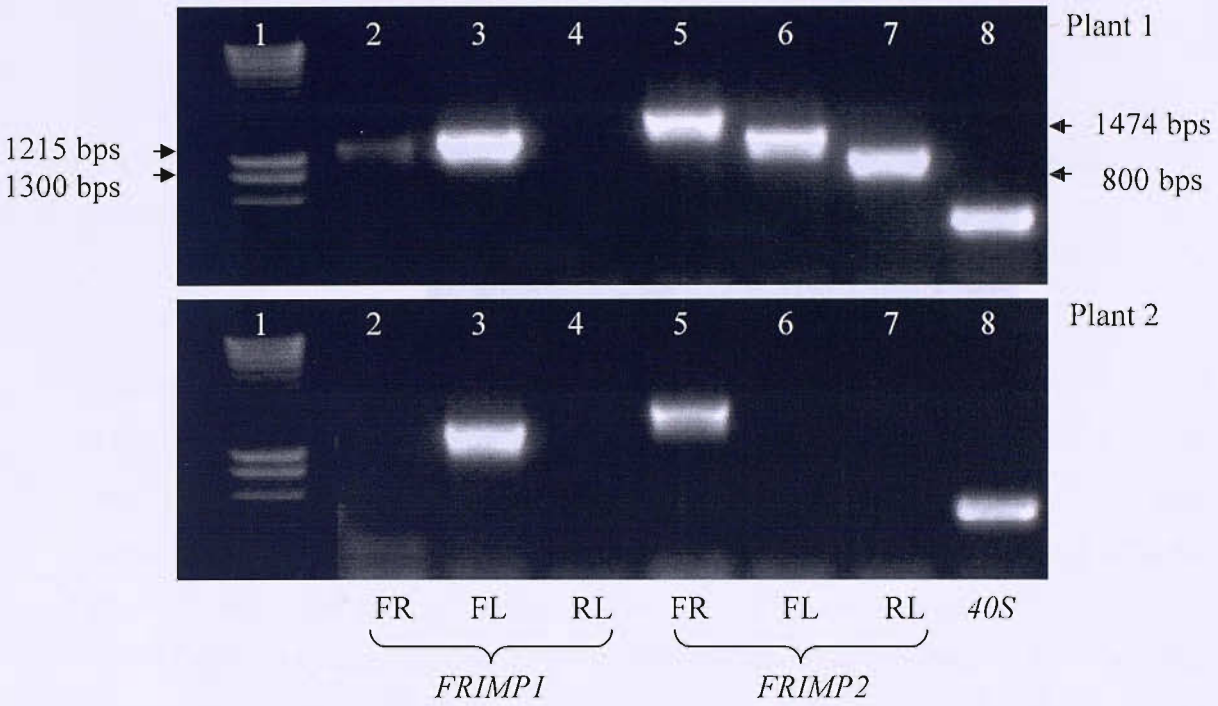

Figure 5.19 Isolation of a *frimp1/frimp2* double mutant. The homozygous *frimp1* mutant was crossed with the homozygous *frimp2* mutant resulting in a series of putative *frimp1/frimp2* double heterozygous mutants. The zygosity of each plant was determined by PCR on genomic DNA extracted from each plant, using gene specific primers to both *FRIMP1* and *FRIMP2* and the T-DNA insert primer Lba1. Three primer pair combinations were used to identify the presence of the T-DNA insert in both genes, gene specific forward primer F2 (F), gene specific reverse primer R2 (R) and T-DNA left border primer Lba1 (L). Refer to Figures 5.4 and 5.6 for location of the primers in *FRIMP1* and *FRIMP2* respectively. See Table 2.5 for primer sequences for both mutants. Lane 1 on both gels contains the molecular weight marker. These plants will have to be self-pollinated in order to obtain a homozygous double mutant.

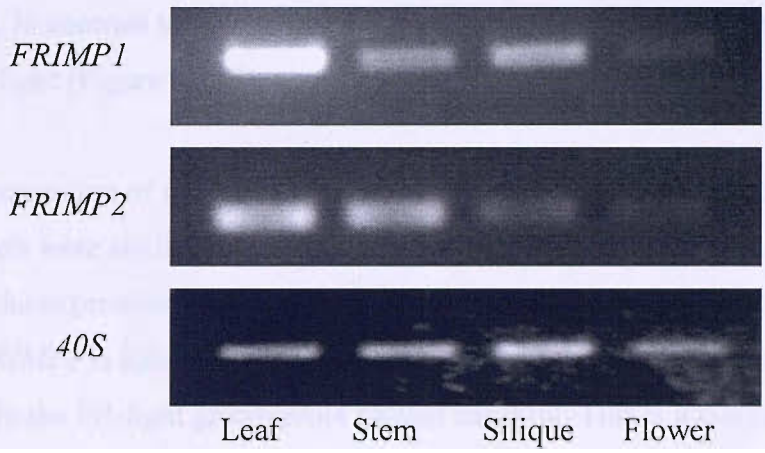

Figure 5.20 RT-PCR showing *FRIMP1* and *FRIMP2* tissue distribution. Tissue distribution of *FRIMP1*, *FRIMP2* and *40S* in leaf, stem, silique and flower tissue. The control gene *40S* is constitutively expressed in all tissues.

5.2.8 Regulation of *FRIMP1* and *FRIMP2* expression

As discussed in chapter 3, *FRIMP1* was induced by FR-light. To further investigate this light response expression of *FRIMP*1 was also examined in other wavelengths. Figure 5.21A shows that *FRIMP1* expression was not induced by either red or blue light and showed some indication of down-regulation under these conditions. This was confirmed by both quantitative real-time PCR and semi-quantitative RT-PCR showing consistency between the two approaches (Figure 5.21A). The light-regulated genes *HEMA1* and *Lhcb1.2* were up-regulated in blue, red and FR-light as shown previously in chapter 4 (Figure 4.23). In contrast to *FRIMP1*, *FRIMP2* showed no change in expression when grown in FR-light (Figure 5.22B).

The expression of *FRIMP1* in the *phyA* mutant was also examined. *FRIMP1* transcript levels were studied in etiolated and FR-light grown *phyA* seedlings, and compared to the expression levels in the wild-type seedlings (Figure 5.21B). As shown previously *FRIMP1* is induced in FR-light grown wild-type seedlings, but interestingly is also induced in the FR-light grown *phyA* mutant seedling. This is a unique response and not shown by any of the other genes studied. Analysis of the control genes *HEMA1* and *Lhcb2.1* show they are FR-light induced and these genes are still dependent on phyA in this experiment (Figure 4.25A-B).

As the FR-light induction of *FRIMP1* expression is intact in the *phyA* mutant it indicates that another photoreceptor must be involved in this response. Real-time RT-PCR was undertaken to look at the transcript levels of *FRIMP1* in other phytochrome mutants (Figure 5.21C). These mutants are in the Ler ecotype background. The expression levels of *FRIMP1* Ler background showed a more subtle induction by FR-light compared to the Col-0 wild-type, thought the control gene *Lhcb1.2* still showed a substantial response to FR-light (Figure 5.21D). However the extent of the induction of *FRIMP1* is reduced in the FR-light grown *phyA* mutant seedling with the Ler background. The same is true for *Lhcb1.2*. The FR-light induction was also retained in the *phyD* and *phyE* mutants. An induction of *Lhcb1.2* was shown in the *phyD* and *phyE* mutants exposed to FR-light.

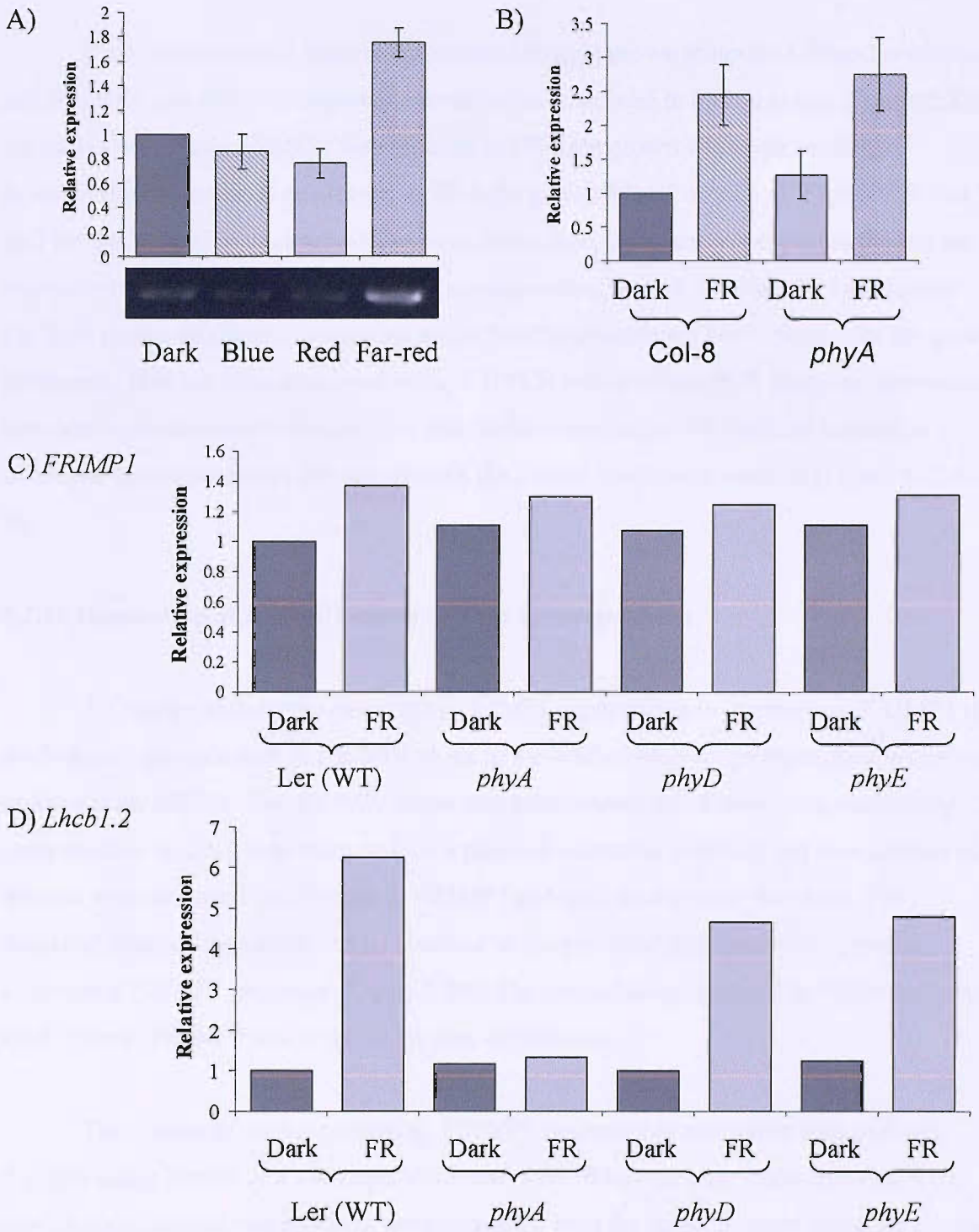

Figure 5.21 Relative expression of *FRIMP1*. Quantitative relative expression of *FRIMP1* in A) etiolated, blue, red and FR-light grown seedlings, where mean ± standard error n = 3. B) Expression of *FRIMP1* in Col-8 and *phyA* etiolated and FR-light (FR) grown seedlings, where mean ± standard error n = 3. Expression of C) *FRIMP1* and D) *Lhcb1.2* in etiolated and FR-light grown wild-type (Ler) and the *phyA*, *phyD* and *phyE* seedlings, where n = 2.

5.2.9 Analysis of gene expression in the *frimp1* and *frimp2* mutants

RNA was extracted from etiolated and FR-light grown *frimp1* and *frimp2* seedlings and *FRIMP1* and *FRIMP2* expression levels were examined in both mutants (Figure 5.22). As shown previously *FRIMP1* was induced in FR-light grown wild-type seedlings, however this induction is not shown in FR-light grown *frimp2* seedlings. *FRIMP2* shows no FR-light induction in either wild-type or in the *frimp1* mutant. As expected there is no expression of *FRIMP1* or *FRIMP2* in its corresponding mutant in either the etiolated or FR-light grown seedlings, confirming again that the mutants are homozygous for the gene of interest. This has been examined using RT-PCR and real-time PCR showing consistency between expression methods. *Lhcb2.1* and *HEMA1* both show FR-light up-regulation in wild-type grown seedlings and also in both the *frimp1* and *frimp2* mutants (Figure 4.21A-B).

5.2.10 Generation of *FRIMP1* constructs for overexpression

To further analyse the function of FRIMP1 experiments to overexpress FRIMP1 in *Arabidopsis* was initiated. A *FRIMP1* clone in a modified blue-script expression vector was ordered from RIKEN. The *FRIMP1* clone was transformed into *E.coli* using chemically competent cells. DNA was extracted via a plasmid extraction protocol and then a series of primers were designed specifically to *FRIMP1* and used to sequence the clone. The sequence obtained was shown to be identical to the predicted sequence from genome sequencing *FRIMP1* sequence (Figure 5.23). The methodology outlined in Figure 5.24 was used to clone *FRIMP1* into a vector for over-expression.

The bluescript vector containing *FRIMP1* has multiple restriction sites and was digested using *Bam*HI and *Xho*I restriction enzymes. When the restriction enzymes were used in combination, two products were generated with the larger product being the excess vector and the smaller product containing the *FRIMP1* clone (Figure 5.25A). The plasmid containing *FRIMP1* was digested firstly with *Xho*I, then blunt ended using Klenow fragments. The product was then digested with *Bam*HI and the product was gel extracted ready for ligation with the pDH51 expression vector. The pDH51 vector was then digested with both *Bam*HI and *Sma*I sequentially due to the different reaction conditions of the restriction enzymes, creating a band of the correct size (Figure 5.25B). The *FRIMP1* clone

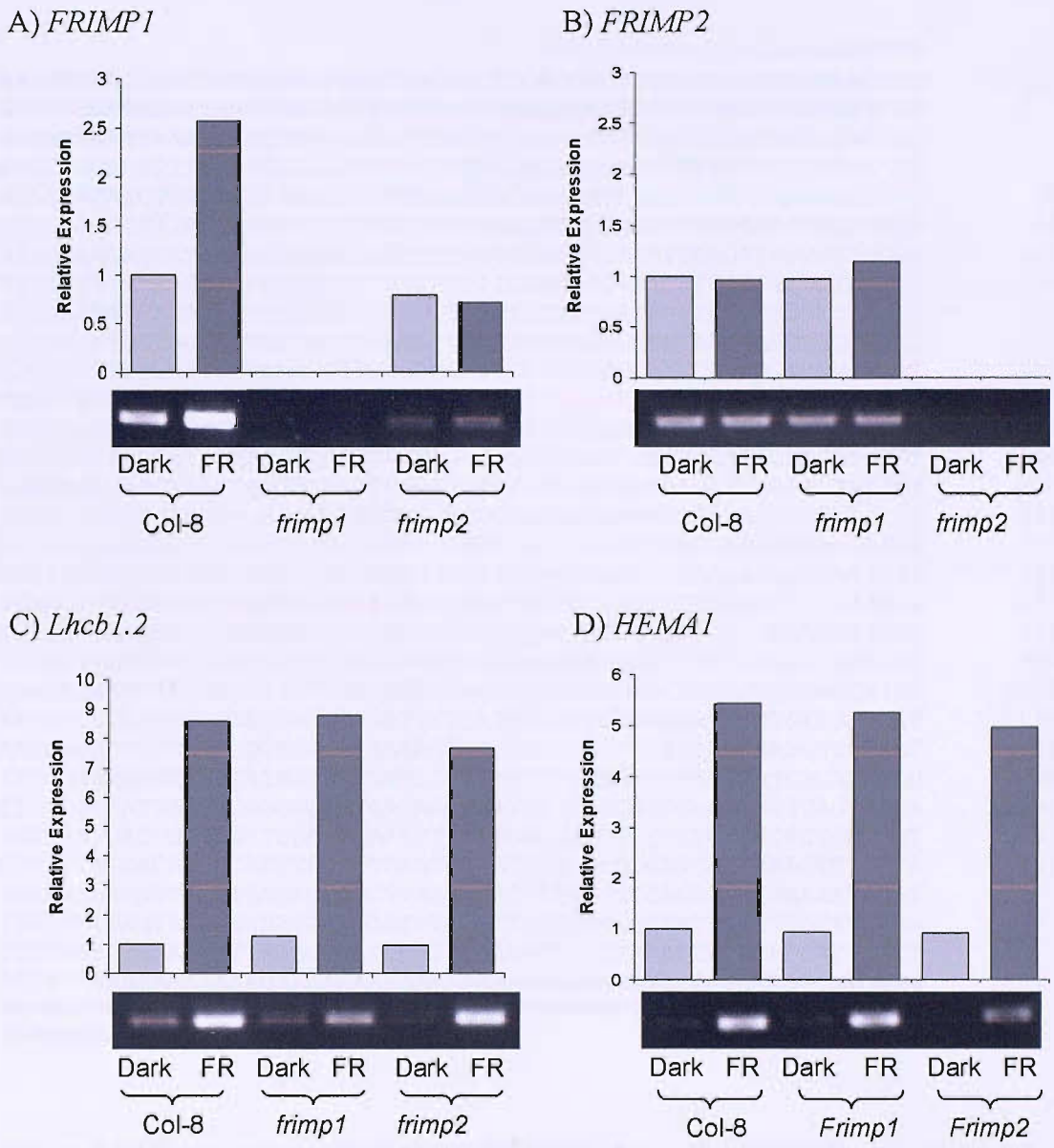

Figure 5.22 Relative expression of *FRIMP1* and *FRIMP2*. Quantitative Real-time PCR and RT-PCR analysis of expression levels of A) *FRIMP1*, B) *FRIMP2*, C) *Lhcb1.2* and D) *HEMA1* in etiolated and FR-light grown, wild-type (Col-8) and the *Frimp1* and *Frimp2* mutant seedlings. Relative expression levels of the genes are normalised to the 40S constitutively expressed control gene. Mean of n =2.

```
                                                TGTAAAACGACGGCCAGTGAATTGT
AATATCGACTCACTATGAGGGCGAATTGGAGCTCCACCGCGGTGGCGGCCGCATAACTTC
GTATAGCATACATTAATACGAAGTTATGGATCAGGCCAAATCGGCCGAGCTCGAATTCGT
CGAGTTAATTAAATTAACCCCCCCCCCCCCCCGATCAAATTCGAATCGAATCGTACAACAG
AAGCTCTGGTGTTGAATCGCCATGAGGTTTTTGCAGATCTGAGGTTTTTTCTCGAGAAGT
AAGAGAGATCTGGAATTTGGCGACATGAGTTACGGATGGGCGATATACGAAGGCACGGT      35
GGTGATAGCTTCACTAAGTCTCTTAGGATGGGCAGGTTTATGGTTTCTTAATCGGAGATT      95
ATACAAAGAGTATGAAGAGAAACGAGCTTTGGTTCAAATCATTTTCAGTGTCGTCTTCGC     155
TTTCTCTTGTAATCTATTGCAGCTCGTTTTGTTCGAGATCATACCTGTTCTCTCTAGAGA     215
GGCAAGGATGATAAACTGGAAGGTGGATCTTTTTTGTTTGATACTTCTTCTGGTTTTCAT     275
GTTGCCGTATTACCATTGCTATTTGATGCTTCGTAATAGTGGTGTAAGAAGGGAGCGTGC     335
CTCTGTTGGGGCTTTCTTATTCTTGTCAGCATTCCTTTACGCATTCTGGCGTATGGGAGT     395
TCATTTCCCTATGCCTTCAGCAGATAAAGGGTTTTTTACCATGCCTCAGCTGGTCAGTAG     455
AATTGGGGTCATTGGTGTGACCTTAATGGCTGTCTTATCAGGATTTGGAGCTGTAAATTT     515
ACCCTACAGCTATATATCCCTCTTCATTAGGGAGATTGAAGAAGCAGATATAATATCTTT     575
GGAAAGGCAACTGATTCAGTCAACTGAGACGTGCATAGCAAAGAAGAAGAAAATTATTTT     635
GTGTCAATTGGAGGTGGAACGAAATCAAGGATCAGAAGAGAATCAGAAACGTAGCTCTTT     695
CTTCAGAAGAATTGTTGGGACTGTTGTGCGGTCGGTTCAAGATGACCAAAAGGAACAAGA     755
CATAAAAATATTGGAAGCGGAGGTGGAAGCCTTAGAGGAGCTGTCAAAACAGTTATTTTT     815
GGAAGTATATGAGCTGCGTCAAGCAAAGGATGCTGCTGCTTATTCTAGAACTTGGAAGGG     875
TCATGTGCAGAACTTACTTGGTTATGCATGTTCCATTTATTGTGTGTATAAAATGTTGAA     935
GTCTCTTCAAAGTGTTGTCTTCAAAGAGGCCGGTACAAAAGATCCTGTCACGACGATGAT     995
CAGCATATTCTTGCGGTTGTTTGATATAGGAGTAGATGCTGCACTCCTCTCACAGTATAT    1055
ATCCCTGCTGTTCATTGGGATGTTGATTGTGATTTCTGTGAGGGGATTCCTGACGAACCT    1115
GATGAAGTTTTTCTTTGCTGTCTCAAGAGTGGGAAGTGGGTCTTCAAGCAATGTTGTACT    1175
TTTCCTATCTGAAATCATGGGAATGTACTTTTTGTCTTCAATTCTTCTTATCAGAAAAAG    1235
CTTGAGAAATGAGTACAGGGGAATCATAACAGATGTGTTGGGTGGAGATATTCAGTTTGA    1295
TTTCTATCATCGATGGTTTGATGCAATTTTTGTGGCGAGTGCTTTTCTTTCTCTCGTTTT    1355
GCTTTCTGCACATTACACGTCTCGTCAATCTGATAAGCACGCCATCGAGTAAGTTTCTTA    1407
TTCAATAATGGTGCCTGAGAGAGTCTTATGATTGTTTGGCCTGACACAACGAAAATCAAT
TTACTACTAGTAAAGGTGACTTAGTGTATAGCTTACAATTGGCTATTTGTTTGTTTTTGA
CGCTTATGTGAAAGATTAAACTGATCAGTTCAAAATTTCTTATACCATAAACGTTGAATT
ATGTTTAAAAAAAAAAAGAAAAAAAAAAAAAAAGAAAAGAGCTCTTGGATCCGGCCATAAGG
GCCTGATCCTTCGAGGGGGGGCCCGGTACCAGCTTTTGTTCCCTTTAGTGAGGGTCTAATTTACGAG
TTGGCGTAATCATGGTCATAGCTGTTTCC
```

Figure 5.23 Sequence analysis of the *FRIMP1* clone. The *FRIMP1* clone from the RIKEN collection was sequenced. The location of the start (**ATG**) and stop (**TAA**) codons are shown with un-translated sequence either side. The bases high-lighted in bold outside the un-translated region represents vector sequence. Five forward primer designed specifically to *FRIMP*1 (F1, F2, F3, F4 and F5 see table 2.6) located within the coding region and the M13 forward and **reverse** primers outside of the coding region are shown. The clone was also sequenced using a selection of gene specific reverse primers to confirm the sequence (primers not shown).

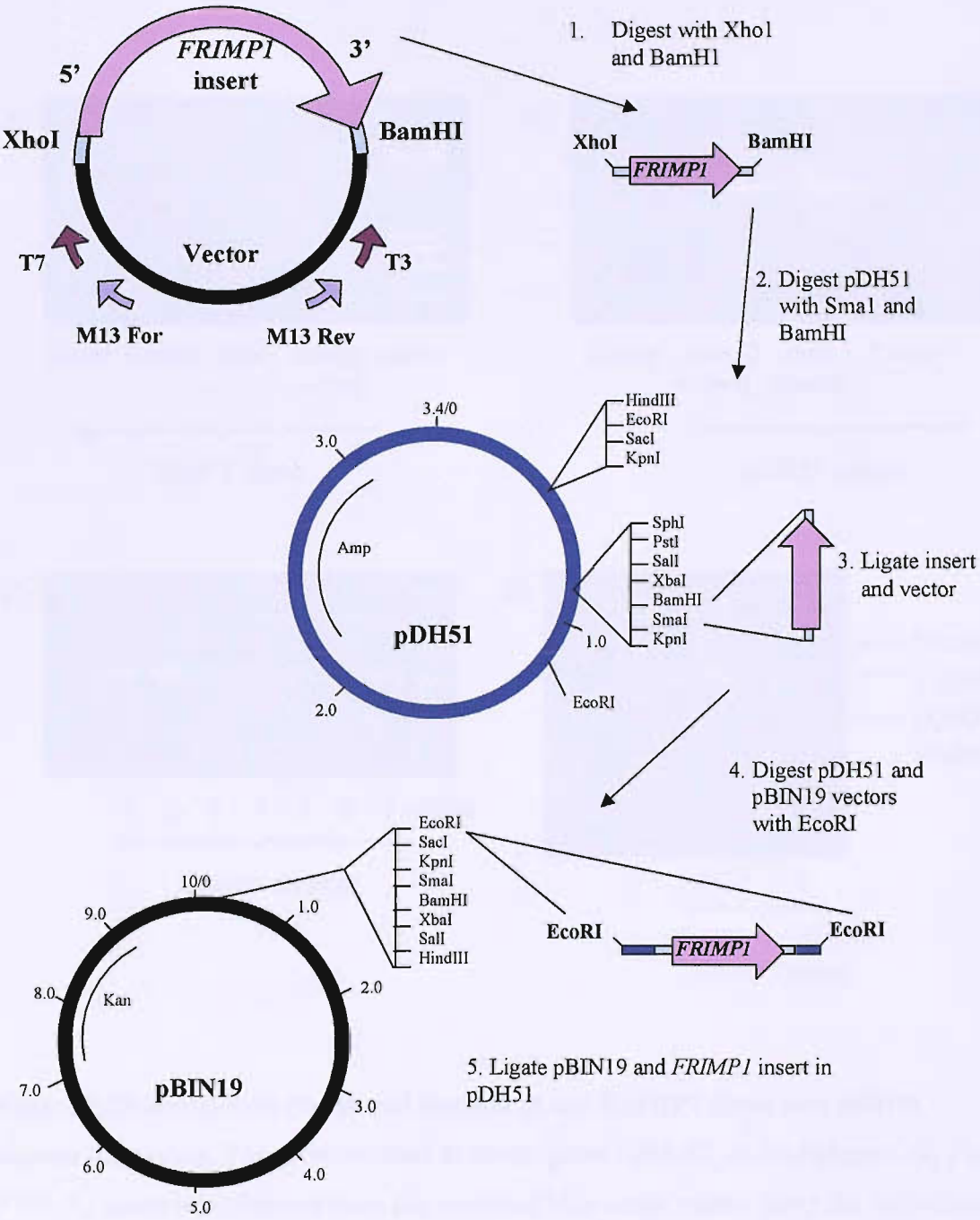

Figure 5.24 Strategy for cloning of *FRIMP1* cDNA for over-expression in *Arabidopsis*. (1) The digestion of the modified bluescript vector containing *FRIMP1* cDNA with *Xho*I, blunted ended with Klenow fragment, then digested with *Bam*HI. (2) The digestion of the pDH51 vector with *Sma*I then *Bam*HI. (3) The ligation of *FRIMP1* cDNA and the pDH51 vector. (4) The digestion of the pDH51 vector containing the *FRIMP1* gene insert with *Eco*RI. (5) Ligation of the pBIN19 expression vector and *FRIMP1* gene insert to give both sense and anti-sense orientation.

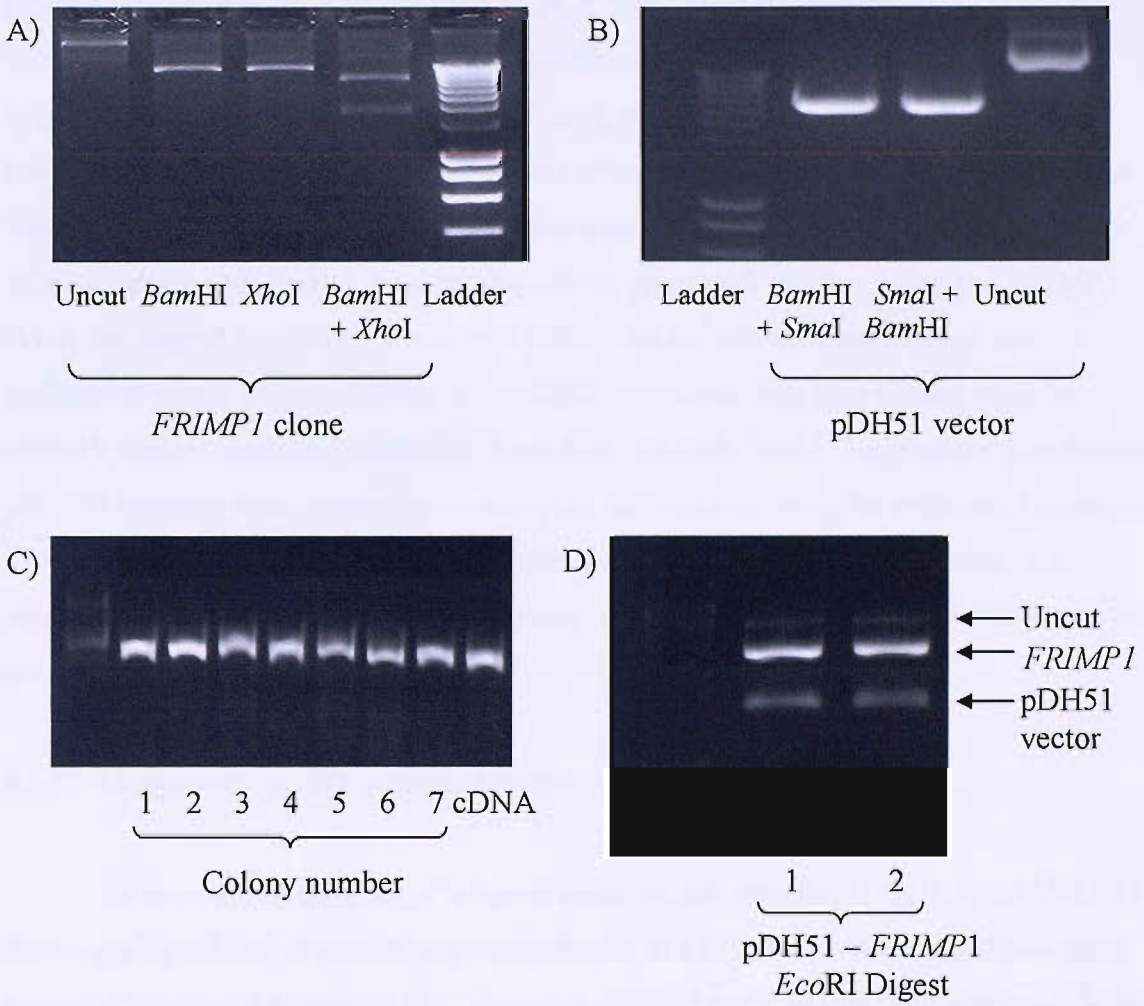

Figure 5.25 Restriction digest and ligation of the *FRIMP1* clone and pDH51 expression vector. The protocol used to overexpress *FRIMP1* in *Arabidopsis*. A) The *FRIMP1* clone was digested from the modified blue-script vector using the restriction enzymes *Bam*HI and *Xho*I individually and in combination. B) The pDH51 vector was digested with *Bam*HI and *Sma*I in two sequential steps. C) The *FRIMP1* clone was ligated with the digested pDH51 vector resulting in 7 positive colonies containing the construct as identified by PCR. D) pDH51–*FRIMP1* construct was digested with *Eco*RI resulting in three bands, the *FRIMP1* fragment containing two *Eco*RI restriction sites, the pDH51 vector and uncut construct.

fragment was then ligated into the pDH51 vector; the blunt end generated by the *Xho*I Klenow fragment was ligated with the SmaI blunt end, and then transferred into chemically competent *E.coli* cells. Seven colonies were generated and the presence of the ligated product was confirmed in all colonies by PCR using primers specific to *FRIMP1* (Figure 5.25C). The colonies were selected using antibiotic resistance as the pDH51 vector contains ampicillin resistance. cDNA was used to indicate the correct band size of full length *FRIMP1*. Plasmid from the newly transformed *E.coli* cells was digested with the EcoR1 restriction enzyme ready for ligation with the second expression vector pBIN19. When digested with EcoR1 three products were generated; the first being the *FRIMP1* clone, the second band being the excess pDH51 vector and the third product was undigested vector (Figure 5.25D). The *FRIMP1* sequence was then ligated with the pBIN19 vector which had previously been digested with EcoR1. No positive transformed pBIN19 colonies were present when selecting for colonies using the antibiotic kanamycin. This was repeated several times, but no colonies were obtained after selection, and unfortunately due to time restrictions cloning of *FRIMP1* into the pBIN19 vector was not completed.

5.2.11 Analysis of FRIMP protein function in *C.elegans* using RNAi

As shown in section 5.1, *C.elegans* contains two proteins, C11H1.2 and Y75B8A showing a significant degree of sequence identity to FRIMP1. To understand how these potential homologues function in *C.elegans* a similar knockout approach was used, in this case taking advantage of RNAi. *E-coli* containing the RNAi feeding vector for C11H1.2 were obtained from Openbiosystems (Huntsville, AL, USA), (http://www.openbiosystems.com). N2 hermaphrodite worms were cultured on NGM plates and fed on *E.coli* containing the RNAi feeding vector. The introduction of double-stranded RNA into a hermaphrodite worm results in specific inactivation of the endogenous gene with corresponding sequence. The progeny produced during the initial feeding period were scored for RNAi phenotypes including body morphology defects, changes in feeding behaviour and changes in body movement. No phenotype was observed in the worms feeding on the RNAi feeding vector in either the first or second generation progeny compared to worms grown on the vector control (Figure 5.26).

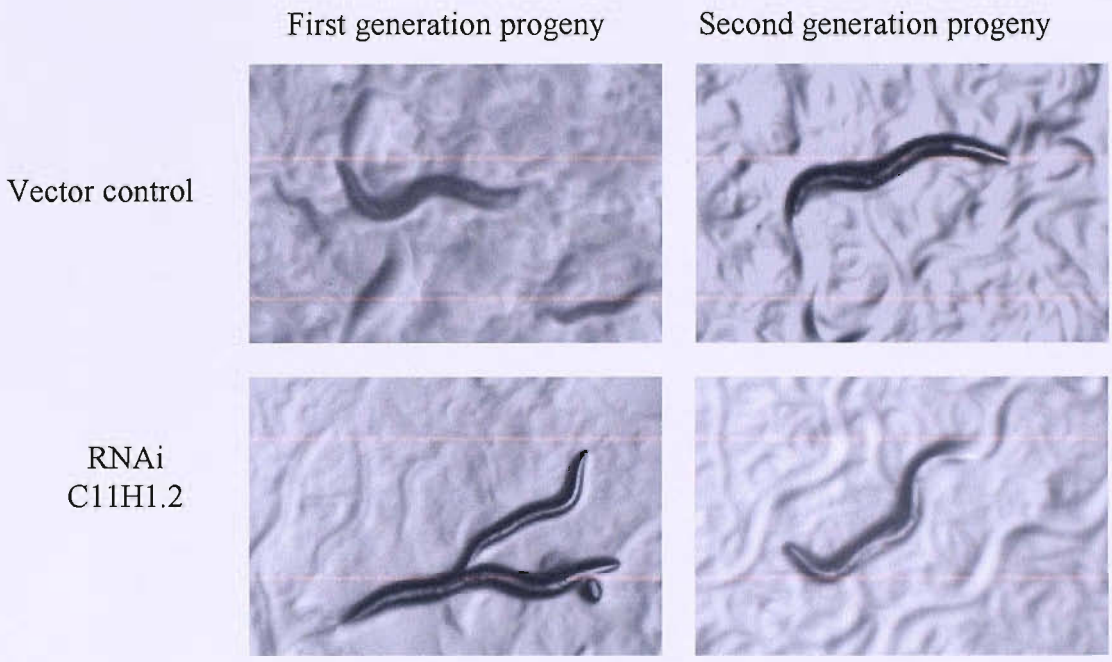

Figure 5.26 Identifying a putative function of C11H1.2 the *C.elegans* homolog to FRIMP1 using RNAi. The phenotype of L4 first and second generation progeny of *C.elegans* fed on the vector control compared to the RNAi feeder containing the C11H1.2 gene. The C11H1.2 protein shows sequence identity to FRIMP1. No phenotypic differences were shown in the C11H1.2 feeder compared to the vector control.

5.2.13 Summary

A summary of observed phenotypes shown by the mutants, changes in photosynthetic pigment levels in the mutants, tissue distribution of the genes and changes in expression levels of the candidate genes in the wild-type seedling grown under different light treatments are shown in Table 5.3. The mutants identified as homozygous for the T-DNA insert for each gene is also highlighted.

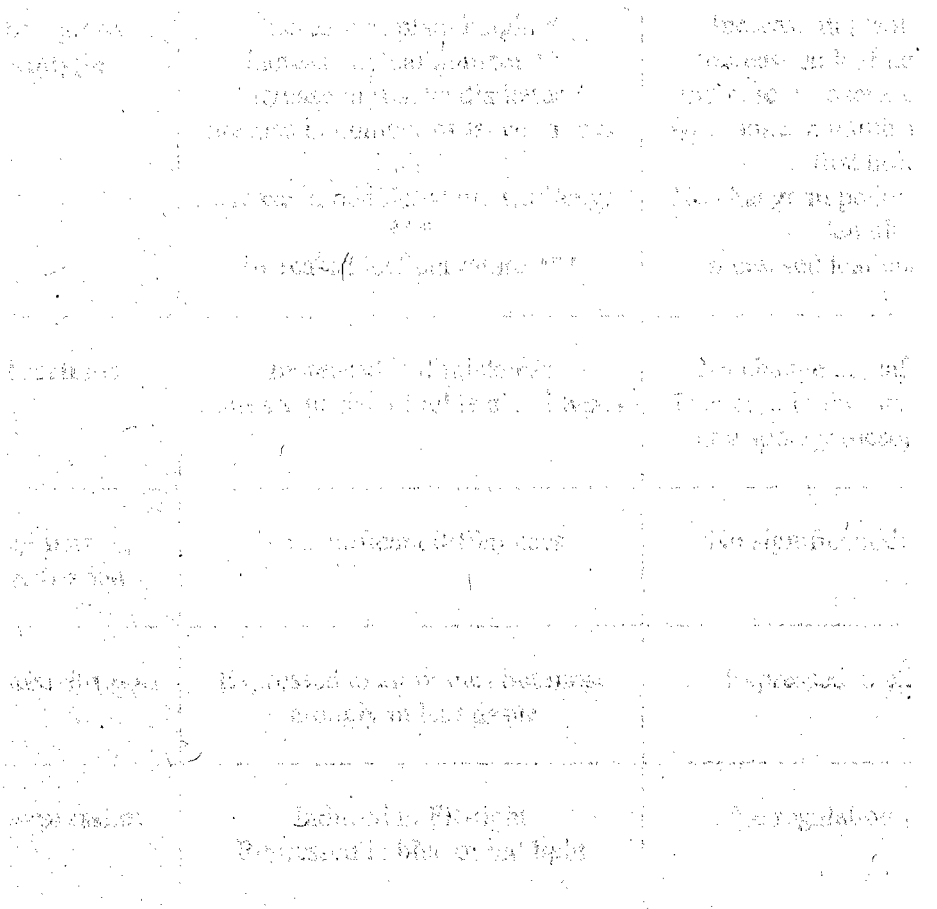

Table 5.3 Summary of the role of FRIMP1 and FRIMP2 in *Arabidopsis*. Phenotypic traits of the *frimp1* and *frimp2* mutants. Summary of *FRIMP1* and *FRIMP2* gene expression, concentration of photosynthetic pigments and tissue distribution. Significance levels * (P<0.05), ** (P<0.01) and *** (P<0.005)

	FRIMP1	FRIMP2
Seedling phenotype of the *frimp* mutants	Increase in hypocotyl length of FR-light seedlings *** Increase in hypocotyl length and cotyledon area of red-light seedlings * No significant change in etiolated, blue or white-light grown seedlings	Decrease in hypocotyl length and cotyledon area of red-light grown seedlings *** No significant change in etiolated, blue, white or FR-light grown seedlings
Mature plant phenotype	Increase in plant height * Increase in leaf number *** Increase in rosette diameter * Increase in number of leaves at first bolt * Increase in petiole/whole leaf length *** Increased leaf curvature ***	Increase in plant height * Increase in leaf number *** Increase in rosette diameter ** No change in number of leaves at first bolt No change in petiole/whole leaf length Increased leaf curvature *
Leaf sections	Increased leaf thickness Increase in size of all leaf cell types	No change in leaf thickness Decrease in the size of palisade and spongy mesophyll cells
Pigment concentration	No significant differences	No significant differences
Tissue distribution	Expressed in all tissues but most strongly in leaf tissue	Expressed in all tissues
Gene expression	Induced in FR-light Repressed in blue or red light Induced in *phyA* FR-light grown seedlings No FR-light induction in *frimp2*	No regulation by light No FR-light induction in *frimp1*

5.3.1 FRIMP1 sequence analyses

Of the 1700 plus predicted transmembrane spanning proteins in *Arabidopsis* the function of a significant proportion is unknown (Bock *et al.*, 2006). This includes the protein encoded by the gene *FRIMP1* which has been identified as being induced by FR-light using microarrays (Wang *et al.*, 2002). Many approaches can be implemented to understand the function of unknown proteins such as FRIMP1. The FRIMP1 protein sequence was used to identity any putative functional domains that could aid in identifying a function. FRIMP1 encodes a predicted membrane protein of 468 amino acids with a predicted molecular mass of 53,546 Da. The protein has no obvious functional motifs with the exception of an ATP-binding site. A protein target prediction database predicts that this protein is targeted to the secretory pathway with a probable signal length sequence of 7 amino acids. Hydropathy plots generated using various transmembrane prediction programs predicted FRIMP1 to have between 7 and 9 transmembrane spanning domains with a long 150 amino acid central loop which is likely to be cytoplasmic (Figure 5.3).

A second protein (FRIMP2) showing 91% sequence identity to FRIMP1 was identified in *Arabidopsis* indicating the possibility of two proteins functioning in a similar way. As the sequence identity is conserved throughout the entire length of the two proteins it is likely that both proteins share the same or similar function in *Arabidopsis*. What was even more interesting was the identification of homologues in a range of other multicellular eukaryotes, including humans, mice, *C.elegans* and rice. As with FRIMP2 the homology is conserved throughout the entire sequence of each protein identified from the different organisms, with each protein showing at least 35% sequence identity to FRIMP1 at the amino acid level. The identification of such homologues can be used to help identify the function of the FRIMP proteins. Unfortunately these proteins have also yet to be assigned a function. The human homolog was predicted to have seven transmembrane spanning domains similar to G-protein coupled receptors (GPCR), so has been referred to as a GPCR. No sequence identity between the human homolog and known any known GPCR has been shown. *Arabidopsis* databases refer to the FRIMP1 proteins as putative GPCRs due to the significant degree of amino acid sequence identity between FRIMP1 and the human protein. No sequence identity was shown between FRIMP1 and any known GPCR

including the only known GPCR in *Arabidopsis*, GPCR1. Although this gives no real basis for a function of the FRIMP proteins as a GPCR, but the possibility cannot be ruled out.

5.3.2 Phenotypic analysis of *frimp1* and *frimp2* homozygous knockout mutants

Knockout mutants were identified and confirmed using a combination of both segregation analysis and PCR for both *FRIMP1* and *FRIMP2* from the SALK collection. Both mutants are recessive with a T-DNA insertion in predicted transmembrane spanning domains of both proteins. As the T-DNA is inserted towards the C-terminal in both proteins, RT-PCR was carried out on both mutants to identify a putative truncated gene product which could result in a partially functional protein. This must be taken in account when interpreting the phenotype of a mutant. Although no truncated product was amplified in *frimp2*, a truncated product was shown in *frimp1*, therefore only *frimp2* in a definite null mutant. Although PCR indicates that the *frimp1* mutant is not a null mutant it does not mean that a truncated protein ever gets produced.

As summarised in Table 5.3 the phenotypic analysis of both mutants gave some interesting phenotypes at both the seedling and plant stage. A significant increase in hypocotyl length was seen in the *frimp1* seedling grown in four days of continuous FR-light compared to the Col-8 wild-type, however *frimp2* was similar to wild-type. However when the FR-light exposure was extended to six days an increase in hypocotyl length was shown in the *frimp2* seedling (Lawrence and Terry, unpublished data). Six days after germination the hypocotyl length is at its maximum and the delay in the longer hypocotyl length of *frimp2* could result from a delay in germination as these seeds showed a reduced germination rate in FR-light. A number of mutants in genes known to be involved in FR-light perception show a marked promotion in hypocotyl elongation compared to the wild-type seedling. These include the *phyA* photoreceptor mutant and the *fhy1* transcription factor mutant (Johnson *et al.*, 1994). The FHY1 (**F**ar-red **E**longated **H**ypocotyl 1) protein which has been defined as a positive regulator of photomorphogenesis in FR-light and *fhy1* has the elongated hypocotyl phenotype (Shen *et al.*, 2005). As the *frimp1* mutant show this elongated hypocotyl phenotype in FR-light it is a good indication that FRIMP1 is vital in FR-light induced de-etiolation and is involved in mediating these morphological changes.

At four days an increase in hypocotyl length was also shown in the *frimp1* seedling grown in red light and a significant decrease in both hypocotyl length and cotyledon area was shown in the *frimp2* mutant. When extended to 6 days of red-light exposure an increase in both hypocotyl length and cotyledon area of *frimp2* seedlings was shown compared to wild-type (Lawrence and Terry, unpublished data). The initial decrease in growth in red-light but not in FR-light at four days, but an increase in growth under both light treatments at six days suggests the possibility of a delay in germination or extended dormancy period of *frimp2* grown under these light conditions. Not all *frimp2* mutant seeds germinated like the wild-type in both red and FR-light as an average of only 60 – 70% of *frimp2* seeds germinated compared to a 100% germination of both the wild-type and *frimp1* seedlings. The germination phenotype shown by the mutants appears to be solely linked with phytochromes as *frimp2* germination was successful when grown in darkness or under blue or white-light. The phenotypes shown by the *frimp* mutants in red and FR-light and the low germination rates of *frimp2* in the same light treatments indicate they are directly involved in the phytochrome signalling pathway or may function as an intersection of light and other signalling pathways.

The *frimp* mutants also displayed a number of interesting phenotypic traits in the mature plants. The most noticeable phenotype of *frimp1* was the epinastic growth of the leaves. This is the lateral down curling and infolding of the leaf margins along the longitudinal axis. The typical curvature ratio of wild-type leaves is 0.9 (Booker *et al.*, 2004), but the ratio of 0.56 of the *frimp1* mutant indicates severe curling of the leaves. The *frimp2* mutant also showed epinastic growth but to a smaller degree. Leaf curling is a common phenomenon and literature searches reveal a number of mutants that show this phenotype. Changes in environmental conditions also produce a similar phenotype. This includes the *Arabidopsis* GPCR, as the *gcr1* mutant shows epinastic growth when treated with 100 or 175 nmol ozone mol^{-1} for 5 days. The elevated ozone concentration causes the epinastic growth of the leaves as a stress response (Booker *et al.*, 2004). This could indeed be the case for the *frimp* mutants, where the leaves are growing epinastically due to light stress. This could be tested further by exposing the *frimp* mutants to different light fluences, both below and above the 120 μmol $m^{-2}s^{-1}$ fluence used in the growth of *Arabidopsis* in this experiment and examining the degree of leaf curvature. The curvature shown in *gcr1* due to ozone stress provides a further possibility that the FRIMP proteins function in signalling pathways, in this case light signalling.

Epinasty has also been shown to result from a high concentration of auxin and ethylene, two examples of phytohormones (Romano *et al.*, 1993). The overproduction of auxin in transgenic plants results in the overproduction of ethylene. Plants overproducing both phytohormones display a number of phenotypic traits including leaf epinasty (Romano *et al.*, 1993). In auxin-overproducing petunia plants, leaf epinasty was shown to be caused by excessive expansion of the adaxial cells of the leaf relative to the abaxial cells (Klee *et al.*, 1987; De Paepe *et al.*, 2005). However such cell expansion could result from either an excess of auxin or ethylene, so a number of mutants either overexpressing auxin or inhibiting ethylene production were crossed and analysed. This allowed *Arabidopsis* plants with elevated auxin and normal ethylene levels to be obtained. Analysis of these plants indicates that leaf epinasty is primarily controlled by auxin rather than ethylene (Romano *et al.*, 1993). This epinastic response has also been shown in the *axr4* mutant, which is an auxin-resistant mutant (Hobbie and Estelle 1995). The *axr4* mutant is specifically resistant to auxin and AXR4 is important for normal auxin sensitivity. This indicates that the resistance to auxin results in the epinastic response (Hobbie and Estelle 1995). A marked epinastic curvature response was shown when tobacco leaves were incubated with indole-3-acetic acid (IAA) the principal form of auxin in plants (Kawano *et al.*, 2003). This provides further evidence that auxin results in the epinastic response. The epinastic phenotype shown in these *Arabidopsis* mutants and when tobacco was treated with IAA indicates that the FRIMP proteins could be functioning as a possible auxin transporter or other membrane protein involved in auxin signalling. This hypothesis would be tested further by inhibiting auxin production in the *frimp* mutants to see if the epinastic response is reduced.

The *frimp* mutants also displayed other phenotypes possibly linked to light stress responses, including an increase in leaf number. Both *frimp1* and *frimp2* showed a significant increase in leaf number compared to wild-type with almost twice as many leaves. This phenotype could be linked to the curling response shown by the leaves. The curling of the leaves results in a decrease in leaf surface area available to obtain light therefore resulting in a possible reduction in photosynthesis and decrease in the rate of plant growth. Another interesting phenotype displayed by *frimp1* is the increase in the length of the petiole. Measurements of the length of the whole leaf and the length of the petiole revealed *frimp1* to have a significant increase in the petiole/whole leaf length compared to wild-type. This response was specific to *frimp1* as *frimp2* had a wild-type

petiole length. This increase in petiole length is a classical light response, for example when *Arabidopsis* wild-type plants are irradiated with FR-light at the end of day photoperiod they exhibit the shade-avoidance syndrome including elongated petioles (Goto *et al.*, 1991). The elongated petiole phenotype has also been shown in many mutants involved in light-signalling mediated plant development. This includes the *phyB* mutant, indicating the phyB-mediated perception of light appears to be controlling factor in the shade-avoidance syndrome (Robson *et al.*, 1993; Tsukaya *et al.*, 2002). The phytochrome *phyAphyBphyD* triple mutant also has elongated petioles in response to end-of-day FR-light. This response by the triple mutant indicated that phyD acts in the shade avoidance syndrome by controlling both flowering time and leaf area (Devlin *et al.*, 1999). Although *frimp1* had a wild-type phenotype with regards to the timing of the development of the plant, both the increase in the number of leaves and the elongated petioles indicate *frimp1* to be involved in light-signalling pathways. In the *frimp1* mutant the petiole supports the leaf blade and the elongation of the petiole delivers the leaf to positions more appropriate for photosynthesis.

A significant increase in rosette diameter of both *frimp1* and *frimp2* was also shown compared to wild-type. The increase in the rosette diameter of *frimp1* results from the elongated petioles. However *frimp2* does not have elongated petioles and instead the increase in rosette diameter of *frimp2* is a result of an increase in the overall length and area of the leaves. This indicates that in terms of leaf development FRIMP2 could be involved in the maintenance of leaf area and size, whereas FRIMP1 is involved in determining petiole length and leaf structure in response to light. However it is unlikely for the proteins to have such different roles in development. The effects of light conditions on the control of leaf blade expansion and petiole elongation are important mechanisms in the light acclimation of plants (Kozuka *et al.*, 2005). It would be interesting to study the number of leaves, leaf blade expansion and petiole elongation in the *frimp* mutants in response to different R/FR ratios, different light levels and monochromatic blue or red-light. This will determine if the leaf responses are specific to a certain wavelength of light and if the FRIMP proteins are linked to the photoreceptors in mediating light-specific growth responses.

The number of leaf abnormalities shown by the *frimp* mutants correlates to the tissue expression of the *FRIMP* genes. *FRIMP1* and *FRIMP2* were expressed in all tissues

examined. However *FRIMP1* and to a lesser extent *FRIMP2* are most strongly expressed in leaves although they are also expressed in stems, silique and very weakly in flower tissue. This strong expression of *FRIMP1* and *FRIMP2* in leaf tissue is consistent with the strong leaf phenotypes shown by both mutants. The expression of the *FRIMP* genes in stem tissue could also implicate the involvement of these proteins in the growth and maintenance of the stem. Again this is consistent with the observed affect of hypocotyl elongation in the *frimp* mutants.

As the *frimp* mutants displayed such a variety of leaf phenotypes; leaf sections of both mutants were taken to investigate how the absence of the proteins affects leaf development at the cellular level. The leaf thickness of *frimp1* was almost twice that of both the wild-type and *frimp2*, and the organisation of the cells types in *frimp1* appears to be lost with a reduction in the air spaces between the cells. The increase in leaf thickness results from an increase in the average size of all four type of leaf cell compared to wild-type. The cell organisation in leaves of the *frimp2* mutant appears to be more organised like the wild-type plant, however there is an decrease in the size of the palisade and spongy mesophyll cells but no change in the upper and lower epidermal cells compared to wild-type. An increase in the epidermal cell area has been shown to correlate with a decrease in epidermal cell number in shaded plants (Cookson and Granier 2006). So it would be interesting to see if there was a change in the number of epidermal cells in the mutants and to see if this correlates with the increase in epidermal cell size in *frimp1*. It appears that both FRIMP proteins, especially FRIMP1, play an important role in cell organisation, and the absence results in disjointed cell organisation and a change in cell size. The unorganised cell arrangement and reduction in air space between the cells in *frimp1* could therefore be responsible for the epinastic growth response shown by the leaves. It would be interesting to use a GFP-fusion protein for both FRIMP1 and FRIMP2 to study further the cell specific localisation of the proteins within the leaf and to see if this correlates with the change in cell phenotype shown by the mutants.

The creation of the *frimp1frimp2* double heterozygous mutant looks promising in establishing a homozygous double mutant. A *frimp1frimp2* double mutant could establish if there is redundancy between the isoforms or if they are working in conjunction to perform their function. On identification of the double mutant it would be interesting to see what phenotypic traits the mutant has in terms of leaf shape and cell structure. Perhaps the

epinastic response could be more dramatic still or maybe the plant may have problems in developing fully functional leaves. It would also be interesting to examine if the FR-light induced hypocotyl elongation is affected in the double mutants. The study of the double mutant will hopefully provide more of an insight to the function of the FRIMP proteins.

In addition to the creation of a double mutant, the *frimp1* mutant was backcrossed with the wild-type plant. This would indicate how much of the phenotype shown was related to the *frimp1* knockout. The loss of the phenotypic traits shown by *frimp1* including the elongated hypocotyl in FR-light and the epinastic response would indicate the traits were as result of the loss of *FRIMP1* and not due to multiple insertions. Unfortunately it appears that the *frimp1* backcross was unsuccessful so this would have to be repeated. This is especially important due of the lack of a second *frimp1* mutant in the coding region. The identification of a second mutant is used to establish if the phenotypic traits shown by the first mutant are as a consequence of the loss of the gene of interest. This is indicated if identical phenotypic traits are shown in both mutants.

5.3.3 Regulation of *FRIMP1* and *FRIMP2* gene expression by light

In Chapter 3 *FRIMP1* was shown to be up-regulated by FR-light. However, this was specific to *FRIMP1* as *FRIMP2* was not up-regulated. *FRIMP1* was also shown to be regulated by other wavelengths of light as PCR reveals *FRIMP1* is down-regulated by red and blue-light. This indicates that like some of the transporter genes discussed in chapter 4, FRIMP1 is involved in a complex light signalling pathway that is mediated by multiple photoreceptors whether they be other phytochromes or blue- light photoreceptors. *HEMA1* and *Lhcb* were used as positive controls to confirm if regulation shown by *FRIMP1* is as a result of the light environment. *HEMA1* and *Lhcb* genes are considered to play key roles during chloroplast development and encode glutamyl-tRNA reductase and chlorophyll a/b-binding proteins respectively (McCormac and Terry 2002). Both *HEMA1* and *Lhcb1.2* are significantly induced in wild-type seedlings grown in FR-light as well as blue and red light (McCormac *et al.*, 2001; McCormac and Terry 2002).

HEMA1 and *Lhcb1.2* expression in photoreceptor deficient mutants showed that induction by FR-light required phyA, but not phyB or the blue light photoreceptors cry1 and cry2 (McCormac and Terry 2002). To identify if *FRIMP1* is truly under the control of

phyA during de-etiolation, the expression profile of *FRIMP1* was examined in the *phyA* null mutant. The most interesting expression profile shown by *FRIMP1* is in the *phyA* mutant. Both *HEMA1* and *Lhcb1.2* transcript levels were induced in the wild-type FR-light grown seedlings. However, this up-regulation is lost in the FR-light grown phyA seedling. In the *frimp1* mutant, the FR-light induction is sustained in the *phyA* mutant. This is a unique expression pattern which has never been reported. This indicates the possible involvement of a second or even multiple photoreceptors regulating the response. The transcript levels of *frimp1* showed a small induction in FR-light grown *phyD* or *phyE* seedlings indicating the possibility of these photoreceptors participating in the response; however these experiments require further investigation. A small induction of *FRIMP1* was also seen in the *phyA* mutant in the Ler background. However, the induction was dramatically reduced compared to the Col-0 response. A different wild-type was used due to the ecotype background of the *phyD* and *phyE* mutant and this could explain the reduction in the extent of the FR-light induction. The induction of *FRIMP1* in both ecotypes indicates that this is a true result. The induction of *FRIMP1* in the initial microarray conducted by Wang *et al.* (2002), was also shown in other wild-type ecotypes including Ler. However the induction of *FRIMP1* in the Ler ecotype was not as significant as the up-regulation in the Col-0 ecotype (Wang *et al.*, 2002) which correlates with the finding shown using PCR.

Phytochrome A is not the only phytochrome to be shown to be involved in FR-light perception as phyE has been shown to control light-induced germination of *Arabidopsis* under these conditions (Hennig *et al.*, 2002). As the *phyE* mutant did not show inhibition of hypocotyl elongation or induction of cotyledon unfolding by FR-light, phyE was not shown to be required for phyA-mediated very low fluence responses (Hennig *et al.*, 2002). However there is strong evidence that phyE does participate directly in R/FR-light reversible germination (Hennig *et al.*, 2002). It has also been shown that phyC in addition to phyA is involved in the photoreception of FR-light in rice (Takano *et al.*, 2005). Under continuous FR-light, the rice *phyA* mutant shows partially impaired de-etiolation, whereas the *phyAphyC* double mutant showed no significant residual phytochrome response. This indicates phyC is involved in perceiving FR-light in rice so perhaps phyC or indeed phyE could be a second photoreceptor involved in the perception of FR-light in Arabidopsis and responsible for the FR-induction of *FRIMP1* in the *phyA* mutant.

The expression profiles of *FRIMP1* and *FRIMP2* were examined in the respective *frimp* mutants. Although *FRIMP1* was up-regulated by FR-light in the wild-type this was not seen in the *frimp2* mutant. It appears that FRIMP2 is essential for the up-regulation of *FRIMP1*. FRIMP2 is not regulated by FR-light in either the wild-type or in the *frimp1* mutant, however it would be interesting to see if *FRIMP2* is regulated by other wavelengths of light. The absence of a *FRIMP1* or *FRIMP2* product in the respective mutant is a positive indication of the homozygous mutant. It would also be interesting to examine the light-regulated expression profiles of the *frimp1frimp2* double mutant, to see if the FR-light regulation is lost or up-regulated further. The expression profiles shown by the FRIMP genes suggests they are mediated by multiple photoreceptor in a complex signalling pathway and as FRIMP2 is required for the up-regulation of *FRIMP1* under FR-light, it appears these the FRIMP proteins work in conjunction in light-mediated plant development.

5.3.4 Generation of *FRIMP1* constructs for overexpression

The phenotypes shown in the *frimp1* knockout would hopefully be complemented by over-expressing *FRIMP1* in *Arabidopsis*. The generation of the over-expressing plant would be useful in providing complementary evidence of FRIMP1 function. It may also complement the *frimp1* mutant confirming that the phenotype is due to the loss of FRIMP1 alone. The phenotypic analysis of the FRIMP1 over-expressing plant could provide a vital insight into the function of the FRIMP proteins. The generation of over-expressing plants was a complicated process and a number of problems were overcome in cloning *FRIMP1* into the first of two expression vectors. The *FRIMP1* clone was successfully cloned into the first expression vector DH51 and this has been confirmed using restriction digests. However further problems arose in cloning into the second expression vector pBIN19 and this was not completed. To over-express *FRIMP1* the second cloning phase will have to be completed or alternatively other cloning strategies could be used, including using the pBECKS expression vector. This is a common binary vector created for use in the *Agrobacterium*-mediated genetic transformation of plants (McCormac *et al.*, 1997).

5.3.5 Analysis of FRIMP protein function in *C.elegans* using RNAi

In *C.elegans* the introduction of double-stranded RNA (dsRNA) results in potent and specific inactivation of an endogenous gene with corresponding sequence (Fire *et al.*, 1998). This technique, known as RNA interference (RNAi) enables rapid, targeted gene inactivation and has become an important tool in identifying gene function. Due to its anatomic and genetic simplicity, the nematode has become an intensively studied simple model system. RNAi has rapidly embraced a reverse genetic tool and has accelerated the pace at which gene functions are discovered (Kamath and Ahringer, 2003). There are three main approaches used in RNAi, but the most common is to feed the worms with *E.coli* expressing target-gene dsRNA (Timmons *et al* 2003). RNAi by feeding is an effective screening tool to determine the loss-of-function phenotype of a gene of interest. Unfortunately a wild-type phenotype was shown in the N2 worms fed on *E.coli* expressing the C11H1.2 gene of interest compared to the vector control. However, as it was not confirmed whether the worms were actually expressing the C11H1.2 gene by PCR, it cannot be assumed that a wild-type phenotype is the true result of the absence of the gene. The phenotype of the worm could be tested further by using a RNAi-supersensitive strain of *C.elegans* which is more likely to take up the RNA and therefore knock out the function of the gene (Kamath and Ahringer, 2003). The main limitation with this approach is that any gene with significant sequence identity to that of the introduced dsRNA may also be silenced. As *C.elegans* contains the gene Y75B8A a homolog to gene C11H1.2 this must be taken into account when the phenotype of the worm is examined. However, RNAi may have the advantage of knocking out the expression of both genes which may help to uncover the phenotype and the function of the genes of interest.

Chapter 6

Final Discussion

Light is one of the most important environmental factors that regulate plant growth and development. Plants have evolved complex signalling pathways to perceive changes in the light environment and adapt their growth to maximise their chance of survival (Sullivan and Deng, 2003). The development of the seedling represents one of the most dramatic changes in plant morphology as a consequence of a change in the light environment (Von Arnim and Deng, 1996). Seedlings that are growing in the dark follow a skotomorphogenic developmental program. However they undergo de-etiolation when they are exposed to light switching to a photomorphogenic program (Fankhauser and Chory, 1997). Changes in light are detected by multiple families of photoreceptors including the phytochromes A-E that perceive red and FR-light (Clack *et al.*, 1994). While phyB is the principal phytochrome for de-etiolation under red light (Reed *et al.*, 1993), mutant studies have shown phyA to the sole photoreceptor involved in the perception of FR-light (Nagatani *et al.*, 1993).

The basis of the research described here is to expand on the knowledge and understanding of the complex light-regulated signalling pathways involved in mediating the morphological changes which occur during seedling de-etiolation. The morphological changes which are a direct result of phytochrome signalling rather than a consequence of photosynthesis were examined. As FR-light grown seedlings are unable to photosynthesize as the activity of POR (NADPH-Pchlide oxidoreductase), a key enzyme in the biosynthesis of chlorophyll requires light (Wettstein *et al.*, 1995; Moulin and Smith, 2005), it was logical to study FR-light induced de-etiolation. This is because changes in gene expression and morphology are as a specific consequence of FR-light and phyA and not due to photosynthesis. Although much is known about the early events of light signalling pathways in terms of the identification of transcription factors, little is understood about the components involved further down the signalling pathway. This includes the specific promoter targets of these transcription factors of multiple downstream genes in the phyA-regulated transcriptional network which are then responsible for the changes in morphology (Tepperman *et al.*, 2001). Target genes could include those encoding membrane proteins

involved in the transport of a variety of compounds. This includes pumps, channels and carriers proteins. Such proteins are responsible for re-distribution, acquisition and compartmentalization of nutrients, photosynthetic products and inorganic ions and for the efflux of metabolic end products and toxic compounds. It could be hypothesised that the regulation of membrane proteins is important during de-etiolation in mediating the morphological changes. This hypothesis has been supported by the data shown in this thesis via the identification of a number of FR-light regulated transporter genes by microarray analysis and RT-PCR and also by the generation of T-DNA knockout mutant plants for these genes.

A transcriptomics approach was undertaken to identify transporter genes involved in phyA-mediated light-signalling pathways and this approach was successful. Genes encoding proteins from multiple families of transporters were identified as being regulated by FR-light using microarray studies. The broad range of transporters identified indicates that transporter proteins are important in mediated light-regulated changes in plant growth and development and confirms the idea that the movement of numerous molecules and compounds is vital for the seedling to change its developmental program. A selection of candidate FR-light regulated genes identified from the array studies of Wang *et al.* (2002) were selected for confirmation by RT-PCR. These included the monosaccharide transporter, *STP1*, a Ca^{2+} ATPase, *ACA2*, the auxin transporter, *PIN4*, a putative anthocyanin transporter *ANM2* and two genes of unknown function, the Niemann-Pick C disease-like protein and *FRIMP1*. These 6 genes were FR-light induced in the array study and this was verified using PCR methods. Three FR-light repressed candidate transporter genes were also selected, *RAN1* an ATP-dependent copper transporter, *CAT4* an amino acid transporter and *AHA2* an H^+-ATPase. Only *AHA2* appeared to show a down-regulation under FR-light, as *RAN1* showed no FR-light regulation and *CAT4* showed an up-regulation. As the majority of the genes showed the expected expression profile under FR-light, the validity of the initial array studies can be confirmed. The likely reason for some of the genes not showing the expected FR-light regulation is due to the difference in the growth conditions of both experiments. The arrays were conducted using RNA extracted from seedlings exposed to 24 hours of darkness followed by 96 hours of FR-illumination, whereas the PCR experiments were carried on seedlings exposed to a shorter FR-light period of only 12 hours after only 48 hours in the dark. The exact growth conditions were

not repeated using RT-PCR as early response transporters genes (under 12 hours) were being examined. This was to identify genes which were regulated early on in the signal transduction and were likely to be specifically regulated as a consequence of phytochrome signalling. This indicates that changes in expression of *CAT4* and *RAN1* may occur only after a prolonged period of FR-light exposure or at a later stage in the development of the seedling.

Some of these genes also showed light-regulation under other light treatments, for example *STP1* was up-regulated by blue light. This indicates that regulation of these transporter proteins could be mediated by other photoreceptors including the cryptochromes and are involved in a highly complex light-signalling pathway. The light-regulation of these transporter proteins indicate they play vital roles in de-etiolation. This has also been shown by the identification of T-DNA knockout mutants for some of the candidate genes. Homozygous mutant plants were identified for *stp1*, *aca2*, *cat4*, *aha2* and *frimp1*. This was confirmed using a combination of antibiotic selection and PCR. This approach was successful in identifying putative roles for some of these transporters in light-regulated seedling development. Some mutants, namely *stp1* and *aha2* showed no phenotypic difference compared to the wild-type plant. This could be because either the plants were grown in normal conditions and require a specific environmental or biological stress to show a phenotype or alternatively it could be due to redundancy between family members/isoforms (Cutler and McCourt, 2005). For example, at least 14 monosaccharide transporters as well as other sugar transporters have been identified in the *Arabidopsis* genome (Buttner and Sauer 2000; Maathius *et al.*, 2003) and it is likely that more that one sugar transporter has a specific function resulting in the *stp1* mutant having a wild-type phenotype. The isolation of double or even triple mutants could aid in identifying a function of proteins such as AHA2 and STP1. Although the identification of *stp1* and *aha2* mutants revealed no indication of a putative function in de-etiolation, putative functions for these proteins can be predicted by looking at the literature. For example *STP1* activity has been shown to be mainly in the roots and is highly up-regulated in response to exogenous sugar (Sherson *et al.*, 2000). So it would be interesting to investigate the phenotype of the *stp1* seedlings supplemented with exogenous sugars when exposed to different light treatments, including red and FR-light. A phenotypic trait could provide an insight into whether *STP* is expressed in the roots of FR-light grown seedlings and if sugar uptake is

required during de-etiolation. A similar scenario could be true for the *aha2* mutant, as *AHA2* has also been shown to accumulate in the roots and promoter-GUS fusions in *Arabidopsis* have suggested that AHA2 is expressed predominately but not exclusively in the root epidermis (Arango *et al.*, 2003). Phenotypic analysis of the roots of seedlings under different light could prove important in understanding the role of AHA2 is seedling development.

The T-DNA knockout approach was more successful in identifying a putative function in the *cat4* mutant. When grown in the dark, *cat 4* resembled the phenotype of the *cop2* and *HSL1* mutants, which are hookless (Raz and Ecker 1999). These hookless mutants are involved in early aspects in the formation of the hook, therefore the amino acid transporter CAT4 maybe involved in the developmental pathway of hook formation and linked to HSL1 and COP2. The treatment of wild-type seedlings with auxin results in a reduced hook curvature and ethylene enhances the curvature of the hook (Ecker., 1995; Lehman *et al.*, 1996). It would therefore be interesting to see if the curvature of the apical hook is rescued in the *cat4* mutant supplemented with ethylene in the dark. This would establish whether CAT4 is linked to the hormone transduction cascade in addition to the skotomorphogenic developmental pathway. CAT4 also appears to play a vital role in cell elongation in the hypocotyl as the *cat4* mutant has a shorter hypocotyl than wild-type. Ethylene has also been shown to reduce cell elongation in the dark grown seeding (Vandenbussche *et al.*, 2005) indicating CAT4 could indeed be linked to the morphological changes that arise due to ethylene production. Alternatively amino acids could just be required for cell growth and CAT4 could be implicated in this process. It would be interesting to identify the specific localization of CAT4 using GPF-fusion proteins to see if this supports the potential role of CAT4.

The *aca2* mutant also showed an interesting phenotype in seedlings grown in continuous blue and white-light. The curling of the roots around the hypocotyl indicates ACA2 is important for normal lateral root growth. This response also appears to be specific to the cryptochrome and/or phototropin blue-light photoreceptors as this response was specific to white and blue-light but not apparent in seedlings grown in red or FR-light. However this response may be more complicated as comparative analysis of expression profiles of various photoreceptor mutants during seedling development in response to blue-

light indicated that phyA plays a limited role in the control of transcription factor gene expression in *Arabidopsis* (Jioa *et al.*, 2003). It is therefore plausible that other genes are regulated by phyA when exposed to blue-light. Calcium is essential for many aspects of plant growth, development and signalling (Sze *et al.*, 2000). One of the most significant roles of Ca^{2+} is as a signal transduction element, and the concentration of cytosolic free Ca^{2+} is critically important in controlling many cellular responses (Sze *et al.*, 2000). An astonishing variety of physiological stimuli elevate cytosolic Ca^{2+} in plant cells, including light (Sanders *et al.*,1999). An elevation in Ca^{2+} causes changes in proteins modulated by Ca^{2+} and their targets that elicit downstream events in such signalling pathways. Changes in the environment of the plant results in the elevation of cytoplasmic calcium concentrations. After the initial response calcium levels must return to the basal level, so therefore an increase in the ACA2 protein may be involved in the efflux of calcium from the cytoplasm to the endoplasmic reticulum during de-etiolation. As ACA2 is located on the endoplasmic reticulum endomembranes it would be interesting to examine the phenotype of the *aca2/eca1* double mutant. ECA1 has also shown to be localised to the endoplasmic reticulum (Axelsen and Palmgren 2001), so it would be interesting to study the seedling and plant phenotype of the *ACA2/ECA1* double mutant.

So far the function of the genes identified as being FR-light regulated are known but their role in seedling de-etiolation has yet to be established. However genes of unknown function were also identified including *FRIMP1*. The *FRIMP1* gene was the most highly FR-light regulated of all the genes identified and was also shown to be down-regulated by blue and red-light. This indicates that, like the transporter proteins previously described, *FRIMP1* is also involved in a complex light signalling pathway mediated by multiple photoreceptors.

Analysis of the FRIMP1 amino acid sequence revealed FRIMP1 protein homologues in a variety of eukaryotic organisms including rice, humans, *C.elegans*, mouse and Drosophila. A second *Arabidopsis* protein was also identified termed FRIMP2 which shows over 90% sequence identity to FRIMP1. Unfortunately the function of none of these genes was known and this provided no insight into a putative function of the FRIMP proteins. Homozygous mutants were identified for both *frimp1* and *frimp2*, both of which displayed a variety of phenotypic traits. Many of the phenotypic observations shown by

these mutants were classical light-regulated traits. These included the elongated hypocotyl shown by *frimp1* seedlings grown in FR-light suggesting a loss of light responsiveness under these conditions. This response is wavelength specific as the hypocotyl length was unaffected in red, blue and white-light. It is interesting that the *frimp1* mutant also results in an increase in cotyledon area when grown under red-light rather than a loss of phytochrome signalling. As *phyB* mutants have reduced cotyledon area under these light conditions this result suggests a hypersensitive response to red-light (Reed *et al.*, 1994). Other phenotypic traits include the elongated petiole length in the *frimp1* mutant and the increase in leaf number of both *frimp1* and *frimp2*. A number of other phenotypic traits were observed including the leaf epinastic curling response of the *frimp1* mutant, the abnormal and irregular cell arrangements shown in *frimp1* and the increase in leaf length and size of the *frimp2* mutant. Some of these observations indicate putative roles for the FRIMP proteins. This includes the epinastic response of leaves of *frimp1*. A number of mutants involved with the phytohormone auxin display the epinastic response, including the *axr4* mutant which is an auxin-resistant mutant and is important for normal auxin sensitivity (Hobbie and Estelle 1995). The overproduction of auxin was also shown to cause epinastic curling in petunia plants (Klee *et al.*, 1987; De Paepe *et al.*, 2005). The epinastic curvature phenotype shown in the *axr4* mutant and tobacco treated with IAA (Kawano *et al.*, 2003) indicates that the FRIMP proteins could be functioning as possible auxin transporters or involved in auxin signalling in some way. This hypothesis could be tested further by inhibiting auxin production in the *frimp* mutants to see if the epinastic response is reduced. The tissue distribution of *FRIMP1* and *FRIMP2* also correlates which the phenotypes shown in the leaves of the respective mutants as both *FRIMPs* were highly expressed in leaf tissue. The identification of a double *frimp1/frimp2* heterozygous mutant looks promising in obtaining a double homozygous mutant. It would be interesting to study the phenotype of the double mutant as it could provide further evidence for the function of the FRIMP proteins.

The most intriguing response shown is the expression profile of *FRIMP1* in the *phyA* mutant, as unlike *HEMA1* and *Lhcb1.2* which are FR-light up-regulated in the wild-type but not in *phyA* (McCormac *et al.*, 2001), the induction of *FRIMP1* is still observed in the *phyA* mutant. This is a unique expression profile and indicates another photoreceptor must be mediating this response. As phyE as been shown in be implicated in FR-light seed

germination in *Arabidopsis* (Hennig *et al.*, 2002), and phyC in the perception of FR-light in rice (Takano *et al.*, 2005), either one of these phytochrome photoreceptors could be responsible for this FR-light induction in the *phyA* mutant. qPCR revealed a small induction was shown in both the *phyA*, *phyD* and *phyE* seedlings grown in FR-light. However due to the reduced up-regulation of *FRIMP1* in the *Langsberg erecta* wild-type compared to Col-0, it would be preferable to repeat such experiments in mutants in the Col-0 background or alternatively extend the studies to the rest of the mutants using the *Langsberg erecta* wild-type to investigate the true regulation of *FRIMP1* in the photoreceptor mutants grown in FR-light.

So where could the FRIMP proteins be involved in a light-signalling pathway? There are many possible explanations to potentially answer this question. Three potential models will be described here (Figure 6.1). Phytochrome has been shown to relocate from the cytoplasm to the nucleus following a light treatment (Nagatani, 2004). The FRIMP proteins could be involved in the cytoplasmic to nucleus transition as they could be localised to the nuclear envelope (Figure 6.1, Model A). Knowing that photoreceptors are often membrane-bound upon signal perception the possibility of phytochromes being associated with cytoplasmic membrane proteins is possible (Moller *et al.*, 2002). Although it has been suggested that phyA is mainly cytosolic some of the Pfr form could possibly be localised to the plasma membrane via protein-protein interaction (Moller *et al.*, 2002). The FRIMP proteins could therefore function as a phytochrome-interacting protein. The FRIMP proteins could act in the cytoplasm thought a non-nuclear phytochrome localised pathway which results in changes in the cellular response (Figure 6.1, Model B). These explanations indicate that the FRIMP proteins act early within the light-signalling pathway. Finally the FRIMP proteins could be implicated further down the phytochrome signalling pathway where they may act as effector proteins. Here the membrane function of the FRIMP proteins could be directly affected by phytochrome signalling (Figure 6.1, Model C).

The next stage would be to use the *frimp* mutants to see if the proteins act directly as a light signalling pathway component between phytochrome and other effector proteins (Models A and B) or if they function as transporters or receptors for a specific signalling molecule (Model C). In conclusion the FRIMP proteins may play either play a direct role in phytochrome signalling or may act as a transporter or receptor and lie as a key intersection

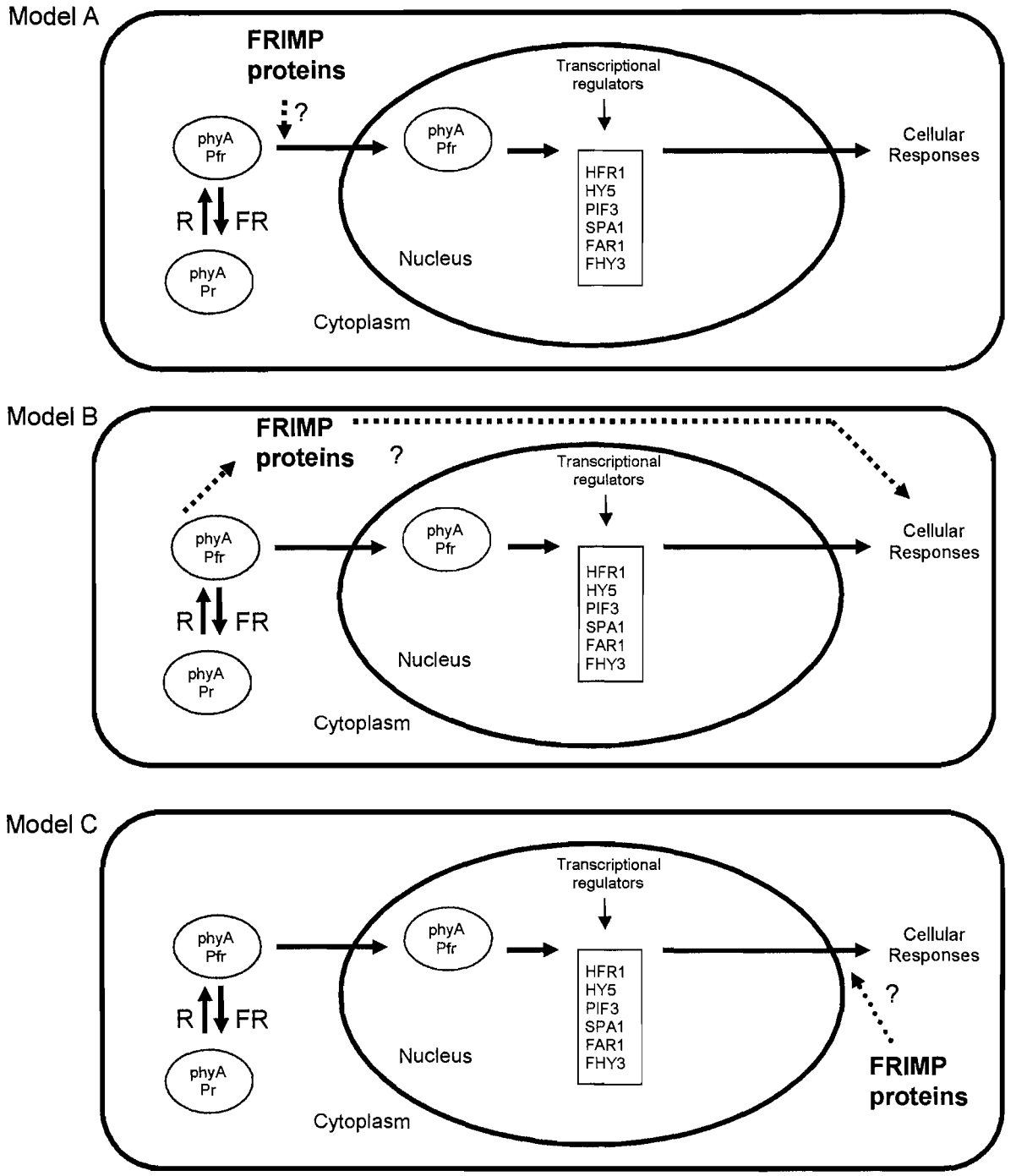

Figure 6.1 Alternative models depicting the involvement of the FRIMP proteins in phytochrome signal transduction. Model A. The FRIMP proteins interact with phytochrome via protein-protein interactions. Model B. The FRIMP proteins act in the cytoplasm thought a non-nuclear phytochrome localised pathway. Both of these models indicate that the FRIMP proteins act early within the light-signalling pathway. Model C. The FRIMP proteins could be implicated further down the phytochrome signalling pathway where they may act as effector proteins as they may function as transporters or receptors for a specific signalling molecule.

with other signalling pathways. To aid in this answering this question a transcriptomics approach using the *frimp1* and *frimp2* mutants as well as the *frimp1frimp2* double mutant will provide an insight into identifying other genes involved in the signalling pathway. The comparison of other data sets with profiles of genes regulated by other signalling pathways showing significant overlap with FRIMP-regulated genes will aid in identifying a function of the FRIMP proteins.

The analysis of some of the mutants has shown that these proteins may not solely be involved in light-signalling pathways as they may also be implicated in phytohormone responses and signalling pathways. For example the epinastic response of the leaves in the *frimp1* mutant as shown by other auxin-related mutants including the *axr4* mutant (Hobbie and Estelle 1995) indicates that FRIMP1 maybe involved in auxin signalling either as a transporter, receptor or other membrane protein. The reduced apical hook in etiolated *cat4* seedlings also suggests that CAT4 maybe involved in either auxin or ethylene signalling pathways as ethylene is known to enhance the curvature of the hook (Ecker., 1995; Lehman *et al.*, 1996). These FR-light regulated genes may be implicated in the light regulation of hormone signalling pathways as there is evidence that photoreceptors regulate phytohormone levels in plant development. Molecular links have been made between light and auxin signalling pathways with direct correlations between light conditions and regulation of auxin (Tian and Reed, 2001) and mutations in genes encoding several transcription factors have been shown to affect both light and auxin responses. Ethylene and auxin have been shown to control responses to decreased light intensities in *Arabidopsis* as ethylene and auxin-insensitive mutants were shown to be impaired in their reaction to shading resulting in a defect in leaf elevation (Vanderbussche *et al.*, 2003). Auxin- inducible genes were also up-regulated in wild-type Arabidopsis in response to a reduction in light intensity indicating both hormones are required in the shading response.

Other phytohormones have also been implicated in light-signalling, for example is has been shown that phyA and cry1 act redundantly to regulate gibberellin levels during de-etiolation in response to blue light in pea seedlings (Foo *et al.*, 2006). Both these photoreceptors are required for the rapid inhibition of hypocotyl elongation in response to transfer from dark to blue light. The inhibition of hypocotyl elongation in blue-light is accompanied by a rapid reduction in the level of gibberellins and this has shown to be

regulated by phyA and cry1 (Foo *et al.*, 2006). It has been shown that hormones are required for light-mediated plant development so it is therefore plausible that the transporter proteins are involved in mediating the light-regulation of hormone levels.

The use of a reverse genetics approach to look for changes in phenotype of a mutant of interest (Krysan *et al.*, 1999) rather than a forward genetics approach by screening mutant populations (Camilleri *et al.*, 1998) has been beneficial in identifying putative functions for some of the genes of interest in seedling de-etiolation. The changes in phenotype observed in some of the mutants may not have been observed when screening such mutant populations. For example the elongated hypocotyl phenotype shown by *frimp1* FR-light grown seedlings may not have been identified via mutant screens. This elongated hypocotyl phenotype forms the basis for screening for mutants involved in phyA signalling (Nagatani *et al.*, 1993; Franklin *et al.*, 2005). The extent of the elongated hypocotyl of *frimp1* may not be as significant as some of the other mutants which show the elongated hypocotyl phenotype so therefore would be missed in mutant screens. The same principle applies for other subtle phenotypes including the straightened apical hook of the dark grown *cat4* seedling, the reduction in size of the *aca2* mutant in blue and white-light and the epinastic response of the *frimp1* leaves. Although a variety of phenotypic traits were observed in the various mutants it is important to confirm that the change in phenotype results specifically from the loss of gene of interest and not due to multiple insertions. It is therefore important to obtain a second mutation in the gene of interest which displays an identical phenotype. Alternatively it is also possible to backcross the mutant with a wild-type to show that a second mutation is not responsible for the phenotype. This was attempted with *frimp1* and *frimp2* however unfortunately the backcrosses were unsuccessful and the repetition of these backcrosses is essential. A wild-type hypocotyl length in the FR-light grown seedlings and the loss of the epinastic response in the F2 progeny would indicate that the differences in the mutant are specifically due to the absence of the *frimp1* gene. The phenotype of a mutant would also ideally by complemented by overexpression analysis. This was initiated for *frimp1* and it would have been very interesting to see the phenotype of a FRIMP1 overexpressing plant and this could further aid the determination of a putative function for this protein.

To summarise, a genomics approach has been successful in identifying transporters and other membrane proteins that are important in mediating the photomorphogenic developmental changes in seedling de-etiolation and plant growth and development. A number of FR-light regulated genes were identified using microarray analysis and verified using PCR. Phenotypic analysis of T-DNA insertional mutants indicated that some of these genes had altered light-responsive phenotypes. This included *frimp1* which had elongated petioles and the FR-light grown seedling had an elongated hypocotyl compared to wild-type. The *cat4* mutant also had a reduced apical hook curvature and a reduction in hypocotyl elongation in the etiolated seedling. The phenotypic traits shown by such mutants indicate that transporters and other potential membrane proteins are vital for light-regulated plant growth and development and provides an insight into the massive potential of transporters in this role. The future potential of the project could branch into a variety of directions including further light and hormone stress studies on the mutants to further characterise their role in plant development and to identify the true function of the FRIMP proteins. The approach can be expanded by undertaking arrays using full genome chips so that all genes are represented and to expand the conditions that have already been tested. Examination of other knockout mutants for other light-regulated candidate genes could also be studied. The aim is to understand the physiological function of these FRIMP membrane proteins by determining what processes and genes they regulate and where they are located and to address if they play a key signalling role in the regulation of plant development by phytochrome. The FR-light induction of *FRIMP1* in the *phyA* seedling questions the hypothesis that phyA is the sole photoreceptor involved in perceiving FR-light and this could be studied further to see if this expression profile shown by *FRIMP1* is true and if the signal transduction pathway under FR-light is more complicated than originally suggested.

References

Aharoni A, Vorst 0. 2001. DNA microarrays for functional plant genomics. *Plant Molecular Biology* **48**:99-118

Ahmad M, Cashmore A.R. 1993. HY4 *of Arabidopsis Thaliana* encodes a protein with characteristics of a blue-light photoreceptor. *Nature* **366**:162-166

Allemeersch J, Durinck S, Vanderhaeghen R, Alard P, Maes R, Seeuws K. 2005. Benchmarking the CATMA microarray. A novel tool for *Arabidopsis* transcriptome analysis. *Plant Physiology* **137**:588-601

Alonso J, Stepanova A, Leisse T, Kim C, Chen H, Shinn P, Stevenson D, Zimmerman J, Barajas P, Cheuk R, Gadrinab C, Heller C, Jeske A, Koesema E, Meyers C, Parker H, Prednis L, Choy N, Deen H, Geralt M, Harazi N, Hom E, Karnes M, Mulholland C, Schmidt I, Guzman P, Carter D, Merchand T, Resseeuw W, Rrogden D, Zeko A, Crosby W, Berry C, Ecker J. 2003. Genome-wide insertional mutagenesis of *Arabidopsis thaliana. Science* **301**:653-657

Alsterfjord M, Sehnke P, Arkell A, Larsson H, Svennelid F, Rosenquist M, ferl R, Sommarin M, Larsson C. 2004. Plasma membrane H^+-ATPase and 14-3-3 isoforms of *Arabidopsis* leaves: Evidence for isoforms specificity in the 14-3-3/H^+-ATPase interaction. *Plant Cell Physiology* **45**:1202-1210

An C, Sawada A, Kawaguchi Y, Fukusaki E, Kobayashi A. 2005. Transient RNAi induction against endogenous genes in *Arabidopsis* protoplasts in vitro-prepared double-stranded RNA. *Bioscience, Biotechnology and Biochemistry* **69**:415-418

Ang L, Deng X. 1994. Regulatory hierarchy of photomorphogenic loci: Allele-specific and light-dependent interaction between the HY5 and COP1 loci. *Plant Cell* **6**:613-628

Ang L, Chattopadhyay S, Wei N, Oyama T, Okada K, Batschaucer A and Deng X. 1998. Molecular interaction between COP1 and HY5 defines a regulatory switch for light control of *Arabidopsis* development. *Molecular Cell* **1**:213-222

Aphalo P.J, Ballare C.L, Scolel A.L. 1999. Plant-plant signalling, the shade avoidance response and competition. *Journal of Experimental Botany* **50**:1629-1634

Arango M, Gevaudant F, Oufattole M, Bounty M. 2003. The plasma membrane proton pump ATPase: the significance of gene subfamilies. *Planta* **216**:355-365

Aukerman M, Hirschfield M, Wester L, Weaver M, Clack T, Amasino R, Sharrock R. 1997. A deletion in the PHYD gene of *Arabidopsis* defines a role for phytochrome D in red/far-red light sensing. *Plant Cell* **9**:1317-1326

Axelsen K, Palmgren M. 2001. Invertory of the superfamily of P-type ion pumps in *Arabidopsis. Plant Physiology* **126**:696-706

Barbier-Brygoo H, Gaymard F, Rolland N, Joyard J. 2001. Strategies to identify transport systems in plants. *Trends in Plant Science* **6**:577-585

Bauer D, Viczian A, Kircher S, Nobis T, Adam E, Fejes E, Schafer E, Nagy F. 2004. Constitutive photomorphogenesis 1 and multiple photoreceptors control degradation of phytochromes interacting factor 3, a transcriptional factor required for light signalling in *Arabidopsis. Plant Cell* **16**:1433-1445

Bock K, Honys D, Ward J, Padmanaban S, Nawrocki E, Hirschi K, Twell D, Sze H. 2006. Integrating membrane transport with male gametophyte development and function through transcriptomics. *Plant Physiology* **140**:1151-1168

Boerjan W, Cervera M, Delaure M, Breekman T, Dewitte W. 1995. Superroot, a recessive mutation in *Arabidopsis*, confers auxin overexpression. *Plant Cell* **7**:1405-1419

Booker F, Burkey K, Overmyer K, Jones A. 2004. Differential response of G-protein *Arabidopsis thaliana* mutants to ozone. *New Phytologist* **162**:633-641

Bosher J, Labouesse M. 2000. RNA interference: genetic wand and genetic watchdog. *Nature Cell Biology* **2**:31-36

Bouche N and Bouchez D. 2001. *Arabidopsis* gene knockout: phenotypes wanted. *Current Opinion in Plant Biology* **4**:111-117

Bovet L, Eggmann T, Meylan-Bettex M. 2003. Transcript levels of *AtMRPs* after cadmium treatment: induction of *AtMRP3*. *Plant Cell and Environment* **26**:371-381

Boyes DC, Zayed AM, Ascenzi R, McCaskill AJ, Hoffman HE, Davis KR, Gorlach J. 2001. Growth stage-based phenotypic analysis of *Arabidopsis*: a model for high through put functional genomics in plants. *Plant Cell* **13**:1499-1510

Boylan M, Quail P. 1991. Phytochrome A overexpression inhibits hypocotyl elongation in transgenic *Arabidopsis*. *PNAS* **88**:10806-10810

Braslavsky S, Gartner W, Schaffner K. 1997. Phytochrome photoconversion. *Plant, Cell and Environment* **22**:700-706

Buch-Pedersen M, Palmgren M. 2003. Mechanism of proton transport by plant plasma membrane proton ATPases. *Journal of Plant Research* **116**:507-515

Bush D.R. 1993. Proton-coupled sugar and amino acid transporters in plant. *Annual Review of Plant Physiology and Molecular Biology*. **44**:513-542

Buttner M, Sauer N. 2000. Monosaccharide transporters in plants: structure, function and physiology. *Biochimica et Biophysica Acta* **1465**:263-274

Camilleri C, Lafleuriel J, Macadre C, Varoquaux F, Parmentier Y, Picard G, Caboche M, Bouchez D. 1998. A YAC contig map of *Arabidopsis thaliana* and chromosome 3. *Plant Journal* **14**:633-642

Carstea E, Morris J, Coleman K. 1997. Niemann-Pick C1 disease gene: Homology to mediators of cholesterol homeostasis. *Science* **277**:228-231

Casal J.J, Sanchez R.A, Botto J,F. 1998. Modes of action of phytochromes. *Journal of Experimental Botany.* **49**:127-138

Chen M, Tao Y, Lim J, Shaw A, Chory J. 2005. Regulation of phytochrome B nuclear localization through light-dependent unmasking of nuclear localization signals. *Current Biology* **15**:637-642

Cheng N, Pittman J, Barkla B, Shigaki T, Hirschi. 2003. The *Arabidopsis cax1* mutant exhibits impaired ion homeostasis, development and hormone responses and reveals interplay among vacuolar transporters. *Plant Cell* **15**:347-364

Cho D, Hong S, Nam H, Soh M. 2003. *FIN5* positively regulates far-red light responses in *Arabisopsis thaliana. Plant Cell Physiology* **44**:565-572

Choi G, Yi H, Lee J, Kwon Y, Soh M, Shin B, Luka S, Song P. 1999. Phytochrome signalling is mediated through nucleoside diphosphate kinase 2. *Nature* **401**:610-613

Chory J, Peto C, Feinbaum R, Pratt L, Ausubel F. 1989. *Arabidopsis thaliana* mutant that develops as a light-grown plant in the absence of light. *Cell* **58**:991-999

Clack T, Matthews S, Sharrock R. 1994. The phytochrome apoprotein family in *Arabidopsis* is encoded by five genes. *Plant Molecular Biology* **25**:413-417

Clough R, Vierstra R. 1997. Phytochrome degradation. *Plant Cell and Environment* **20**:713-721

Clough R, Jordan-Beebe E, Lohman K, Marita J, Walker J, Gatx C, Vierstra R. 1999. Sequences within both the C and N-terminal domains of phytochrome A are required for the Pfr ubiquitination and degradation. *Plant Journal* **17**:155-167

Cookson S, Granier C. 2006. A dynamic analysis of the shade-induced plasticity in *Arabidopsis thaliana* rosette leaf development reveals new components of the shade-adaptive response. *Annals of Botany* **97**:443-452

Cosgrove D.J. 1994. Photomodulation of growth. *In photomorphogenesis in plants, 2nd edition* pp 631-658, Kluwer Academic Publishers

Curran A, Hwang I, Corbin J, Martinez S, Rayle D, Sze H, Harper J. 2000. Autoinhibition of a calmodulin-dependent calcium pump involves a structure in the stalk that connects the transmembrane domain to the ATPase catalytic domain. *Journal of Biological Chemistry* **275**:30301-30308

Cutler S, McCourt P. 2005. Dude, Where's my phenotype? Dealing with redundancy in signalling networks. *Plant Physiology* **138**:558-559

De Paepe A, Grauwe L, Bertrand S, Smalle J, Van Der Straeten D. 2005. The *Arabidopsis* mutant *eer2* has enhanced ethylene responses in the light. Journal of experimental botany **56**:2409-2420

Deforce L, Tomizawa K, Farrens D, Song P, Furuya M. 1991. In vitro assembly of apophytochrome and apophytochrome deletion mutants expressed in yeast with phycocyanobilin. *Proceedings of the National Academy of Sciences USA* **88**:10392-10396

Deng X, Caspar T, Quail P. 1991. *cop1* : A regulatory locus involved in light-controlled development and gene expression in *Arabidopsis*. *Genes and Development* **5**:1172-1182

Deprez R, Ruijter J, Moorman A. 2002. Sensitivity and accuracy of quantitative real-time PCR using SYBR green 1 depends on cDNA synthesis conditions. *Analytical Biochemistry* **307**:63-69

Devlin P, Patel S, Whitelam G. 1998. Phytochrome E influences internode elongation and flowering time in Arabidopsis. *Plant Cell* **10**:1479-1487

Devlin P, Robson R, Patel S, Goosey L, Sharrock R, Whitelam G. 1999. Phytochrome D acts in the shade-avidance syndrome in *Arabidopsis* by controlling elongation growth and flowering time. *Plant Physiology* **119**:909-915

Devlin P, Yanovsky M, Kay S. 2003. A genomic analysis of the shade avoidance response in *Arabidopsis. Plant Physiology* **133**:1617-1629

Donson J, Fang Y, Volkmuth W. 2002, Comprehensive gene expression analyses by transcript profiling. *Plant Molecular Biology* **48**:75-97

Dreyer I, Horeay C, Lemaillet G, Zimmermann S, Bush D, Schachtmann D, Spalding E, Sentenac H, Gaber R. 1999. Identification and characterization of plant transporters using heterologous expression systems. *Journal of Experimental Botany* **50**:1073-1087

Duek P, Fankhauser C. 2003. HFR1, a putative bHLH transcription factor, mediates both phytochromes A and cryptochrome signalling. *Plant Journal* **34**:827-836

Duek P, Fankhauser C. 2005. bHLH class transcription factors take stage in phytochrome signalling. *Trends in Plant Science* **10**:51-54

Ecker J. 1995. The ethylene signal transduction pathway in plants. *Science* **268**:667-675

Eraso P, Portillo F. 1994. Molecular mechanism of regulatory of yeast plasma facultative metallophyte *Arabidopsis halleri. Plant Cell and Environment* **29**:950-963

Fankhauser C, Casal J. 2004. Phenotypic characterization of a photomorphogenic mutant. *Plant Journal* **39**:747-760

Fankhauser C, Yeh K, Lagarias J, Zhang H, Elich T, Chory J. 1999. PSK1, a substrate phosphorylated by phytochromes that modulates light signalling in *Arabidopsis*. *Science* **28**:1539-1541

Fankhauser C, Chory J. 1997. Light control of plant development. *Annual Review of Cell Developmental Biology* **13**:203-229

Fire A, Xu S, Montgomery M, Kostas S, Driver S, Mello C. 1998. Potent and specific genetic interference by double-stranded RNA in *Caenorhabditis elegans*. *Nature* **391**:806-811

Fischer W.N, Kwart M, Hummel S, Frommer W.B. 1995. Substrate specificity and expression profile of amino acid transporters (AAPs) in *Arabidopsis*. *Journal of Biological Chemistry* **270**:16315-16320

Foo E, Platten J, Weller J, Reid J. 2006. PhyA and cry1 act redundantly to regulate gibberellin levels during de-etiolation in blue light. *Physiologica Plantarum* **127**:149-156

Franklin K, Praekelt U, Stoddart W, Vierstra R and Whitelam G. 2003a. Phytochromes B, D and E act redundantly to control multiple physiological responses in *Arabidopsis*. *Plant Physiology* **131**:1340-1346

Franklin K, Davis S, Stoddart W, Vierstra R, Whitelam G. 2003b. Mutant analyses define multiple roles for phytochromes C in *Arabidopsis thaliana* photomorphogenesis. *Plant Cell* **15**:1981-1989

Franklin K, Larner V, Whitelam G. 2005. The signal transducing photoreceptors of plants. *Int. J. Dev. Biol* **49**:653-664

Freeman W, Walker S, Vrana K. 1999. Quantitative RT-PCR: Pitfalls and potential. *Biotechniques* **20**:112-125

Friml J, Vieten A, Sauer M. 2002. Efflux-dependent auxin gradients as a common module for plant organ formation. *Cell* **115**:591-602

Friml J. 2003. Auxin transport – shaping the plant. *Current Opinions in Plant Biology* **6**:7-12

Frommer W, Ninnemann O. 1995. Heterologous expression of genes in bacterial, fungal, animal and plant cells. *Annual Review of Plant Physiology and Plant Molecular Biology* 46:419-444

Fuchs I, Philippar K, Ljung K, Sandberg G, Hedrich R. 2003. Blue light regulates an auxin-induced K^+ channel gene in the maize coleoptile. *Proceedings of the National Academy of Sciences USA* **100**:11795-11800

Fuglsang A, Borch J, Bych K, Jahn T, Roepstorff P, Palmgren M. 2003. The binding site for regulatory 14-3-3 protein in plant plasma membrane H^+-ATPase. *Journal of Biological Chemistry* **24**:42266-42272

Furuya M, Song P.1994. Assembly and properties of holophytochrome. In *Photomorphogenesis in plants 2nd edn* 105-140, Kluwer Academic Publishers

Gazzarrini S, Lejay L, Gogon A, Ninnemann O, Frommer W, Wiren N. 1999. Three functional transporters for constitutive, diurnally regulated and starvation induced uptake of ammonium into *Arabidopsis* roots. *Plant Cell* **11**:937-947

Geelen D, Lurin C, Franchisse J, Courtial B, Maural C. 2000. Disruption of a putative anion channel gene *AtCLC-a* in *Arabidopsis* suggests a role in the regulation of nitrate content. *The Plant Journal* **21**:259-267

Geisler M, Aelsen K, Harper J, Palmgren M. 2000. Molecular aspects of higher plant P-type Ca^{2+} ATPases. *Biochim. Biophys. Act* **1465**:52-78

Geisler M, Murphy A. 2006. The ABC of auxin transport: The role of p-glycoproteins in plant development. *FEBS letters* **580**:1094-1102

Ghassemian M, Lutes J, Tepperman J, Chang H, Zhu T, Wang X, Quail P, Markus-Lange B. 2006. Integrative analysis of transcript and metabolite profiling data sets to evaluate the regulation of biochemical pathways during photomorphogenesis. *Archives of Biochemistry and Biophysics* **448**:45-59

Gilliland L, Pawloski L, Kandasamy M. 2003. *Arabidopsis* actin gene ACT7 plays an essential role in germination and root growth. *Plant Journal* **32**:319-328

Goto N, Kumagi T, Koornneef M. 1991. Flowering responses to light-breaks in photomorphogenic mutants of *Arabidopsis thaliana*, a long-day plant. *Plant Physiology* **83**:209-215

Grossman and Takahashi. 2001. Macronutrient utilization by photosynthetic eukaryotes and the fabric of interactions. *Annu. Rev. Plant Physio. Plant Mol. Biol.* **52**:163-210

Harada K, Fukusaki E, Kobayashi A. 2006. Pressure-assisted capillary mass spectrometry for metaolomics anion analysis. *Journal of Bioscience and Bioengineering* **101**:403-409

Harper J, Hong B, Hwang I, Stoddard R, Huang J, Palmgren M, Sze H. 1999. A novel calmodulin-regulated Ca^{2+} ATPase (ACA2) from *Arabidopsis* with an N-terminal autoinhibitory domain. *Journal of Biological Chemistry.* **273**:1099-1106

Hechenberger M, Schwappach B, Fischer W, Frommer W, Jentsch T, Steinmeyer K. 1996. A family of putative chloride channels from *Arabidopsis* and functional complementation of a yeast strain with a CLC gene disruption. *Journal of Biological chemistry* **271**:33632-33638

Hennig L, Funk M, Whitelam G, Schafer E. 1999. Functional interaction of cryptochrome 1 and phytochromes D. *Plant Journal* **20**:289-294

Hennig L, Stoddart W, Dieterle M, Whitelam G, Schafer E. 2002. Phytochrome E controls light-induced germination of *Arabidopsis*. *Plant Physiology* **128**:194-200

Hirschfield M, Tepperman J, Clack T, Quail P, Sharrock R. 1998. Co-ordination of phytochrome levels in phyB mutants of *Arabidopsis* as revealed by apoprotein specific monoclonal antibodies. *Genetics* **149**:523-535

Hobbie L, Estelle M. 1995. The *axr4* auxin-resistant mutants of *Arabidopsis thaliana* define a gene important for root gravitropism and lateral root initiation. *Plant Journal* **7**:211-220

Hoecker U. 2005. Regulated proteolysis in light signalling. *Current Opinions in Plant Biology* **8**:469-476

Holtorf H, Guitton M, Reski R. 2002. Plant functional genomics. *Naturwissenschaften* **89**:235-249

Hong B, Ichida A, Wang Y, Gens J, Pickard B, Harper J. 1999. Identification of a calmodulin-regulated Ca^{2+}-ATPase in the endoplasmic reticulum. *Plant Physiology* **119**:1165-1175

Hsieh H, Okamoto H, Wang M, Ang L, Matsui M, Goodman H, Deng X. 2000. FIN219, an auxin-related gene, defines a link between phytochrome A and the downstream regulator COP1. *Genes and Development* **14**:1958-1972

Hua J, J Meyerowitz EM. 1998. Ethylene responses are negatively regulated by a receptor gene family in *Arabidopsis thaliana. Cell* **94**:261-271

Huq E. 2006. Degradation of negative regulators: a common theme in hormone and light signalling networks? *Trends in Plant Science* **11**:4-7

Hwang I, Harper J, Liang F, Sze H. 2000a. Calmodulin activation of an endoplasmic reticulum-located calcium pump involves an interaction with the N-terminal autoinhibitory domain. *Plant Physiology* **122**:157-167

Hwang I, Sze H, Harper J. 2000b. A calcium-dependent protein kinase can inhibit a calmodulin-stimulated Ca^{2+} pump (ACA2) located in the endoplasmic reticulum of *Arabidopsis. Proceedings of the National Academy of Sciences USA* **97**:6224-6229

Ikonen E, Holtta-Vuori. 2004. Cellular pathology of Niemann-Pick type C disease. *Seminars in Cell and developmental Biology* **15**:445-454

Jiang K, Feldman L. 2002. Root meristems establishment and maintenance: The role of auxin. *Journal of Plant Growth Regulation* **21**:432-440

Jiao Y, Yang H, Ma L, Sun N, Yu H, Liu T, Gao Y, Gu H, Chen Z, Wada M, Gerstein M, Zhao H, Qu L, Wang-Deng X. 2003. A Genome-Wide analysis of the blue-light regulation of *Arabidopsis* transcription factor gene expression during seedling development. *Plant Physiology* **133**:1480-1493

Jiao Y, Ma L, Strickland E, Deng XW. 2005. Conservation and divergence of light-regulated genome expression patterns during seedling development in rice and *Arabidopsis. Plant Cell* **17**:3239-3256

Johnson E, Bradley M, Harberd P, Whitelam G. 1994. Photoresponses of light-grown *phyA* mutants of *Arabidopsis. Plant Physiology* **105**:141-149

Kagawa T, Sakai T, Suetsugu N, Oikawa K, Ishiguro S, Wada M. 2001. *Arabidopsis* NPL1: a prototropin homolog controlling the chloroplast high-light avoidance response. *Science* **291**:2138-2141

Kaiser B, Rawat S, Siddiqi Y, Masle J, Glass A. 2002. Functional analysis of an *Arabidopsis* T-DNA knockout of the high-affinity ammonium transporter *AtAMT1-1*. *Plant Physiology* **130**:1263-1275

Kamath R, Ahringer J. 2003. Genome-wide RNAi screening in *Caenorhabditis elegans*. *Science* **30**:313-321

Kasai M, Muto S. 1990. Ca^{2+} pump and Ca^{2+}/H^{+} antiporter in plasma membrane vesicles isolated. *Journal of Membrane Biology* **114**:3452-2471

Kawano N, Kawano T, Lapeyrie F. 2003. Inhibition of the Indole-3-acetic acid-induced epinastic curvature in Tobacco leaf strips by the 2,4-dichlorophenoxyacetic acid. *Annals of Botany* **91**:465-471

Kazan K, Schenk P, Wilson I, Manners. 2001. DNA microarray: new tools in the analysis of plant defence responses. *Molecular Plant Pathology*. **2**:177-185

Keurentjes J, Fu J, Lommen A, Hail R, Bion R, Jansen R, Koornneef M. 2006. The genetics of plant metabolism. *Nature and Genetics* **38**:842-849

Kim B, von Arnim A.G. 2006. The early dark-response in *Arabidopsis thaliana* revealed by cDNA microarray analysis. *Plant Molecular Biology* **60**:321-342

Kircher S, Kozma-Bognar L, Kim L, Adam E, Harter K, Schafer E, Nagy F. 1999. Light quality-dependent nuclear import of the plant photoreceptors phytochromes A and B. *Plant Cell* **11**:1445-1456

Klee H, Horsch R, Hinchee M, Hein M, Hoffmenn N. 1987. The effects of two *Agrobacterium tumefaciens* T-DNA auxin biosynthetic gene products in transgenic petunia plants. *Genes and Development* **1**:86-96

Koornneef M, Rolff E, Spruitt C. 1980. Genetic control of light-inhibited hypocotyl elongation in *Arabidopsis thaliana. Molecular Genetics* **100**:147-160

Kozuka T, Horiguchi G, Kim G, Ohgishi M, Sakai T, Tsukaya H. 2005. The different growth responses of the *Arabidopsis thaliana* leaf blade end and petiole during shade avoidance are regulated by photoreceptors and sugar. *Plant Cell Physiology* **46**:213-223

Krysan S, Young JC, Sussman MR. 1999. T-DNA as an insertional mutagen in *Arabidopsis. Plant Cell* **11**:2283-2290

Kuo W, Jenssen T, Butte A. 2002. Analysis of matched mRNA measurements from two different microarray technologies. *Bioinformatics* **18**:405-412

Kwon S, Choi E, Choi Y, Ahn J, Park O. 2006. Proteomics studies of post-translational modifications in plants. *Journal of Experimental Botany* **57**:1547-1551

Lahner B, Gong J, Smith E, Abid K, Rogers E, Guerniot M, Harper J, Ward J, McIntyre L. 2003. Genomic scale profiling of nutrient and trace elements in *Arabidopsis thaliana. Nature and Biotechnology* **21**:1215-1221

Largarias J, Mercurio F. 1995. Structure functions studies on phytochromes. *Journal of Biological Chemistry* **260**:2415-2423

Le J, Vanderbussche F, De Cnodder T, Verbelen J. 2005. Cell elongation and microtubule behavior in the *Arabidopsis* hypocotyl: Responses to ethylene and auxin. *Journal of Plant Growth and Regulation* **24**:166-178

Lehman A, Black R, Ecker J. 1996. HOOKLESS1, an ethylene responsive gene is required for differential cell elongation in the *Arabidopsis* hypocotyl. *Cell* **85**:183-194

Lemoine R. 2000. Sucrose transporters in plants: update on function and structure. *Biochimica et Biophysica Acta* **1465**:246-262

Li H, Altschmeid L, Chory J. 1994. *Arabidopsis* mutants define downstream branches in the phototransduction pathway. *Genes and Development* **8**:339-349

Li H, Johnson P, Stepanova A, Alonso J, Ecker J. 2004. Convergence of signalling pathways in the control of differential cell growth in *Arabidopsis. Developmental Cell* **7**:193-204

Li H, Washburn T, Chory J. 1993. Regulation of gene expression by light. *Opinions in CellularBiology* **5**:455-460.

Liscum E, Hangarter R. 1993a. Light stimulated apical hook opening in wild-type *Arabidopsis thaliana* seedlings. *Plant Physiology* **101**:567-572

Liscum E, Hangarter R. 1993b. Photomorphogenic mutants of *Arabidopsis thaliana* reveal activities of multiple photosensory systems during light-stimulated apical hook opening. *Planta* **191**:214-211

Lockhart D, Dong H, Brown E. 1996. Expression monitoring by hybridisation to high-density oligonucleotide arrays. *Nature Biotechnology* **13**:1675-1680

Ludewig U, Frommer W. 2002. Gene and proteins for solute transport and sensing. *The Arabidopsis Book.*

Lui X, Bush D. 2006. Expression and transcriptional regulation of amino acid transporters in plants. *Amino Acids* **30**:113-120

Luoni L, Bonza MC, Michelis M. 2006. Calmodulin/Ca^{2+} ATPase interaction at the *Arabidopsis thaliana* plasma membrane is dependent on calmodulin isoform showing isoform-specific Ca^{2+} dependencies. *Physiologia Plantarum* **136**:175-186

Luoni L, Meneghelli S, Bonza M, DeMichelis M. 2004. Auto-inhibition of *Arabidopsis thaliana* plasma membrane Ca^{2+}-ATPase involves an interaction of the N-terminus with the small cytoplasmic loop. *FEBS letters* **574**:20-24

Ma L, Li J, Qu L, Hager J, Chen Z, Zhao H, Deng X. 2001. Light control of *Arabidopsis* development entails coordinated regulation of genome expression and cellular pathways. *Plant Cell* **13**:2589-2607

Maathius F, Amtmann A *et al.*, 2003. Transcriptome analysis of root transporters reveals participation of multiple gene families in the response to cation stress. *Plant Journal* **35**:675-692

Maathius F, Sanders D. 1994. Mechanism of high affinity potassium uptake in roots of *Arabidopsis thaliana. Proceedings of the National Academy of Sciences USA* **91**:9272-9276

Mancinelli A.L. 1994. The physiology of phytochrome actions. *In photomorphogenesis in plants, 2nd edition* pp 211-270, Kluwer Academic Publishers

Martienssen R. 1998. Functional genomics: probing plant gene function and expression with transposons. *Proceedings of the National Academy of Sciences USA* **95**:2021-2026

Martinioa E, Klein M, Geisler M, Bovet L, Forestier C. 2002. Multifunctionality of plant ABC transporters – more than just detoxifiers. *Planta* **214**:345-355

Matsushita T, Mochizuki N, Nagatani A. 2003. Dimers of the N-terminal domain of phytochrome B are functional in the nucleus. *Nature* **424**:571-574

McCormac A, Elliot M, Chen D. 1997. pBECKS – A flexible series of binary vectors for *Agrobacterium*-mediated plant transformation. *Molecular Biotechnology* **8**:199-205

McCormac A, Fisher A, Kumar A, Soll D, Terry M. 2001. Regulation of *HEMA1* expression by phytochromes and a plastid signal during de-etiolation in *Arabidopsis thaliana. The Plant Journal* **25**:549-561.

McCormac A, Smith H, Whitelam G. 1993. Photoregulation of germination in seeds of a transgenic line of tobacco and *Arabidopsis* which express an introduced cDNA encoding phytochrome A or phytochrome B. *Planta* **191**:386-393

McCormac AC, Terry MJ. 2002. Light-signalling pathways leading to the co-ordinated expression of *HEMA1* and *Lhcb* during chloroplast development in *Arabidopsis thaliana. The Plant Journal* **32**:549-559

Mc Dowell J, An Q, Huang S. 1996. The *Arabidopsis* ACT7 gene is expressed in rapidly developing tissues and respond to several external stimuli. *Plant Physiology* **111**:669-711

McKinney E, Ali N, Traut A, Feldman K, Belostotsky D, McDowell J, Meagher R. 1995. Sequence based identification of T-DNA insertion mutations in *Arabidopsis* Actin mutants act2-1 and act2-4. *Plant Journal* **8**:613-650

Meagher R, Kandasamy M, Deal R. 2004 Nuclear actin-related proteins modulate multiple diverse developmental pathways in *Arabidopsis. Molecular Cell Biology* **15**:328-345

Möller S, Ingles S. 2000. The cell biology of phytochromes signalling. *New Phytologist* **154**:553-590

Möller S, Ingles S, Whitelam G. 2002. The cell biology of phytochromes signalling. *New Phytologist* **154**:553-590

Monte E, Alsonso J, Ecker J, Zhang Y, Li X, Young J, Austin-Philips S, Quail P. 2003. Isolation and characterisation of *phyC* mutants in *Arabidopsis* reveals complex crosstalk between phytochromes signalling pathways. *Plant Cell* **15**:1962-1980

Montomery B, Lagarias J. 2002. Phytochrome ancestry. Sensors of bilins and light. *Trends in Plant Science* 7:357-366

Moran R, Porath D. 1980. Chlorophyll determination in intact tissues using N,N-Dimethylformamide. *Plant Physiology* **65**:478-479.

Moulin M, Smith A. 2005. Regulation of tetrapyrrole biosynthesis in higher plants. *Biochemical Society Transaction* **33**:737-742

Murshige T, Skoog F. 1962. A revised medium for rapid growth and Bio assays with Tobacco tissue cultures. *Physiologica Plantarum* **15**:473-497

Murphy J, Largarias J. 1997. The phytofluors: a new class of fluorescent protein probes. *Current Biology* 7:870-876

Nacry P, Camilleri C, Courtial B, Caboche M, Bouchez D. 1998. Major chromosomal rearrangements induced by T-DNA transformation in *Arabidopsis*. *Genetics* **149**:641-659

Nacry P, Camilleri C, Courtial B, Caboche M, Bouchez D. 1998. Major chromosomal rearrangements induced by T-DNA transformation in *Arabidopsis*. *Genetics* **149**:641-659

Nagatani A, Chory J, Furuya M. 1991. Phytochrome B is not detectable in the *hy3* mutant of *Arabidopsis*, which is deficient in responding to end-of-day far-red light treatments. *Plant Cell Physiology* **32**:1119-1122

Nagatani A, Reed J, Chory J. 1993. Isolation and initial characterisation of *Arabidopsis* mutants that are deficient in functional phytochromes A. *Plant Physiology* **102**:269-277

Nagatani A. 2004. Light-regulated nuclear localization of phytochromes. *Current Opinion in Plant Biology* **7**:708-711

Nagy F, Schafer E. 2002. Phytochromes control photomorphogenesis by differentially regulated, interacting signalling pathways in higher plants. *Annual Review of Plant Biology* **53**:329-355

Nagy F, Kircher D, Schafer E. 2000. Nucelo-cytoplasmic partitioning of the photoreceptor phytochromes. *Cell Development and Biology* **11**:505-510

Nakanishi Y, Yabe I, Maeshima M. 2003. Patch clamp analysis of a H^+ pump heterologously expressed in giant yeast vacuoles. *Journal of Biochemistry* **134**:615-623

Neff M, Chory J. 1998. Genetic interaction between phytochrome A, phytochrome B and cryptochrome 1 during *Arabidopsis* development. *Plant Physiology* **118**:27-36

Ni M, Tepperman J, Quail P. 1998. PIF3, a phytochrome-interacting factor necessary for normal photo-induced signal transduction, is a novel basic helix-loop-helix protein. *Cell* **95**:657-667

Niittyle T, Messerli G, Trevisan M, Chen J, Smith A, Zeeman S. 2004. A previously unknown maltose transporter essential for starch degradation in leaves. *Science* **2**:87-89

Oka Y, Matsushita T, Mochizuki N, Suzuki T, Nagatani A. 2004. Functional analysis of a 450-amino acid N-terminal fragment of phytochrome B in *Arabidopsis*. *Plant Cell* **16**:2104-2116

Okumoto S, Koch W, Tegeder M, Fischer W, Biehl A, Leister D, Frommer W. 2004. Root phloem-specific expression of the plasma membrane amino acid proton co-transporter AAP3. *Journal of Experimental Botany* **55**:2155-2168.

Ortiz-Lopez, Chang H.C, Bush D,R. 2000. Amino acid transporters in plants. *Biochimica et Biophysica Acta* **1465**:275-280

Osterlund M, Hardtke C, Wei N, Deng X. 2000. Targeted destabilization of HY5 during light regulated development of *Arabidopsis*. *Nature* **405**:462-466

Palmgram M.G, Harper J.F. 1999. Pumping with plant P-type ATPases. *Journal of Experimental Botany* **50**:883-893

Palmgren M. 2001. Plasma membrane H^+ ATPases: Powerhouses for nutrient uptake. *Annu Rev. Plant Physiol. Plant Mol. Biol.* **52**:817-845

Parinov S, Sundaresan V. 2000. Functional genomics in *Arabidopsis*: large-scale insertional mutatgenesis complements the genome sequencing project. *Current Opinion in Biotechnology* **11**:157-161

Parinov S, Sevugen M, Ye D, Yang WC, Kumaran M, Sundaresan V. 1999. Analysis of flanking sequences from dissociation insertion lines: a database for reverse genetics in *Arabidopsis*. *Plant Cell* **11**:2263-2270

Park E, Kim J, Lee Y, Oh E, Chung W, Lia J, Choi G. 2004. Degradation of phytochrome interacting factor 3 in phytochrome-mediated light signalling. *Plant Cell Physiology* **136**:968-97

Park O. 2004. Proteomic studies in plants. *Journal of Biochemistry and Molecular Biology* **37**:133-138

Patterson M, Vanier M, Morris J, Carstea E, Neufold E. 2001. Niemann-Pick disease C: a lips trafficking disorder. *The Metabolic and Molecular basis of Inherited Diseases* **34**:2625-2639

Pfaffl M. 2001. A new mathematical model for relative quantification in Real-time RT-PCR. *Nucleic Acids Research* **29**:952-963

Poerik R, Cuppens M, Voesenek L, Visser E. 2004. Interactions between ethylene and gibberellins in phytochrome-mediated shade avoidance responses in Tobacco. *Plant Physiology* **136**:2928-2936

Ponting C, Aravind L. 1997. PAS: A multifunctional domain family comes to light. *Current Biology* 7:674-677

Pylatuik J, Fobert P. 2005. Comparison of transcript profiling on *Arabidopsis* microarray platform technologies. *Plant Molecular Biology* **58**:609-624

Quail P. 1991. Phytochrome: A light-activated molecular switch that regulates plant gene expression. *Annual Review of Genetics* **25**:389-409

Quail P. 1997. An emerging molecular map of the phytochromes. *Plant, Cell and Environment* **20**:657-665

Quail P. 2002. Phytochrome photosensory signalling networks. *Nature Review of Moecular Cell Biology* **3**:85-93

Radhamony RN, Prasad A, Srinivasan R. 2005. T-DNA insertional mutagenesis in *Arabidopsis*: a tool for functional genomics. *Journal of Biotechnology* **8**:81-95

Raina S, Mahalingam R, Chen F, Fedoroff. 2002. A collection of sequenced and mapped Ds transposon insertion sites in *Arabidopsis thaliana. Plant Molecular Biology* **50**:93-110

Ramachandran S, Sundaresan V. 2001. Transposons as tools for functional genomics. *Plant Physiol Biochemistry* **39**:243-252

Raven P, Every R, Eichhorn S. 2005. Biology of Plants seventh edition. *W.H Freeman and Company Publishers*

Raz V, Ecker J. 1999. Regulation of differential growth in the apical hook of *Arabidopsis. Development* **126**:3661-3668

Raz V, Koornneef M. 2001. Cell division activity during apical hook development. *Plant Physiology* **125**:219-226

Reed J, Nagatani A, Elich T, Fagan M, Chory J. 1994. Phytochrome A and phytochrome B have overlapping but distinct functions in *Arabidopsis* development. *Plant Physiology* **104**:1139-1149

Reed J, Nagpal P, Poole D, Furuya M, Chory J. 1993. Mutations in the gene for the red/far-red light receptor phytochromes B alter cell elongation and physiological responses throughout *Arabidopsis* development. *Plant Cell* **5**:147-157

Ringli C, Baumberger N, Diet A. 2002. ACTIN2 is essential for bulge site selection and tip growth during root hair development of *Arabidopsis. Plant Physiology* **129**:1464-1472

Robertson W, Clark C, Young J, Sussman M. 2004. An *Arabidopsis thaliana* plasma membrane proton pump is essential for pollen development. *Genetics* **168**:1677-1687.

Robson P, Whitelam G, Smith H. 1993. Selected components of the shade-avoidance syndrome are displayed in a normal manner in mutants of *Arabidopsis thaliana* and *Brassica rapa* deficient in phytochrome B. *Plant Physiology* **102**:1179-1184

Rockwell N, Lagarias J. 2006. The structure of phytochrome: A picture is worth a thousand spectra. *The Plant Cell* **18**:4-14

Rockwell N, Su Y, Lagarias J. 2006. Phytochrome structure and signalling mechanisms. *Annual Review of Plant Biology* **57**:837-858

Romano C, Cooper M, Klee H. 1993. Uncoupling auxin and ethylene effects in transgenic Tobacco and *Arabidopsis* plants. *The Plant Cell* **5**:181-189

Saier M.H et al. 1999. The major facilitator superfamily. *Journal of Molecular Microbiology & Biotechnology* **1**:257-259

Saijo Y, Sullivan J, Wang H, Yang J, Shen Y, Rubio V, Ma L, Hoecker U, Deng X. 2003. The COP1-SPA1 interaction defines a critical step in phytochrome A-mediated regulation of HY5 activity. *Genes and Development* **17**:2642-2647

Sakamoto k, Nagatani A. 1996. Nuclear localisation activity of phytochromes B. *Plant Journal* **10**:859-868

Salt D. 2004. Update on plant ionomics. *Plant Physiology* **136**:2451-2456

Sambrook J, Fritsch E, Maniatis T. 1989. Molcular Cloning – A laboratory manual 2nd edition. Cold Spring Habour Laboratory Press, New York.

Sanders D, Brownlee C, Harper J. 1999. Communicating with calcium. *Plant Cell* **11**:691-706

Sauer N, Baier K, Gahrtz M, Stadler R, Stolz J, Truenit E. 1994. Sugar transport across the plasma membrane of higher plants. *Plant Molecular Biology* **26**:1671-1679

Sauer N, Friedlander K, Graml-Wicke U.1990. Primary structure, genomic organisation and heterozygous expression of a glucose transporter from *Arabidopsis thaliana*. *EMBO* **9**:3045-3050

Sauer N, Stolz J. 1994. SUC1 and SUC2, two sucrose transporters from *Arabidopsis thaliana*; expression and characterisation in bakers yeast. *Plant Journal* **6**:67-77

Schena M. 1996. Genome analysis with gene expression microarrays. *Bioessays* **18**:427-431

Schiott M, Romanowsky S, Baekgaard L, Palmgren M, Harper J. 2004. A plant plasma membrane Ca^{2+} pump is required for pollen tube growth and fertilization. *Proceedings of the National Academy of Sciences USA* **101**:9502-9507.

Scholz-Starke J, Buttner M, Sauer N. 2003. AtSTP1, a new pollen-specific H^{+}-monosaccharide symporter from *Arabidopsis*. *Plant Physiology* **131**:70-77

Schuzle A, Downward J. 2001. Navigating gene expression during miroarrays – a technology review. *Nature Cell Biology* **13**:61-72

Schwacke R, Schneider A, van der Graaff E, Fischer K. 2003. Aramemnon a novel database for *Arabidopsis* integral membrane proteins. *Plant Physiology* **131**:16-26

Seki M, Narusaka M, Ishida J. 2002. Monitoring the expression profiles of 7000 *Arabidopsis* genes under drought and cold stresses by using a full-length cDNA microarray. *Plant Cell* **13**:279-292

Seo H, Yang J, Ishikawa M, Bolle C, Ballesteros M, Chau N. 2003. LAF1 ubiquitination by COP1 controls photomorphogenesis and is stimulated by Spa1. *Nature* **423**:995-999

Shahmuradov I, Solovyev V, Gammerman A. 2005. Plant promoter prediction with confidence estimation. *Nucleic Acids Research* **33**:1069-1076

Sharrock R, Quail P. 1989. Novel phytochromes sequences in Arabidopsis thaliana: structure, evolution and differential expression of a plant regulatory photoreceptor family. *Genes and Development* **3**:1745-1757

Shen Y, Feng S, Ma L, Lin R, Qu L, Chen Z, Wang H, Deng X. 2005. *Arabidopsis* FHY1 protein stability is regulated by light via phytochrome A and 26S proteasome. *Plant Physiology* **10**:1104-1112

Sherson S, Hemmann G, Wallace G, Forbes S. 2000. Monosaccharide/proton symporter AtSTP1 plays a major role in uptake and response of *Arabidopsis* seeds and seedlings to sugar. *The Plant Journal* **24**:849-857

Shigaki T, Sreevidya C, Hirshi K. 2001. Analysis of the Ca^{2+} domain in the *Arabidopsis* H^{+}/Ca^{2+} antiporters CAX1 and CAX3. *Plant Molecular Biology* **50**:475-483

Shinomura T, Nagatani A, Chory J, Furuya M. 1994. The induction of seed germination in *Arabidospis thaliana* is regulated principally by phytochrome A and secondary by phytochrome A. *Plant Physiology* **104**:363-371

Shinomura T, Nagtani A, Kubota M, Watanabe M, Furuya M. 1996. Action spectra for phytochrome A and B-specific photoinhibition of seed germination in *Arabidopsis thaliana. Proceedings of the National Academy of Sciences USA* **93**:8129-8133

Smith H, Whitelam G. 1997. The shade avoidance syndrome: Multiple responses mediated by multiple phytochromes. *Plant Cell and Environment* **13**:695-707

Smith H. 2000. Phytochromes and light signal perception by plants – an emerging synthesis. *Nature* **407**:585-591

Somers D, Sharrock R, Tepperman J, Quail P. 1991. The *hy3* long hypocotyls mutant of *Arabidopsis* is deficient in phytochromes B. *Plant Cell* **3**:1263-1274

Songergaard T, Schulz A, Palmgren MG. 2004. Energization of transport processes in plants. Roles of the plasma membrane H^{+}-ATPase. *Plant Physiology* **136**:2475-2482

Speulman E, Metz PL, Van Arkel G, Lintel B, Stiekema WJ, Pereira A. 1999. A two-component enhancer-inhibitor transposon mutagenesis system for functional analysis of the Arabidopsis genome. *Plant Cell* **11**:1853-1866

Stadler R, Buttner M, Ache P, Hedrich R, Sauer N. 2003. Diurnal and light-regulated expression of AtSTP1 in guard cells of *Arabidopsis. Plant Physiology* **133**:1-10

Su Y, Frommer W, Ludewig. 2004. Molecular and functional characterization of a family of amino acid transporters in *Arabidopsis. Plant Physiology* **136**:3104-3113

Sullivan J, Wang Deng X. 2003. From seed to seed: the role of photoreceptors. *Developmental Biology* **260:**289-297

Symons G, Reid J. 2003. Interactions between light and plant hormones during de-etiolation. *Journal of Plant Growth and Regulation* **22**:3-14

Sze H, Liang F, Hwang I. 2000. Diversity and regulation of plant Ca^{2+} pumps: Insights from the expression in yeast. *Annu Rev. Plant Physiol. Plant Mol. Biol* **51**:433-462

Takano M, Inagaki N, Xie X, Yuzurihara N, Hihara F, Ishizuka T, Yano M, Nishimura M, Miyao A. 2005. Distinct and cooperative functions of phytochromes A. B, and C in the control of de-etiolation and flowering in rice. *The Plant Cell* 17:3311-3325

Tanako M, Kanegae H, Shinomura T, Miyao A, Furuya M. 2001. Isolation and characterisation of rice phytochromes A mutants. *Plant Cell* **13**:521-534

Tasler R, Mioises T. 2005. Biochemical and spectroscopic characterization of the bacterial phytochrome. *Journal of Biological Chemistry* **272**:1927-1936

Taylor B, Zhulin I. 1999. PAS domains: Internal sensors of oxygen, redox potential and light. *Microbiology Molecular Biology Research* **2**:479-487

Tepperman J, Hudson M, Khanna R, Chang S, Wang X, Quail P. 2004. Expression profiling of the phyB mutant demonstrates substantial contribution of other phytochromes to red-light regulated gene expression during seedling de-etiolation. *Plant Journal* **38**:725-739

Tepperman J, Zhu T, Chang H, Wang X, Quail P. 2001. Multiple transcription-factor genes are early targets of phytochrome A signalling. *PNAS* **98**:9437-9442

Terry MJ, Wahleithner J, Lagarias JC. 1993. Biosynthesis of the plant photoreceptor phytochromes. *Arch. Biochem. Biophys* **306**:1-15

Terzaghi W.B. & Cashmore A.R. 1995. Light-regulated Transcription. *Annual Review of Plant Physiology and Plant Molecular Biology* **46**:445-474

Thain S, Vandenbussche F, Laarhoven L, Dowson-Day M, Wang Z, Tobin E, Harren F, Millar A. 2004. Circadian rhythms of ethylene emission in *Arabidopsis. Plant Physiology* **136**:3751-3761

Theologis A, Ecker J, Palm C. 2000. Sequence and analysis of chromosome 1 of the plant *Arabidopsis thaliana. Nature* **408**:616-820

Tian Q, Reed W. 2001. Molecular links between light and auxin signalling pathways. *Journal of Plant Growth and Regulation* **20**:271-280

Tiaz L, Zeiger E. 2006. Plant Physiology fourth edition. *Sinauer Associates Inc. Publishers*

Timmons L, Tabara H, Mello C, Fire A. 2003. Inducible systematic RNA silencing in *Caenorhabditis elegans. Molecular Biology of the Cell* **14**:2972-2983

Toledo-Ortiz G, Huq E, Quail P. 2003. The *Arabidopsis* basic/helix-loop-helix transcription factor family. *Plant Cell* **15**:1749-1770

Torii K, Deng X. 1997. The role of COP1 in light control of *Arabidopsis* seedling development. *Plant Cell and Environment* **20**:728-733

Tsukaya H, Kozuka, T, Kim G. 2002. Genetic control of petiole length in *Arabidopsis thaliana. Plant Cell Physiology* **43**:1221-1228

Vandenbussche F, Verbelen J, Van Der Straeten D. 2005. Of light and length:regulation of hypocotyl growth in *Arabidopsis*. *Bioessays* **27**:275-284

Vanderbussche F, Vriezen W, Smalle J, Laarhoven L, Harren F, Van Der Straeten D. 2003. Ethylene and auxin control the *Arabidopsis* response to decreased light intensity. *Plant Physiology* **133**:517-527

Verwoerd T, Dekker B, Hoekema A. 1989. A small-scale procedure foe the rapid isolation of plant RNAs. *Nature* **17**:2362-2365

Vogel J, Zarka D, Van Buskirk H, Fowler S, Thomashow M. 2005. Roles of the CBF2 and Zat12 transcription factors in configuring the low temperature transcriptome of *Arabidopsis*. *Plant Journal* **41**:195-211

Von Arnim A & Deng X. 1996. Light control of Seedling development. *Annual Review Plant Physiology and Plant Molecular Biology* **47**:215-243

Wagner J, Brunzelle J, Forest K, Vierstra R, 2005. A light-sensing knot revealed by the structure of the chromophore-binding domain of phytochrome. *Nature* **438**:325-331

Wang H, Ma L, Habashi J, Zhao H, Deng X. 2002. Analysis of far-red light-regulated genome expression profiles of the phytochrome A pathway mutants in *Arabidopsis. Plant Journal* **32**:723-733

Wang H, Ma L, Li J, Zhao H, Deng X. 2001. Direct interaction of *Arabidopsis* cryptochromes with COP1 in light control development. *Science* **294**:154-158

Wang R, Guegler K, Labrie S, Crawford N. 2000. Genomic analysis of a nutrient response in *Arabidopsis* reveals diverse expression patterns and novel metabolic and potential regulatory genes induced by nitrate. *Plant Cell* **12**:1491-1509

Ward J. 2001. Identification of novel families of membrane proteins from the model plant *Arabidopsis thaliana. Bioinformatics* **17**:560-563

Weber M, Trampczynska A, Clemens S. 2006. Comparative transcriptome analysis of toxic metal responses in *Arabidopsis thaliana* and the Cd^{2+}-hypertolerant membrane H^{+}-ATPases by glucose. Interaction between domains and identification of regulatory sites. *Journal of Biological Chemistry* **269**:10393-10399

Wei N, Chamovitz D, Deng X. 1994. *Arabidopsis* COP9 is a component of a novel signalling complex mediating light control of development. *Cell* **78**:117-124

Wettstein D, Gough S, Kannangara C. 1995. Chlorophyll biosynthesis. *The Plant Cell* 7:1039-1057

White P, Broadley M. 2003. Calcium in plants. *Annals of Botany* **92**:487-511

Whitelam G, Devlin P. 1997. Roles of different phytochromes in *Arabidopsis* photomorphogenesis. *Plant Cell and Environment* **20**:752-758

Whitelam G, Harberd N. 1994. Action and function of phytochromes family members revealed through the study of mutant and transgenic plants. *Plant Cell and Environment* **16**:564-572

Whitelam G, Patel S, Devlin P. 1998. Phytochrome and photomorphogenesis in *Arabidopsis. Phil. Trans R. Soc. London* **353**:1445-1453

Williams L, lemoine R, Sauer N. 2000a. Sugar transporters in higher plants – a diversity of roles and complex regulation. *Trends in Plant Science* **5**:283-290.

Williams L, Pittman J, Hall J. 2000b. Emerging mechanisms for heavy metal transport in plants. *Biochimica et Biophysica Acta* **1464**:104-126

Williams L, Mills R. 2005. P1B-ATPases- an ancient family of transition metal pumps with diverse functions in plants. *Trends in Plant Science* **10**:1360-1375

Williams LE, Mills, R.F. 2005. The P 1B -ATPases – an ancient family of transition metal pumps with diverse functions in plants. *Trends in Plant Science* **10**:492-502

Woeste K, Kieber J. 2000. A strong loss-of-function mutation in RAN1 results in constitutive activation of the ethylene response pathway as well as a rosette-lethal phenotype. *Plant Cell* **12**:443-455

Wullschliger S, Difazio S. 2003. Emerging use of gene expression microarrays in plant physiology. *Comparartive and Functional Genomics* **4**:216-224

Yamamoto Y, Matsui M, Ang L, Deng X. 1998. Role of a COP1 interactive protein in mediating light-regulated gene expression in *Arabidopsis. Plant Cell* **10**:1083-1094

Yang K, Kim Y, Lee S, Song P, Soh M. 2003. Overexpression of a mutant basic helix-loop-helix protein HFR1, HFR1 activates a branch pathway of light signalling in *Arabidopsis. Plant Physiology* **133**:1630-1642

Yang J. 2005. Light regulates COP1-mediated degradation of HFR1, a transcriptional factor essential for light signalling in *Arabidopsis* . *Plant Cell* **17**:804-821

Young CJ, Krysan PJ, Sussmann MR. 2001. Efficient screening of *Arabidopsis* T-DNA insertion lines using degenerate primers. *Plant Physiology* **125**:513-518

Yu H, Hogan P, Sundaresan V. 2005. Analysis of the female gametophyte transcriptome of *Arabidopsis* by comparative expression profiling. *Plant Physiology* **139**:1853-1869

Zhu T and Wang X. 2002. Large-scale profiling of the *Arabidopsis* transcriptome. *Plant Physiology* **124**:1472-1476

Zimmermann P, Hirsch-Hoffmann, Hennig L, Gruissem W. 2004. GENEVESTIGATOR. *Arabidopsis* microarray database and analysis toolbox. *Bioinformatics* **136**:2621-2632